EXPLORATION OF THE DETERMINANTS OF SUBSTRATE AND REACTION SPECIFICITY IN THE PYRIDOXAL 5'-PHOSPHATE-DEPENDENT ENZYMES OF THE TRANSSULFURATION PATHWAYS

By

Pratik Lodha, B.Sc.H.

A thesis submitted to the Faculty of Graduate and Postdoctoral Affairs in partial fulfillment of the requirements for the degree of

Doctor of Philosophy

in

Biology

Department of Biology

Ottawa-Carleton Institute of Biology

Carleton University

Ottawa, Ontario

April 2011

Your file Votre référence
ISBN: 978-0-494-81584-7
Our file Notre référence
ISBN: 978-0-494-81584-7

ABSTRACT

A common feature of the diverse enzymes catalyzing transformations of amino acids is their reliance of the pyridoxal 5'-phosphate (PLP) cofactor. The adaptability and plasticity of their protein scaffold has allowed enzymes to regulate the chemistry of PLP to take advantage of its remarkable catalytic versatility. The enzymes cystathionine γ-synthase (CGS) and cystathionine β-lyase (CBL) of the plant and bacterial transsulfuration pathway and cystathionine β-synthase (CBS) and cystathionine γ-lyase (CGL) of the yeast and mammalian reverse transsulfuration pathway interconvert L-cysteine and L-homocysteine. These enzymes, which catalyze distinct side-chain rearrangements of similar amino-acid substrates, comprise an ideal model system for investigation of the structure-function relationships that allow enzymes to regulate the specificity of PLP-catalyzed reactions. The focus of the studies described in this thesis is the investigation of the roles of active-site residues of *Escherichia coli* CGS (eCGS) and CBL (eCBL) and yeast CBS (yCBS) as determinants of substrate and reaction specificity. Site-directed replacements of 26 residues, proposed to interact with the substrates and/or the PLP cofactor, in the active sites of yCBS, eCBL and eCGS were characterized. The results indicate that residues K112 and Y248 of yCBS interact indirectly with the L-Ser and L-Hcys substrates of this enzyme, while the drastic effect of the G247S substitution on the kinetic parameters of yCBS, in combination with *in silico* modeling of the corresponding disease-associated, G307S mutation of human CBS, demonstrate this residue impacts cofactor binding and orientation within the active site. Residue yCBS-N84 also interacts with the PLP cofactor and substitution with alanine, histidine and aspartate revealed roles in both substrate binding and reaction specificity, *via* shielding of

the reactive aminoacrylate intermediate. The enzymes eCBL and eCGS share 38% amino acid sequence identity, a common quaternary structure and several active site residues. Additionally, the L-cystathionine product of eCGS is the substrate of eCBL. The ability of these two enzymes to enforce strict reaction specificity is a function of the identity, position and conformation of key active-site residues. The role of a pair of conserved arginine residues in binding the dicarboxylic substrates of both enzymes was demonstrated. However, none of the nine active-site residues investigated, conserved in bacterial CGS sequences, are involved in binding the L-Cys substrate of eCGS. A unique role in modulating reaction specificity is proposed for a serine residue, conserved in both eCGS (S326) and eCBL (S339), *via* a tethering interaction that guides the catalytic base. The results of this exploration of the factors that allow the enzymes of the transsulfuration pathways to control the substrate and reaction specificity of the PLP cofactor will enable future studies attempting to modify these properties for biotechnology applications as well as the development of novel classes of therapeutic and antimicrobial compounds.

PREFACE

This thesis follows the integrated thesis format and, as such, the main chapters represent work that has already been published in a peer-reviewed journal (chapters 3-5) at the time of submission of this thesis, or will soon be submitted for publication. I have included a methods section to provide additional detail for techniques common to more than one research chapter.

Status of manuscripts corresponding to research chapters at time of thesis submission

Chapter 3:

P.H. Lodha, H. Shadnia, C.M. Woodhouse, J.S. Wright and S.M. Aitken. Investigation of residues Lys112, Glu136, His138, Gly247, Tyr248 and Asp249 in the active site of yeast cystathionine β-synthase, Biochemistry and Cell Biology. 87 (2009) 531-540.

Chapter 4:

P.H. Lodha, E.M.S. Hopwood, A.L. Manders and S.M. Aitken. Residue N84 of yeast cystathionine β-synthase is a determinant of reaction specificity, Biochimica et Biophysica Acta Proteins and Proteomics. 1804 (2010) 1424-1431.

Chapter 5:

P.H. Lodha, A.F. Jaworski and S.M. Aitken. Characterization of site-directed mutants of residues R58, R59, D116, W340 and R372 in the active site of *E. coli* cystathionine β-lyase, Protein Science. 19 (2010) 383-391.

Chapter 6:

P.H. Lodha and S.M. Aitken. Characterization of the side-chain hydroxyl moieties of residues Y56, Y111, Y238, Y338 and S339 as determinants of specificity in *E. coli* Cystathionine β-Lyase. To be submitted to the journal Biochemistry. Expected date of submission: May, 2011.

Chapter 7:

P.H. Lodha and S.M. Aitken. Exploration of the active site of *E. coli* cystathionine γ-synthase. To be submitted to the journal Protein Science. Expected date of submission: June, 2011.

Chapter 8:

The general conclusions chapter has been composed to synthesize and reflect upon the body of research work presented in this thesis. It also includes some material published in a recent review paper, for which I am the second author:

S.M. Aitken, P.H. Lodha and D.J.K. Morneau. The Enzymes of the transsulfuration pathways: active site characterizations. Biochimica et Biophysica Acta Proteins and Proteomics. In press.

Statement of contributions

My contributions to the research described in this thesis include:

1. development of the research questions, in partnership with Dr. S.M. Aitken,
2. responsibility for experimental design and the collection and analysis of data,
3. the co-supervision, in collaboration with Dr. S.M. Aitken, of five undergraduate students: Heidi Los and Navya Kalidindi, who participated in purification of the site-directed variants described in chapters 5 and 6, Adrienne Manders, who participated in the purification and characterization of enzymes described in chapter 4 and the construction and purification of site-directed variants described in chapter 7, Colleen Woodhouse, who constructed and purified one of the enzymes described in chapter 3 and Emily Hopwood, who participated in the pre-steady state characterization of the three site-directed variants described in chapter 4.
4. the preparation of drafts of the manuscripts, in collaboration with Dr. S.M. Aitken, which comprise the research chapters of this thesis.

I formally acknowledge the contributions of the co-authors of the manuscripts that comprise the research chapters of my thesis. My supervisor, Dr. S.M. Aitken, contributed her expertise by guiding me in the formulation of the research questions and experimental design and by assisting with the analysis and interpretation of data and the preparation of manuscripts for each of the five research chapters of my thesis. Dr. Hooman Shadnia (postdoctoral fellow) and Dr. James S. Wright (Dept of Chemistry, Carleton University) are co-authors of the published article corresponding to chapter 3. Dr. Shadnia performed

computer analysis and homology modeling under the supervision of Dr. Wright. Allison Jaworski (Ph.D. candidate, Aitken lab, Dept. of Biology), constructed, purified and performed the preliminary characterization of one of the site-directed variants described in chapter 5. The contributions of former and current undergraduate students is described above.

I have obtained copyright permission from each publisher to reproduce published manuscripts and from each of my co-authors to use collaborative works in this thesis.

ACKNOWLEDGEMENTS

The monumental task of completing this Ph.D. thesis, spanning the duration of five years, cannot be solely done by one person. The culmination of this vast project is a result of the collaborative efforts of many people whom I would like to thank from the bottom of my heart. I would like to begin by thanking the undergraduate students with whom I had the privilege to work: Adrienne Manders, Sherwin Habibi, Navya Kalidindi and Heidi Los. These students were some of the brightest minds I have ever encountered and training them was an extremely rewarding experience. My fellow graduate students, Faraz Quazi, Muluken Belew Shambel, Colleen Woodhouse, Jennifer Skanes, Dominique Morneau, Allison Jaworski and Edgar Abou-Assaf, were always willing to provide assistance with my work and created an invigorating learning experience by challenging me constantly. I would also like to thank the administrative staff of the Biology Department, Marija Gojmerac, Laura Thomas and Michelle O'Farrell, who handled all the laborious paper work and were always helpful with administrative tasks.

Special parts of this long experience were the close friendships I shared with Nikita Rayne, Vishwanath Sollapura, Emily Hopwood, Andrew Robinette, Justin Kicks and Ali Farsi, who tolerated my shortcomings and accepted me with my many quirks. They have made my life enjoyable, providing memorable moments with ample laughter.

This thesis would not have been accomplished without the unconditional love and support of my entire family. In addition to providing financial assistance, my father, Hemant Lodha, constantly motivated and guided me along the right path, and my mother, Prabha Lodha, always believed in my abilities to succeed even when I did not. In the past three years my wife, Vaishali Jain, has pushed me to work harder towards my goals.

Her unwavering support in sustaining my health and well-being during this period is something I appreciate and will be eternally grateful for. I thank my sister Prachi Daga and her husband Navin Daga, for always showing support and curiosity in my work. To my extended family, I offer my sincere gratitude for being understanding of my absence during important events.

I would also like to extend my deepest thanks to my committee members, Dr. Owen Rowland and Dr. Douglas A. Johnson, who were always willing to provide me with their brilliant ideas, feedback and words of wisdom during committee meetings and my qualifying exam. In addition, I thank Dr. Susan M. Aitken, without whom this reality would be just a dream. Dr. Aitken was not only my supervisor but a role model, a parental figure, and a friend throughout the years I have known her. Apart from providing advice for my career and thesis, she never deterred me when I approached her with personal matters. She has shown an immense level of patience towards my weaknesses and has worked relentlessly to improve them. I appreciate the path she has paved for me and any success I encounter in the future can be attributed to the hard work and support that she has given me during my graduate studies. With sincere gratitude, I would like to thank her for always believing in me and for providing me the rare and valuable opportunity to work in her laboratory.

DEDICATION

In loving memory of my Grandfather,
Mr. Chanchal Mal Lodha

TABLE OF CONTENTS

LIST OF TABLES

Page

LIST OF FIGURES

Page

ABBREVIATIONS

A. thaliana	*Arabidopsis thaliana*
AA	Aminoacrylate
AATase	Aspartate aminotransferase
ALAS	5-aminolevulinate synthase
AMPSO	N-(1,1-Dimethyl-2-hydroxyethyl)-3-amino-2-hydroxypropanesulfonic acid
APPA	DL-E-2-amino-5-phosphono-3-pentenoic acid
AtCBL	*A. thaliana* cystathionine β-lyase
AVG	Aminoethoxyvinylglycine
BSA	Bovine serum albumin
C. freundii	*Citrobacter freundii*
CAPS	N-cyclohexyl-3-aminopropanesulfonic acid
CBL	Cystathionine β-lyase
CBS	Cystathionine β-synthase
CfTPL	*Citrobacter freundii* tyrosine phenol lyase
CGL	Cystathionine γ-lyase
CGS	Cystathionine γ-synthase
CO	Carbon Monoxide
CTCPO	5-carboxymethylthio-3-(3'-chlorophenl)-1,2,4-oxadiazol
dCBS	*Drosophila melanogaster* cystathionine β-synthase
DMSO	Dimethyl sulfoxide
DNA	Deoxyribonucleic acid

DTNB	5,5'-Dithiobis-(2-nitrobenzoic acid)
DTT	Dithiothreitol
E. coli	*Escherichia coli*
E.C.	Enzyme Commission
E-AA	Enzyme-aminoacrylate
eAATase	*Escherichia coli* aspartate aminotransferase
eCBL	*Escherichia coli* cystathionine β-lyase
eCGS	*Escherichia coli* cystathionine γ-synthase
EDTA	Ethylenediaminetetraacetic acid
H_2S	Hydrogen sulfide
hCBS	Human cystathionine β-synthase
hCGL	Human cystathionine γ-lyase
HGL	Homocysteine γ-lyase
HO-HxoDH	D-2-Hydroxyisocaproate dehydrogenase
IPTG	Isopropyl- β-*D*-thiogalactopyranoside
KCl	Potassium Chloride
L-Cth	L-Cystathionine
L-Cys	L-Cysteine
L-Hcys	L-Homocysteine
LDH	L-lactate dehydrogenase
L-LDH	L-lactate dehydrogenase
L-Met	L-Methionine
L-OAS	*O*-acetyl-L-serine

L-OPHS	*O*-phospho-L-homoserine
L-OSHS	*O*-succinyl-L-homoserine
L-Ser	L-Serine
meALAS	Murine erythroid aminolevulinate synthase
MGL	Methionine γ-lyase
MVG	Methoxyvinylglycine
NAD^+	Nicotinamide adenine dinucleotide, oxidized form
NADH	Nicotinamide adenine dinucleotide, reduced form
NaOH	Sodium Hydroxide
nCGS	*Nicotiana tabacum* cystathionine γ-synthase
Ni-NTA	Ni-nitrilo triacetic acid
OAHSS	*O*-acetylhomoserine sulfhydrylase
OASS	*O*-acetyl- L-serine sulfhydrylase
OE-PCR	Overlap-extension polymerase chain reaction
OSHSS	*O*-succinylhomoserine sulfhydrylase
PAG	Propargylglycine
PCR	Polymerase chain reaction
PLP	Pyridoxal 5'-phosphate
PMP	Pyridoximine
PPCA	3-(phosphonomethl)pyridine-2-carboxylic acid
rcALAS	*Rhodobacter capsulatus* 5-aminolevulinate synthase
S. cerevisiae	*Saccharomyces cerevisiae*
S. typhimurium	*Salmonella typhimurium*

SAH	*S*-adenosyl-homocysteine
SAM	*S*-adenosyl-methionine
SDS	Sodium dodecyl sulfate
SDS-PAGE	Sodium dodecyl sulfate polyacrylamide gel electrophoresis
stOASS	*Salmonella typhimurium O*-acetylserine sulfhydrylase
stTrpS	*Salmonella typhimurium* tryptophan synthase
T. denticola	*Treponema denticola*
T. vaginalis	*Trichomonas vaginalis*
TAPS	N-Tris(hydroxymethyl)methyl-3-aminopropanesulfonic acid
tMGL	*Trichomonas vaginalis* methionine γ-lyase
TNB	5'thionitrobenzoic acid
Tris	Tris-[hydroxymethyl]aminomethane
TrpS	Tryptophan synthase
UV	Ultraviolet
yCBS	Yeast cystathionine β-synthase
ytCBS	Truncated yCBS (residues 1-353)
ytCBSc	Closed conformation of ytCBS
ytCBSo	Open conformation of ytCBS

1. INTRODUCTION

1.1 Antibiotics: a brief historical perspective

The serendipitous discovery of the antibiotic penicillin by the Scottish scientist Sir Alexander Fleming has revolutionized modern medicine. The concept of anti-infectious agents however is much older and can be dated back to ancient civilizations such as those of the Indus valley, through the *Ayurveda*, and the Chinese and Egyptians, *via* their use of herbal medicines. The concept that infection is caused by agents that cannot be seen by the naked eye was understood by these civilizations. Through trial and error they determined which fungal and plant materials possess anti-infective properties and used them to make medicines. The *Ayurveda* went as far as proposing methods of sterilization to perform surgeries thorough the use of honey, which is now known to contain antimicrobial agents, and fumigation by burning *Azadirachta indica* (the Neem tree) leaves, which are reported to have antimicrobial, antiviral and anti-diabetic properties (Subapriya and Nagini, 2005).

The modern search for antimicrobial compounds dates to the mid-19th century when critical insights into the spread of airborne infection were made by Robert Williams, John Tyndall, Louis Pasteur, and Ferdinand Cohen. In the mid-1870s, Robert Williams and John Tyndall also identified and investigated the antibacterial properties of *Penicillium* mould (Roberts, 1874; Tyndall, 1876). The pace of research on anti-infective agents slowed in the early 20th century due to World War I and it was not until 1928 that the antimicrobial properties of *Penicillium* mould were characterized by Alexander Fleming (Fleming, 1929). Although it was another ten years before researchers isolated

the active penicillin compound, the commercialization of it as a drug was rapid, due to the needs of soldiers during World War II.

The present anti-infective industry generates billions of dollars in revenue annually (Shlaes, 2010). The increased rate of bacterial resistance, caused by the inappropriate and extensive use of antibiotics, poses a major challenge for researchers and physicians (Pankey and Sabath, 2004). However, this also presents scientists with the opportunity to develop new antibiotics with novel modes of action. Given the pressures of increasing global population growth and growing antibiotic resistance, it is imperative that the development of new antibacterial drugs, first introduced only six decades ago, continues with unabated vigor.

Anti-infective agents targeting bacteria, whether synthetic or natural, are divided into two groups. Bacteriostatic compounds inhibit bacterial growth, while those with bactericidal properties kill bacteria (Pankey and Sabath, 2004). These antibacterial agents are further categorized into 17 different classes of drugs that disrupt five major bacterial cellular processes: the biosynthesis of cell wall components, DNA replication, transcription of RNA, translation of proteins and the folic acid cycle (Chopra *et al.*, 2002; Hurdle *et al.*, 2011). Current antibiotics do not target biosynthetic pathways that are involved in amino acid production (Hurdle *et al.*, 2011). Amino acid metabolism presents an untapped opportunity for the development of new anti-infective agents because, while bacteria and plants synthesize the full complement of proteinogenic amino acids *de novo*, humans and non-ruminant animals rely upon diet for approximately half, which are referred to as the essential amino acids. Therefore, the amino acid biosynthetic pathways

that are not present in mammals provide potential targets for the development of antibacterial therapeutics because disrupting them will pose fewer side effects to humans.

1.2. Enzymes

Cellular metabolism is dependent on the ability of biological catalysts, enzymes, to drastically accelerate the rates of specific biological reactions by lowering their activation energy. The importance of enzymes in cellular metabolism is illustrated by the large number of human genetic diseases linked to mutations in genes encoding enzymes. Of the 923 genes associated with human genetic diseases, 31% encode enzymes (Jimenez-Sanchez *et al.*, 2001). Examples of metabolic disorders caused by mutation(s) in the gene encoding specific enzymes include homocystinuria (cystathionine β-synthase; MIM ID# 236200), methylmalonic acidemia (methylmalonyl-CoA mutase; MIM ID# 251000) and phenylketonuria (phenylalanine hydroxylase; MIM ID# 261600) (Jimenez-Sanchez *et al.*, 2001).

In the context of modern biotechnology, the exquisite specificity and enantioselectivity of enzymes allow them to be employed in the production of chemicals and in industrial processes. Applications of amino acids in the chemical and pharmaceutical industries are developing rapidly and currently comprise a billion-dollar market (Hermann, 2003; Leuchtenberger *et al.*, 2005). Recent awareness of global pollution has also brought enzymes into the limelight for their potential to increase efficiency and reduce waste, in industries from pharmaceuticals to pulp and paper, and for environmental remediation applications. The use of enzymes for economic and industrial purposes over the past three decades has been a driving factor for development

of the relatively new field of protein engineering, where properties of proteins such as thermostability and specificity are modified to achieve specific goals (Fersht, 2008).

Despite the vast amount of information on enzymes and their structure-function relationships available today, the plasticity of macromolecular structure presents a considerable challenge for engineering *via* rational design, in which specific residues are targeted for mutagenesis based on structural, biochemical and bioinformatic data, with the goal of altering a specific property of the protein (Dunaway-Mariano, 2008). The induced-fit model of of substrate binding, proposed by Daniel Koshland, provided early insight into the dynamic nature of structure-function relationships and researchers continue to probe the underlying principles with the goal of facilitating rational redesign studies (Koshland, 1958; Glasner *et al.*, 2006; Khersonsky *et al.*, 2006; Dunaway-Mariano, 2008). A valuable opportunity to probe the structure-function relationships of proteins is presented by enzyme families that share common structural features, but have evolved to catalyze distinct reactions. For example, enzymes catalyzing transformations of amino acids are generally reliant on the ubiquitous pyridoxal 5'-phosphate (PLP) cofactor. Phylogenetic analysis has demonstrated that functional specificity had arisen in PLP-dependent enzymes by the time that the biological kingdoms diverged, between 1 and 1.5 billion years ago (Christen and Mehta, 2001).

1.3. Pyridoxal 5'-Phosphate (PLP) Cofactor

The side chains of the 20 amino acids found in proteins do not provide the variety of chemical tools required for all of the reactions catalyzed by enzymes. Cofactors are

small molecules, which may be metal ions or organic molecules that help enzymes catalyze biochemical transformations (Voet *et al.*, 2002). Cofactors generally bind within the active site of an enzyme and participate in catalysis, but are not considered a substrate since they are returned to their original state upon completion of the catalytic cycle (Bryce, 1979). The terms apoenzyme and holoenzyme are applied to the protein component of an enzyme and the protein-cofactor complex of the same enzyme, respectively. Examples of compounds employed as enzyme cofactors include flavin, heme, nicotinamide and PLP.

Pyridoxine, commonly known as vitamin B_6, is the precursor of PLP, the ubiquitous, water-soluble cofactor employed by enzymes that catalyze transformations of amino acids (Christen and Mehta, 2001). Vitamin B_6 was identified by Paul György while researching the effects of riboflavin and vitamin B_1 on mice raised on a vitamin B-deficient diet (György, 1934). The first crystallization of vitamin B_6 by Lepkovsky (1938) was followed by the elucidation of its structure in 1939 (Harris and Folkers, 1939; Harris *et al.*, 1939; Kuhn *et al.*, 1939). Early research by Kuhn and Wendt (1938) on enzyme-bound pyridoxine suggested that PLP may be a cofactor. This was supported by studies investigating the conversion of glutamate to other amino acids in pigeon muscles, started in 1936 by the Russian enzymologist Alexander E. Braunstein, which demonstrated that these reactions were catalyzed by pyridoxine-dependent enzymes (Braunstein and Kritzman, 1946). The ensuing discovery of the variety of reactions catalyzed by PLP-dependent enzymes, including transamination (Cammarata and Cohen, 1950; Meister, 1955; Jenkins and Sizer, 1957), racemization (Wood and Gunsalus, 1951), decarboxylation (Mandeles *et al.*, 1954; Rothberg and Steinberg, 1957) and side-chain

elimination or rearrangement (Yanofsky and Reissig, 1953; Matsuo, 1958), was the starting point for research investigating the catalytic versatility of PLP and the mechanism whereby the protein component of the enzyme regulates cofactor chemistry (Snell, 1953; Ikawa and Snell, 1954; Longenecker, 1957a; Longenecker *et al.*, 1957b) . These early studies, in the 1930-1950 period, were seminal because they confirmed that PLP is the active agent of enzymes performing transformations of amino acids and demonstrated that the PLP-catalyzed reactions of distinct enzymes share common mechanistic elements (Metzler *et al.*, 1954).

The structure of PLP and its functional groups are shown in Figure 1.1 A. The 3' hydroxyl and 4' formyl groups (Figure 1.1 A) are involved in catalysis. In contrast, the phosphate moiety linked to the 5' position (Figure 1.1 A) is required for binding and positioning of the coenzyme by the protein component of the enzyme (Metzler *et al.*, 1954). The pyridinum nitrogen, situated at position 1 (Figure 1.1 A), participates in resonance stabilization of the carbanion formed during catalysis (Perault *et al.*, 1961). Research in the 1950s by the labs of Braunstein, Metzler and Snell led to the proposal that the mechanism of PLP-catalyzed transformation of amino acid substrates begins with the formation of a Schiff base between the formyl group of PLP and the α-amino group of the amino acid substrate (Braunstein and Shemyakin, 1953; Metzler *et al.*, 1954). Subsequent weakening and cleavage of one of the bonds of the α-carbon, to either the H^+ (Figure 1.1B, bond 1), COOH (Figure 1.1B, bond 2) or R groups (Figure 1.1B, bond 3), will determine the type of reaction performed. For example, if the leaving group is the α-carboxylate the result is decarboxylation, while abstraction of the C_α proton can result in

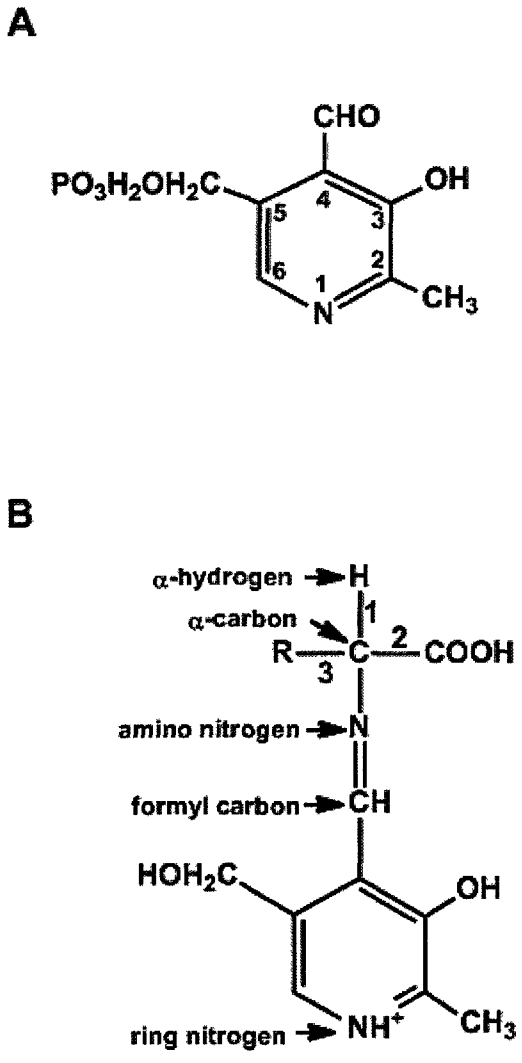

Figure 1.1. (**A**) The functional groups of the PLP cofactor: (1) pyridine nitrogen at the N1 position of the heterocyclic aromatic ring, (2) C2' methyl group, (3) phenolic hydroxyl group (O3' position); (4) formyl group (C4' position); and (5) hydroxylmethyl phosphate ester (Metzler *et al.*, 1954). (**B**) Resonance stabilization of the carbanion formed following cleavage of the carbon-α bond of the amino acid substrate, perpendicular to the plane of the pyridinum ring (Dunathan, 1966).

racemization, side-chain elimination or rearrangement or transamination. Subsequent hydrolysis of the bond between the formyl carbon and the amino group of the α-carbon allows release of the final reaction product (Metzler *et al.*, 1954). Expansion of this theory was required to clarify the mechanism of selection and cleavage of the Cα bond to be broken. The work performed by Perault and colleagues (1961) contributed to our understanding of the conjugated system of PLP and its effects on the Cα bonds. However, the question of how enzymes modulate the chemistry of the versatile PLP cofactor to perform a specific reaction remained. In 1966, Dunathan proposed that PLP-dependent enzymes orient the substrate, in Schiff–base linkage with the cofactor, such that the bond to be broken is perpendicular to the plane of the aromatic ring of the cofactor (Figure 1.1 B) (Dunathan, 1966).

The detailed chemical characterization of PLP, performed by Braunstein, Snell and Dunathan, began the race to understand the mechanisms employed by enzymes to modulate the chemistry of PLP. The research groups of Kaplan, Snell, Braunstein and Dunathan began to probe different PLP-dependent enzymes, including glutamate aspartate transaminase (Dunathan *et al.*, 1968), dialkyl amino-acid transaminase (Bailey *et al.*, 1970), L-glutamate decarboxylase (Sukhareva *et al.*, 1971) and serine hydroxymethylase (Voet *et al.*, 1973). The discovery that many PLP-dependent enzymes share common mechanistic steps, such as transfer of the Cα proton of the substrate to the C4' position of the PLP cofactor, led researchers to postulate that all PLP enzymes originated from a single ancestral protein, a theory that was subsequently disproven (Dunathan and Voet, 1974). Since the 1970s, work on PLP-dependent enzymes has grown substantially, with pioneering contributions on model enzymes, such as tryptophan

synthase and aspartate aminotransferase, from many labs, including Miles, Christen, Kirsch and Toney (Miles, 1995; Christen *et al.*, 1990; Kirsch and Toney, 1990). During this period the crystal structure of the PLP-dependent enzyme aspartate aminotransferase in complex with phosphopyridoxal-aspartate was also published, which confirmed the Dunathan hypothesis (Jansonius *et al.*, 1984; Kirsch *et al.*, 1984).

Analysis of the crystal structures of a variety of PLP-dependent enzymes, in concert with mechanistic studies, has resulted in a general model of the reactions catalyzed by the versatile PLP cofactor. It is now understood that the cofactor is bound covalently to an active-site lysine residue *via* an aldimine linkage, also referred to as a Schiff base. When the substrate enters the catalytic cleft the α-amino group of the substrate replaces the ε-amino group of the active-site lysine residue, *via* a transaldimination reaction, to form the external aldimine intermediate. Regulation of reaction specificity follows the formation of the external aldimine, a step common to all PLP-dependent enzyme catalyzing transformations of amino acids. Interestingly, this control is not only achieved by accelerating the specified reaction, but by also preventing all other possible side reactions (Hayashi, 1995; John, 1995; Christen and Mehta, 2001; Eliot and Kirsch, 2004; Toney, 2005).

The 2001 study on the evolution of PLP enzymes by Christen and Mehta demonstrated that functional specificity had arisen by 1500 million years ago, prior to divergence of eukaryotes, archaebacteria and eubacteria. As the number of reported PLP-dependent enzymes grew to more than 140 distinct Enzyme Commission (EC) numbers in 2003, analysis by Percudani and Peracchi (2003) showed that the diversity of reactions

catalyzed by these enzymes is such that they are found in five of the six enzyme classes (EC 2 – transferases, EC 3 – hydrolases, EC 4 – lyases, EC 5 – isomerases and EC 6 – ligases) defined by the Enzyme Nomenclature Committee of the International Union of Biochemistry and Molecular Biology (Christen and Mehta, 2001; Eliot and Kirsch, 2004).

PLP-dependent enzymes are classified according to five distinct structural fold-types (Percudani and Peracchi, 2003), corresponding to five independent evolutionary lineages (Christen and Mehta, 2001). Fold-type I, the largest family of enzymes, also referred to as the α-family, is catalytically diverse and includes enzymes that perform transamination, decarboxylation and side-chain rearrangements, *via* α,β and α,γ-elimination or replacement reactions. These enzymes function as homodimers, or homotetramers, in which the two active sites of each dimer are located at the subunit interface and are comprised of residues from both monomers, as exemplified by the prototypical fold-type I enzyme aspartate aminotransferase (Eliot and Kirsch, 2004). The enzymes of fold-type II, also referred to as the β-family, carry out α,β-elimination and/or replacement reactions, as exemplified by tryptophan synthase and cystathionine β-synthase (Jansonius, 1998; Christen and Mehta, 2001). In contrast with fold-type I enzymes, the active-sites of fold-type II enzymes are comprised of residues from a single monomer. Fold-type II enzymes may also possess a regulatory domain, as exemplified by eukaryotic cystathionine β-synthase and plant threonine synthase, which are both regulated by *S*-adenosylmethionine (Koutmos *et al.*, 2010). Alanine racemase and a subset of amino-acid decarboxylases comprise fold-type III, while fold-type IV enzymes are D-amino acid aminotransferases in which the PLP cofactor is bound in a mirror-image

conformation to that observed for fold-type I and II enzymes (Sugio, 1995). The glycogen and starch phosphorylases of fold-type V are distinct from the enzymes of the other fold-types because they use the phosphate group of the PLP for catalysis (Sugio *et al.*, 1995; Eliot and Kirsch, 2004). The diversity of PLP-dependent enzymes illustrates the versatility of the cofactor as well as the plasticity of the protein scaffold, which focuses its catalytic power to provide substrate and reaction specificity, and demonstrates that PLP-dependent enzymes represent a rich resource for the engineering of enzyme properties, including substrate and reaction specificity, for industrial applications.

1.4. The transsulfuration and reverse transsulfuration pathways

Among the twenty proteinogenic amino acids only two, L-cysteine (L-Cys) and L-methionine (L-Met), contain sulfur. The discovery of L-Cys dates back to 1810 when Wollaston isolated a sulfur-based compound from the bladder stones of his patients and called it cystic oxide (Wollaston, 1810). The accurate elemental formula and the name cysteine were later reported by Berzelius (1833). Within three years of Mörner's 1899 discovery of L-Cys in animal proteins (Mörner, 1899), it was clear that L-Cys was not the only sulfur-containing component of proteins since it could not account for their total sulfur content (Osborne, 1902). Methionine was identified as the second sulfur-containing amino acid when Mueller isolated it while studying bacterial growth in different culture broths using trypsin-digested casein and meat extracts (Mueller, 1922a; Mueller, 1922b; Mueller, 1923). Almost a century separated the discovery of cysteine and methionine but in the first half of the 20th century many more sulfur-containing amino acids, including L-homocysteine (L-Hcys), L-homocystine and L-cystathionine (L-

Cth), were identified and their roles in cellular sulfur metabolism proposed (Butz and du Vigneaud, 1932; Brown and du Vigneaud, 1941). This work, including studies that traced the metabolic fate of ^{35}S-radiolabelled L-Met in rats, underlies our current understanding that L-Met is an essential amino acid for mammals, from which the semi-essential L-Cys is derived (Jackson and Block, 1932; Tarver and Schmidt, 1939). Experiments with other ^{35}S-labeled amino acids, such as L-Hcys and L-Cth, elucidated the transmethylation and transsulfuration pathways, which recycle L-Hcys to L-Met or converts it to L-Cys, respectively, in mammals (Figure 1.2) (du Vigneaud *et al.*, 1939a; du Vigneaud *et al.*, 1939b; Mackenzie *et al.*, 1949; Reed *et al.*, 1949). The flux of L-Hcys, the branch point intermediate between these two pathways, is regulated by *S*-adenosylmethionine, the ubiquitous cellular methyl donor (Finkelstein, 2000).

The importance of L-Met as a precursor of protein biosynthesis and DNA replication, *via* the thiamine biosynthesis pathway, and the roles of L-Cys in forming disulfide bonds in proteins, to stabilize tertiary and quaternary structure, and as a precursor for glutathione, a primary compound in the maintenance of cellular redox status, are well understood (Tomlinson *et al.*, 1967; Tazuya *et al.*, 1987). In their 2005 review, Wirtz and Droux highlight the central importance of L-Met and L-Cys in metabolic networks of all organisms (Wirtz and Droux, 2005). Our understanding of sulfur amino acid metabolism has grown remarkably over the past sixty years. The pathway converting L-Hcys to L-Cys, which occurs in mammals and baker's yeast (*Saccharomyces cerevisiae*), is now referred to as the reverse transsulfuration pathway and is comprised of the enzymes cystathionine β-synthase (CBS) and cystathionine γ-lyase (CGL). In contrast, L-Cys is synthesized *de novo* by plants and bacteria and is

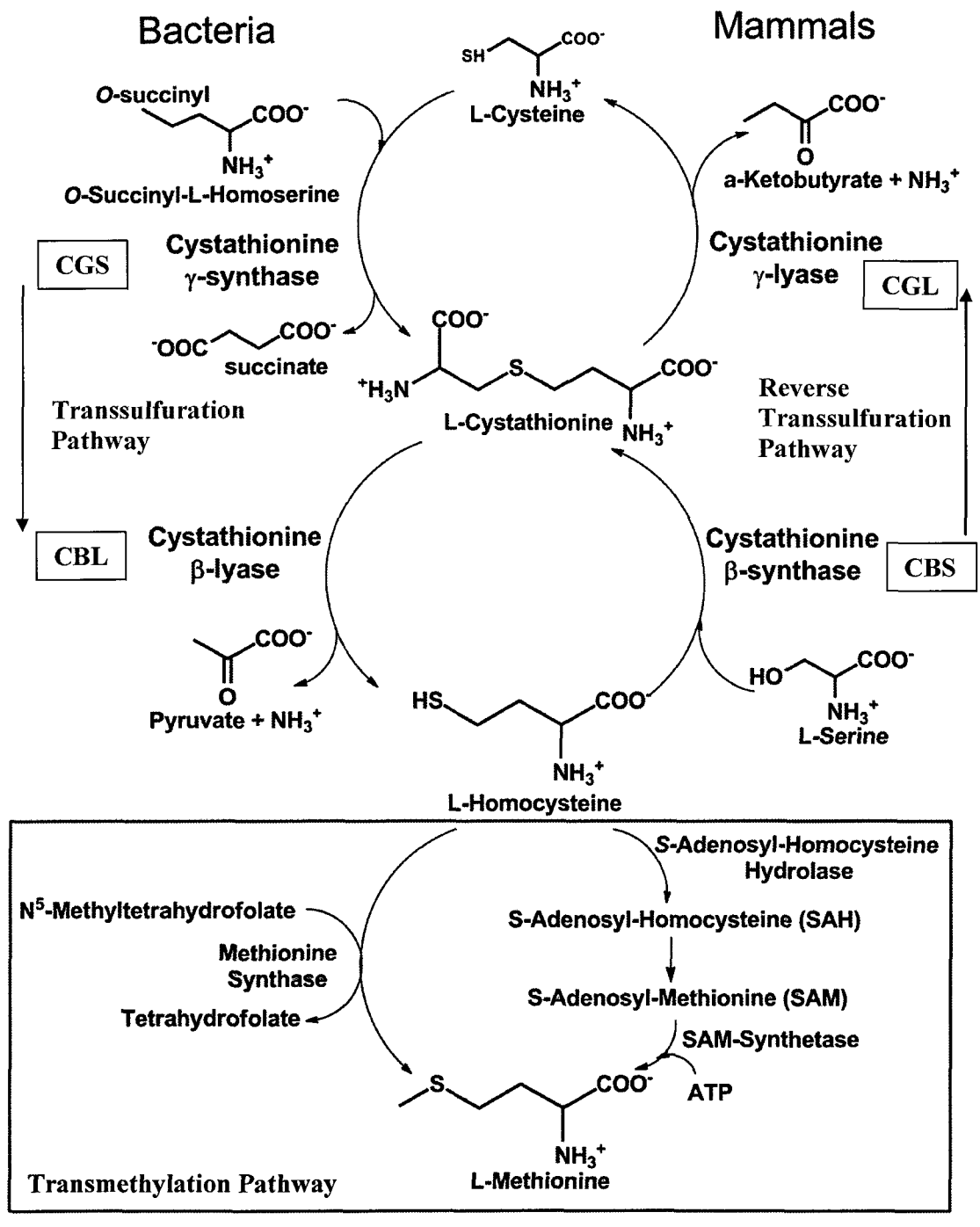

Figure 1.2. The transsulfuration pathway of bacteria, and the reverse transsulfuration and transmethylation pathways of mammals.

converted to L-Hcys, the immediate precursor of L-Met, *via* the action of cystathionine γ-synthase (CGS) and cystathionine β-lyase (CBL), the enzymes of the transsulfuration pathway (Figure 1.2). The subsequent sections of this thesis elucidate the aforementioned PLP-dependent enzymes of the transsulfuration pathways.

1.5. Cystathionine γ-Synthase

In bacteria, sulfide is derived from the reduction of sulfate and is incorporated into L-Cys, which is subsequently converted to L-Hcys, the immediate precursor of L-Met. This contrasts with the mammalian reverse transsulfuration pathway in which L-Hcys is converted to L-Cys (Reed *et al.*, 1949). Cystathionine γ-synthase (CGS) is the first enzyme of the transsulfuration pathway in bacteria and plants (Figure 1.2). Encoded by the *metB* gene in *Escherichia coli* (*E. coli*) (Bachmann, 1976), CGS catalyzes a PLP-dependent, α,γ-replacement reaction in which L-Cys and *O*-succinyl-L-homoserine (L-OSHS) are condensed to produce L-Cth and succinate (Rowbury and Woods, 1964; Kaplan and Flavin, 1965). The Flavin group was the first to isolate a bacterial CGS, from *Salmonella typhimurium* (*S. typhimurium)*, and published a series of reports between 1966 and 1971 describing the spectral, kinetic and mechanistic characterization of *S. typhimurium* CGS (Guggenheim and Flavin, 1969a; Guggenheim and Flavin, 1969b; Kaplan and Flavin, 1966b). A survey of CGS activity in eleven species of higher plants, including two gymnosperms and nine angiosperms, demonstrated that the transsulfuration pathway of plants is similar to that of bacteria, with the exception that substrates for plant and bacterial CGS are *O*-phospho-L-homoserine (L-OPHS) and L-OSHS, respectively (Datko *et al.*, 1974).

Recent studies have demonstrated that there are a number of important applications for research on CGS and the related enzymes of the transsulfuration pathway. For example, since CGS is found only in bacteria and plants, it is a target for the development of antimicrobial compounds (Guggenheim and Flavin, 1969b; Kerr and Flavin, 1969; Kong *et al.*, 2008a; Kong *et al.*, 2008b) and herbicides (Thompson *et al.*, 1982; Clausen *et al.*, 1999; Steegborn *et al.*, 2001). Another application for CGS research is in mammalian nutrition, as the seeds of some crop plants, such as the grain legumes, chickpea and lentil, are deficient in L-Met, from the perspective of human nutrition. The overexpression or modification of CGS has been explored as a method of increasing the L-Met content of plants (Avraham *et al.*, 2005; Hacham *et al.*, 2007; Dancs *et al.*, 2008; Hacham *et al.*, 2008). The role of CGS in the production of ethylene, a plant hormone derived from *S*-adenosylmethionine (SAM) and required for fruit ripening, has also been investigated as a mechanism of regulating fruit ripening in agricultural production (Katz *et al.*, 2006). The development of an increased understanding of the role of active-site residues in CGS substrate and reaction specificity will provide insight useful for each of these distinct applications.

1.5.1. Structure

The structures of CGS from *E. coli* (eCGS) (Figure 1.3) and *Nicotiana tabacum* (nCGS) were solved to a resolution of 1.5 and 2.9 Å, respectively, by Clausen and colleagues (Clausen *et al.*, 1998; Steegborn *et al.*, 1999). Typical of members of the γ-subfamily of fold-type I enzymes, which includes CGS, CBL and CGL, of the transsulfuration pathways, eCGS is a homotetramer composed of two dimers. The two active sites of each catalytic dimer are ~20 Å apart and are comprised of residues from

Figure 1.3. Cartoon representation of the eCGS tetramer. Each monomer is coloured differently, and PLP is shown in yellow. (PDB: **1CS1**)(Clausen *et al.*, 1998)

both subunits. The eCGS monomer contains three domains: the N-terminal domain (residues 1 – 51) is composed of a helix and an extended loop and forms part of the active site of the neighboring subunit, the PLP-binding domain (residue 52 – 247) and the C-terminal domain (residues 248 – 385). The PLP ligand is covalently bonded, *via* a Schiff-base linkage, to the active-site lysine residue (eCGS-K198) (Clausen *et al.*, 1998). The microbial and plant CGS enzymes share several common features, but also differ in their active site architecture. The nCGS active-site is more confined, corresponding to the smaller L-OPHS substrate, than that of the L-OSHS-specific eCGS in which the extended loop structure adopted by residues 36* to 45* (where the asterisk indicates a residue from the second subunit) provides a larger active site. Probing the L-OSHS binding site of eCGS will further highlight these differences and improve the understanding of substrate specificity observed in CGS.

1.5.2. Kinetic Mechanism

The bacterial CGS enzyme catalyzes an α,γ-replacement reaction to synthesize L-Cth from L-Cys and L-OSHS. If L-Cys is not present, an α,γ-elimination side reaction generating succinate, α-ketobutyrate and ammonia from L-OSHS is detectable (Kaplan and Flavin, 1966a). Brzovic *et al.* (1990) determined that the common intermediate of the CGS-catalyzed α,γ-replacement and α,γ-elimination reactions is a β,γ-unsaturated ketimine. The first step of the CGS mechanism is replacement of the ε-amino group of the active-site lysine (eCGS-K198) in Schiff-base linkage with the PLP cofactor (internal aldimine, intermediate I of Figure 1.4) with the α-amino group of the L-OSHS substrate (external aldimine, intermediate II of Figure 1.4). The catalytic base, eCGS-K198, is

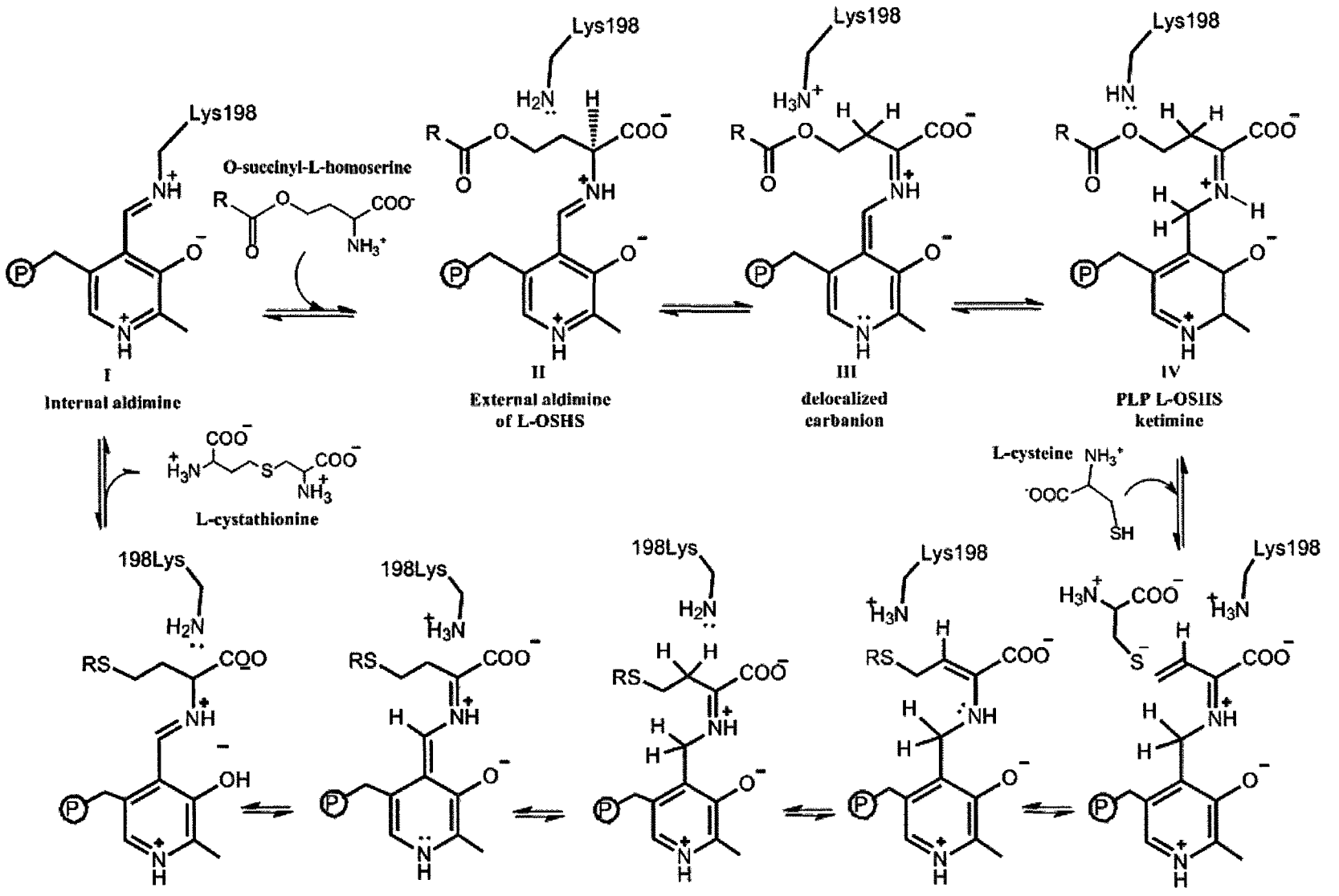
Lys198
O-succinyl-L-homoserine
I
Internal aldimine
II
External aldimine of L-OSHS
III
delocalized carbanion
IV
PLP L-OSHS ketimine
L-cystathionine
L-cysteine
198Lys

Figure 1.4. Schematic representation of the reaction mechanism proposed for plant and bacterial CGS. Internal aldimine (I); external aldimine of L-OSHS (II); delocalized carbanionic intermediate (III); PLP L-OSHS ketimine derivative (IV); βγ-unsaturated ketimine (V); αβ-unsaturaded ketimine (VI); ketimine intermediate (VII); delocalized carbanion intermediate (VIII); and external aldimine of L-Cth (IX). (Steegborn *et al.*, 1999)

proposed to perform a proton transfer from C_α of L-OSHS to C4` of PLP *via* a transient carbanion intermediate (intermediate III of Figure 1.4). The same lysine residue is then proposed to abstract a proton from the C_β position of the substrate, to enable the γ-elimination of succinate to produce the β,γ-unsaturated ketimine (intermediate V of Figure 1.4). A role for the active-site tyrosine residue (eCGS-Y101) that overlays the aromatic ring of the PLP cofactor in facilitating the release of succinate has been proposed (Clausen *et al.*, 1998). Attack of L-Cys on the γ-position of the β,γ-unsaturated ketimine results in the external aldimine of L-Cth, which is released *via* a reverse transaldimination reaction (intermediates VI to IX of Figure 1.4), thus regenerating the internal aldimine form of the CGS enzyme (Brzovic *et al.*, 1990; Clausen *et al.*, 1998; Steegborn *et al.*, 1999).

The ping-pong mechanism of the CGS-catalyzed α,γ-replacement reaction, in which the binding of L-Cys and the release of L-Cth is preceeded by the binding of L-OSHS and release of succinate, proposed by (Holbrook *et al.*, 1990) did not consider the α,γ-elimination activity of CGS. To further investigate the complex mechanism of this enzyme Aitken *et al.*, (2003) developed a novel, continuous assay for both activities and carried out a detailed steady-state kinetic characterization of eCGS. In contrast with the value of 1.5 reported by Holbrook *et al.* (1990) for the ratio of k_{cat} values for the α,γ-replacement and α,γ-elimination activities of eCGS, the value reported by (Aitken *et al.*, 2003) is 67. The k_{catR} and k_{catE} values, at 25 °C, for the α,γ-replacement and elimination activities are 121 and 1.8 s^{-1}, respectively. The corresponding $K_{mR}^{L\text{-}OSHS}$ and $K_{mE}^{L\text{-}OSHS}$ values are similar (2.5 and 1.3 mM, respectively), while the $K_{mR}^{L\text{-}Cys}$ (0.11 mM) is 23-fold lower than $K_{mR}^{L\text{-}OSHS}$ for the α,γ-replacement reaction (Aitken *et al.*, 2003).

1.6. Cystathionine β-lyase

Cystathionine β-lyase (CBL) follows CGS in the transsulfuration pathway of bacteria and plants (Figure 1.2). Encoded by the *metC* gene in *E. coli* (Bachmann *et al.*, 1976), CBL hydrolyzes L-Cth to produce L-Hcys, pyruvate and ammonia. The *E. coli* CBL (eCBL) enzyme was first cloned and purified by Dwivedi *et al.* (1982b) and the gene sequenced by Belfaiza *et al.* (1986). Studies by the Flavin lab investigating the transsulfuration pathway of *Neurospora crassa* identified a PLP-dependent enzyme that hydrolysed L-Cth and co-purified with CGS. Investigations of these *N. crassa* isolates were complicated by their mixed α,β/α,γ-elimination activities. Consequently, the Flavin group focused on the bacterial CBL enzyme, which exclusively catalyzes the α,β-elimination of L-Cth, with no detectable α,γ-elimination activity. (Flavin and Slaughter, 1964; Delavier-Klutchko and Flavin, 1965b). CBL also has the ability to hydrolyze other sulfur-containing substrates such as L-cystine, L-homolanthionine, L-*meso*-lanthionine and L-dienkolic acid *via* elimination reactions, although the K_m values of these substrates is one to two orders of magnitude higher than that of L-Cth (Dwivedi *et al.*, 1982a). The hydrolysis of L-Cys, to produce hydrogen sulfide, pyruvate and ammonia, has also been reported (Delavier-Klutchko and Flavin, 1965a; Delavier-Klutchko and Flavin, 1965b; Dwivedi *et al.*, 1982a). The CBL enzyme from several species including *S. typhimurium* (Park and Stauffer, 1987), *Bordetella avium* (Gentry-Weeks *et al.*, 1995), *Spinacia oleracea L.* (Droux *et al.*, 1995), *Lactococcus lactis* (Alting *et al.*, 1995) and *Arabidopsis thaliana* (*A. thaliana*) (Ravanel *et al.*, 1996) has been subsequently characterized.

Cystathionine β-lyase, like CGS, is only found in plants and bacteria and thus has been identified as a target for antimicrobials and herbicides. Aminoethoxyvinyl-glycine

(AVG) and rihzobitoxine are naturally occurring, slow-binding inhibitors of eCBL. Both possess an α-carboxylate group akin to the L-Cth substrate, but the sulfur group is replaced with oxygen, these compounds lack a distal carboxylate group, and the distal amino group of L-Cth and AVG is replaced by CH_2OH in rhizobitoxine (Owens *et al.*, 1968; Clausen *et al.*, 1997). Recently a pair of synthetic eCBL inhibitors, N-hydrazinocarbonylmethyl-4-Nitrobenzamide (IC_{50} = 25 μM) and N-hydrazinocarbonyl-methyl-2-trifluoromethylbenzamide (IC_{50} = 0.08 μM), were identified from a library of 50, 000 molecules (Ejim *et al.*, 2007). However, their inability to inhibit bacterial growth demonstrates that further refinement of these compounds is required to develop effective anti-microbial agents that could be investigated as therapeutics. The crystal structures of eCBL in complex with of AVG (IC_{50} = 1.7 μM (Lodha *et al.*, 2010)), N-hydrazino-carbonylmethyl-4-Nitrobenzamide and N-hydrazinocarbonylmethyl-2-trifluoromethyl-benzamide identified the amino acids interacting with the α-carboxylate moiety of L-Cth, but do not provide insight into the nature of interactions with the distal carboxylate of the substrate (Clausen *et al.*, 1997; Ejim *et al.*, 2007). Studies probing the roles of active-site residues in substrate and inhibitor binding will assist in the development of improved inhibitors for CBL.

1.6.1. Structure

The structures of the *E. coli* and *A. thaliana* CBL enzymes and the eCBL-AVG complex, solved to a resolution of 1.8-2.3 Å (Figure 1.5), have confirmed the homotetrameric structure and provided insight into the mechanism of this enzyme (Clausen *et al.*, 1996; Clausen *et al.*, 1997; Breitinger *et al.*, 2001). Typical of fold-type I enzymes, each monomer contains a PLP cofactor covalently bound to the side-chain of a

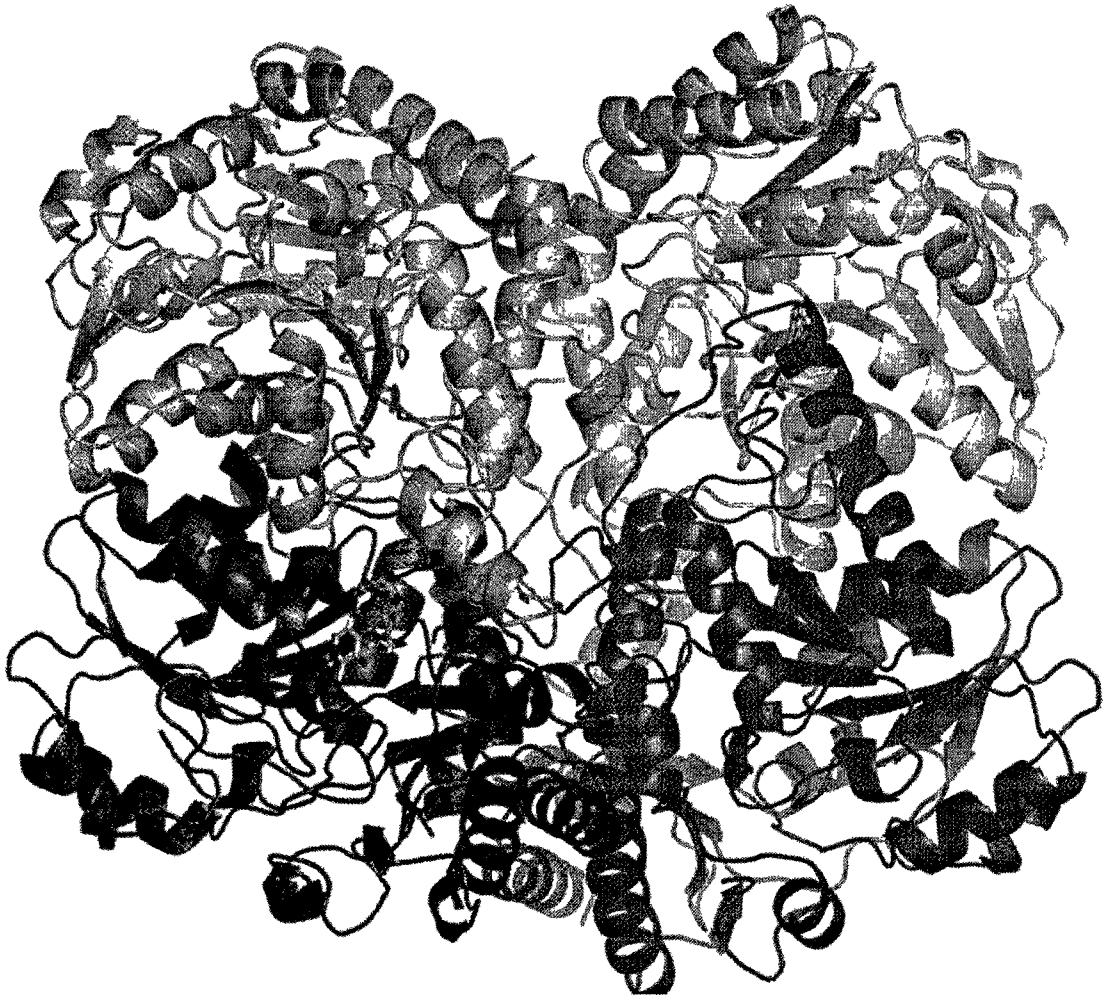

Figure 1.5. The eCBL tetramer, represented in stick and cartoon form. Each monomer is displayed in a different colour and PLP is shown in yellow. (PDB: **1CL1**) (Clausen *et al.*, 1996).

lysine residue (eCBL-K210) and the active sites, situated at the interface of the catalytic dimer, and are composed of residues from both of the subunits. The eCBL monomer is comprised of three domains: the N-terminal extended arm (residues 1 – 60), which forms part of the active site of the neighboring subunit, the PLP-binding domain (residues 61 – 256) and the C-terminal domain (residues 257 – 395) (Clausen *et al.*, 1996).

1.6.2. Kinetic Mechanism

The CBL-catalyzed α,β-elimination of L-Cth, the physiological substrate, yields L-Hcys, pyruvate and ammonia. Alternative substrates of CBL include L-Cys and disulfides such as L-cystine, L-homolanthionine, L-*meso*-lanthionine and L-dienkolic acid (Delavier-Klutchko and Flavin, 1965b; Dwivedi *et al.*, 1982a). The hydrolysis of L-Cth starts with transaldimination, a step common to all PLP enzymes catalyzing transformations of amino acids, to release the ε-amino group of the active-site lysine and form the external aldimine of L-Cth (intermediate II of Figure 1.6). Subsequent abstraction of the Cα proton by the catalytic base (eCBL-K210) produces a carbanion that is resonance-stabilized by the PLP cofactor (intermediate III of Figure 1.6). The elimination of L-Hcys produces a PLP-bound aminoacrylate (intermediate IV of Figure 1.6), which is released *via* a final transaldimination step to regenerate the internal aldimine form of the enzyme (intermediate I of Figure 1.6). The released iminopropionate quickly breaks down in the presence of water, releasing pyruvate and ammonia (Clausen *et al.*, 1997).

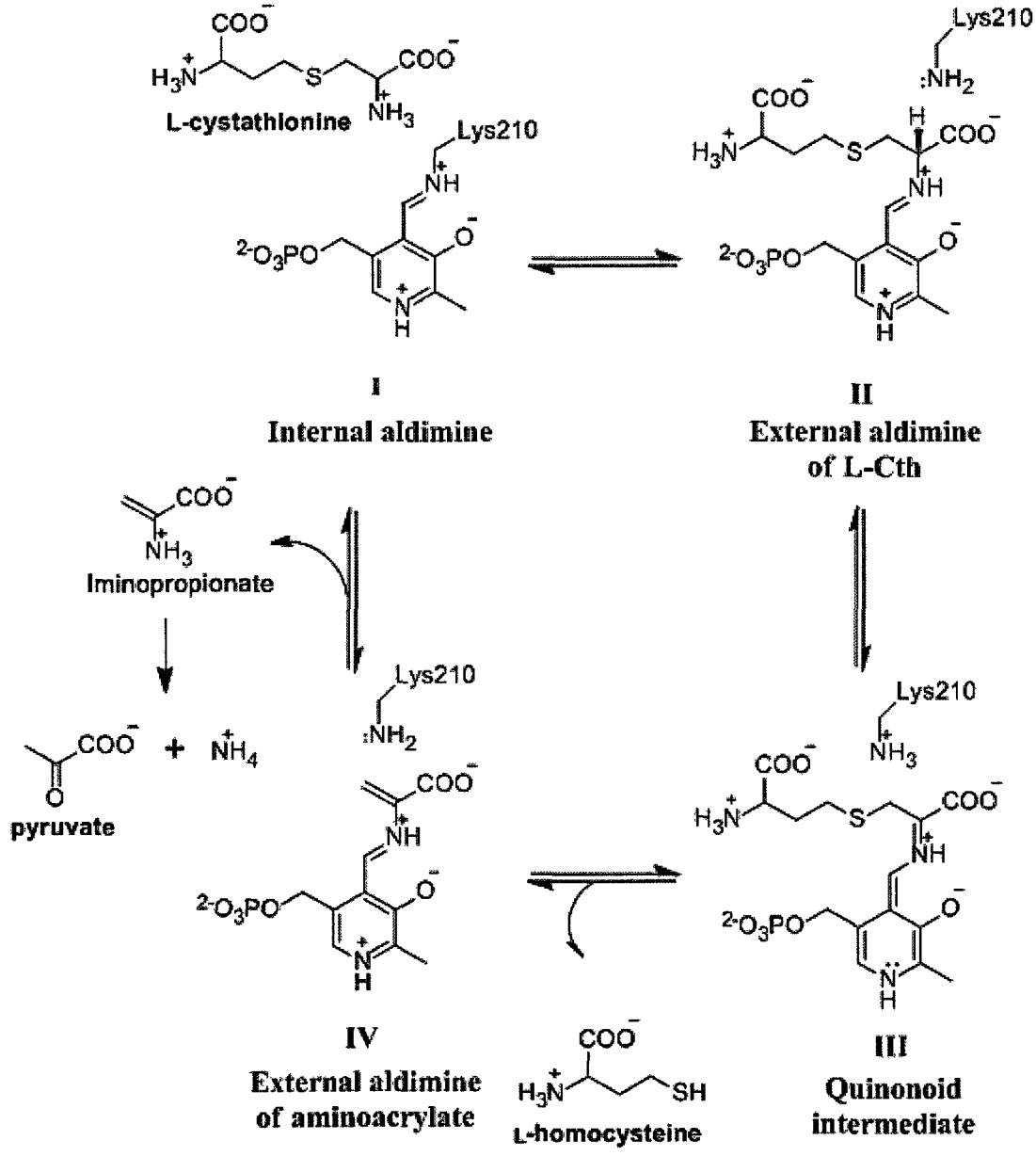

Figure 1.6. Schematic representation of the reaction mechanism proposed for CBL from bacteria and plants. Internal aldimine (I); external aldimine L-Cth (II); resonance-stabilized carbanionic intermediate (quinonoid) (III); and external aldimine of aminoacrylate (IV). (Clausen *et al.*, 1997)

1.7. Cystathionine β-Synthase

Cystathionine β-Synthase (EC 4.2.1.22) (CBS) is the first enzyme of the reverse transsulfuration pathway, found in both fungi and mammals (Figure 1.2), and catalyzes a PLP-dependent, α,β-replacement reaction in which L-serine (L-Ser) and L-Hcys are condensed to yield L-Cth. It is encoded by the *CYS4* gene in yeast, *Saccharomyces cerevisiae* (*S. cerevisiae*) (Ono *et al.*, 1988), and is located on chromosome 21 in humans (Munke *et al.*, 1988). Reports of L-Cth synthesis by enzymes were first published by researchers working on sulfur metabolism in mammals. Francis Binkley, working at the University of Utah, was the first person not only to extract and crystallize CBS from rat livers, but to confirm that L-Cth is synthesised from L-Ser and L-Hcys and to show that CBS is a PLP-dependent enzyme (Binkley, 1951; Binkley *et al.*, 1952). Selim and Greenberg (1959) confirmed Binkley's finding and reported that CBS can also perform the deamination of L-Ser, in absence of L-Hcys, to produce pyruvate and ammonia. However, the importance of this enzyme in human metabolism was only realized after Irish scientists reported characterization of the amino acid profiles of urine samples of 2081 mentally challenged patients. They observed two female siblings (ages 5 and 7) with unusually high amounts of L-Hcys and termed the disorder homocystinuria (MIM ID# 236200) (Carson and Neill, 1962; Carson *et al.*, 1963). Working independently, a group of American scientists reported a similar elevation of the L-Hcys level in the urine of a one year old male child d isplaying similar symptoms to the patients in the Irish study (Gerritsen *et al.*, 1962).

S. Harvey Mudd, who was previously working on characterizing the enzymes of the transsulfuration, reverse transsulfuration and transmethylation pathways, was approached by Leonard Laster and James D. Finkelstein, who suspected homocystinuria was caused by enzymatic defects. In 1964, they confirmed this hypothesis by demonstrating that the CBS enzyme isolated from the liver biopsy of a child suffering from homocystinuria lacked activity (Mudd *et al.*, 1964). These researchers went on to demonstrate the role of CBS in regulating the flux of sulfur in the human reverse transsulfuration and transmethylation pathways. When the level of L-Met is sufficient to meet the demands of cellular metabolism, excess L-Hcys is shunted into the transsulfuration pathway for L-Cys production. In contrast, when CBS activity is deficient, as in the case of patients with homocystinuria, excess L-Hcys is converted to L-Met, which increases the concentration of the latter, a common side effect of this disease (Laster *et al.*, 1965). These studies demonstrate the complex integration of the transsulfuration pathways and the folate cycle to regulate and modulate the concentration of important sulfur-containing amino-acid metabolites.

In contrast with CGS and CBL, CBS was isolated from *N. crassa* and *S. cerevisiae* but is not found in bacterial extracts. These findings led to the realization that bacteria and plants convert L-Cys to L-Hcys, *via* the transsulfuration pathway, while fungi and mammals convert L-Hcys to L-Cys, *via* the reverse transulfuration pathway (Delavier-Klutchko and Flavin, 1965a; Finkelstein, 1974). Following the identification of the CBS gene (*CYS4*) from *S. cerevisiae* in 1988, Ono *et al.* characterized the *in vivo* role of the enzyme (Ono *et al.*, 1988; Ono *et al.*, 1992; Ono *et al.*, 1994). The *S. cerevisiae* CBS (yCBS) enzyme is generally used as a model enzyme for the human CBS (hCBS)

because it can be recombinantly purified in large quantities, 20 - 40 mg/L, from bacterial cultures (Aitken and Kirsch, 2003; Aitken and Kirsch, 2004; Lodha *et al.*, 2009) and does not contain a heme-binding domain, which is common to CBS from higher eukaryotes. The Soret absorbance of the heme group of hCBS masks the absorbance of the PLP cofactor, thereby complicating pre-steady state investigations (Aitken and Kirsch, 2003; Aitken and Kirsch, 2004; Lodha *et al.*, 2009; Quazi and Aitken, 2009). In addition, the 41% sequence identity shared between yCBS and hCBS in the catalytic region allows yCBS to be used as a model for characterization of the active-site and to study the effects of homocystinuria-associated amino acid substitutions that impede hCBS activity.

Cystathionine β-synthase is associated with homocystinuria and Down syndrome. Mutation within the gene encoding CBS is the most prevalent cause of homocystinuria, while the location of hCBS gene on the 21st chromosome results in increased expression of CBS, and many other genes, in patients with Down syndrome (Pogribna, 2001). The clinical manifestations of homocystinuria include *ectopia lentis*, skeletal abnormalities, vascular disease, and mental retardation. Similarly an increase in the concentration of L-Hcys in the plasma, commonly observed with aging, has been linked to arteriosclerosis and an elevated level of L-Hcys has been identified as an independent risk factor for cardiovascular disorders (McCully, 2004).

A database maintained by Jan Kraus at the University of Colorado, Denver catalogues ~150 homocystinuria-associated mutations (as of March 2011) in the human gene encoding CBS that have been identified from patients diagnosed with homocystinuria (http://cbs.lf1.cuni.cz/index.php) (Kraus *et al.*, 1999). This database has been maintained for over a decade since the seminal paper identifying 92 distinct hCBS

alleles was published by an international consortium of 12 different labs (Kraus *et al.*, 1999). Two thirds of the reported mutations are nucleotide substitutions, or missense mutations, resulting in a change in the encoded amino acid, for which the associated residues are located throughout the protein. The remaining ~50 reported homocystinuria-associated mutations are deletions, insertions, nonsense mutations resulting in a stop codon, or substitutions resulting in aberrant splicing events. The three most common substitutions in hCBS that result in homocystinuria are I278T, T191M and G307S, in order of decreasing prevalence. The G307S variant accounts for greater than 70% of homocystinuria alleles in patients of Celtic origin. Patients with the G307S mutation do not respond to additional vitamin B_6, which is the medical approach normally employed to treat homocystinuria. In contrast, B_6 treatment is effective for patients with the I278T allele (Kraus *et al.*, 1999). Understanding the structure-function relationships that underlie homocystinuria-associated mutations as well as the role of active-site residues as determinants of substrate and reaction specificity in CBS will provide the necessary framework for the development of therapeutics for the diseases associated with this enzyme.

1.7.1. Structure

CBS is unique among the enzymes within the transulfuration and reverse transulfuration pathways because it is the only one classified as a fold-type-II PLP-dependent enzyme, whereas CGS, CBL and CGL are fold-type I enzymes. The similarity of the catalytic domain and the active site of hCBS with that of *O*-acetylserine sulfhydrylase (OASS) from *Salmonella typhimurium* allowed the crystal structure of hCBS to be solved, using the OASS structure as a model, *via* molecular replacement

(Meier *et al.*, 2001) (Figure 1.7A). This structure was the truncated form of hCBS, residues 1-413, because the full-length hCBS enzyme tends to aggregate, thereby precluding the generation of high-quality crystals required for structure determination. The first structure of the full-length form of CBS, from *Drosophila melanogaster,* (dCBS) was reported by Koutmos *et al.* in 2010 (Figure 1.7B). The hCBS and yCBS enzymes are reported to exist as homotetramers in solution, but the dCBS structure demonstrates that the enzyme is a stable homodimer (Stipanuk, 1986; Ono *et al.*, 1994; Koutmos *et al.*, 2010). Although the crystal structure of yCBS has yet to be solved, the ~41% amino acid sequence identity between the catalytic domains of hCBS and dCBS and yCBS, allows these structures to be used as a model for the yeast enzyme (Aitken and Kirsch, 2004).

The crystal structures of hCBS and dCBS show that each monomer is composed of an N-terminal heme binding domain (yCBS does not possess this domain), the PLP–binding catalytic domain and the C-terminal regulatory domain (Jhee *et al.*, 2000b; Koutmos *et al.*, 2010; Maclean *et al.*, 2000; Meier *et al.*, 2001; Taoka *et al.*, 2002). The role of the heme cofactor in CBS from higher eukaryotes, including hCBS, is a topic of active debate, and catalytic, regulatory and structural roles have been proposed. The ~25-Å distance between the heme and PLP cofactors in hCBS and dCBS and the absence of a heme-binding domain in CBS from lower eukaryotes, such as *S. cerevisiae*, suggests that the heme cofactor likely does not play a role in catalysis or enzyme folding (Jhee *et al.*, 2000a; Maclean *et al.*, 2000; Meier *et al.*, 2001; Taoka *et al.*, 2002; Koutmos *et al.*, 2010). The theory that holds the most promise proposes that the heme cofactor is a redox regulator which is linked, *via* the L-Cys product of the reverse transsulfuration pathway,

A

B

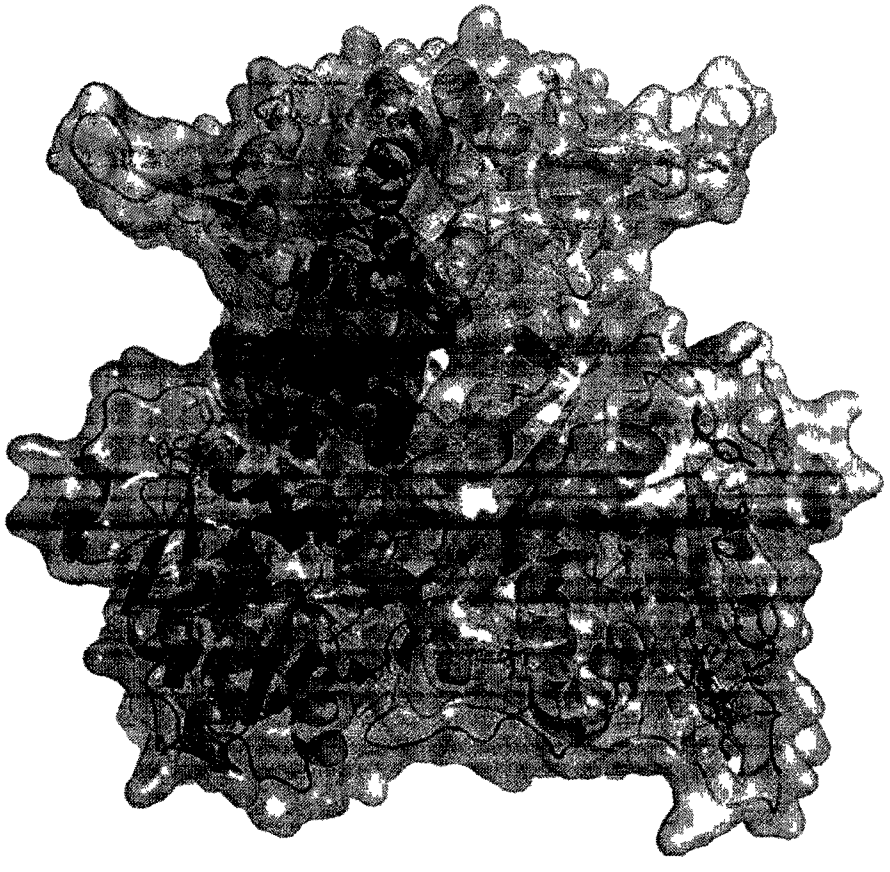

Figure 1.7. Stick and cartoon depiction of CBS enzymes. (A) The hCBS dimer, lacking the C-terminal regulatory domain, depicted in stick and cartoon form. PLP is shown in yellow and the heme cofactor located at the edge of the dimer is shown in red. (PDB: **1JBQ**) (Meier *et al.*, 2001). (B) Surface view of the *Drosophila melanogaster* CBS dimer. The C-terminal regulatory domain is shaded in green, the catalytic and heme domains are shaded in blue, and the linker between the regulatory and catalytic domains is shaded in pink. (PDB: **3PC2**) (Koutmos *et al.*, 2010).

to the important redox-regulatory compound glutathione. The heme cofactors of the bacterial transcription factor CooA and human guanylate cyclase, which bind CO and NO, respectively, exemplify a potential regulatory role for the heme cofactor of hCBS (Severina, 1998; Aono *et al.*, 2000). However, heme-mediated changes in hCBS activity have only been observed under non-physiological conditions (Cherney *et al.*, 2007; Weeks *et al.*, 2009; Singh *et al.*, 2007). The C-terminal, regulatory domain of hCBS is the binding site of the allosteric activator, *S*-adenosylmethionine (SAM), which results in a ~2 fold increase in enzyme activity (Finkelstein *et al.*, 1975; Kabil and Banerjee, 1999; Janosik *et al.*, 2001). *S*-adenosylmethionine is inhibitor of methylenetetrahydrofolate reductase and methionine adenosyl-transferase (Kutzbach and Stokstad, 1971). Therefore, SAM modulates the flux of L-Hcys between the transmethylation and transsulfuration pathways, which recycle L-Hcys to L-Met or convert it to L-Cys, respectively (Finkelstein *et al.*, 1975; Finkelstein and Martin, 1984). Removal of the regulatory domain from CBS results in a truncated, dimeric enzyme form that is SAM-insensitive and is ~2-fold more active than the full-length, tetrameric form of the enzyme (Kery *et al.*, 1998). In contrast with the human enzyme, yCBS and dCBS, which possess similar C-terminal domains as hCBS, are reported to be unresponsive to SAM (Jhee *et al.*, 2000b; Maclean *et al.*, 2000; Koutmos *et al.*, 2010;). However, removal of the regulatory domain of yCBS results in a truncated, dimeric enzyme form (ytCBS) that is also ~2-fold more active when compared to the full-length tetrameric form (Jhee *et al.*, 2000b). Therefore, as no allosteric activator of yCBS or dCBS has been reported, the role of the regulatory domain in the context of these enzymes is unclear.

Members of the β-family of PLP-dependent enzymes, CBS (Meier *et al.*, 2001), OASS (Burkhard *et al.*, 1998), tryptophan synthase (Hyde *et al.*, 1988), threonine deaminase (Gallagher *et al.*, 1998) and aminocyclopropane deaminase (Yao *et al.*, 2000)

share a similar fold type. Both yCBS and OASS perform a β-replacement reaction mechanism in which L-Ser and O-acetylserine are first substrates, respectively. An overlay of the 25 most conserved residues between these two enzymes resulted in a root mean square deviation of only 1.6 Å at the C_α position. The identification of residues involved in L-Ser binding in ytCBS was facilitated by comparison with the structure of OASS-K41A in complex with L-Met (Burkhard *et al.*, 1998; Aitken and Kirsch, 2004). However, as hydrogen sulfide (H_2S) is the second substrate of OASS the same method could not be employed to predict residues involved in L-Hcys binding to CBS.

1.7.2. Kinetic Mechanism

The CBS-catalyzed condensation of L-Ser and L-Hcys follows a ping-pong mechanism in which L-Ser binding preceeds that of L-Hcys ((Flavin and Slaughter, 1964; Jhee *et al.*, 2000b). The common endpoint assay for CBS activity, employed since 1965, relies upon separation of ^{14}C-labeled L-Cth product from the ^{14}C-L-Ser substrate, with subsequent quantification (Mudd *et al.*, 1965; Ono *et al.*, 1994; Jhee *et al.*, 2000b). In 2003, a coupled-coupled assay was developed by Aitken and Kirsch to reduce cost and improve data quality (Aitken and Kirsch, 2003). This continuous assay employs CBL to hydrolyze the L-Cth produced by CBS, regenerating L-Hcys and producing ammonia and pyruvate, which is subsequently reduced by L-lactate dehydrogenase (L-LDH) to lactate, with concomitant oxidation of nicotinamide adenine dinucleotide (NADH) to NAD^+ (ε_{340} = 6200 $M^{-1}cm^{-1}$). This assay relieved product inhibition that had previously resulted in an over- and under-estimation of $K_m^{L\text{-}Ser}$ and k_{cat}, respectively (Aitken and Kirsch, 2003). Employing the CBL-LDH and 5,5'-dithiobis-2-nitrobenzic acid (DTNB) assays for the physiological condensation of L-Ser and L-Hcys and the reverse-physiological hydrolysis

of L-Cth, respectively, Aitken and Kirsch determined the catalytic efficiency of both reactions ($k_{cat}/K_m^{L\text{-}Ser}$ = 1.8 x 10^4 $M^{-1}s^{-1}$, $k_{cat}/K_m^{L\text{-}Hcys}$ = 7.2 x 10^4 $M^{-1}s^{-1}$ and $k_{cat}/K_m^{L\text{-}Cth}$ = 6.7 x 10^3 $M^{-1}s^{-1}$) and confirmed that the equilibrium of this reaction favors the production of L-Cth *in vivo*.

The α,β-replacement mechanism of CBS is divided into two stages or half reactions (Jhee *et al.*, 2001). Typical of PLP-dependent enzymes that catalyze transformations of amino acids, the initial step of the first half reaction is transaldimination, in which the ε-amino group of an active-site lysine residue is replaced by the α-amino group of the amino acid substrate, in Schiff-base linkage with the PLP cofactor, thereby converting the internal aldimine (intermediate I of Figure 1.8) to the external aldimine (intermediate III of Figure 1.8) form of the enzyme. This reaction occurs *via* formation of a geminal diamine intermediate (intermediate II of Figure 1.8). The ε-amino group of the displaced Lys residue then abstracts the C_α proton from the L-Ser substrate to facilitate α,β-elimination of the hydroxyl leaving group, thereby resulting in formation of the external aldimine of aminoacrylate (intermediate IV of Figure 1.8), to complete the first half reaction. The involvement of a quinonoid, in the conversion of intermediate III to IV, has been proposed but not observed under pre-steady state or equilibrium conditions (Koutmos *et al.*, 2010). The second half reaction commences with the nucleophilic attack of the aminoacrylate intermediate by the thiolate group of L-Hcys. Following reprotonation of C_α of the resulting external aldimine of of L-Cth (intermediate V of Figure 1.8), transaldimination releases the L-Cth produce and regenerates the internal aldimine form of the yCBS (Jhee *et al.*, 2001; Koutmos *et al.*, 2010).

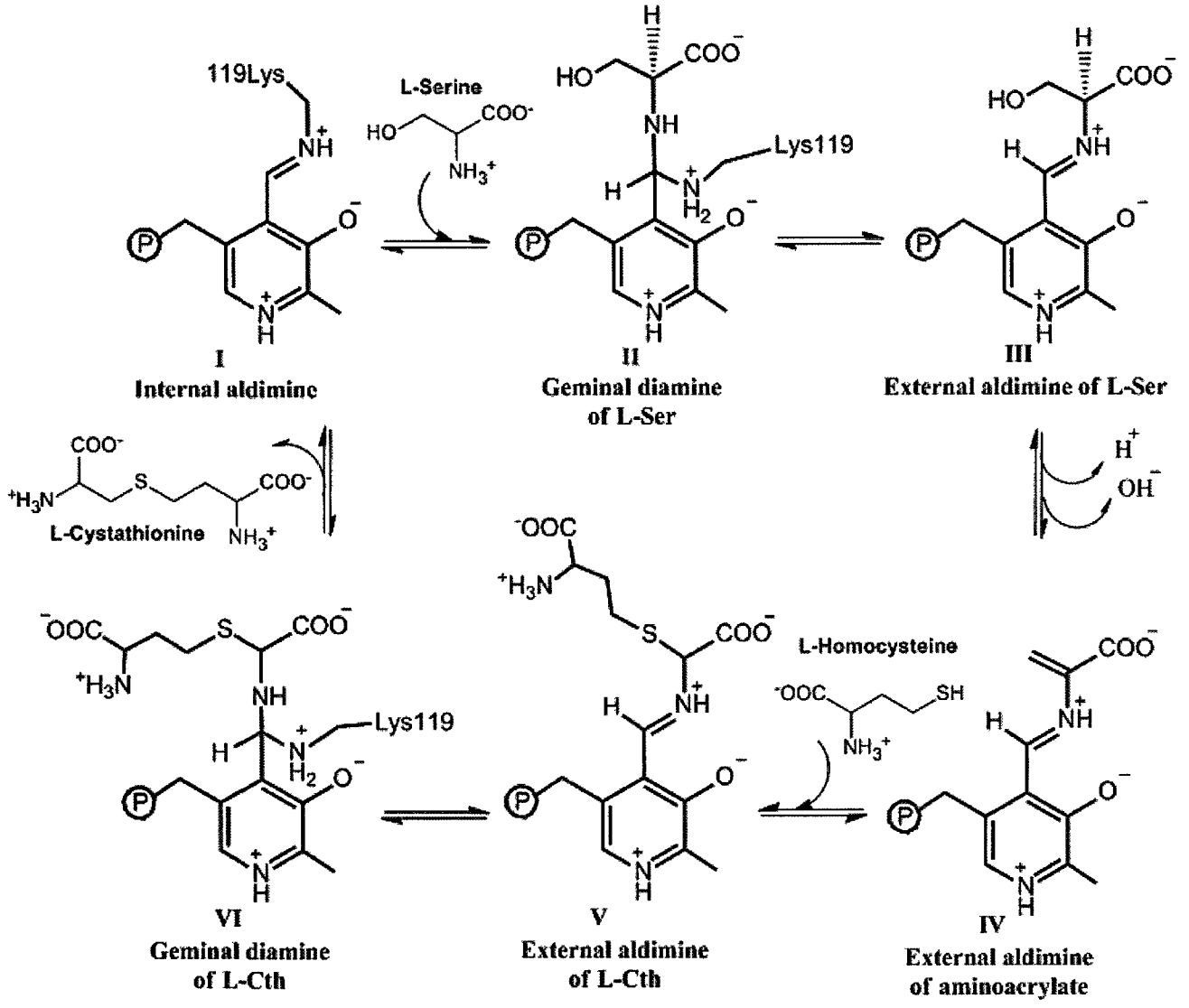
119Lys
L-Serine
Lys119
I
Internal aldimine
II
Geminal diamine of L-Ser
III
External aldimine of L-Ser
L-Cystathionine
H+
OH−
L-Homocysteine
Lys119
VI
Geminal diamine of L-Cth
V
External aldimine of L-Cth
IV
External aldimine of aminoacrylate

Figure 1.8. Schematic representation of the reaction mechanism proposed for CBS. Internal aldimine (I); geminal diamine of L-Ser (II); external aldimine of L-Ser (III); external aldimine of aminoacyrlate (IV); geminal diamine of L-Cth (V); external aldimine of L-Cth. (Jhee *et al.*, 2001)

1.8. Cystathionine γ-Lyase

Cystathionine γ-lyase (EC 4.4.1.1) is the second enzyme of the reverse transsulfuration pathway of yeast and animals (Figure 1.2). CGL is encoded by the *CYS3* gene in *S. cerevisiae* (Ono *et al.*, 1988) and by the *CTH* gene located on human chromosome 1 (as mapped by the International Radiation Hybrid Mapping Consortium (stSG39248)). The PLP-dependent α,γ-elimination of L-Cth catalyzed by CGL yields L-Cys, α-ketobutyrate and ammonia (Carroll *et al.*, 1949). Increased concentration of L-Cth in the urine of human patients was reported as early as 1959 and was linked to a diseased called cystathioninuria (Harris *et al.*, 1959). When reports of homocystinuria began to surface in 1962, a relation between these two diseases was suspected as both L-Cth and L-Hcyc are intermediates of the same pathway. Research on these diseases occurred simultaneously (Brenton *et al.*, 1965; Levy *et al.*, 1975) and involved many of the same scientists discussed in the earlier CBS section, such as Vincent du Vigneaud, Martin Flavin, Francis Binkley, S. Harvey Mudd, and James Finkelstein. Cystathioninuria (MIM ID #219500) was eventually determined to be an autosomal recessive disorder with minor symptoms such as pale liver of small size and increased L-Cth levels in urine (Frimpter, 1965).

Early CGL research focused on exploring the relationship between the reverse transsulfuration pathway and cystathioninuria. However, since the mid-1990s the role of H_2S as a neuromodulator and smooth muscle relaxant and the roles of CBS and CGL in H_2S production have revived interest in research on CGL (Awata *et al.*, 1995; Abe and Kimura, 1996; Eto *et al.*, 2002; Robert *et al.*, 2003; Teague *et al.*, 2002; Dominy and Stipanuk, 2004; Huang *et al.*, 2010).

The structural similarities between the three fold-type I enzymes (CGS, CBL and CGL) of the transsulfuration pathways pose challenges for the development of enzyme-specific inhibitors. Reported inhibitors for eCGS, propargylglycine (2-amino-4-pentynoic acid) and eCBL, AVG, have been also been observed to inhibit CGL (Johnston *et al.*, 1979; Clausen *et al.*, 1997; Steegborn *et al.*, 1999; Sun *et al.*, 2009). These studies demonstrated that promising lead compounds of novel antibiotics can produce unanticipated side effects if used as therapeutics. Therefore, cystathionine γ-lyase can be utilized as a control for development of inhibitors of CGS and CBL and is thus pertinent to the theme of this thesis.

1.8.1. Structure

The crystal structures of both yeast CGL (yCGL) (Figure 1.9) and human CGL (hCGL) have been solved (Messerschmidt *et al.*, 2003; Sun *et al.*, 2009). The yeast and human enzymes share 50% amino acid sequence identity. Typical of the γ-subfamily of fold-type I of PLP-dependent enzymes, which includes CGS and CBL, CGL is a homotetramer. Each monomer comprises an N-terminal domain, a PLP-binding domain, and a C-terminal domain. The PLP cofactor is bound to an active-site lysine (yCGL-K203 and hCGL-K212) *via* a Schiff-base linkage. The π-stacking interaction between the pyridine ring of PLP and a conserved Tyr residue, present in both eCGS and eCBL, is also observed in yCGL (Y103) and hCGL (Y114) (Messerschmidt *et al.*, 2003; Sun *et al.*, 2009).

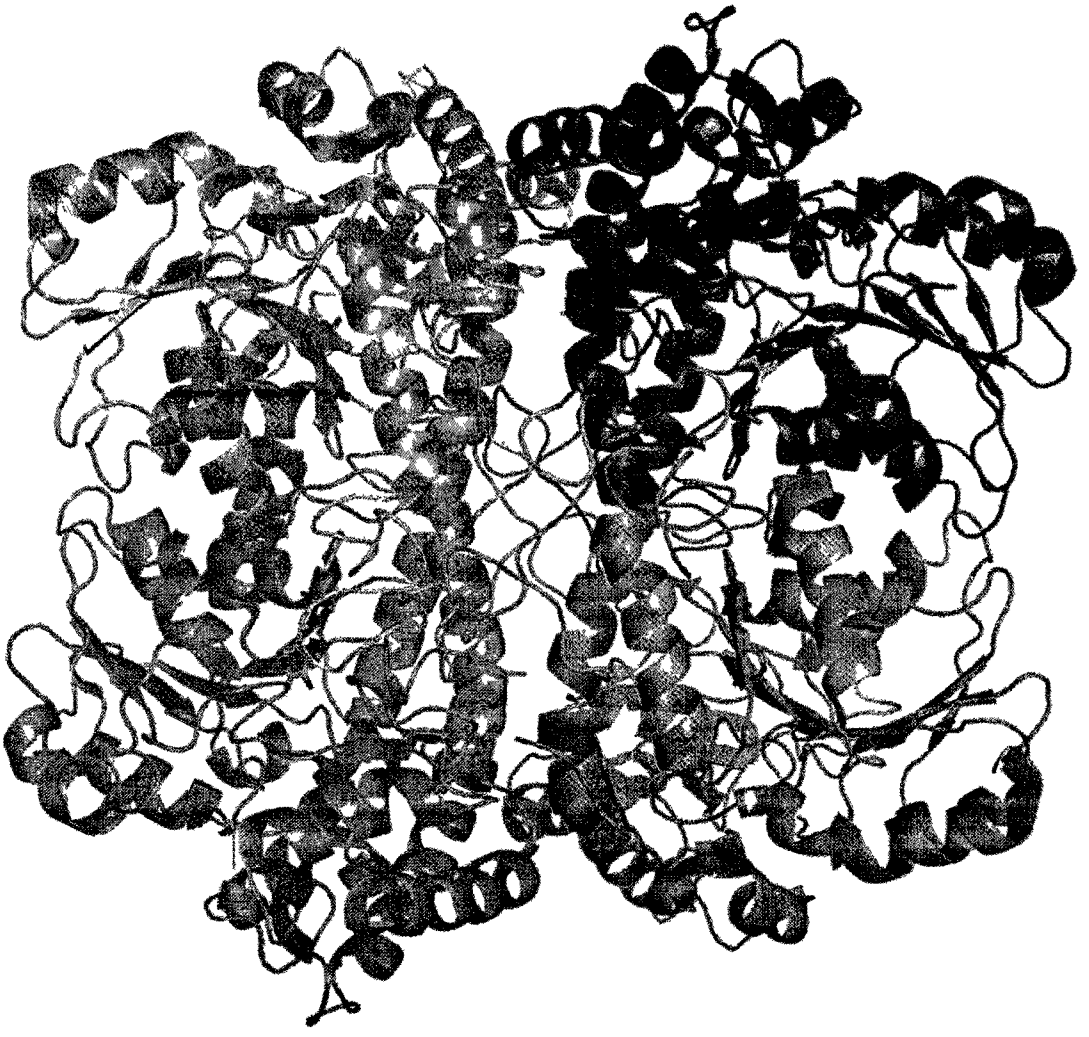

Figure 1.9. The yCGL tetramer, represented in stick and cartoon form. Each monomer is depicted in a different colour, and PLP is shown in yellow. (PDB: **1N8P**) (Messerschmidt *et al.*, 2003)

1.8.2. Kinetic Mechanism

The α,γ-elimination reaction mechanism of CGL enzyme is identical to the α,γ-elimination of L-OSHS by eCGS (Figure 1.4), with the exception that the substrate of CGL is L-Cth (Brzovic *et al.*, 1990; Aitken *et al.*, 2003; Chiku *et al.*, 2009). Compared to the other fold-type I enzymes of the transsulfuration pathways CGL has the lowest catalytic efficiency. The $k_{cat}/K_m^{L\text{-}Cth}$ of eCBL ((1.52 ± 0.09) x 10^5 mol·L^{-1}·s^{-1}) is 30-fold higher than that of yCGL ((1.98 ± 0.08) x 10^3 mol·L^{-1}·s^{-1}) and, while the $k_{cat}/K_m^{L\text{-}OSHS}$ of the minor eCGS α,γ-elimination activity ((3.2 ± 0.4) x 10^3 mol·L^{-1}·s^{-1}) is comparable to the catalytic efficiency of yCGL, the $k_{cat}/K_m^{L\text{-}OSHS}$ of the eCGS α,γ-replacement ((3.0 ± 0.6) x 10^4 mol·L^{-1}·s^{-1}) activity is 8-fold greater than the catalytic efficiency of the α,γ-elimination of L-Cth by yCGL (Farsi *et al.*, 2009). Yamagata *et al.* proposed, based on comparison of yCGL activity with various homoserine derivatives, that the reaction specificity of eCGS and yCGL is the result of *in vivo* substrate availability rather than a property of the enzymes (Yamagata *et al.*, 1993). Farsi *et al.* (2009) refuted this theory by demonstrating that their substrate specificity, as the k_{cat}/K_m for L-Cth is 150-fold lower for eCGS than yCGL and k_{cat}/K_m for L-OSHS is 200-fold higher for eCGS than to yCGL. These studies demonstrate that although eCGS, eCBL and yCGL are structurally similar, they differ in reaction and substrate specificity. Investigation of the determinants of specificity in these closely related enzymes will provide the necessary insight to design specific inhibitors for each enzyme and to modify their activities for potential industrial applications.

1.9 Enzymes of the transsulfuration pathways: similarities and differences.

Among the four enzymes of the transsulfuration pathways, CBS is structurally distinct as a member of fold-type II of PLP-dependent enzymes. In contrast, CGS, CBL, and CGL belong to the γ-subfamily of fold-type I. The differences between fold-types I and II in the mode of cofactor and substrate binding are illustrated by these enzymes. For example, CBS employs hydrogen-bonding networks to interact with the phosphate moiety of PLP and the carboxylate groups of substrates and products (Aitken and Kirsch, 2004; Koutmos *et al.*, 2010). In contrast, CGS, CBL and CGL employ arginine residue(s) for this purpose (Clausen *et al.*, 1996; Clausen *et al.*, 1997; Clausen *et al.*, 1998; Messerschmidt *et al.*, 2003; Ejim *et al.*, 2007). Although CGS and CBS both catalyze the PLP-dependent synthesis of L-Cth, the mechanisms and substrates employed are distinct. Probing the active site residues that are responsible for these differences will contribute to our understanding of the ways different PLP-dependent enzymes achieve reaction and substrate specificity.

The crystal structures of eCBL, eCGS and yCGL are so similar that the r.m.s deviation of their least squares superposition is only ~1.5 Å for 350 C_α atoms of the peptide backbone (Messerschmidt *et al.*, 2003). Several, but not all, active-site residues are also conserved between the three enzymes, suggesting that subtle changes in the identity and position of key residues determine the substrate and reaction specificity of these enzymes. For example, the common pseudosymmetric L-Cth substrate of CGL and CBL is hydrolyzed *via* α,γ- and α,β-elimination mechanisms, respectively. When comparing the active sites of eCBL, eCGS and yCGL, (Messerschmidt *et al.*, 2003) observed that two hydrophobic residues in eCBL (F55 and Y338) are replaced by acidic

residues in eCGS (D48 and E325) and yCGL (E48 and E333) and subsequently proposed that these residues are determinants of α,β *versus* α,γ reaction specificity. However, the interconversion of these amino acids in eCBL, eCGS and yCGL is not sufficient to modify the *in vivo* reaction specificity of these enzymes (Farsi *et al.*, 2009). While yCGL catalyzes α,β-elimination and α,γ-replacement reactions, in addition to physiological α,γ-elimination of L-Cth, the strict specificity of eCBL and eCGS is demonstrated by their inability to complement methionine-auxotrophic *E. coli* strains lacking the *metB* and *metC* genes, encoding CGS and CBL, respectively (Farsi *et al.*, 2009). Interestingly, residue E333 of yCGL was proposed to regulate the orientation of L-Cth in the active site by interaction with the sulfur atom of the substrate (Messerschmidt *et al.*, 2003). However, the yCGL-E333Y variant, in contrast with wild-type yCGL, does not rescue the Δ*metC* strain, lacking eCBL activity. The ~30-fold reduction in the catalytic efficiency of the E333A and E333Y variants of yCGL is dominated by an increase in $K_m^{L\text{-}Cth}$, suggesting a role for this residue in binding the distal amino group of L-Cth. The catalytic efficiency of the corresponding eCBL Y338E (44.5 ± 0.4 $mol \cdot L^{-1} \cdot s^{-1}$) variant decreased by four orders of magnitude compared to the wild-type eCBL ((1.52 ± 0.09) x 10^5 $mol \cdot L^{-1} \cdot s^{-1}$) enzyme (Farsi *et al.*, 2009). The *in vivo* and *in vitro* results of this study indicate that while this pair of residues (corresponding to F55 and Y338 of eCBL) may participate in determining specificity, they must act in concert with other active-site residue. Farsi *et al.*, (2009) concluded that exploration of the roles that active-site residues play in each enzyme is essential to provide the information required for projects with the goal of altering the reaction and substrate specificity of these enzymes.

Inhibition of eCBL and eCGS by two naturally occurring inhibitors, AVG and propargylglycine (2-amino-4-pentynoic acid) (PAG), respectively, has provided insight into the mechanistic details of these enzymes. (Johnston *et al.*, 1979; Clausen *et al.*, 1997; Steegborn *et al.*, 1999; Sun *et al.*, 2009). However, the discovery of these promising mechanism-based inhibitors has not led to the production of novel antibiotics because they also inhibit yeast and human CGL (Steegborn *et al.*, 1999; Sun *et al.*, 2009). This example illustrates the need for studies characterizing the active sites of these enzymes to provide the knowledge required to guide the design of enzyme-specific inhibitors.

The residues proposed to be involved in substrate binding and catalysis in eCGS eCBL and yCGL (Figures 1.10, 1.11 and 1.12, respectively) demonstrate that Y56, R58, Y101, S339 and R372 (eCBL numbering) are conserved (Figure 1.13) between these three enzymes. Conversely, residues F55 and Y338 in eCBL are replaced by acidic residues in eCGS and yCGL, R59 is conserved in eCBL and eCGS, but replaced by a serine in yCGL, and residues D116, Y238 and W340 in eCBL are substituted by a conserved arginine, asparagines and leucine residues in eCGS and yCGL. Exploring the roles of these residues and their interactions with the cofactor and substrates of eCBL, eCGS and yCGL will provide insight into the determinants of substrate and reaction specificity in the γ-subfamily of PLP-dependent enzymes.

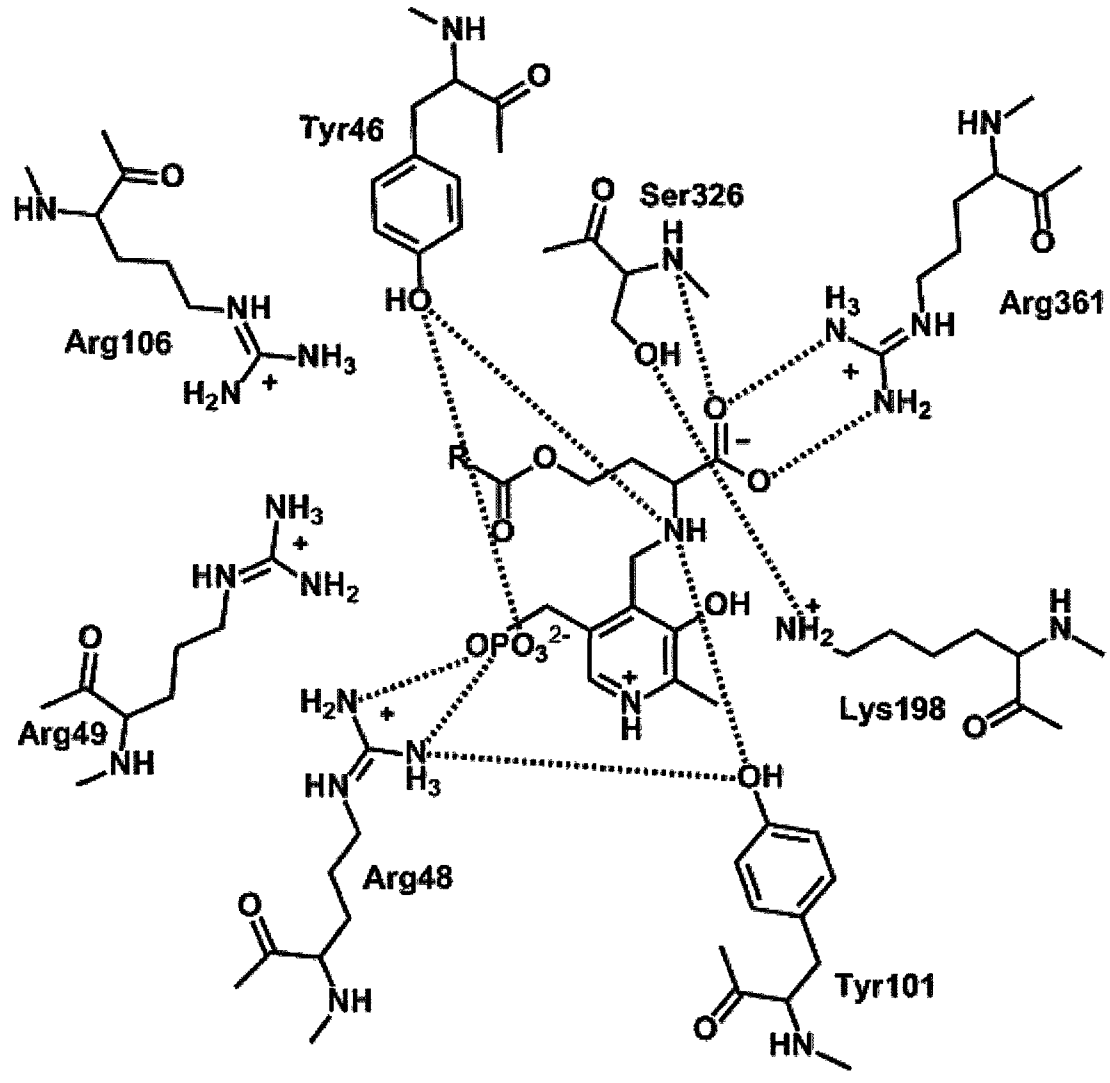

Figure 1.10. The key active site residues proposed to be involved in L-OSHS substrate binding in the eCGS enzyme. Shown in a schematic representation (Clausen *et al.*, 1998).

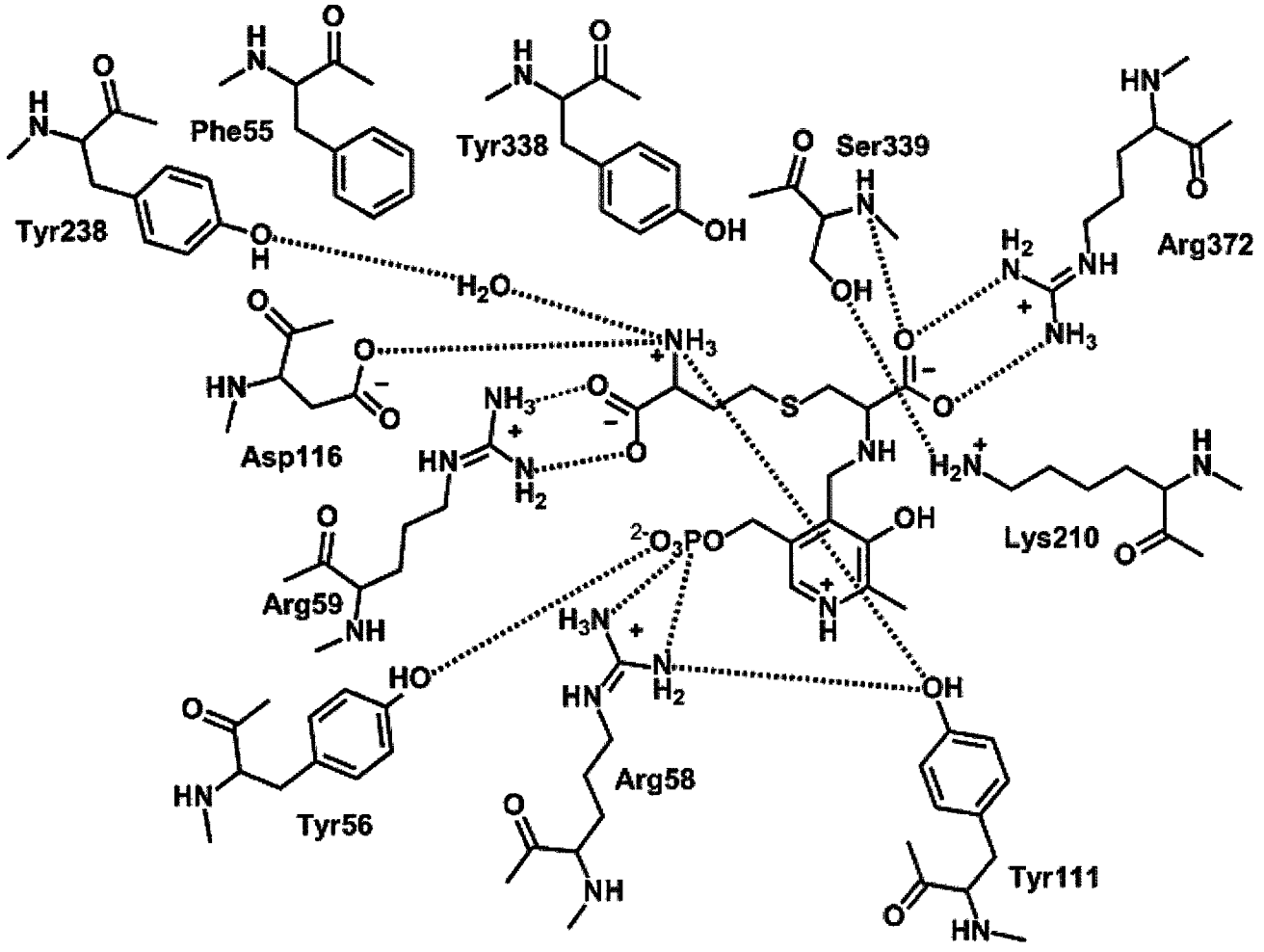

Figure 1.11. The key active site residues proposed to be involved in L-Cth substrate binding in the eCBL enzyme. Shown in a schematic representation (Clausen *et al.*, 1997).

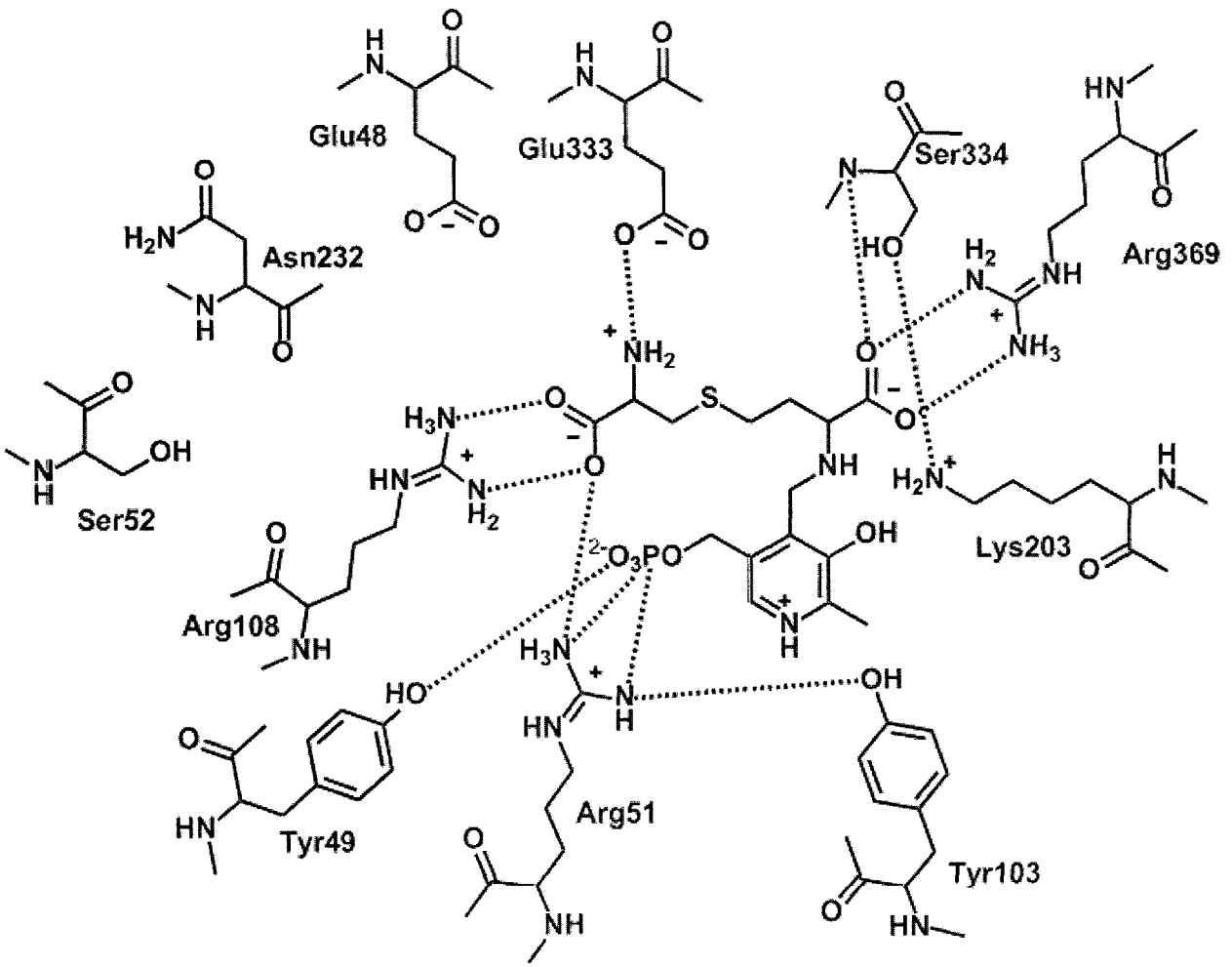

Figure 1.12. The key active site residues proposed to be involved in L-Cth substrate binding in yCGL enzyme. Shown in a schematic representation (Messerschmidt *et al.*, 2003).

Figure 1.13: ClustalW2 (Chenna *et al.*, 2003) alignment of the amino acid sequences of eCGS (P00935), eCBL (P06721) and yCGL (P31373). Active-site residues conserved in these three enzymes are highlighted in green, while non-conserved residues and the catalytic lysine, which forms a Schiff base with the PLP cofactor, are highlighted in blue and pink, respectively.

1.10. Objective

The enzymes of the transsulfuration pathways, with their structural similarities and mechanistic differences, provide an excellent model system for investigating the structure-function relationships of PLP-dependent enzymes. The chemical versatility of the PLP cofactor is well-documented. However, a complete understanding of how PLP-dependent enzymes enforce reaction specificity remains elusive. The purpose of the research described in this thesis is to explore, *via* site-directed mutagenesis, the active site residues proposed to participate in substrate and reaction specificity in the enzymes of the transsulfuration (CGS and CBL) and reverse transsulfuration (CBS and CGL) pathways of *E. coli* and *S. cerevisiae*, respectively. The goal is to understand how these structurally similar enzymes employ the PLP cofactor to catalyze distinct reactions. This knowledge will aid in the design of specific inhibitors and novel antibiotics. Furthermore, a greater understanding of how these enzymes modulate reaction and substrate specificity will provide the knowledge base that is required to alter them for specific protein engineering applications.

2. METHODS

This section provides the general methods utilized in all research chapters, including site-directed mutagenesis, protein purification and steady-state measurement of enzyme activity. The variations and details specific to each experiment are described in the appropriate thesis chapters.

2.1 Site directed mutagenesis

All of the site-directed mutants in this study were constructed using the modified DNA mutagenesis protocol designed by Higuchi (Figure 2.1) (Aitken *and* Kirsch, 2004; Higuchi, Krummel, *and* Saiki, 1988). The protocol employs overlap-extension polymerase chain reaction (OE-PCR) to create single or multiple amino acid substitutions in the gene of interest. The 5'-flanking and the reverse mutagenic primers and the forward mutagenic and 3'-flanking primers, are used in separate polymerase chain reactions (PCR) to produce overlapping 5' and 3' amplicons, respectively, of the target template sequence. Following recombination of these segments, *via* OE-PCR, the resulting full-length sequences are inserted into the appropriate expression vector. Site-directed mutants are subsequently sequenced to verify the presence of the targeted alteration and to ensure no unanticipated mutations are present.

2.2 Affinity Protein Purification

Cells expressing wild-type and site-directed variants of 6-His, affinity-tagged ytCBS, eCBL and eCGS were grown and harvested according to the protocols described by (Aitken *and* Kirsch, 2004; Farsi *et al.*, 2009). The harvested cell pellets were re-suspended in 100-150 mL of buffer A (50 mM K phosphate, pH 7.8 and 10 mM

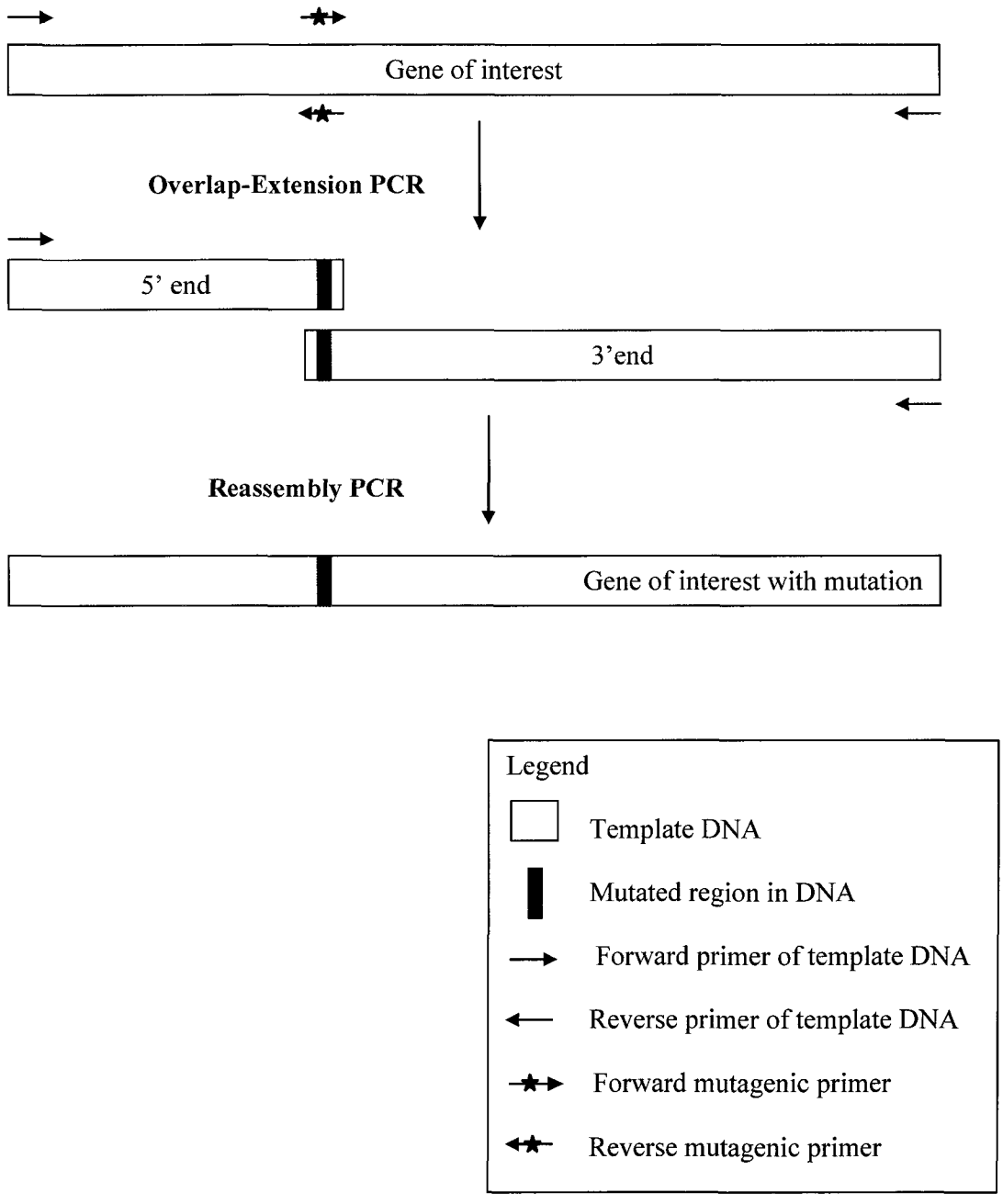

Figure 2.1: A schematic representation of site-directed mutagenesis protocol employed in this study. (Aitken *and* Kirsch, 2004; Higuchi *et al.*, 1988)

imidazole) containing one complete EDTA-free tablet (Roche) and 20 μg/mL DNAse I. The cells were lysed by incubation with 1 mg/mL lysozyme on ice for 20 min followed by repeated (8 x 30 s) cycles of sonication (Sonic and Material, Inc. Vibra Cell sonicator). The centrifuged crude lysate was loaded on a ~10 mL column of Ni-nitrilo triacetic acid (Ni-NTA) resin (Qiagen), equilibrated with buffer A. The column was washed with 10-column volumes of buffer A and eluted with a 200-mL linear gradient of 10-200 mM imidazole in buffer A. The protein fractions (~5 mL each) were tested for purity *via* sodium dodecal sulfate polyacrylamide gel electrophoresis (SDS-PAGE). The fractions with no other protein bands visible were pooled, concentrated, and dialyzed against dialysis buffer (50 mM potassium phosphate, pH 7.8, 1 mM EDTA, 1 mM DTT, 20 μM PLP). The protein concentration was determined *via* the Bradford assay (Bradford, 1976), using bovine serum albumin (BSA) as a standard, after addition of ~20% (v/v) glycerol for storage at -80 °C.

2.3. Steady-state kinetics enzyme assays

Enzyme activity was measured in a total volume of 100 μL at 25 °C on a Spectramax 340PC Molecular Devices spectrophotometer. The assay buffer comprised 50 mM Tris (pH 8.6) and 20 μM PLP for ytCBS enzymes, 50 mM Tris (pH 8.5) and 20 μM PLP for eCBL enzymes and 50 mM Tris (pH 7.8) and 20 μM PLP for eCGS enzymes. A background rate, for all components except the test enzyme, was recorded for

each sample before initiating the reaction by the addition of the test enzyme. Data was fit by nonlinear regression with the program SAS (SAS Institute, Cary, NC).

2.3.1. L-Cystathionine hydrolysis assay with 5,5'-Dithiobis-2-Nitrobenzic Acid (DTNB).

The DTNB assay was used to monitor the hydrolysis of L-Cth to L-Hcys by ytCBS and eCBL enzymes. DTNB reacts with the free thiol product, L-Hcys, releasing the TNB thiolate ion which absorbs at 412 nm (Aitken *et al.*, 2003; Ellman, 1959; Yamagata *et al.*, 1993). Reactions were carried out in assay buffer containing 2 mM DTNB (20 µL of a 100 mM stock of DTNB in DMSO) and 0.05 – 6.6 mM L-Cth, as substrate. The reactions were initiated by the addition of either wild-type or variant ytCBS or eCBL enzyme. Absorbance changes were monitored at 412 nm ($\Delta\varepsilon 412$ = 13 600 M^{-1} cm^{-1}). The data was fit to the Michaelis-Menten equation (equation 2.1), to derive the k_{cat} and $K_m^{L\text{-}Cth}$ values, and $k_{cat}/K_m^{L\text{-}Cth}$ was obtained independently from equation 2.1 and 2.2 (Aitken *et al.*, 2003).

$$\frac{v}{[E]} = \frac{k_{cat} \times [\text{L}-\text{Cth}]}{K_m + [\text{L}-\text{Cth}]} \qquad (2.1)$$

$$\frac{v}{[E]} = \frac{{}^{k_{cat}}/_{K_m} \times [\text{L}-\text{Cth}]}{1 + {}^{[L-Cth]}/_{K_m}} \qquad (2.2)$$

2.3.2. Coupled-Coupled enzyme assay with nicotinamide adenine dinucleotide (NADH).

The coupled-coupled enzyme assay was employed for determination of the kinetic parameters for the synthesis of L-Cth by ytCBS and eCGS. The optimal concentrations of coupling enzymes was confirmed before each experiment to verify that the rates of reactions measured would not be limited by insufficient coupling enzyme. The two coupling enzymes that were used most commonly in this study were eCBL and L-lactate dehydrogenase (LDH). The concentration of the eCBL and LDH coupling enzymes for

the wild-type and site-directed variant enzymes were determined to be 0.4 and 1.3 μM, respectively, for ytCBS and 0.8 μM and 2 μM, respectively, for eCGS. Reactions were carried out in assay buffer containing 1.5 mM NADH. The concentrations of the L-Hcys and L-Ser substrates of ytCBS and the L-Cys and L-OSHS substrates of eCGS were selected depending on the kinetic parameters of the specific variant to ensure that a range of substrate was within ~0.1–20-fold of the K_m. Reactions were initiated by the addition of target enzyme, and the conversion of NADH to NAD^+, corresponding to L-Cth production, was monitored at 340 nm ($\Delta\varepsilon 340$ = 6200 M^{-1} cm^{-1}). The rate of NADH oxidation in the CBL/LDH continuous assay is linearly dependent on ytCBS or eCGS concentration at the concentrations used in the assays. This linear range was determined independently for each variant. The values of the kinetic parameters were determined from the fit of the data to models described by Jhee *et al,*. (2000a) for ytCBS and Aitken *et al.*, (2003) for eCGS.

Chapter 3. Investigation of Residues K112, E136, H138, G247, Y248, and D249 in the Active Site of Yeast Cystathionine β-Synthase

3.1. Abstract

Cystathionine β-synthase (CBS), the first enzyme of the reverse transsulfuration pathway, catalyzes the pyridoxal 5'-phosphate-dependent condensation of L-serine and L-homocysteine to form L-cystathionine. A model of the L-cystathionine complex of the truncated form of yeast CBS (ytCBS), comprising the catalytic core, was constructed to identify residues involved in the binding of L-homocysteine and the distal portion of L-cystathionine. Residue K112 was selected for site-directed mutagenesis based on the results of the *in silico* docking of L-cystathionine to the modeled structure of ytCBS. Residues E136, H138, Y248 and D249 of ytCBS were also targeted as they correspond to identical polar residues lining the mouth of the active site in the structure of human CBS. A series of eight site-directed variants was constructed and their order of impact on the ability of ytCBS to catalyze the β-replacement reaction is G247S ≈ K112Q > K112L ≈ K112R >> Y248F > D249A ≈ H138F > E136A. The β-replacement activity of yCBS G247S, which corresponds to the homocystinuria-associated hCBS G307S variant of human CBS, is undetectable. The $K_m^{L\text{-}Ser}$ of the K112L and K112R variants is increased by 50 and 90-fold, respectively, while $K_m^{L\text{-}Hcys}$ is increased only 2 and 4-fold, respectively. The $K_m^{L\text{-}Hcys}$ of H138F and Y248F is increased 8 and 18-fold, respectively. The results indicate that while the targeted residues are not direct determinants of L-Hcys binding, G307, Y248 and K112 play essential roles in the maintenance of appropriate active-site conformation.

3.2. Introduction

Cystathionine β-synthase (CBS, E.C. 4.2.1.22) catalyzes the condensation of L-serine (L-Ser) and L-homocysteine (L-Hcys) to form L-cystathionine (L-Cth) in the first step of the reverse transsulfuration pathway. Elevated plasma L-Hcys is a risk factor for cardiovascular disease and deficiency of CBS activity in humans is the most common cause of homocystinuria, the clinical manifestations of which include thromboembolism and connective tissue defects (Kraus *et al.,* 1999; McCully, 2005). Mammalian CBS is unique among pyridoxal 5'-phosphate (PLP)-dependent enzymes as it also contains a heme cofactor, bound by a domain comprised of residues ~1-70 (Meier *et al.,* 2001). In contrast, the yeast enzyme, typical of CBS from lower eukaryotes, lacks the amino-terminal domain and the heme cofactor, which masks the absorbance of PLP intermediates in human CBS (hCBS), thereby providing an effective model system for mechanistic studies (Jhee *et al.,* 2000; Jhee *et al.,* 2000).

The structure of the truncated form of hCBS, lacking the carboxy-terminal, regulatory domain, was solved, *via* molecular replacement, using the closely-related *O*-acetylserine sulfhydrylase (OASS) from *Salmonella typhimurium* as a model (Meier *et al.* 2001). Both CBS and OASS employ a β-replacement mechanism in which the hydroxyl group of L-Ser or the acetate of *O*-acetyl-L-serine, respectively, is eliminated to form a PLP-bound aminoacrylate intermediate in the first half reaction. Residues in the yeast CBS (yCBS) active site involved in L-Ser binding were identified, based on the structure of the L-Met complex of the K41A variant of OASS, and their roles in L-Ser binding and catalysis were characterized (Burkhard *et al.,* 1999; Aitken and Kirsch 2004). However, limited information about the nature of the L-Hcys binding site of CBS can be inferred by

analysis of OASS, as the corresponding substrate of the latter is hydrogen sulfide. Taoka *et al.* (Taoka *et al.*, 2002) observed that a number of angles of approach are possible for L-Hcys and that the mouth of the hCBS active site is lined by the polar residues E201, H203, Y308 and D309 (conserved as E136, H138, Y248 and D249, respectively in yCBS). These residues, with side chains capable of forming hydrogen bonds to the α-amino and α-carboxylate moieties of bound L-Hcys, or the corresponding groups of the distal portion of the L-Cth product, and which are not conserved between CBS and OASS, were targeted for site-directed mutagenesis in yCBS (E136A, H138F, Y248F, and D249A) to probe their involvement in L-Hcys binding.

The catalytic domain of yCBS is 31% and 47% identical to that of OASS and hCBS, respectively, thereby enabling these enzymes to serve as scaffolds for homology modeling of the open and closed conformations of the yeast enzyme. Docking of L-Cth to the modeled structures of truncated yCBS (ytCBS), comprising the catalytic domain, suggested roles for S82 and Y158, which have been previously investigated (Aitken and Kirsch 2004), and K112 in hydrogen bonding to the distal amino and carboxylate groups of L-Cth. Therefore, the K112L,Q,R site-directed variants were constructed to probe the effect of modification/removal of the hydrogen-bonding capacity of the side-chain amine moiety of this residue, while minimizing changes in nonpolar interactions. The development of a more complete understanding of structure-activity relationships in the active site of CBS will provide the framework for the discovery of therapeutics to modulate cellular L-Hcys concentration.

3.3. Materials and Methods

3.3.1. Reagents.

L-Cth [*S*-(2-amino-2-carboxyethyl)-L-homocysteine], L-lactate dehydrogenase (LDH), β-nicotinamide adenine dinucleotide (β-NADH, reduced form), L-Ser and L-Hcys thiolactone were obtained from Sigma. L-Hcys was prepared from the thiolactone (Kashiwamata and Greenberg, 1970). Protease inhibitor (Complete EDTA-free) tablets were a Roche product. Nickel-nitrilotriacetic acid (Ni-NTA) resin and 5,5'-dithio-bis-(2-nitrobenzoic acid) (DTNB) were from Qiagen and Pierce, respectively. Cystathionine β-lyase (CBL) was expressed and purified as described previously (Aitken and Kirsch, 2003).

3.3.2. Construction, expression and purification of site-directed variants.

The pT-SECb-his construct, expressing ytCBS with a carboxy-terminal, 6-histidine tag, described by Aitken and Kirsch (Aitken and Kirsch, 2004), was employed for the construction of the site-directed mutants. Mutations were introduced by overlap-extension PCR (Higuchi, 1990). Wild-type ytCBS and site-directed variants were expressed and purified as described previously (Aitken and Kirsch, 2004).

3.3.3. Enzyme Assays.

Enzyme activity was measured in a total volume of 100 μL at 25 °C with a Spectramax 340PC Molecular Devices spectrophotometer. The assay buffer comprised 50 mM Tris, pH 8.6, and 20 μM PLP. The β-replacement activity was measured in assay buffer containing 1.5 mM NADH ($\Delta\varepsilon_{340}$ = 6,200 M^{-1} cm^{-1}), 0.4 μM CBL, 1.3 μM LDH,

0.3-31.3 μM wild-type or site-directed variants of ytCBS and varying concentrations of L-Hcys and L-Ser substrates (Aitken and Kirsch, 2003). A background rate, for all components except the ytCBS enzyme, was recorded for each sample. Data were fit by nonlinear regression with the program SAS (SAS Institute, Cary, NC). Kinetic parameters were determined from the fit of the data to equation 3.1, in which the F subscript denotes the physiological reaction in which L-Cth is produced and $K_{iF1}^{L\text{-}Hcys}$ and $K_{iF2}^{L\text{-}Hcys}$ are the inhibition constants for substrate inhibition by L-Hcys (Jhee *et al.*, 2000a). Equation 3.1 was modified by removal of the $K_{iF2}^{L\text{-}Hcys}$ term, as required, for the site-directed variants.

(3.1)

$$\frac{v}{[E]} = \frac{k_{catF}[L-Ser][L-Hcys]}{K_m^{L-Hcys}[L-Ser] + K_m^{L-Ser}[L-Hcys]\left(1+\frac{[L-Hcys]}{K_{iF1}^{L-Hcys}}\right) + [L-Ser][L-Hcys]\left(1+\frac{[L-Hcys]}{K_{iF2}^{L-Hcys}}\right)}$$

The hydrolysis of L-Cth, producing L-Ser and L-Hcys, was detected *via* reaction of the latter with DTNB ($\Delta\varepsilon_{412}$ = 13,600 M^{-1} cm^{-1}). Reactions were carried out in assay buffer containing 2 mM DTNB, 0.008-6.0 mM L-Cth and 1.0-28 μM ytCBS. The data were fit to the Michaelis-Menten equation and to equation 3.2, to obtain an independent value for $k_{catR}/K_{mR}^{L\text{-}Cth}$. The R subscript denotes the reverse-physiological hydrolysis of L-Cth (Aitken and Kirsch, 2003).

$$\frac{v}{[E]} = \frac{k_{catR}/K_m^{L-Cth}[L-Cth]}{1+[L-Cth]/K_m^{L-Cth}} \qquad (3.2)$$

3.3.4. Homology Modeling.

The crystal structure of the truncated form of hCBS (PDB: 1JBQ (Meier *et al.* 2001)) served as the template for construction, *via* homology modeling with the MOE software package (MOE reference version 2006.02, CCG Inc.), of a structural model of the open conformation of ytCBS (ytCBSo). There are no available structures of CBS in complex with a substrate or inhibitor. Therefore, the structure of the L-Met complex of the K41A variant of the closely-related OASS from *S. typhimurium* (OASS-K41A/L-Met, PDB: 1D6S) was employed as a template for the closed conformation of ytCBS (ytCBSc), as Burkhard *et al.*, (1999) demonstrated that it is a suitable model of the closed conformation of the OASS active site. The structural similarity of these two enzymes is such that the crystal structure of hCBS was solved using molecular replacement with OASS (Meier *et al.,* 2001), thereby providing a precedent for modeling of ytCBSc based on the structure of the OASS-K41/L-Met complex. Comparison of the hCBS and OASS-K41/L-Met structures demonstrated differences in the placement of the peptide backbone and the secondary structure of residues 192-203 of hCBS (corresponding to residues 127-138 of yCBS), which includes hCBS residues 194-200 that are not resolved in the crystal structure, in the region corresponding to the mobile subdomain of OASS (Burkhard *et al.,* 1999). The initial step in construction of a model of ytCBSc was modeling of the targeted mobile region, comprising residues 122-154, which includes the yCBS 127-138 core sequence and corresponds to residues 107-138 of OASS (Burkhard *et al.,* 1999). Sequence alignment of these segments was completed using *MOE-Align* with a blosum62 matrix and gap open and extend penalties of 7 and 1, respectively. The *MOE-Homology* module (parameters: outgaps ignored) was subsequently employed to build a family of

3D models. All structures were energy minimized and the 10 models with a RMSD ≤0.005 were chosen for analysis, *via* the *best intermediate* method, to select the lowest energy model.

The crystal structures of the hCBS and OASS-K41A/L-Met templates were prepared for modeling by the addition of hydrogen atoms and the assignment of polarities to charged residues. Each structure was then subjected to gradual thawing, to relax it to a local energy minimum. The energy minimization procedure, employing a MMFF94s force field and Born solvation model, was performed sequentially, with tether forces applied to reduce the repositioning of non-target atoms (Halgren, 1999a; Halgren, 1999b; Bashford and Case, 2000; Shadnia *et al.* 2009). Initially only the introduced hydrogen atoms were optimized. This was followed by a partial relaxation of side chain atoms, including all but hydrogen (tether constant = 10) and with protein backbone atoms fixed, with subsequent energy minimization of hydrogen atoms (tether constant = 0). Side chains were then fully relaxed, while protein backbone atoms were tethered (tether constant = 10), prior to relaxation of all atoms, with no tethering. The use of this gradual thawing method produced relaxed structures that correspond closely to the crystal structure template and have a RMSD (crystal structure of template *versus* optimized structure of model) 80% lower than those produced *via* a fully unconstrained optimization.

3.3.5. Docking Studies.

Appropriate ligand conformations of L-Ser and L-Cth were selected using the *Builder* module of MOE and the stochastic conformer search method (Ferguson and

Raber, 1989). Non-redundant conformers up to 7 Kcal/mol from the global minimum were retained, resulting in a set of 20 conformers of L-Ser and 90 of L-Cth. Docking studies were performed using U-Dock (version 1.6), designed in SVL language for implementation in the MOE software package (version 2006.02, CCG Inc.) (Navidpour *et al.,* 2007). Random orientations of all conformers of the L-Ser and L-Cth ligands were generated inside a virtual docking box, with dimensions of 60 20 66 Å , such that it is large enough to accommodate the PLP cofactor, L-Cth or L-Ser ligand and the entrance to the active site (Figure 3.1).

The L-Cth ligand was docked to the open and closed conformations of ytCBS and L-Ser was docked to ytCBSo. The U-Dock software employs a layered-shell model to simulate protein flexibility. The first (S1) and second (S2) shells were defined as complete residues having at least one atom within 6 Å or 10.5 Å, respectively, of the active-site surface. Residues comprising S1 were excluded from the S2 set. The remaining atoms were deleted (217 amino acids, 2918 atoms) and residues adjacent to broken peptide bonds, which were capped with hydrogen atoms, form the third shell (S3). The S1 set of residues comprises 36 amino acids (494 atoms) and includes all of the active site, while S2 includes 118 residues (1086 atoms) and S3 contains 90 incomplete residues (181 atoms). A random orientation was assigned to each ligand conformer and the enzyme-ligand complex was energy minimized. During the docking procedure S3 was fixed, S2 was semi-flexible and S1 and ligand were relaxed (fully flexible). Semi-flexibility was simulated with a tether constant of 30 for S2. The Born solvation model was not employed during docking, as deletion of amino acids beyond S3 creates a new

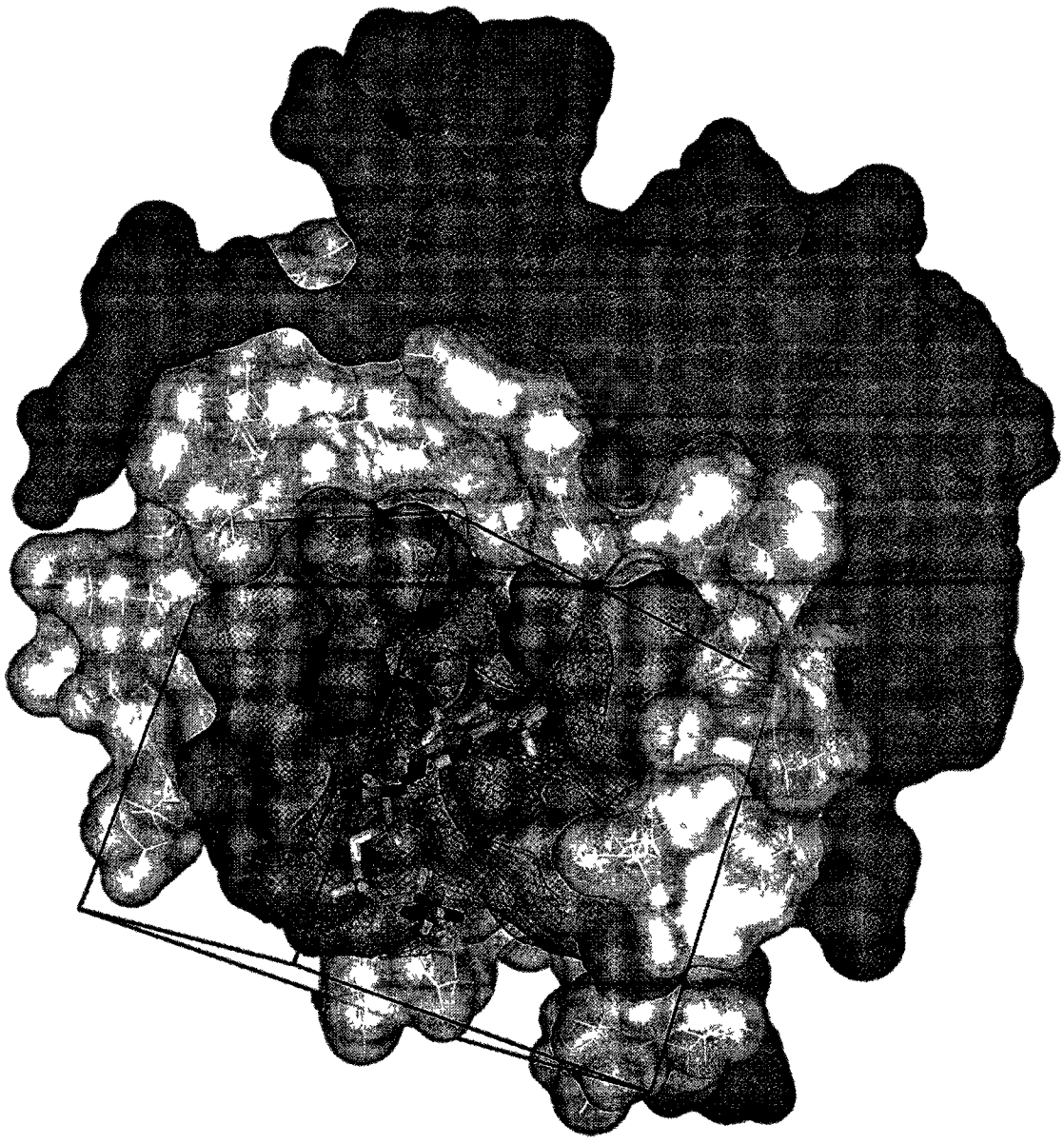

Figure 3.1. Model of the open conformation of ytCBS with L-Cth docked at the active site. The shells of residues considered in docking are shown: S1 (orange) - active site, S2 (white) - buffer shell, comprising those residues contacting active-site amino acids, and S3 (green) – residues situated between S2 and the rest of the protein (grey). The active site surface is rendered in dark blue mesh, and the docking box is displayed in red.

front for the model that is unrealistically close to the active site and to amino acids comprising S1and S2. Each ligand conformer was used to create up to 200 complexes. The force field energies of the fully flexible part of the complex (ligand plus S1) were used to rank the optimized complexes and the 5-10 lowest-energy structures were interpreted as optimum binding mode. The effect of the homocystinuria-associated hCBS-G307S mutation, which corresponds to ytCBS-G247S, was investigated by *in silico* mutation of the hCBS structure (1JBQ). The enzyme structure was prepared, as described above, the hydrogen side chain of G307 was replaced with that of serine and energy minimization was performed in three steps with flexible shells, as described in the docking procedure.

3.4. Results

3.4.1. Homology modeling of ytCBS and substrate docking.

Comparison of the open and closed conformations of ytCBS demonstrates that residues T128-S138 adopt a helical structure in the open conformation, which is lost in the closed conformation (Figure 3.2). In ytCBSo a pair of α-helices, comprising residues T128-S134 and I139-E148, are connected via residues P135-H138, which adopt a left-handed helix conformation. The strain resulting from the formation/unfolding of the α-helical structure of residues T128-S134 is absorbed by a corresponding conformational change in residues P135-H138, which also lose their left-handed helical structure in the closed conformation of the active site (Figure 3.1).

Comparison of the mode of binding of L-Cth to the open and closed conformations of the ytCBS model structures suggests that the α-carboxylate group of the L-Cth (Figure 3.3), or L-Ser, ligand is within hydrogen-bonding distance of G83, N84 and T85 in the open and closed conformations of ytCBS. A putative hydrogen bond (2.4 Å) between the distal carboxylate of L-Cth and S82 is also observed in the open and closed conformations of the enzyme. The distal amino group of L-Cth likely interacts with the G245 and Y158, *via* water-mediated H-bonds, in the open conformation and directly with the backbone carbonyl groups of G245, I246 and G247 and the side-chain hydroxyl group of Y158 in the closed conformation (Figure 3.3). Characterization of the T81A, S82A and Y158F variants of ytCBS was reported by Aitken and Kirsch, (2004). In the closed conformation, the side-chain of K112 is shifted by approximately 3.0 Å, compared to the ytCBSo-L-Cth complex, and approaches to within 3.8 Å of the

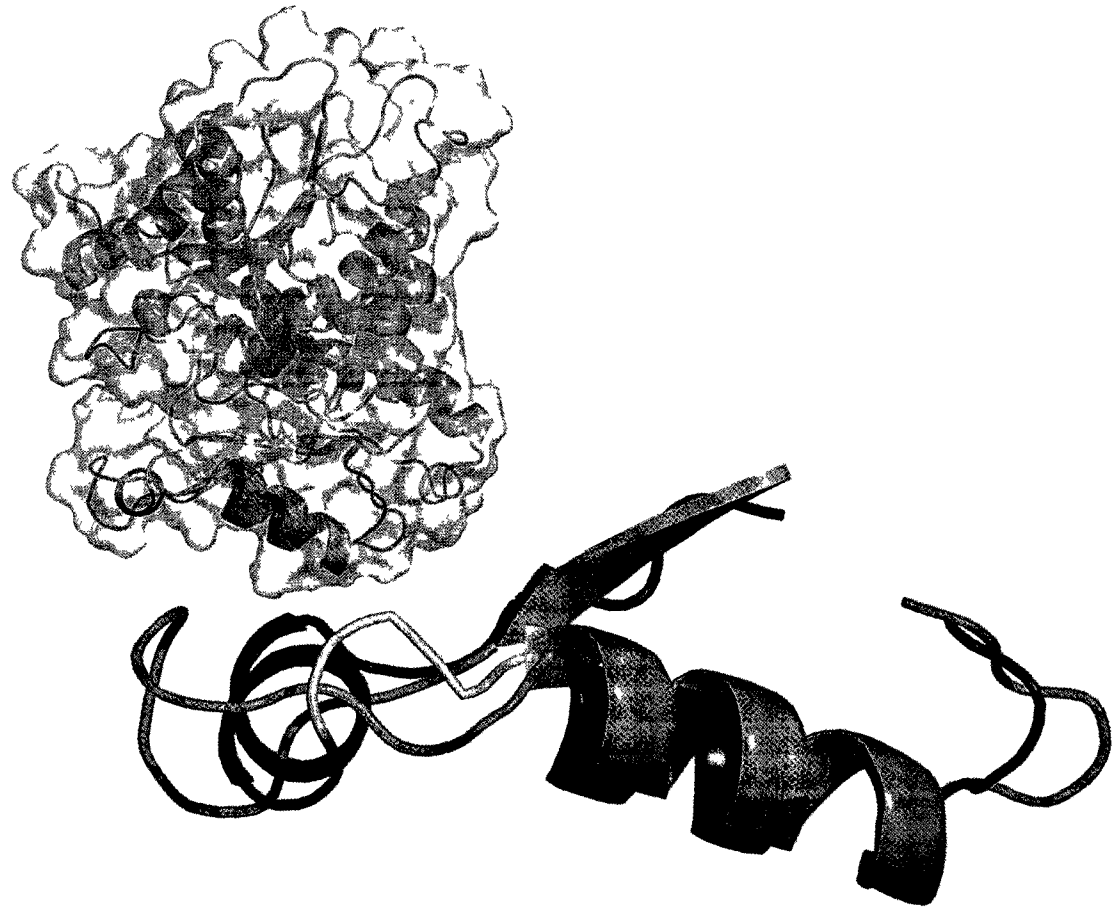

Figure 3.2. Comparison of modeled open (red and yellow) and closed (cyan) conformations of ytCBS. The PLP cofactor is shown in green in space-filling representation.

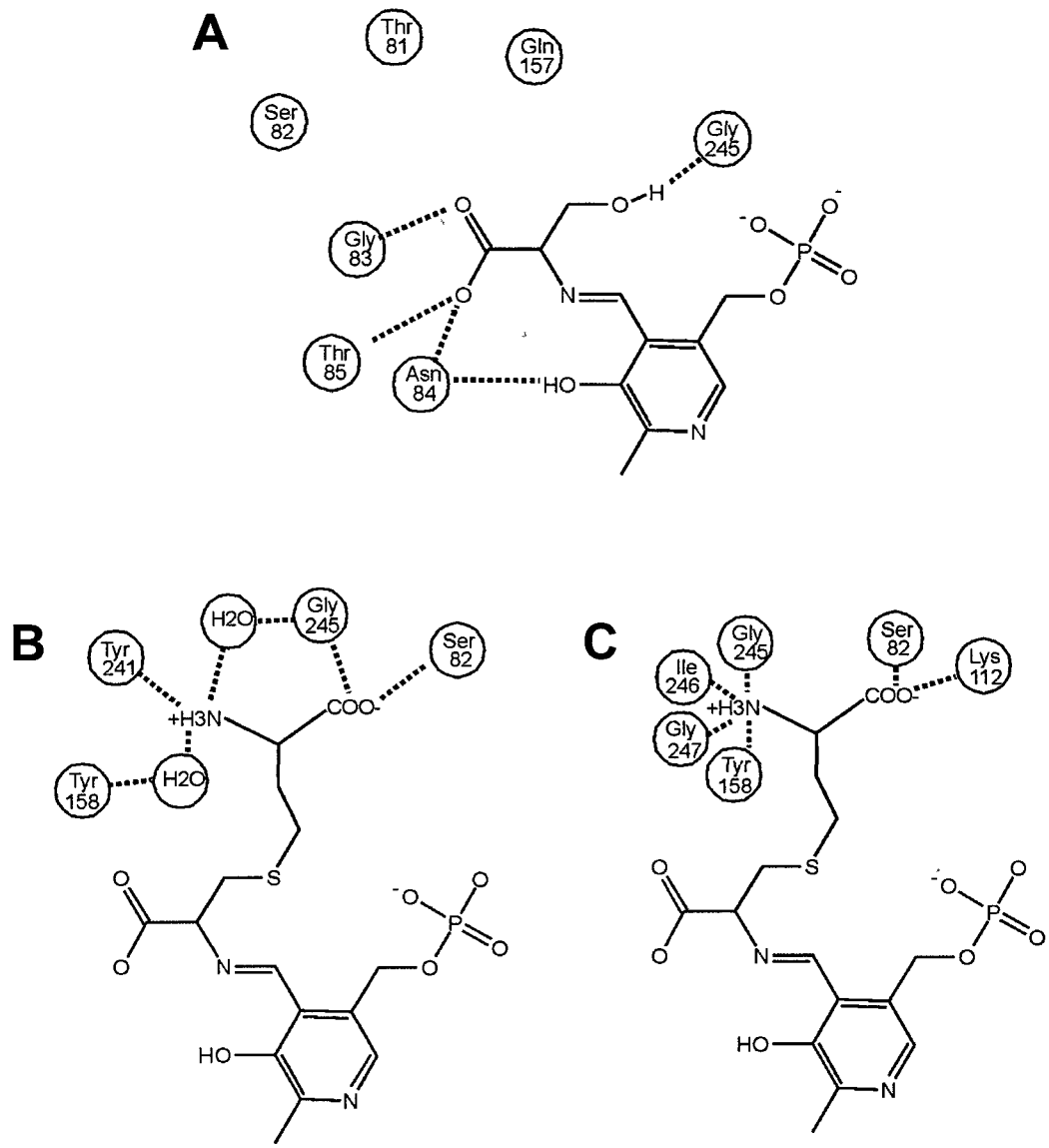

Figure 3.3. Schematic diagrams of L-Ser and L-Cth binding to the ytCBS models. Residues interacting with the ligand are shown for the docked (**A**) ytCBSo-L-Ser, (**B**) ytCBSoL-Cth and (**C**) ytCBScL-Cth complexes.

distal carboxylate of the L-Cth ligand (Figures 3.3 and 3.4). Although no interactions between the docked L-Cth ligand and residues E136, H138, Y248 or D249 were observed in the 20 lowest-energy conformations of the complex of L-Cth with either ytCBSo or ytCBSc (Figure 3.4), these residues were targeted for mutagenesis, in addition to K112, as they are the only polar residues within the mouth of the yCBS active site. These four residues are also of interest as E136 and H138 are included in the left-handed helical turn (P135-H138) of ytCBSo, the conformation of which is changed in ytCBSc (Figure 3.2), while residues Y248 and D249 are immediately adjacent to G247, which is predicted to interact with the distal amino group of L-Cth (Figure 3.3) and corresponds to G307 of hCBS, a residue associated with a prevalent homocystinuria-linked mutation.

3.4.2. Kinetic characterization.

The activity of all enzymes was measured at 25 °C and comparison of the kinetic parameters of wild-type ytCBS with those determined at 37 °C (Aitken and Kirsch, 2004) demonstrates that $K_m^{L\text{-}Ser}$ and $K_m^{L\text{-}Hcys}$ of the physiological, condensation reaction and $K_m^{L\text{-}Cth}$ of L-Cth hydrolysis are unchanged (Table 3.1). The k_{catF} and k_{catR} values, where the F and R subscripts denote kinetic parameters of the condensation and L-Cth hydrolysis reactions, respectively, are decreased by 2.8 and 3.1-fold, respectively, at 25 °C, in keeping with the ~2.4-fold decrease expected for the 12-°C difference in temperature. No β-elimination activity was detectable for the wild-type enzyme, as reported previously (Aitken and Kirsch, 2003), or the eight site-directed variants. The kinetic parameters of the H138F and Y248F variants were determined from the fit of the data to equation 3.1.

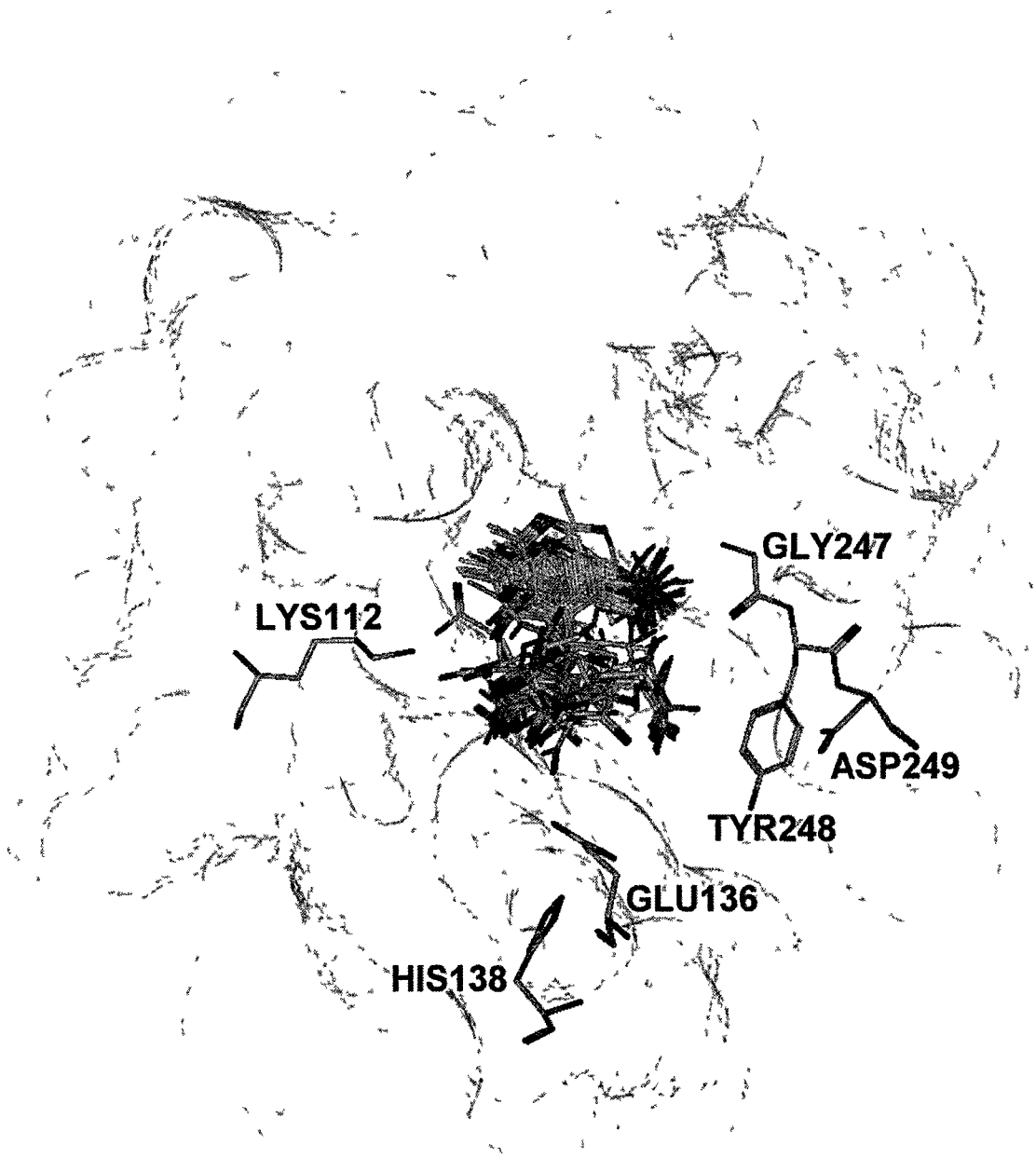

Figure 3.4. Location of targeted active-site residues with respect to the 20 lowest energy ligand conformations in the ytCBSc-L-Cth complex.

Table 3.1. Steady-state kinetic parameters for wild-type ytCBS and the E136A, H138F, Y248F and D249A site-directed variants.

	ytCBS (37 °C)[a]	ytCBS (25 °C)	E136A	H138F	Y248F	D249A
L-serine + L-homocysteine → L-cystathionine[b]						
k_{catF} (s^{-1})	17 ± 1	6.0 ± 0.3	11 ± 1	5.3 ± 0.7	0.035 ± 0.001	3 ± 2
$K_{mF}^{L\text{-}Ser}$ (mM)	1.2 ± 0.1	0.8 ± 0.2	1.0 ± 0.3	1.6 ± 0.6	1.2 ± 0.3	4 ± 3
$K_{mF}^{L\text{-}Hcys}$ (mM)	0.30 ± 0.03	0.39 ± 0.04	0.21 ± 0.06	7 ± 1	0.19 ± 0.02	4 ± 2
$k_{catF}/K_{mF}^{L\text{-}Ser}$ ($M^{-1}s^{-1}$)	(2.5 ± 0.6) 10^4	(8 ± 2) 10^3	(1 ± 0.3) 10^4	(8.1 ± 0.6) 10^2	30 ± 8	(8 ± 3) 10^2
$k_{catF}/K_{mF}^{L\text{-}Hcys}$ ($M^{-1}s^{-1}$)	(8 ± 1) 10^4	(1.6 ± 0.1) 10^4	(5 ± 1) 10^4	(3 ± 1) 10^3	(1.8 ± 0.2) 10^2	(8 ± 1) 10^2
$K_{iF1}^{L\text{-}Hcys}$ (mM)	1.0 ± 0.4	0.9 ± 0.3	0.6 ± 0.2	1.5 ± 0.6	1.2 ± 0.5	1.6 ± 0.8
$K_{iF2}^{L\text{-}Hcys}$ (mM)	15 ± 4	4.8 ±0.6	2.7 ± 0.6	9 ± 2		2 ± 1
$K_{iF}^{L\text{-}Ser}$ (mM)			4 ± 1	78 ± 17		31 ± 8
L-cystathionine → L-homocysteine + L-serine[c]						
k_{catR} (s^{-1})	1.03 ± 0.02	0.329 ± 0.003	0.274 ± 0.004	0.116 ± 0.002	(3.40±0.09) 10^{-3}	0.101 ± 0.004
$K_{mR}^{L\text{-}Cth}$ (mM)	0.09 ± 0.02	0.069 ± 0.004	0.041 ± 0.004	0.31 ± 0.02	0.036 ± 0.006	0.15 ± 0.02
$k_{catR}/K_{mR}^{L\text{-}Cth}$ ($M^{-1}s^{-1}$)	(7.5 ± 0.4) 10^3	(4.7 ± 0.2) 10^3	(6.7 ± 0.6) 10^3	(3.7 ± 0.2) 10^2	90 ± 10	(6.9 ± 0.9) 10^2

[a]Reference (Aitken and Kirsch 2004).

[b]Data were fit to equations 3.1 (H138F and Y248F) and 3 (E136A and D249A). The F subscript denotes kinetic parameters of the β-replacement reaction.

[c]Data were fit to the Michaelis-Menten equation and equation 3.2. The R subscript denotes kinetic parameters of the reverse, L-Cth hydrolysis, reaction.

The k_{catF} of the H138F variant is unchanged, compared to the wild-type enzyme, while that of Y248F is reduced 250-fold. In contrast, the $K_m^{L\text{-}Ser}$ and $K_m^{L\text{-}Hcys}$ values of the H138F variant are increased by 9 and 18-fold, respectively, while those of Y248F are unchanged. The $k_{catR}/K_m^{L\text{-}Cth}$, for the reverse-physiological, hydrolysis of L-Cth, of the H138F and Y248F variants are reduced by 13 and 57-fold, respectively, changes that are dominated by the increase in the $K_m^{L\text{-}Cth}$ of H138F and decrease in the k_{catR} of Y248F, similar to the trend observed for the condensation reaction.

The activity of the E136A and D249A variants was observed to decrease at elevated L-Ser concentration. Therefore, equation 3.1. was modified, incorporating a term for substrate inhibition by L-Ser ($K_{iF}^{L\text{-}Ser}$), to produce equation 3.3, to which the data for the E136A and D249A variants were fit.

$$\frac{v}{[E]} = \frac{k_{catF}[L-Ser][L-Hcys]}{K_m^{L-Hcys}[L-Ser]*F_1 + K_m^{L-Ser}[L-Hcys]*F_2 + [L-Ser][L-Hcys]*F_3} \quad (3.3)$$

The F_1, F_2 and F_3 terms in the denominator of equation 3.3 denote (1 + [L-Ser]/$K_{iF}^{L\text{-}Ser}$), (1 + [L-Hcys]/$K_{iF1}^{L\text{-}Hcys}$) and (1 + [L-Hcys]/$K_{iF2}^{L\text{-}Hcys}$), respectively. The substrate inhibition of the E136A and D249A variants by L-Ser is mild as the $K_{iF}^{L\text{-}Ser}$ values determined are 4 and 31 mM, respectively (Table 3.1). The kinetic parameters of the E136A variant are within 2-fold of the wild-type ytCBS. The $K_m^{L\text{-}Ser}$ and $K_m^{L\text{-}Hcys}$ of ytCBS-D249A are increased by 5 and 8-fold, respectively, and the k_{catF} and k_{catR} are reduced by only 2-3-fold. The spectra of the PLP cofactor of the E136A, H138F and D249A variants are identical to the wild-type enzyme and the intensity of the 412-nm, internal-aldimine peak of Y248F is reduced by 20%.

The β-replacement activity of the G247S variant is undetectable and the hydrolysis of L-Cth is drastically reduced. The 10^4-fold reduction in the $k_{catR}/K_{mR}^{L\text{-}Cth}$ (0.45 ± 0.03 $M^{-1}s^{-1}$) of G247S is dominated by a 1400-fold reduction in k_{catR} [k_{catR} = (2.42 ± 0.03) 10^{-4} s^{-1} and $K_{mR}^{L\text{-}Cth} = 0.32 \pm 0.02$ mM]. The corresponding G307S mutation was modeled in the context of the hCBS crystal structure (Meier *et al.,* 2001) and the side chain of the substituted S307 is observed to form a hydrogen bond with that of Y301. This interaction causes movement of the peptide backbone with concomitant loss of the hydrogen bonds between oxygen atoms of the cofactor phosphate moiety and the backbone of G256 and side chain of T257. This results in a ~1.4 Å movement of the phosphate group and a corresponding ~1 Å shift in the position of the cofactor within the active site (Figure 3.5). The effect of this mutation is also evidenced by the 40% decrease in the 412-nm peak of the internal aldimine, in the absence of substrate, and the lack of a 460-nm peak, corresponding to the external aldimine of aminoacrylate, upon reaction of 20 μM ytCBS-G307S with 50 mM L-Ser (Figure 3.6).

Residue K112, targeted for site-directed mutagenesis on the basis of the proposed interaction with the distal carboxylate group of L-Cth (Figures 3.3 and 3.4), was converted to residues of similar size that either differ in their hydrogen-bonding capacity (K112Q and K112R) or lack the ability to form hydrogen bonds (K112L). An upper limit of ≤0.02 s^{-1} is estimated for the k_{catF} of the β-replacement activity of the K112Q variant, a reduction of ≥300-fold, and the $k_{catR}/K_m^{L\text{-}Cth}$ of the reverse-physiological reaction is correspondingly decreased by ~10^5-fold (Table 3.2). The K112L and K112R variants have a near-identical effect, resulting in decreases of ~400 and ~20-fold in $k_{catR}/K_m^{L\text{-}Ser}$ and $k_{catR}/K_m^{L\text{-}Hcys}$, respectively, although the 5.8×10^5-fold reduction in the $k_{catR}/K_m^{L\text{-}Cth}$

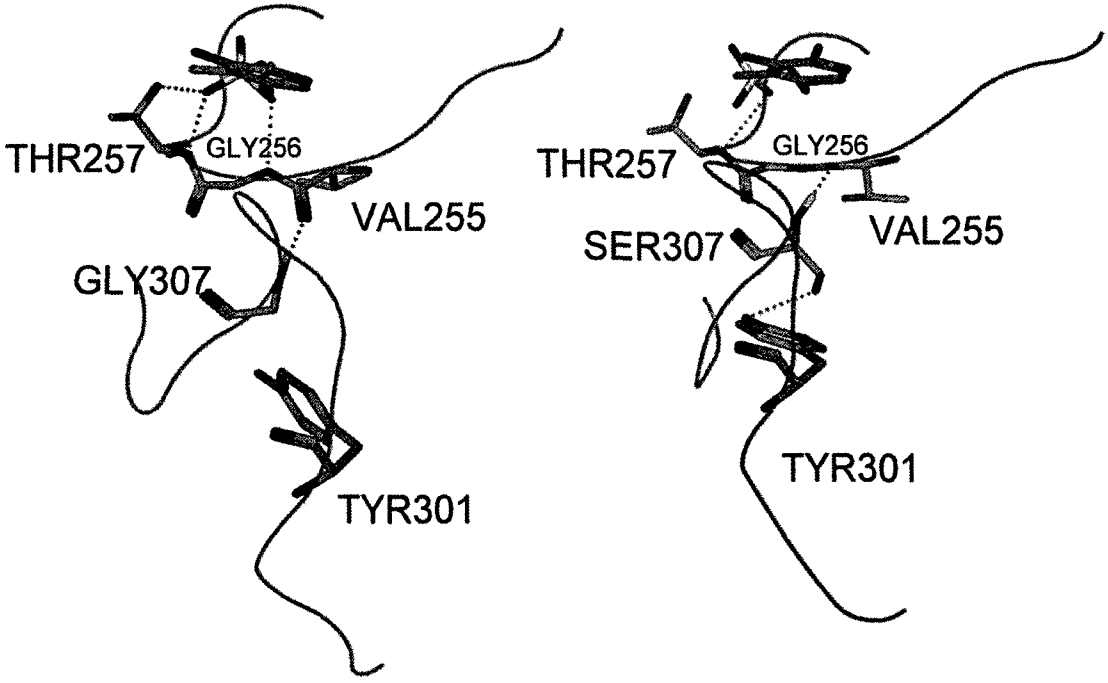

Figure 3.5. Effect of the G307S mutation in the context of the hCBS active site. Gradual energy minimization of the modified enzyme (right) resulted in formation of a hydrogen bond, between the side-chain hydroxyl moieties of S307 and Y301, that is not present in the wild-type enzyme (left). The presence of the S307-Y301 hydrogen bond results in movement of the peptide backbone such that the hydrogen bonds between oxygen atoms of the cofactor phosphate and residues G256 and T247, present in the wild-type enzyme, are lost in the G307S variant.

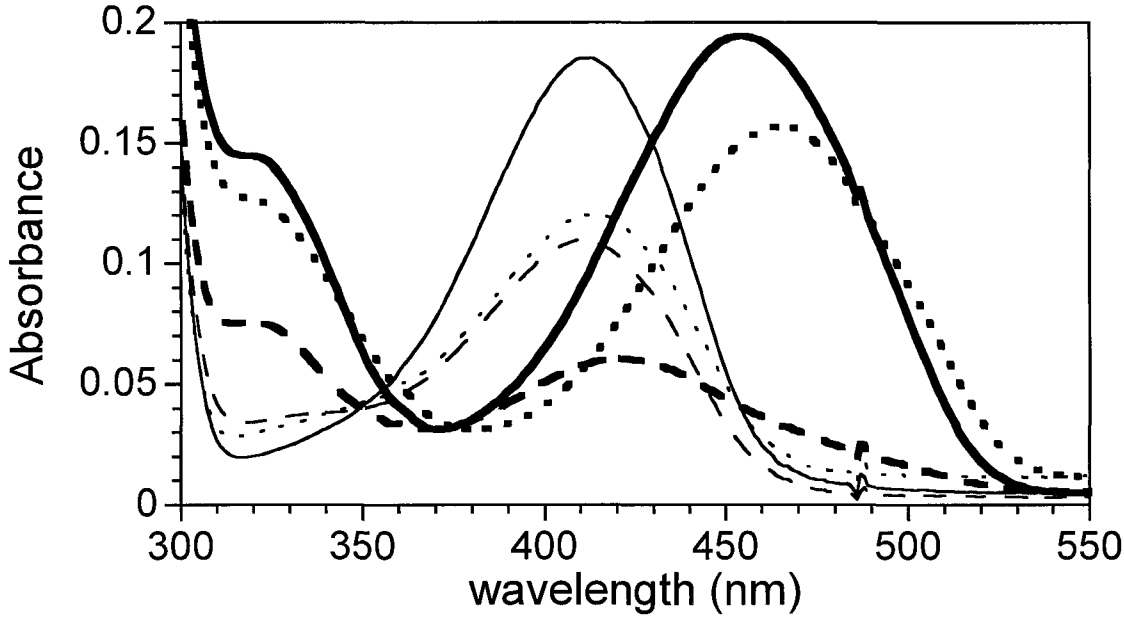

Figure 3.6. Spectra of the PLP cofactor of wild-type ytCBS (solid line), G247S (dashed line) and K112L (dotted line) alone and following a 10-min incubation with 50 mM L-Ser (thick lines).

Table 3.2. Steady-state kinetic parameters for K112 site-directed variants.[a]

	K112L	K112Q	K112R
L-serine + L-homocysteine → L-cystathionine[b]			
k_{catF} (s^{-1})	1.1 ± 0.1	≤ 0.02	1.2 ± 0.2
$K_{mF}^{L\text{-}Ser}$ (mM)	43 ± 7	n.d.	69 ± 13
$K_{mF}^{L\text{-}Hcys}$ (mM)	0.8 ± 0.3	n.d.	1.5 ± 0.3
$k_{catF}/K_{mF}^{L\text{-}Ser}$ ($M^{-1}s^{-1}$)	23 ± 2	n.d.	17 ± 1
$k_{catF}/K_{mF}^{L\text{-}Hcys}$ ($M^{-1}s^{-1}$)	(1.1 ± 0.4) 10^{3}	n.d.	(8 ± 2) 10^{2}
$K_{iF1}^{L\text{-}Hcys}$ (mM)	6.2 ± 0.6	n.d.	7.2 ± 0.7
$K_{iF2}^{L\text{-}Hcys}$ (mM)		n.d.	
$K_{iF}^{L\text{-}Ser}$ (mM)	5 ± 2	n.d.	17 ± 5
L-cystathionine → L-homocysteine + L-serine[c]			
k_{catR} (s^{-1})	n.s.	n.s.	n.s.
$K_{mR}^{L\text{-}Cth}$ (mM)	n.s.	n.s.	n.s.
$k_{catR}/K_{mR}^{L\text{-}Cth}$ ($M^{-1}s^{-1}$)	1.41 ± 0.04	(3.9 ± 0.6) 10^{-2}	(8.1 ± 0.9) 10^{-2}

[a]n.d. indicates that activity was not detectable, n.s. indicates that saturation was not achieved within the solubility limit of L-Cth.

[b]Data were fit to equation 3.3. The F subscript denotes kinetic parameters of the β-replacement reaction.

[c]Data were fit to the Michaelis-Menten equation and equation 3.2. The R subscript denotes kinetic parameters of the reverse, L-Cth hydrolysis, reaction.

of K112R, compared to wild-type ytCBS, is two orders of magnitude greater than that of K112L. Similar to G247S, the 412-nm absorbance of the internal aldimine of the three K112 variants is reduced by ~40%. However, in contrast with G247S, the 460-nm peak, characteristic of the aminoacrylate intermediate, is evident upon reaction of the K112 variants with 50 mM L-Ser, as exemplified by K112L in Figure 3.6.

3.5. Discussion

Cystathionine β-synthase is unique among the enzymes of the transsulfuration pathways as it is a member of fold type II of PLP-dependent enzymes. In contrast, cystathionine γ-synthase (CGS) and cystathionine β-lyase (CBL), which comprise the bacterial/plant transsulfuration pathway and cystathionine γ-lyase, which follows CBS in the reverse transsulfuration pathway of yeast and animals, belong to the γ-subfamily of fold type I (Christen and Mehta, 2001). An active-site arginine residue interacts with the α-carboxylate group of the amino acid substrate, bound in aldimine linkage to the PLP cofactor, in fold type I enzymes, as exemplified by the structures of inhibitor complexes of CGS and CBL (Clausen *et al.,* 1997; Steegborn *et al.,* 2001; Ejim *et al.,* 2007). In contrast, the crystal structure of the L-Met complex of OASS-K41A, demonstrates that, typical of fold type II enzymes, a conformational change occurs upon substrate binding to form a hydrogen-bonding network between active-site residues and the α-carboxylate group of the substrate bound in aldimine linkage to the PLP cofactor (Burkhard *et al.,* 1999). Although the only available structures of CBS are of the unliganded form of the human enzyme (Meier *et al.,* 2001; Taoka *et al.,* 2002), the structural similarity of CBS and OASS enabled the K41A/L-met complex of the latter to be employed as a model to identify active-site residues involved in L-Ser binding to ytCBS (Figure 3.3.A) (Aitken and Kirsch, 2004). However, as the second substrate of OASS is H_2S, the same approach cannot be employed to identify yCBS residues involved in L-Hcys binding. Therefore, two strategies were employed to identify putative L-Hcys-binding residues as targets for site-directed mutagenesis. In the first approach, polar residues situated at the mouth of the hCBS active site, and non-conserved between OASS and CBS, were targeted to probe

their role in L-Hycs binding. The ytCBS residues E136, H138, Y248 and D249, which correspond to K117, M119, A231 and G232, respectively, of OASS, were selected for site-directed mutagenesis. The site-directed variants were constructed in the model ytCBS enzyme, which lacks the heme cofactor and is expressed in *E. coli* at a level sufficient to facilitate kinetic characterization (Aitken and Kirsch, 2004). One of the most prevalent homocystinuria-associated mutations of hCBS is G307S. As the corresponding G247 of yCBS is immediately adjacent in sequence to the targeted polar residues Y248 and D249 and is one of three residues (G245-I246-G247) proposed to interact with the distal amino group of the ligand in the docked ytCBSc-L-Cth complex (Figure 3.3), the ytCBS-G247S site-directed variant was constructed to probe the effect of this mutation in the model yeast enzyme.

An *in silico* strategy of modeling and docking was also employed to identify key active-site residues. The L-Cth product was docked to models of the open and closed conformations of ytCBS, which were based on the structures of hCBS and OASS-K41A/L-Met, respectively (Burkhard *et al.,* 1999; Meier *et al.,* 2001). Analysis of the modeled ytCBS-L-Cth complexes indicated three residues that may form hydrogen bonds to the distal amino (S82 and Y158) and carboxylate (K112) groups of ytCBS. A series of three site-directed variants of K112 were constructed to investigate the role of this residue by elimination and modification of the hydrogen bonding interactions formed by the ε-amino group of its side chain (K112L, K112Q and K112R). The roles of S82 and Y158 have been described by Aitken and Kirsch (Aitken and Kirsch, 2004). The side chain hydroxyl group of S82, which is within ~2.9 Å of the α-carboxylate of L-Ser or L-Cth docked at the active site of the ytCBS models (Figure 3.3), is involved in L-Ser

binding, as demonstrated by the ~70-fold increase in the $K_{d(app)}^{L\text{-}Ser}$ of ytCBS-S82A (Aitken and Kirsch, 2004). However, the S82A mutation has no effect on $K_{mF}^{L\text{-}Hcys}$ and increases the $K_{mR}^{L\text{-}Cth}$, of the L-Cth hydrolysis reaction, by only ~7-fold. Mutation of Y158 (Y158F), which is replaced with a conserved phenylalanine in OASS, results in reduction of the $k_{catF}/K_{mF}^{L\text{-}Ser}$ and $k_{catF}/K_{mF}^{L\text{-}Hcys}$ of the β-replacement reaction by ~3-fold and a 5-fold decrease in the $k_{catR}/K_{mR}^{L\text{-}Cth}$ of the L-Cth hydrolysis reaction, demonstrating that the hydroxyl group of Y158 is not a major factor in binding or catalysis. However, while mutation of S82 and Y158 does not impede L-Hcys or L-Cth binding, these residues play a role in maintenance of the equilibrium between the open and closed conformations of the enzyme, thereby acting as determinants of reaction specificity (Aitken and Kirsch, 2004).

3.5.1. E136A and H138F.

Comparison of the OASS and OASS-K41A/L-Met structures, representing the open and closed conformations of the active-site, respectively, demonstrates the rigid-body movement of a subdomain of the enzyme upon closure of the active site. In the closed conformation one end of the active-site cleft is sealed by contact between the amino-terminus of helix 4 and residues on the opposite side of the active site (Burkhard *et al.,* 1999). This helical segment corresponds to positions 128-134 in ytCBS, immediately adjacent to the left-handed helical turn containing residues E136 and H138 (Figure 3.2). Therefore, a similar movement in ytCBS could be expected to reduce the distance between E136 and H138 and opposing residues in the active-site cleft (Figure 3.4). The negligible effect of the E136A mutation on the kinetic parameters of ytCBS suggests that this residue, located at the outside edge of the catalytic cleft (Figure 3.4), is

apparently too far from the PLP cofactor to interact with the L-Hcys substrate or L-Cth product. Substrate inhibition by L-Ser was observed for E136A, indicating a subtle change in the ytCBS active site to enable the binding of L-Ser to the L-Hcys site without changing the $K_m^{L\text{-}Hcys}$. The 18 and 4-fold increases the $K_m^{L\text{-}Hcys}$ and $K_m^{L\text{-}Cth}$, and corresponding change of less than 3-fold in k_{catF}, k_{catR} and $K_m^{L\text{-}Ser}$, of the H138F variant suggest that this residue plays a minor or indirect role in L-Hcys binding. Residues E136 and H138 are not predicted to be within hydrogen-bonding distance of the L-Cth ligand in the open or closed conformations of ytCBS (Figure 3.3). The side chains of the corresponding E201 and H203 of hCBS do not interact with any other active-site residues in the open conformation of the enzyme and are ≥8 Å from residues on the opposite side of the active-site cleft. A number of water molecules are found within the active sites of hCBS and OASS (Burkhard *et al.*, 1998; Meier *et al.*, 2001; Taoka *et al.*, 2002). Therefore, water molecules in the ytCBS active site can be expected to mediate interactions, and changes in the hydrogen-bonding network of water molecules in the active site of the E136A and H138F variants, which both eliminate the hydrogen-bonding capacity of the targeted residues, may explain the subtle changes in kinetic parameters observed.

3.5.2. Y248F and D249A.

The k_{catF} and k_{catR} of the Y248F variant are decreased by two orders of magnitude, while the K_m values for L-Ser, L-Hcys and L-Cth are unchanged. In contrast, the kinetic parameters of D249A are within 5-fold of the wild-type enzyme, with the exception of a 10-fold increase in $K_m^{L\text{-}Hcys}$. Neither the docked L-Cth ligand, nor any active-site residues are within hydrogen-bonding distance of the side chains of Y248 or D249 in either the

open or closed conformations of ytCBS. Similarly, no contacts to other residues are apparent for the corresponding Y308 and D309 of hCBS (Meier *et al.,* 2001). In contrast, a hydrogen bond is formed between the backbone carbonyl of A231 (corresponding to ytCBS-Y248) and the ε-amino group of K119 in OASS-K41A/L-Met. This interaction is enabled by the 5.3-Å movement of K119, situated at the amino-terminus of helix 4 within the mobile subdomain, between the open and closed conformations of the OASS active site. However, in the OASS-K41A/L-Met structure no interactions are evident for G232, which corresponds to ytCBS-D249. Therefore, the observed ~100-fold reduction in k_{cat} and 10-fold increase in $K_m^{L\text{-}Hcys}$ of the Y248F and D249A variants, respectively, of ytCBS are likely due to subtle changes in active-site conformation and dynamics resulting from the loss of direct or water-mediated hydrogen bonds to opposing groups of the mobile subdomain. The effect of the Y248F variant is unique, suggesting that the latter does not interact primarily with either E136 or H138.

3.5.3. G247S.

Docking of L-Cth to the closed conformation of ytCBS identified interactions between the distal amino moiety of the ligand and the backbone carbonyl groups of residues G245, I246 and G247. One of the most prevalent homocystinuria-associated mutations of hCBS is G307S (Kraus *et al.,* 1999). Residue G307, which corresponds to G247 of yCBS, is situated within the active-site and individuals with the G307S mutation are pyridoxine non-responsive and suffer severe clinical manifestations. Meier *et al.,* (2003) proposed that the side-chain of serine in the G307S variant may result in a conformational change that restricts the access channel of the active site and impairs L-Hcys binding. Modeling of G307S in the active site of hCBS indicates that the hydrogen

bonds between phosphate oxygen atoms and the backbone amide of G256 and side-chain hydroxyl group of T257 of the wild-type enzyme are lost in the variant as a result of formation of a hydrogen bond between the side chains of S307 and Y301 (Figure 3.5). As a result, the PLP cofactor, which is shifted ~1 Å toward the mouth of the active site, is likely bound in a catalytically non-productive position. This is supported by the marginal formation of the aminoacrylate intermediate upon reaction of the corresponding ytCBS-G247S with 50 mM L-Ser (Figure 3.6), as well as the lack of β-replacement activity and the 10^4-fold reduction in the $k_{catR}/K_{mR}^{L\text{-}Cth}$ of L-Cth hydrolysis of this variant.

3.5.4. K112 variants.

Docking of L-Cth, the product of the ytCBS-catalyzed condensation of L-Ser and L-Hcys, to the models of the open and closed forms of the enzyme enabled comparison of the active-site interactions in the two conformations. While the side chain of S82 is predicted to form a hydrogen bond to the distal carboxylate of L-Cth in both conformations, the water-mediated interaction between Y158 and the distal amino group of the ligand in ytCBSo-L-Cth is replaced with a direct hydrogen bond in the ytCBSc-L-Cth model (Figure 3.3). The only predicted side chain interaction unique to the closed conformation is that between the distal carboxylate group of L-Cth and the ε-amino group of K112. A series of three variants were constructed to alter (K112Q and K112R) or eliminate (K112L) the hydrogen-bonding capacity, while maintaining packing interactions, of the K112 side chain. While the k_{catF} and $K_m^{L\text{-}Hcys}$ of K112L and K112R are within 5-fold of the wild-type, $K_m^{L\text{-}Ser}$ is increased 50 and 90-fold, respectively,

suggesting a role for K112 in L-Ser, but not L-Hcys binding. The corresponding K177 of hCBS is involved in a hydrogen-bonding network (S147-K177-E304-K384) that bridges the two sides of the active-site cleft by linking the mobile loop of residues 146-150, which interacts with the α-carboxylate group of the L-Ser substrate (Aitken and Kirsch, 2004), with loops 296-316 and 374-388, which cover a large portion of the active-site surface. The residues of the K177 hydrogen-bonding network and L-Ser-binding loop of hCBS are conserved in yCBS as S82-K112-E244-K327 and T81-S82-G83-N84-T85, respectively. The corresponding K112 hydrogen-bonding network of ytCBS is present in the structures of the modeled open and closed conformations of the enzyme. The 20 and 50-90-fold increases in the $K_m^{L\text{-}Ser}$ of the S82A and K112L/R variants of ytCBS are of similar magnitude, supporting an interaction between the two residues that is eliminated by mutation of either one (Table 3.2) (Aitken and Kirsch, 2004). The lack of detectable β-replacement activity of the K112Q variant, in comparison with K112L, may be due to unanticipated interactions formed by the side chain of glutamine. The ~400-fold reduction in the $k_{catF}/K_m^{L\text{-}Ser}$ of the K112L and K112R site-directed variants, which correspond to hCBS-K177, also sheds light on the E176K and K384E/N homocystinuria-associated mutations of hCBS. These amino acids belong to a circular network of five residues linked by covalent and hydrogen bonds in which residue E176, immediately adjacent to K177, is hydrogen bonded to T383 and both the neighboring K384 and K177 are hydrogen bonded to E304. Therefore, the naturally-occurring K384E/N and E176K mutations would be expected to disrupt the hydrogen bonding network that participates in holding together the 146-150, 296-316 and 374-388 loops, which comprise much of the surface of the active-site entrance of hCBS.

3.6. Conclusions

The results of this study provide insight into the effect of the homocystinuria-associated G307S, E176K and K384E/N mutations within the context of the hCBS structure. However, the five targeted ytCBS residues (K112, E136, H138, Y248 and D249), selected on the basis of their polar side chains, location within the active site and *in silico* docking predictions, are not direct determinants of L-Hcys binding. The α-carboxylate and α-amino of L-Hcys, and the corresponding distal carboxylate and amino groups of L-Cth, may be bound by interactions with the backbone of active-site residues, such as G245, I246 and G247 (Figure 3.3), or *via* water-mediated hydrogen bonds. A structure of the closed conformation of the hCBS/K119A-L-Cth complex, in which the active-site lysine residue is mutated to prevent L-Cth cleavage, would provide a useful model to guide further explorations of the active site. Comparison of this structure with that of OASS-K41A/L-Met would provide insight into the determinants of substrate specificity that distinguish these structurally and mechanistically-similar enzymes.

Chapter 4. Residue N84 of Yeast Cystathionine β-Synthase is a Determinant of Reaction Specificity

4.1. Abstract

Cystathionine β-synthase (CBS) catalyzes the pyridoxal 5'-phosphate (PLP)-dependent condensation of L-serine and L-homocysteine to form L-cystathionine in the first step of the reverse transsulfuration pathway. Residue N84 of yeast CBS (yCBS), predicted to form a hydrogen bond with the hydroxyl moiety of the PLP cofactor, was replaced with alanine, aspartate and histidine. The truncated form of yCBS (ytCBS, residues 1-353) was employed in this study to eliminate any effects of the C-terminal, regulatory domain. The $k_{cat}/K_m^{L\text{-}Ser}$ of the N84A, N84D and N84H variants for the β-replacement reaction are reduced by a factor of 230, 11000 and 640, respectively. Fluorescence resonance energy transfer between tryptophan residue(s) of the enzyme and the PLP cofactor, observed in the wild-type enzyme and N84A variant, is altered in N84H and absent in N84D. PLP saturation values of 73%, 30% and 67% were observed for the alanine, aspartate and histidine variants, respectively, compared to 98% for the wild-type enzyme. A marginal β-elimination activity was detected for N84D ($k_{cat}/K_m^{L\text{-}Ser}$ = 0.23 ± 0.02 $M^{-1}s^{-1}$) and N84H ($k_{cat}/K_m^{L\text{-}Ser}$ = 0.34 ± 0.06 $M^{-1}s^{-1}$), in contrast with wild-type ytCBS and the N84A variant, which do not catalyze this reaction. The ytCBS-N84D enzyme is also inactivated upon incubation with L-serine, via an aminoacrylate-mediated mechanism. These results demonstrate that residue N84 is essential in maintaining the orientation of the pyridine ring of the PLP cofactor and the equilibrium between the open and closed conformations of the active site.

4.2. Introduction

Cystathionine β-synthase (CBS; E.C. 4.2.1.22.) catalyzes the pyridoxal 5'-phosphate-(PLP) dependent condensation of L-serine (L-Ser) and L-homocysteine (L-Hcys) to form L-cystathionine (L-Cth) (Borcsok and Abeles, 1982). The first half reaction of the CBS-catalyzed β-replacement comprises abstraction of the C_α proton of L-Ser, followed by β-elimination of the hydroxyl group. Reaction of the resulting aminoacrylate intermediate with L-Hcys and release of the L-Cth product regenerates the internal aldimine form of the enzyme (Jhee *et al.*, 2000a). Mechanistic studies relying on the spectral properties of catalytic intermediates are precluded in human CBS (hCBS) because of the overlapping absorbance spectra of the PLP and heme cofactors. Therefore, as yeast CBS (yCBS; CYS4/Ygr155w) catalyzes the same reaction as the human enzyme and shares 47% amino acid sequence identity in the catalytic domain, but does not contain heme, it provides a useful proxy for the human enzyme (Jhee *et al.*, 2000a; Maclean *et al.*, 2000). The structure of the truncated form of hCBS, lacking the C-terminal, regulatory domain, provides a model for studies on yCBS, for which no structure is available (Meier *et al.*, 2001; Taoka *et al.*, 2002).

The interactions between PLP and active-site residues, which maintain a catalytically-productive orientation of the cofactor, include hydrogen bonds to N1 (the pyridinium nitrogen), O3' (the hydroxyl moiety) and the phosphate group (Eliot and Kirsch, 2004). The residue that interacts with the N1 position of the cofactor plays a central role in modulating the electronic properties of the pyridine ring (Eliot and Kirsch, 2004). In PLP-dependent enzymes of the β-family this residue is a serine, as exemplified by hCBS and *Salmonella typhimurium* *O*-acetylserine sulfhydrylase (stOASS) and

tryptophan synthase (stTrpS) (Burkhard *et al.*, 1998; Hyde *et al.*, 1988; Meier *et al.*, 2001; Taoka *et al.*, 2002). While the residue that interacts with N1 is strongly conserved within each of the fold types of PLP enzymes, greater variability is found at the position that interacts with O3'. For example, crystal structures show that the phenolic group of the PLP cofactor is within hydrogen-bonding distance of a histidine (H217) in *Rhodobacter capsulatus* 5-aminolevulinate synthase (rcALAS) and a tyrosine (Y225) in *Escherichia coli* aspartate aminotransferase (eAATase), which both belong to the large, α-family of PLP-dependent enzymes, an asparagine in hCBS (N149) and stOASS (N71), both members of the β-family, and an arginine (R136) in *Bacillus stearothermophilus* alanine racemase, of the small alanine racemase family (Astner *et al.*, 2005; Burkhard *et al.*, 1998; Christen and Mehta, 2001; Jager, *et al.*, 1994; Meier *et al.*, 2001; Shaw *et al.*, 1997). The specific role of the residue interacting with PLP-O3' depends on the nature of the reaction catalyzed. For example, while Y225 of eAATase lowers the pK_a of the internal aldimine, β-subunit residue Q114 (βQ114) is involved in the partitioning of the reactive aminoacrylate intermediate and allosteric communication in stTrpS (Blumenstein *et al.*, 2007; Goldberg, *et al.*, 1991). The N84A,D,H site-directed variants were constructed to probe the role of this residue in yCBS. The truncated form of yCBS (ytCBS, residues 1-353) was employed to avoid sample heterogeneity caused by cleavage of the labile regulatory domain and to facilitate interpretation of the data in the context of other studies that have investigated the roles of specific active-site residues of ytCBS (Aitken and Kirsch, 2004; Quazi and Aitken, 2009). The histidine and aspartate substitutions of ytCBS-N84 were selected to maintain the potential for polar contacts within the active-site, in contrast with N84A, while modifying the capacity of this residue

to form hydrogen bonds. Characterization of these variants demonstrates that residue N84 is involved in binding of the L-Ser substrate and plays an important role in maintaining a catalytically-productive orientation of the PLP cofactor and partitioning of the reactive aminoacrylate intermediate.

4.3. Materials and Methods

4.3.1. Reagents.

L-Cth [*S*-(2-amino-2-carboxyethyl)-L-homocysteine], β-nicotinamide adenine dinucleotide (NADH, reduced form), N-(1,1-Dimethyl-2-hydroxyethyl)-3-amino-2-hydroxypropanesulfonic acid (AMPSO), N-cyclohexyl-3-aminopropanesulfonic acid (CAPS), N-Tris(hydroxymethyl)methyl-3-aminopropanesulfonic Acid (TAPS), L-Ser and L-Hcys thiolactone were purchased from Sigma. Dithiothreitol (DTT), ampicillin, 5,5'-dithio-bis-(2-nitrobenzoic acid) (DTNB) and imidazole were obtained from Fisher Scientific and L-lactate dehydrogenase (LDH) and protease inhibitor (Complete EDTA-free) tablets were from Roche Diagnostics. Restriction endonucleases and T4 DNA ligase were from New England Biolabs. Nickel-nitrilotriacetic acid (Ni-NTA) resin was from Qiagen. L-Hcys was prepared from the thiolactone according to the method of Kashiwamata and Greenberg, (1970). Cystathionine β-lyase (CBL) was expressed and purified as described previously (Aitken and Kirsch, 2003).

4.3.2. Construction, Expression and Purification of ytCBS variants.

Overlap-extension polymerase chain reaction (PCR), with the pSECseq1 (CGG TTC TGG CAA ATA TTC TGA AAT GAG CTG) and pSECseq7r (GCC CGC CAC CCT CCG GGC CGT TGC TTC GC) flanking primers and either the N84Af (CCT ACT TCT GGT GCG ACC GGT ATC GGT CTA GC), N84Df (CCT ACT TCT GGT GAT ACC GGT ATC GGT CTA GC) or N84Hf (CCT ACT TCT GGT CAT ACC GGT ATC GGT CTA GC) mutagenic primers and their reverse complements, was employed to introduce the N84A, N84D and N84H site-directed mutations in the pTSECb-His

plasmid. This plasmid contains the gene encoding the truncated form of yCBS (ytCBS; residues 1-353), lacking the regulatory domain, and with a C-terminal, 6-His affinity tag (Aitken and Kirsch, 2004). The amplification product was digested with *Bam*HI and *Pst*I, inserted at the corresponding sites of the pT-SECb-His vector and transformed into the *Escherichia coli* strain DH10B (Gibco BRL) *via* electroporation (Gene Pulser, BioRad). The N84A, N84D and N84H site-directed variants were expressed and purified via Ni-NTA affinity chromatography (Qiagen), as previously described for the heterologous expression of 6-His tagged ytCBS (Aitken and Kirsch, 2004).

4.3.3. Steady-State Kinetics.

Enzyme activity was measured in a total volume of 1 mL with a model HP8453 spectrophotometer (Agilent) or in 0.1 mL with a Spectramax model 340 microtiter plate spectrophotometer (Molecular Devices) at 37 °C. The assay buffer was comprised of 50 mM Tris, pH 8.6, and 20 μM PLP. A background rate, for all components except the ytCBS enzyme, was recorded for each sample before initiating the reaction with the addition of ytCBS. Data was fit by nonlinear regression with the program SAS (SAS Institute, Cary, NC). The assay employing cystathionine β-lyase and lactate dehydrogenase (CBL-LDH) as coupling enzymes, in which formation of L-Cth is detected continuously, was employed to monitor the ytCBS β-replacement activity. The LDH and 5,5'-Dithiobis-(2-Nitrobenzoic Acid) (DTNB) assays were employed to monitor the β-elimination of L-Ser, producing pyruvate and NH_3, and the hydrolysis of L-Cth, to L-Ser and L-Hcys, respectively (Aitken and Kirsch, 2004; Aitken and Kirsch, 2003). The k_{catE} and $K_{mE}^{L\text{-}Ser}$ and the k_{catR} and $K_{mR}^{L\text{-}Cth}$ for the β-elimination of L-Ser and

the L-Cth hydrolysis reactions, respectively, were determined from the fit of the data to the Michaelis-Menten equation. The R and E subscripts denote the reverse-physiological L-Cth-hydrolysis and the β-elimination of L-Ser, respectively. The k_{cat}/K_m for each reaction was obtained independently from equation 4.1.

$$\frac{v}{[E]} = \frac{k_{cat}/K_m \times [L-Cth]}{1 + [L-Cth]/K_m} \tag{4.1}$$

The kinetic parameters of the β-replacement reaction of ytCBS-N84A were determined from the fit of the data to equation 4.2, where the F subscript denotes the physiological, β-replacement activity and $F_1^{L\text{-}Hcys}$ = 1 + [L-Hcys]/$K_{1F1}^{L\text{-}Hcys}$ and $F_2^{L\text{-}Hcys}$ = 1 + [L-Hcys]/$K_{1F2}^{L\text{-}Hcys}$ (Jhee *et al.*, 2000b). Equation 4.2 was rearranged by dividing all terms by $K_{mF}^{L\text{-}Ser}$ or $K_{mF}^{L\text{-}Hcys}$ to obtain independent values for $k_{catF}/K_{mF}^{L\text{-}Ser}$ and $k_{catF}/K_{mF}^{L\text{-}Hcys}$, respectively.

$$\frac{v}{[E]} = \frac{k_{catF}[L-Ser][L-Hcys]}{K_{mF}^{L-Hcys}[L-Ser] + K_{mF}^{L-Ser}F_1^{L-Hcys}[L-Hcys] + F_2^{L-Hcys}[L-Ser][L-Hcys]} \tag{4.2}$$

The kinetic parameters for the β-replacement reactions of the N84D and N84H variants were determined from the fit of the data to equation 4.3, which incorporates terms (k_{catE} and $K_{mE}^{L\text{-}Ser}$) for the β-elimination activity observed for these enzymes (Aitken and Kirsch, 2004). The E subscript denotes the non-physiological, β-elimination of L-Ser, to produce pyruvate and ammonia. The values of k_{catE} and $K_{mE}^{L\text{-}Ser}$, determined via the β-elimination assay, were substituted into equation 4.3., thereby reducing the number of kinetic parameters to be determined. Equation 4.3 was rearranged by dividing

all terms by $K_{mF}^{L\text{-}Ser}$ or $K_{mF}^{L\text{-}Hcys}$ to obtain independent values for $k_{catF}/K_{mF}^{L\text{-}Ser}$ and $k_{catF}/K_{mF}^{L\text{-}Hcys}$, respectively.

$$\frac{v}{[E]} = \frac{k_{catE} K_{mF}^{L-Hcys}[L-Ser] + k_{catF}[L-Ser][L-Hcys]}{K_{mE}^{L-Ser} K_{mF}^{L-Hcys} + K_{mF}^{L-Hcys}[L-Ser] + K_{mF}^{L-Ser} F_1^{L-Hcys}[L-Hcys] + F_2^{L-Hcys}[L-Ser][L-Hcys]} \quad (4.3)$$

4.3.4. Fluorescence Spectroscopy.

Fluorescence spectra were acquired with a Cary Eclipse spectrofluorimeter (Varian) at 37 °C in 50 mM Tris, pH 8.6. To investigate the possibility of energy transfer from one or more of the four tryptophan residues of ytCBS to the PLP, a probe of cofactor orientation, the fluorescence spectrum (λ_{ex} = 298 nm) of 20 μM enzyme was recorded from 480-560 nm, with excitation and emission slit widths of 5 nm, in the absence and presence of 50 mM L-Ser (McClure and Cook, 1994). Differences in the efficiency of energy transfer from tryptophan residues to the PLP cofactor have been observed in several PLP-dependent enzymes. For example, Frederiuk and Shafer (1983) and McClure *et al.* (1994), working on D-serine dehydratase and stOASS, respectively, have both suggested that formation of the external aldimine results in a change in the conformation of the cofactor within the active site which increases energy transfer from tryptophan residues of the protein to the PLP cofactor. Therefore, energy transfer from tryptophan residues to the PLP cofactor provides a probe of changes to cofactor orientation for investigations of the role of active-site residues. The apparent dissociation constant for the enzyme-aminoacrylate (E-AA) complex due to L-Ser association with free enzyme ($K_{d(app)}^{L\text{-}Ser}$) was determined by the protocol described by Jhee *et al.* (2000b), where a 1.0 μM solution of ytCBS enzyme was titrated with aliquots of L-Ser, and the

increase in fluorescence at 540 nm (λ_{ex} = 460 nm), due to formation of the aminoacrylate (AA) intermediate, was monitored. The change in fluorescence at 540 nm (ΔF_{max}) was plotted *versus* [L-Ser] and fit to equation 4.4 (Jhee *et al.*, 2000b).

$$\Delta F = \frac{\Delta F_{\max}[L-Ser]}{K_{d(app)}^{L-Ser} + [L-Ser]} \tag{4.4}$$

The method of Adams (1969) was adapted for determination of the PLP saturation of wild-type and variant enzymes. The enzymes were diluted (to 10 μM) in 200 μL of 5mM phosphate buffer, pH 7.4. Following the addition of an equal volume of 11 % trichloroaceteic acid and incubation for 15 min at 50°C, 140 μL of 3.3 M K_2HPO_4 and 50 μL of 0.02 M KCN were added and samples incubated at 50°C for a further 25 min prior to the addition of 70 μL of 28% H_3PO_4 and 640 μL of 2 M potassium acetate, pH 3.8. The PLP concentration of the samples was determined from comparison of the fluorescence intensity at 425 nm (λ_{ex} = 325 nm) to a standard curve of 0-20 μM PLP. The PLP saturation of each enzyme was determined from the ratio of the PLP concentration to the concentration of enzyme monomer.

4.3.5. Absorbance Spectroscopy.

Spectra were recorded from 250-1100 nm with a model HP8453 spectrophotometer (Agilent) at 37 °C. The internal aldimine of wild-type ytCBS and the N84A, N84D and N84H site-directed variants were titrated *versus* pH. The pH of a solution of enzyme in 5 mM TAPS (p*K*a 8.4, pH 7.2), containing 0.5 M KCl, was varied by successive additions of 0.5 M AMPSO (p*K*a 9.0, pH 10.6) below pH 9.0, 0.5 M CAPS (p*K*a 10.4, pH 11.5) between pH 9.0- 10.5 and 1.0 M NaOH above pH 10.5. The enzyme

solution was drawn through a 0.2-μm filter, to reduce light scattering from precipitate, and the pH of the solution was determined prior to each absorbance measurement. The reaction of a 14 μM solution of each of the N84 variants with 0.1-100 mM L-Ser in 50 mM Tris, pH 8.6, was monitored for 120 min to observe the formation of the reaction intermediates.

4.4. Results

4.4.1. Steady state kinetic parameters.

The protein expression levels of the N84A (84 mg/L), N84D (162 mg/L) and N84H (83 mg/L) site-directed variants were comparable to wild-type ytCBS (36 mg/L), demonstrating that the variants adopt a stable, folded conformation. The $k_{catF}/K_{mF}^{L\text{-}Ser}$ of the β-replacement activity is reduced by 230, 11000 and 640-fold, respectively, for ytCBS-N84A, N84D and N84H, compared to the wild-type enzyme (Table 4.1) The subscripts F, E and R in the kinetic parameters listed in Table 4.1 denote the physiological β-replacement reaction, the β-elimination of L-Ser, not catalyzed by the wild-type enzyme, and the reverse-physiological hydrolysis of L-Cth, respectively. The ~2 order-of-magnitude decrease in the $k_{catF}/K_{mF}^{L\text{-}Ser}$ of N84A is the result of an 11-fold increase in $K_{mF}^{L\text{-}Ser}$ and 20-fold decrease in k_{catF}. In contrast, the $K_{mF}^{L\text{-}Hcys}$ value of N84A is only 2-fold greater than the wild-type enzyme (Table 4.1), suggesting that while residue N84 interacts directly or indirectly with L-Ser, the L-Hcys binding site of this variant is unperturbed. The $K_{d(app)}^{L\text{-}Ser}$ of the N84A variant is increased 2-fold, compared to the wild-type enzyme, suggesting an indirect role for N84 in substrate binding (Table 4.1). The k_{catR} of the reverse-physiological L-Cth hydrolysis reaction is reduced 145-fold for both the N84A and N84D variants and 100-fold for N84H. Although the N84D ($k_{catE}/K_{mE}^{L\text{-}Ser}$ = 0.23 ± 0.02 $M^{-1}s^{-1}$) and N84H ($k_{catE}/K_{mE}^{L\text{-}Ser}$ = 0.34 ± 0.06 $M^{-1}s^{-1}$) variants possess a marginal β-elimination activity, the k_{catE} of this reaction is 25 and 1300-fold, respectively, lower than the k_{catF} of the β-replacement reaction. The N84A variant, like the wild-type enzyme, does not catalyze the conversion of L-Ser to pyruvate and ammonia (Table 4.1).

Table 4.1. Steady-state kinetic parameters for ytCBS and the N84A, N84D and N84H variants.[a]

	ytCBS[b]	N84A[c]	N84D[c]	N84H[c]
L-serine + L-homocysteine → L-cystathionine				
k_{catF} (s^{-1})	17 ± 1	0.87 ± 0.09	0.0205 ± 0.0006	1.2 ± 0.1
$K_{mF}^{L\text{-}Ser}$ (mM)	0.7 ± 0.2	8 ± 2	9 ± 1	30 ± 7
$K_{mF}^{L\text{-}Hcys}$ (mM)	0.21 ± 0.04	0.46 ± 0.09	0.08 ± 0.01	0.7 ± 0.1
$k_{catF}/K_{mF}^{L\text{-}Ser}$ ($M^{-1}s^{-1}$)	(2.5 ± 0.6) x 10^4	110 ± 20	2.3 ± 0.3	39 ± 7
$k_{catF}/K_{mF}^{L\text{-}Hcys}$ ($M^{-1}s^{-1}$)	(8 ± 1) x 10^4	1900 ± 200	250 ± 30	1700 ± 100
$K_{iF1}^{L\text{-}Hcys}$ (mM)	1.0 ± 0.4	10 ± 7	8 ± 5	5 ± 2
$K_{iF2}^{L\text{-}Hcys}$ (mM)	15 ± 7	5 ± 1	n.d.	11 ± 4
$K_{d(app)}^{L\text{-}Ser}$ (mM)[d]	15.1 ± 0.6	34 ± 4	n.d.	n.d.
L-serine → pyruvate + NH_3				
$k_{catE}^{L\text{-}Ser}$ (s^{-1})	n.d.	n.d.	0.00082 ± 0.00002	0.00094 ± 0.00004
$K_{mE}^{L\text{-}Ser}$ (mM)	n.d.	n.d.	3.5 ± 0.4	2.7 ± 0.5
$k_{catE}/K_{mE}^{L\text{-}Ser}$ ($M^{-1}s^{-1}$)	n.d.	n.d.	0.23 ± 0.02	0.34 ± 0.06
L-cystathionine → L-homocysteine + L-serine				
k_{catR} (s^{-1})	1.03 ± 0.02	0.0071 ± 0.0002	0.0072 ± 0.0009	0.0104 ± 0.0007
$K_{mR}^{L\text{-}Cth}$ (mM)	0.14 ± 0.01	0.022 ± 0.004	5 ± 1	2.1 ± 0.3
$k_{catR}/K_{mR}^{L\text{-}Cth}$ ($M^{-1}s^{-1}$)	(7.5 ± 0.4) x 10^3	330 ± 50	2.4 ± 0.1	5.0 ± 0.5

[a]Kinetic parameters for the β-replacement, β-elimination and L-Cth hydrolysis activities are denoted by the subscripts F, E and R, respectively. Kinetic measurements were carried out in 50 mM Tris, pH 8.6, containing 20 μM PLP at 37 °C. n.d. denotes that activity was not detectable.
[b]From reference (Aitken and Kirsch, 2004).
[c]β-replacement conditions: 0.4 μM CBL, 1.4 μM LDH, 300 μM NADH, 0.041-11.6 mM L-Hcys, 0.25-180 mM L-Ser, and 7.7 μM N84A, 51-103 μM N84D or 5.1-10.3 μM N84H. Data were fit to eq 4.2 (N84A) and eq 4.3 (N84D and N84H). β-elimination conditions: 1.25 mM NADH, 1.3 μM LDH, 0.1-120 mM L-Ser and 33 μM ytCBS, 15 μM N84A, 46 μM N84D or 23 μM N84H. Hydrolysis of L-Cth to L-Ser and L-Hcys conditions: 2 mM DTNB, 0.01-6.4 mM L-Cth and 15 μM N84A, 46 μM N84D or 23 μM N84H. β-elimination and L-Cth hydrolysis data were fit to the Michaelis-Menten equation and eq 4.1.
[d]$K_{d(app)}^{L\text{-}Ser}$ values were determined by the increase in fluorescence at 540 nm (λex = 460 nm), due to the formation of AA, resulting from a titration of 1.0 μM ytCBS enzyme with aliquots of L-Ser (Jhee *et al.*, 2000b). Data were fit to eq 4.4.

4.4.2. Formation of the aminoacrylate intermediate.

The degree of PLP saturation of the wild-type, N84A, N84D and N84H enzymes is 98%, 73%, 30% and 67%, respectively, demonstrating that binding of the cofactor to the variants is impaired, but not precluded. Comparison of the spectra of the wild-type and N84A variant (Figure 4.1) demonstrates that while the 412-nm peak, corresponding to the ketoenamine tautomer of the PLP cofactor, of N84A is only 53% the intensity of the same peak in the wild-type enzyme, the absorbance of N84A at 330 nm, corresponding to the enolamine tautomer, is 62% greater than the wild-type enzyme. A role for the corresponding N149 of hCBS in maintaining the balance between the ketoenamine and enolamine tautomers has also recently been suggested based on investigation of the Fe^{II}-CO complex of human CBS (Weeks *et al.*, 2009). Weeks *et al.* (2009) proposed that the tautomeric shift observed in hCBS is caused by loss of the hydrogen bond between O3' of the PLP cofactor and the side chain residue N149 due to disruption of a series of interactions resulting from reduction of the heme iron and switching of the C52 axial ligand for CO.

In contrast with the wild-type enzyme and the N84A and N84H variants, formation of the aminoacrylate intermediate, with characteristic peaks at 320 and 460 nm, is not observed for the N84D variant at L-Ser concentrations up to 100 mM and over a period of 2 h (Figure 4.1). The broad, unresolved PLP spectrum of ytCBS-N84D decreases in intensity at ~412 nm, corresponding to the internal aldimine, and increases at ~320 nm upon reaction L-Ser (Figure 4.2). The possibility that the ~320-nm species is indicative of substrate-induced inactivation, previously reported for the Q157H and

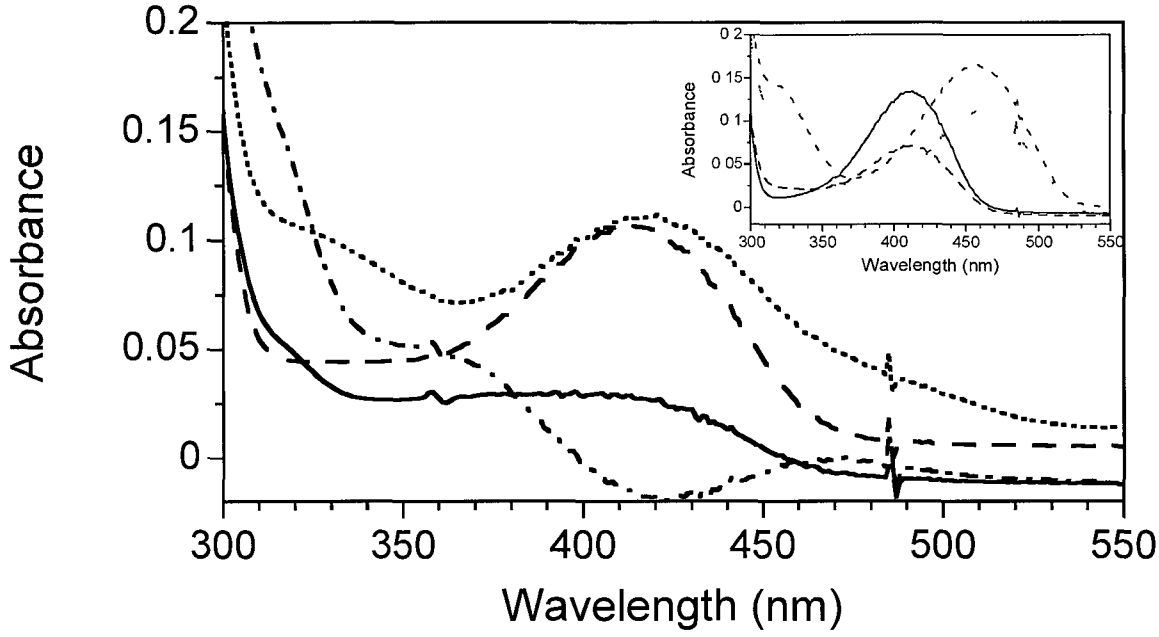

Figure 4.1. Spectra of 14 μM ytCBS-N84D (—) and N84H (- - -) alone and after 2 h incubation with 50 mM L-Ser (- · - · - · N84D; · · · N84H). Inset: wild-type ytCBS (—) and N84A (- - -) alone and after 2 h incubation with 50 mM L-Ser (- · - · - · ytCBS; · · · N84A). Conditions: ytCBS or N84A,D,H variants (14 μM) in 50 mM Tris, pH 8.6 at 37 °C.

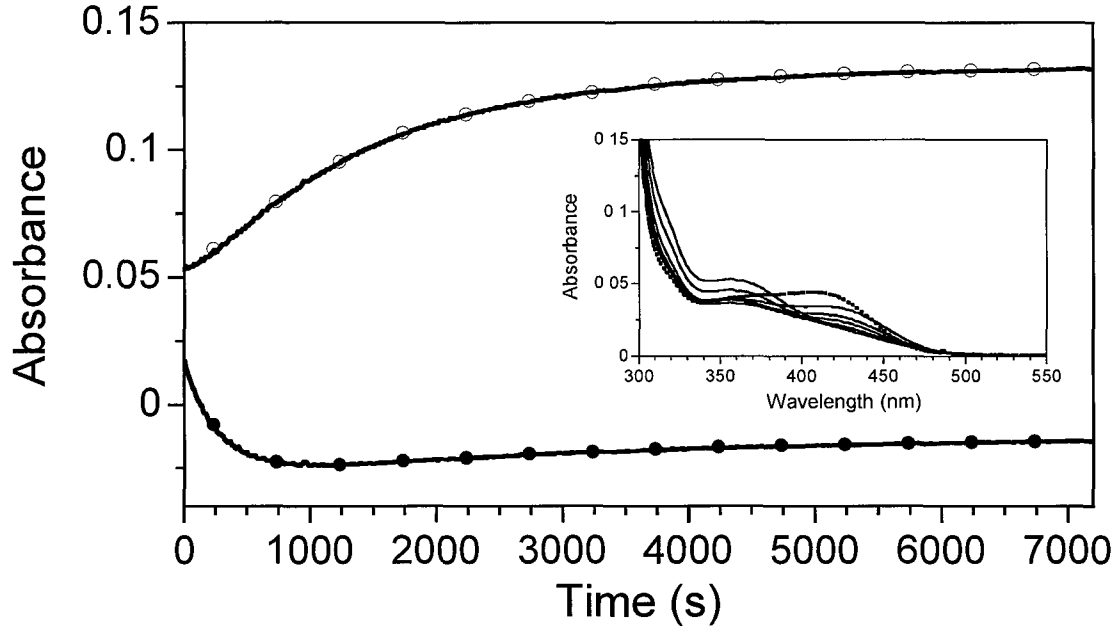

Figure 4.2. The time course of the reaction of N84D with L-Ser. Absorbance was monitored at 320 nm (open circles) and 412 nm (closed circles) following the addition of 50 mM L-Ser to 14 μM N84D. Inset: time-resolved spectra immediately prior to the addition of L-Ser (dotted line) and 0.2, 1, 2, 3.5, 11, and 24 min (solid lines) after the addition of 50 mM L-Ser. Conditions as in Figure 4.1.

Y158F variants of ytCBS, was investigated (Aitken and Kirsch, 2004). Following a 3-h incubation of 20 μM N84D with 50 mM L-Ser, the remaining L-Ser was removed by dialysis in 5 mM Tris, pH 8.6. The spectrum of the enzyme was unchanged by the dialysis step. The pH was subsequently adjusted to 11.5 and an increase in absorbance at 424 nm, resulting from a vinylglyoxylic acid moiety linked to the C4' atom of the cofactor, was recorded (Ahmed *et al.*, 1991; Likos *et al.*, 1982; Ueno *et al.*, 1982). The presence of the diagnostic 424-nm band following alkaline treatment, observed for ytCBS-N84D, but not the wild-type, N84A or N84H enzymes, demonstrates that N84D alone undergoes substrate-mediated inactivation. Addition of 0.1-100 mM L-Ser to the N84A and N84H variants results in a decrease in absorbance at 412 nm and a concomitant increase in intensity at 460 and 320 nm, consistent with formation of the external aldimine of aminoacrylate (Figure 4.1), as observed for the wild-type enzyme (Jhee *et al.*, 2001). The linear increase in intensity at 320 nm, upon reaction of ytCBS-N84H with 50 mM L-Ser (Figure 4.3), not observed for the wild-type and ytCBS-N84A enzymes, is due to the accumulation of pyruvate resulting from the β-elimination activity of this enzyme (Table 4.1). The N84D variant possesses a similar level of β-elimination activity as N84H, but the increase in intensity at 320 nm (Figure 4.2) observed for N84D is also due to the mechanism-based inactivation of this variant. The 460-nm peak observed upon incubation of ytCBS-N84H with 50 mM L-Ser (Figure 4.3) decreased over the course of the 2-h incubation with a concomitant increase in intensity in the 410-420-nm region.

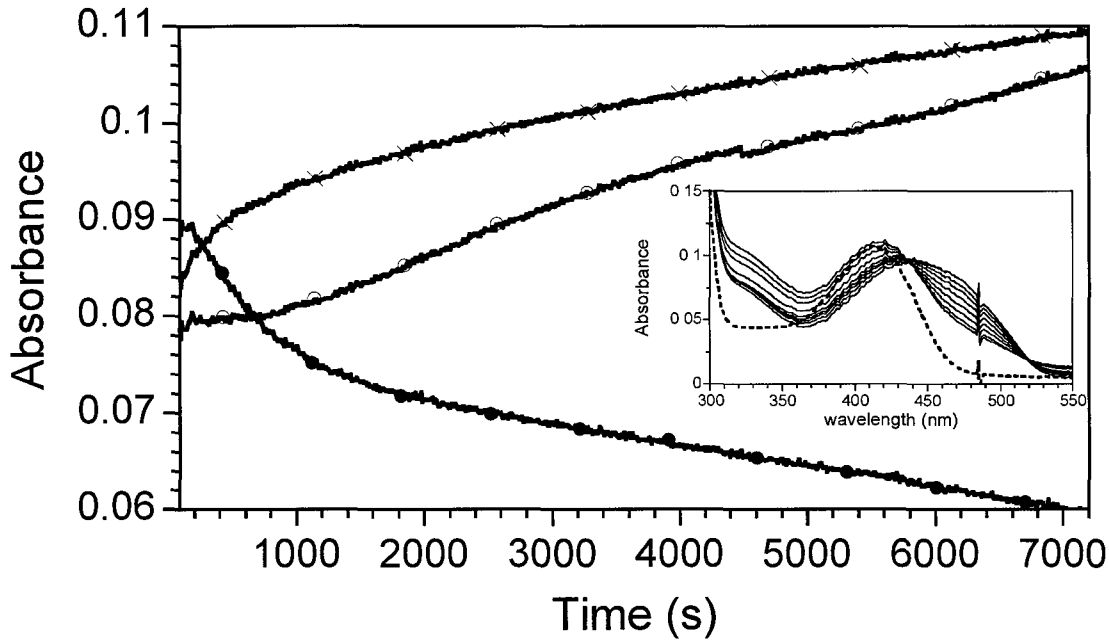

Figure 4.3. The time course of the reaction of N84H with L-Ser. Absorbance was monitored at 320 nm (open circles), 412 nm ( ) and 460 nm (closed circles) following the addition of 50 mM L-Ser to 14 μM N84H. Inset: time-resolved spectra immediately prior to the addition of L-Ser (dotted line) and 0.7, 2.3, 6, 10, 17, 33, 67, 100 and 120 min (solid lines) after the addition of 50 mM L-Ser. Conditions as in Figure 4.1.

4.4.3. Equilibrium spectroscopic studies.

Absorbance spectra of the N84A, N84D and N84H site-directed variants were recorded over the pH range of 7.1-12.5. The pK_a of the Schiff base nitrogen of the internal aldimine of ytCBS, which is >11 for the wild-type enzyme, is unchanged in the N84 variants (Aitken and Kirsch, 2003). Similar results were observed for the alanine and aspartate variants of residue S289, which interacts with N1 of the cofactor, while the corresponding S377D mutation in stTrpS results in a reduction of the pK_a of the internal aldimine to 7.63 ± 0.06 (Quazi and Aitken, 2009; Jhee *et al.*, 1998). The decrease in absorbance at 412 nm, corresponding to the ketoenamine form of the internal aldimine, at pH >11 is concomitant with the appearance of the ~330-nm absorbance of the enolamine form, for the wild-type, N84A (Figure 4.4) and N84H enzymes. In contrast, at elevated pH an increase in absorbance at ~412 nm is observed for ytCBS-N84D (Figure 4.4). The appearance of a similar, ~406-nm absorbance observed at pH ~13 for the Q114N variant of the β-subunit of stTrpS (stTrpS-βQ114N) was shown to be comprised of 390 and 424-nm peaks, corresponding to the enolamine form of the internal aldimine and aminoacrylate-inactivated cofactor, respectively (Blumenstein *et al.*, 2007).

Fluorescence spectra (λ_{ex} = 298 nm and λ_{em} = 460-560 nm) of the wild-type and variant enzymes were recorded in the absence and presence of 50 mM L-Ser (Figure 4.5). Upon excitation at 298 nm, a peak is observed at ~500 nm in the emission spectrum of the wild-type enzyme that is likely the result of Förster energy transfer from tryptophan residue(s) of the enzyme to the PLP cofactor. A similar effect has been observed for stOASS (McClure and Cook, 1994). The ~500-nm peak of the N84A variant is identical to the wild-type enzyme, while that of N84H shows a 67% increase in intensity (Figure 4.5),

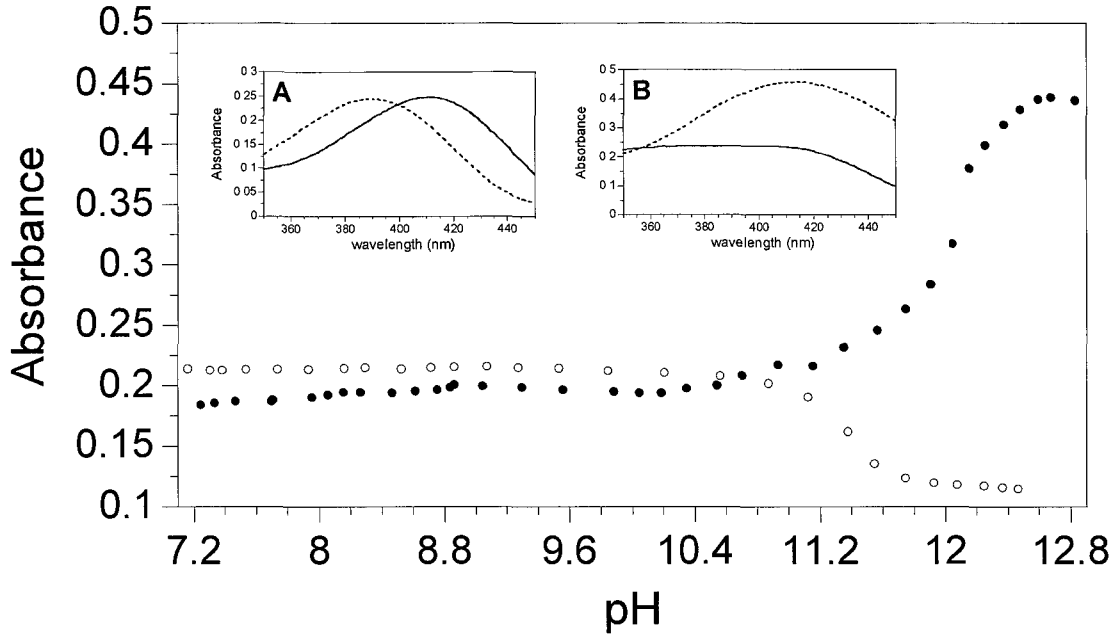

Figure 4.4. Spectrophotometric titration of 35.5 μM ytCBS-N84A (open circles) and N84D (closed circles) versus pH at 425 nm. (Inset A) UV-visible spectra of ytCBS-N84A at pH 7.5 (—) and 12.5 (- - -). (Inset B) UV-visible spectrum of ytCBS-N84D at pH 7.5 (—) and 12.5 (- - -).

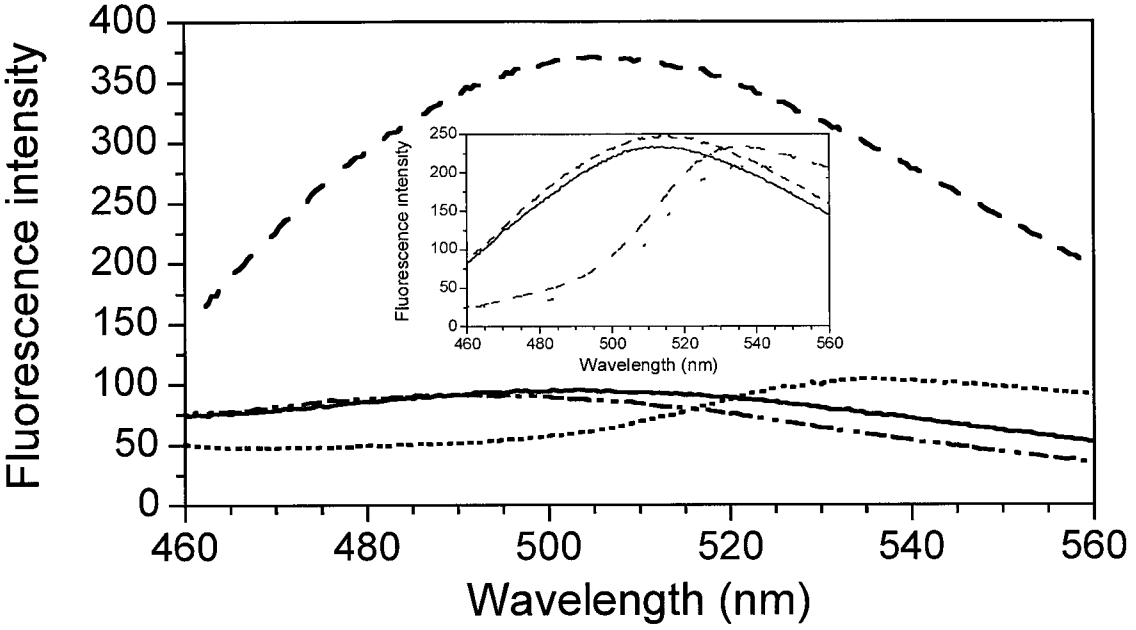

Figure 4.5. Fluorescence spectra (λ_{ex} = 298 nm) of 20 μM ytCBS-N84D (—) and N84H (– – –) alone and in the presence of 50 mM L-Ser (– · – · – · N84D; · · · N84H). Inset: wild-type ytCBS (—) and N84A (– – –) alone and in the presence of 50 mM L-Ser (– · – · – · ytCBS; · · · N84A). Conditions as in Figure 4.1.

suggesting that the orientation of the cofactor is altered by replacement of N84 with histidine. This corresponds to the observed β-elimination activity of ytCBS-N84H, but not N84A. The ~500-nm fluorescence intensity of ytCBS-N84D is 43% of the wild-type enzyme, in agreement with the 30% PLP saturation of this variant. Addition of 50 mM L-Ser to the wild-type and N84A and N84H enzymes results in a shift in the fluorescence emission peak from 500 to 540 nm (Figure 4.5). The ratio of the intensity of the 500 and 540-nm peaks, corresponding to the internal aldimine and the external aldimine of aminoacrylate, respectively, of the wild-type, N84A and N84H enzymes is 0.95, 1.1 and 3.5, respectively, providing further evidence of differences in the orientation of the PLP cofactor within the ytCBS-N84H active site. The shift in fluorescence emission to 540 nm is not observed for the N84D variant, which does not form an observable aminoacrylate intermediate upon reaction with L-Ser (Figures 4.2 and 4.3).

4.5. Discussion

The amino acids that interact with the N1 and O3' positions of PLP regulate the distribution of electrons within the cofactor as well as its position within the active site (Kirsch *et al.*, 1984). An interaction between the pyridinium nitrogen of the cofactor and a conserved aspartate or serine residue is common to PLP enzymes of the α and β-families, respectively (Burkhard *et al.*, 1998; Hyde *et al.*, 1988; Kack, *et al.*, 1999; Meier *et al.*, 2001). In contrast, there is variation in the identity of the amino acid which hydrogen bonds to the phenolic O3' atom. Characterization of the eAATase-Y225F, eAATase-N194A, meALAS-H282A and stTrpS-βQ114N site-directed variants has demonstrated that the specific role of the residue interacting with PLP-O3' is variable and may include modulation of the pK_a of the Schiff base nitrogen, substrate and cofactor binding and maintenance of the equilibrium between the open and closed conformations of the active site (Blumenstein *et al.*, 2007; Goldberg *et al.*, 1991; Turbeville *et al.*, 2007; Yano *et al.*, 1993). Given the diversity of roles proposed and the differences in the interactions observed for hCBS-N149 and stTrpS-βQ114, the ytCBS-N84A,D,H variants were constructed to probe the function of this residue in yCBS.

The catalytic efficiency of ytCBS-N84A is reduced, as demonstrated by the 230 and 145-fold decreases in the $k_{catF}/K_{mF}^{L\text{-}Ser}$ and $k_{catR}/K_{mR}^{L\text{-}Cth}$ of the β-replacement and L-Cth hydrolysis reactions, respectively (Table 4.1). A similar effect is observed for the corresponding meALAS-H282A and eAATase-Y225F variants demonstrating that removal of the hydrogen bond to O3' of the PLP cofactor reduces the catalytic capacity of these enzymes (Turbeville *et al.*, 2007; Goldberg *et al.*, 1991). Turbeville *et al.*, (2007) suggest that the hydrogen bonding network of meALAS-H282, which interacts with PLP-

O3', assists in maintaining a catalytically productive orientation of the cofactor within the active site. While a 20-fold increase in $K_m^{L\text{-}Ser}$ and an 11-fold decrease in k_{cat} are observed for ytCBS-N84A (Table 4.1), no β-elimination or substrate-induced inactivation are detected. Additionally, the fluorescence resonance energy transfer from tryptophan residue(s) to the internal aldimine and the external aldimine of aminoacrylate forms of the cofactor is similar to that of the wild-type enzyme (Figure 4.5). This suggests that, despite the loss of the hydrogen bond to O3' of the cofactor, the orientation of PLP in the internal aldimine and the external aldimine of aminoacrylate, as well as the equilibrium between the open and closed conformations of the active site, of the N84A variant is similar to that of the wild-type enzyme (Figure 4.5). Therefore, while elimination of the hydrogen bond between PLP-O3' and N84 of ytCBS likely alters the movement and orientation of the cofactor during the catalytic cycle, the change is subtle. The observed change in the kinetic parameters of ytCBS-N84A may also be due to repositioning of the backbone of this residue as a result of elimination of the tethering hydrogen bonds of the N84 side chain. This could cause the weakening or loss of the proposed hydrogen bond between the α-carboxylate of the substrate and the backbone NH moiety of N84 (Burkhard *et al.*, 1999).

The histidine and aspartate substitutions of ytCBS-N84 were selected to modify the capacity of this residue to form hydrogen bonds. The 640 and 100-fold reductions in the $k_{catF}/K_{mF}^{L\text{-}Ser}$ and $k_{catR}/K_{mR}^{L\text{-}Cth}$ of the β-replacement and reverse-physiological activities of N84H are similar to those observed for N84A (Table 4.1). However, a change in the orientation of the PLP cofactor within the active site, compared to the wild-type enzyme and ytCBS-N84A, are observed for N84H (Figure 4.5). A marginal β-

elimination activity ($k_{catE}/K_{mE}^{L\text{-}Ser}$ = 0.34 ± 0.06 $M^{-1}s^{-1}$) is also detected for ytCBS-N84H, suggesting a corresponding change in active-site dynamics.

The $k_{catF}/K_{mF}^{L\text{-}Ser}$ and $k_{catR}/K_{mR}^{L\text{-}Cth}$ of N84D are reduced by 3 and 4 orders of magnitude, respectively. This drastic reduction in catalytic efficiency, compared to the wild-type enzyme and the N84A and N84H variants, the 3-fold reduction in PLP-saturation, the lack of accumulation of an aminoacrylate intermediate (Figures 4.2 and 4.3) and the observed inactivation of this variant demonstrate that the cofactor is not bound in a productive orientation and that the equilibrium between the open and closed conformations of the active site is disrupted. The side chain $O_{\delta 1}$ and $N_{\delta 2}$ atoms of hCBS-N149, which corresponds to N84 of yCBS, are 3.24 and 3.28 Å from N380 ($N_{\delta 2}$) (yCBS-S323) and the carboxylate moiety of D376 (yCBS-D319), respectively (Figure 4.6) (Meier *et al.*, 2001). The introduction of a carboxylate group in place of the amide moiety of N84 would disrupt the hydrogen bonding network, linking the mobile loop of residues (T81-S82-G83-N84-T85), which binds the α-carboxylate group of the substrate, with residues D319, R322, S323 and Y324 at the C-terminus of the catalytic domain (Figure 4.6). It is interesting to note that although >100 distinct homocystinuria-associated mutations of hCBS have been reported, only one of these nine residues (G83) corresponds to the site of a disease-linked mutation (hCBS-G148R) (Kraus *et al.*, 1999). A common feature of the ytCBS-N84D and stTrpS-βQ114N variants is that they both undergo mechanism-based inactivation and are purified as a mixture of active and inactivated enzyme, due to reaction with serine during expression or purification (Figure 4.4) (Blumenstein *et al.*, 2007). The partitioning of aminoacrylate between nucleophilic attack on C4' of the PLP cofactor, resulting in inactivation, and the reaction with water to

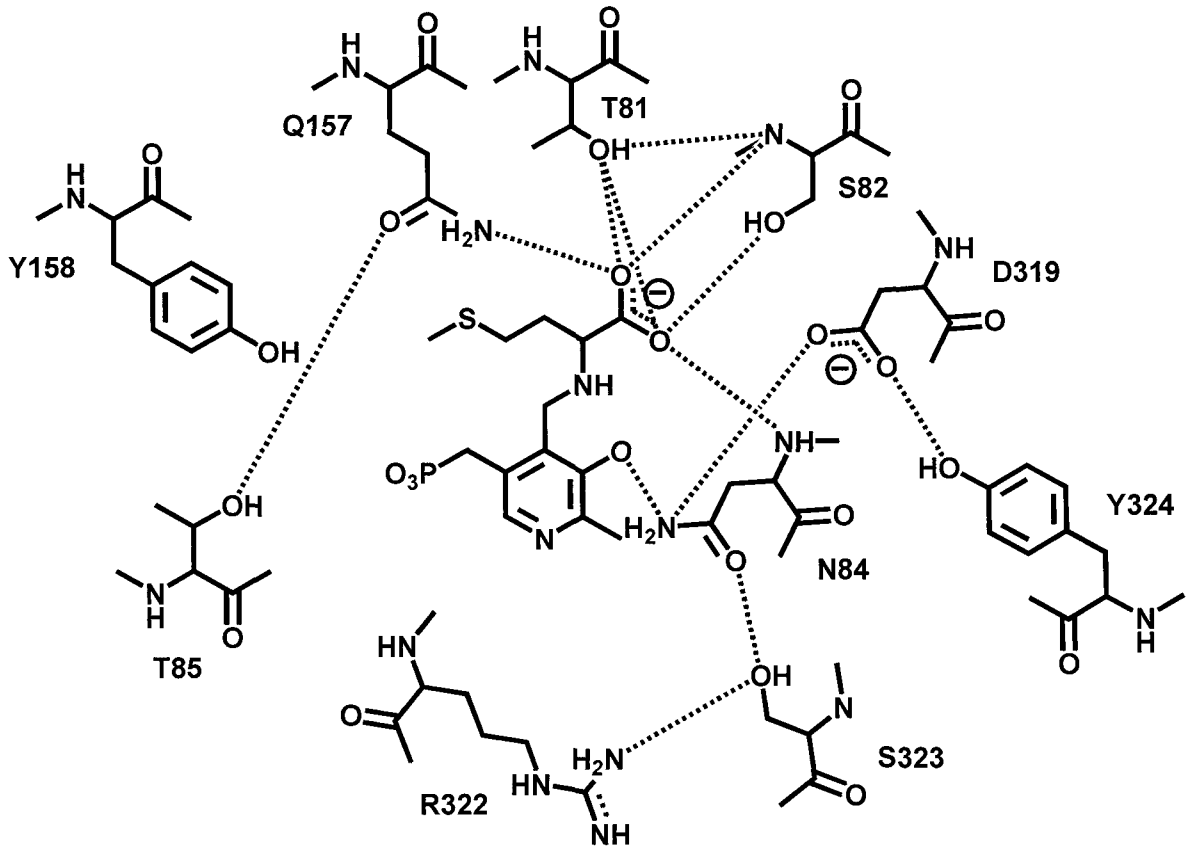

Figure 4.6. Proposed active site contacts in the L-Met external aldimine yCBS complex. The interactions are based on the structures of hCBS and the stOASS-K41A variant complex with L-Met (Burkhard *et al.*, 1999; Meier *et al.*, 2001). The dotted lines represent putative hydrogen bond distances of ≤ 3.3 Å between heteroatoms. Residue labels are those of yCBS.

produce pyruvate and ammonia is dependent on active-site dynamics that enable the release of aminoacrylate (Blumenstein *et al.*, 2007). Although an active-site residue could facilitate the attack of aminoacrylate on the PLP cofactor, this explanation was discounted as an inactivation mechanism for the βQ114N variant of stTrpS because there are no carboxylate residues suitably placed to enable electrostatic catalysis in the active site of this enzyme (Blumenstein *et al.*, 2007). Therefore, the observed inactivation of the stTrpS-βQ114N variant by aminoacrylate is likely due to a change in the equilibrium between the open and closed conformations of the active site, as proposed for the Q157H and Y158F variants of ytCBS (Aitken and Kirsch, 2004). Blumenstein *et al.* (2007) suggest that, although wild-type stTrpS and the βQ114N variant possess a similar level of β-elimination side reaction activity, the variant is uniquely inactivated because it lacks the ability to efficiently release aminoacrylate from the active site (Blumenstein *et al.*, 2007). In contrast with stTrpS-βQ114N, the carboxylate moiety of the aspartate side chain of the ytCBS-N84D variant may stabilize the developing positive charge of the enamine nitrogen during the attack of aminoacrylate on C4' of the PLP cofactor, thereby facilitating the inactivation of the enzyme.

4.6. Conclusion

While a β-elimination activity has been observed for 10 (T81A, S82A, N84D, N84H, T85A, Q157A, Q157E, Q157H, Y158F and S289) of the 20 site-directed variants, targeting 13 active-site residues (Figure 4.6), reported for ytCBS, aminoacrylate-mediated inactivation has been reported for only three (N84D, Q157H and Y158F) (Aitken and Kirsch, 2004; Lodha *et al.*, 2009; Quazi and Aitken, 2009). PLP enzymes catalyzing β-replacement reactions have evolved to facilitate the transaldimination reaction with substrates and products, but not aminoacrylate, thereby minimizing the β-elimination side reaction, which produces pyruvate and ammonia, and inactivation by aminoacrylate. The ability to selectively facilitate the transaldimination of substrates and products and diminish the corresponding reaction with aminoacrylate is likely a function of conformational constraints imposed by the enzyme (Blumenstein *et al.*, 2007). The data presented demonstrate that residue N84 of ytCBS is a determinant of cofactor positioning and of reaction specificity, via its role in the regulation of aminoacrylate partitioning to favor the β-replacement reaction over the release of aminoacrylate, via β-elimination.

Chapter 5. Characterization of Site-Directed Mutants of Residues R58, R59, D116, W340 and R372 in the Active Site of *E. coli* Cystathionine β-Lyase

5.1. Abstract

Cystathionine β-lyase (CBL) catalyzes the hydrolysis of L-cystathionine to produce L-homocysteine, pyruvate and ammonia. A series of active-site variants of *Escherichia coli* CBL (eCBL) was constructed to investigate the roles of residues R58, R59, D116, W340 and R372 in catalysis and inhibition by aminoethoxyvinylglycine (AVG). The effects of these mutations on the $k_{cat}/K_m^{L\text{-}Cth}$ for the β-elimination reaction range from a reduction of only 3-fold for D116A and D116N to 6 orders of magnitude for the R372L and R372A variants. The order of importance of these residues for the hydrolysis of L-Cth is: R372 >> R58 > W340 ≈ R59 > D116. Comparison of the kinetic parameters for L-Cth hydrolysis with those for inhibition of eCBL by AVG demonstrates that residue R58 tethers the distal carboxylate group of the substrate and confirms that residues W340 and R372 interact with the α-carboxylate moiety. The increase in the pK_a of the acidic limb and decrease in the pK_a of the basic limb of the $k_{cat}/K_m^{L\text{-}Cth}$ versus pH profiles of the R58K and R58A variants, respectively, support a role for this residue in modulating the pK_a of an active-site residue.

5.2. Introduction

Cystathionine β-lyase (CBL) catalyses the hydrolysis of L-cystathionine (L-Cth) to produce L-homocysteine (L-Hcys), pyruvate and ammonia. This reaction is the second step in the transsulfuration pathway, which converts L-cysteine (L-Cys) to L-Hcys, the immediate precursor of L-methionine (Figure 5.1). The two enzymes of the transsulfuration pathway, cystathionine γ-synthase (CGS) and CBL, are unique to plants and bacteria (Aitken and Kirsch, 2005). These enzymes are attractive targets for the development of novel anti-microbial compounds, to address the growing challenge of antibiotic resistance by microbial pathogens, because methionine is a precursor for protein biosynthesis as well as thiamine biosynthesis, via the ubiquitous methyl donor *S*-adenosylmethionine, thereby providing a link to DNA replication (Ejim *et al.*, 2007). A detailed study of the mechanism of slow-binding inhibition of eCBL by the β,γ-unsaturated amino acid aminoethoxyvinylglycine (AVG) and the structure of the eCBL-AVG complex were reported by Clausen *et al.*, (1997). This work provides a solid foundation for investigation of the roles of active-site residues and the design of inhibitors, as exemplified by the novel, slow-binding inhibitors of eCBL, with IC_{50} values in the μM and sub-μM range, recently developed by Ejim et al., (2007).

The structures of *Escherichia coli* CBL (eCBL), yeast cystathionine γ-lyase (yCGL), the second enzyme of the reverse transsulfuration pathway of mammals and yeast, and *E. coli* CGS (eCGS) are so similar that the r.m.s. deviation in their least squares superposition is only ~1.5 Å between ~350 C_α atoms of the protein backbone (Clausen *et al.*, 1996; Clausen *et al.*, 1998; Messerschmidt *et al.*, 2003). Therefore, these enzymes provide a useful model system to investigate determinants of specificity, as

differences in their substrate and reaction specificity are likely the result of differences in the placement and mobility of active-site residues (Clausen *et al.*, 1996; Clausen *et al.*, 1998; Messerschmidt *et al.*, 2003).

The active site of the homotetrameric eCBL enzyme is situated at the subunit interface of the catalytic dimer and is comprised of residues from each subunit (Clausen *et al.*, 1996). The crystal structures of eCBL in complex with AVG, N-hydrazinocarbonylmethyl-2-nitrobenzamide and N-hydrazinocarbonylmethyl-2-trifluoro-methylbenzamide provide valuable insight into the active site and mechanism of this enzyme (Figure 5.1) (Clausen *et al.*, 1996; Clausen *et al.*, 1997; Ejim *et al.*, 2007). The α-carboxylate group of AVG interacts with the side chains of W340 and R372 (Figure 5.2) (Clausen *et al.*, 1997). Although AVG lacks the distal carboxylate group of L-Cth, an interaction is observed between R58 and the trifluoromethyl moiety of the N-hydrazinocarbonylmethyl-2-trifluoromethylbenzamide inhibitor designed by Ejim *et al.*, (2007). The side chains of R58 and R59, which approach the bound inhibitor in the eCBL-AVG complex to within 3.6 and 6.7 Å, respectively, have both been proposed to interact with the distal carboxylate group of the L-Cth substrate (Clausen *et al.*, 1996; Clausen *et al.*, 1997; Messerschmidt *et al.*, 2003). A series of site-directed variants of the eCBL active-site residues R58, R59, D116, W340 and R372 was constructed to probe the specific roles of these residues (Figure 5.2). The observed reduction in the activity of the R58A,K, W340F and R372A,K,L site-directed variants and the differences in their kinetic parameters for hydrolysis of L-Cth and inhibition by AVG identify R58, W340 and R372 as residues interacting with the distal and α-carboxylate groups of the L-Cth substrate.

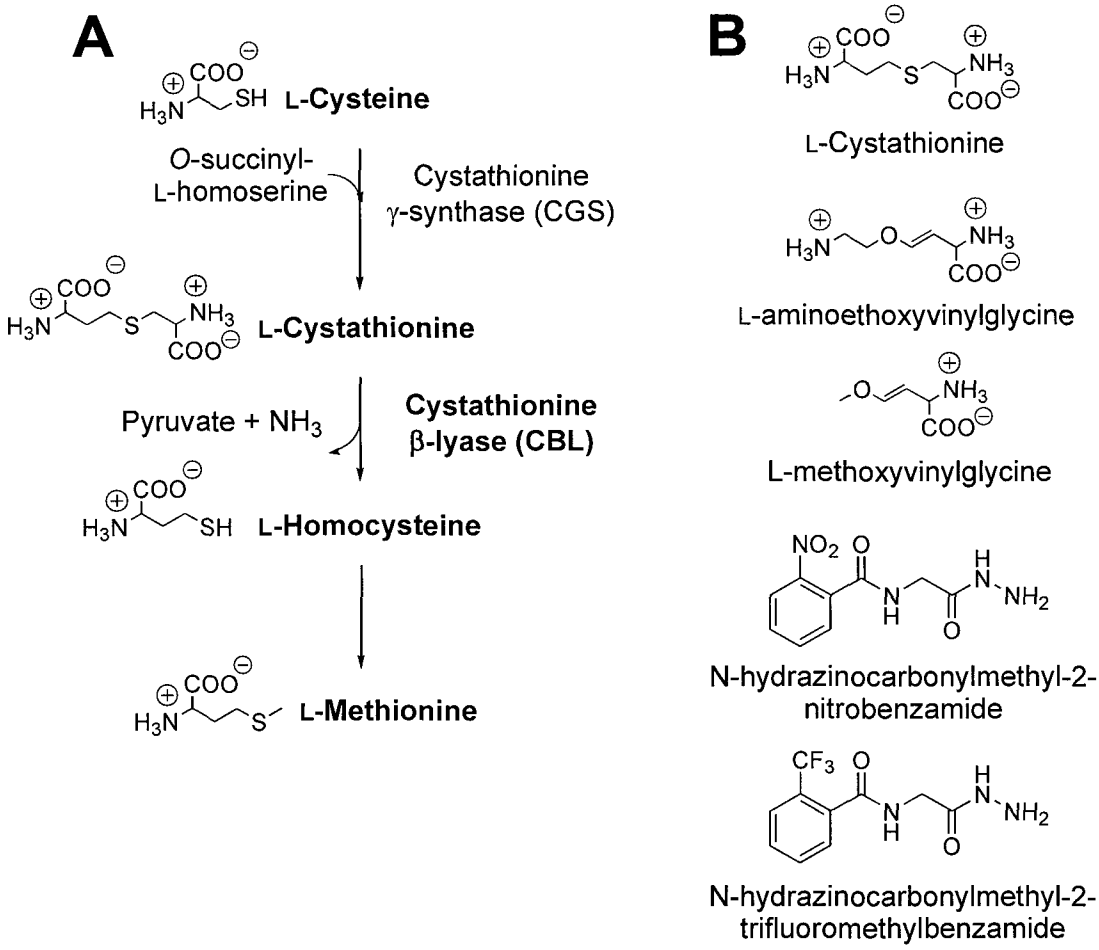

Figure 5.1. (**A**) The enzymes and metabolites of the transsulfuration pathway. (**B**) The structures of the L-Cth substrate and slow-binding inhibitors of eCBL (Clausen *et al.*, 1997; Ejim *et al.*, 2007).

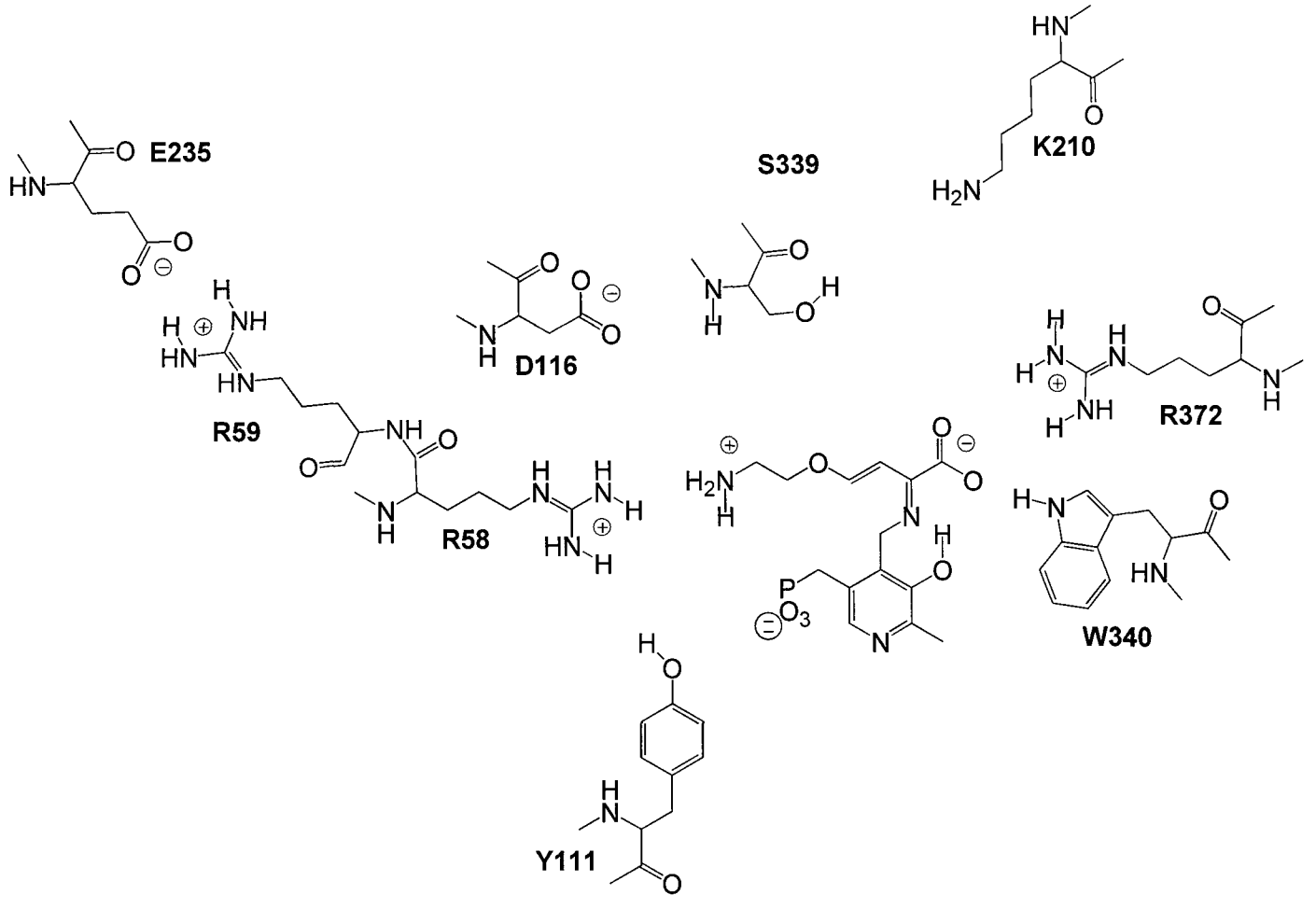

Figure 5.2. Observed contacts of AVG in the active-site of eCBL (Clausen *et al* , 1997). The dotted lines represent putative hydrogen bond distances of ≤ 3.3 Å between heteroatoms. The image was constructed using ChemDraw and PDB entry 1CL2.

5.3. Materials and Methods

5.3.1. Reagents.

L-Cth and L-aminoethoxyvinylglycine (AVG) were purchased from Sigma. Protease inhibitor (Complete, EDTA-free) tablets were obtained from Roche. Ni-NTA resin was a Qiagen product. 5,5'-Dithiobis(2-nitrobenzoic acid) (DTNB) was from Pierce. Oligonucleotide primers were synthesized by Integrated DNA Technologies and mutants were sequenced by DNA Landmarks prior to expression and purification.

5.3.2. Construction, expression and purification of site-directed variants.

Site-directed mutants were constructed by overlap-extension polymerase chain reaction and inserted into the pTrc-99aAF plasmid, which encodes an N-terminal, 6-His tag and linker (Farsi *et al.*, 2009). Farsi *et al.,* demonstrated that the presence of this affinity tag does not alter the kinetic properties of eCBL (Farsi *et al.*, 2009). The *E. coli* KS1000 *metC::cat* strain, in which the gene encoding eCBL is replaced by that of chloramphenicol acetyltransferase, was employed for expression of the site-directed mutants to avoid contamination with the wild-type *E. coli* enzyme (Farsi *et al.*, 2009). The wild-type and site-directed variants of eCBL were expressed and purified as described by Farsi *et al.,* (2009).

5.3.3. Determination of steady-state kinetic parameters.

Enzyme activity was measured in a total volume of 100 μL at 25 °C using a Spectramax 340 microtiter plate spectrophotometer (Molecular Devices). The assay

buffer was comprised of 50 mM Tris, pH 8.5, containing 20 μM PLP, and the hydrolysis of L-Cth (0.01-6.25 mM) was detected (ε_{412} = 13,600 $M^{-1}s^{-1}$) via the reaction of 5,5'-dithiobis-(2-nitrobenzoic acid) (DTNB) with the free thiol of the L-Hcys product (Aitken *et al.*, 2003; Ellman, 1959; Farsi *et al.*, 2009). A background reading was recorded before initiation of the reaction by the addition of eCBL (0.068-6.6 μM, depending on the activity of the particular site-directed variant) for all assays. Values of k_{cat} and $K_m^{L\text{-}Cth}$ for the hydrolysis of L-Cth were obtained by fitting of the data to the Michaelis-Menten equation and $k_{cat}/K_m^{L\text{-}Cth}$ was obtained independently from equation 5.1. Data were fit by nonlinear regression with the SAS software package (SAS Institute, Cary, NC).

$$\frac{v}{[E]} = \frac{k_{cat}/K_m \times [S]}{1 + [S]/K_m} \tag{5.1}$$

5.3.4. Evaluation of the pH dependence of wild-type and site-directed variants of eCBL.

The pH dependence of L-Cth hydrolysis by eCBL was determined using the continuous DTNB assay in a three-component buffer, comprised of 50 mM MOPS (pK_a = 7.2), 50 mM Bicine (pK_a = 8.3) and 50 mM proline (pK_a = 10.7) (Jhee *et al.*, 2000; Peracchi *et al.*, 1996). The kinetic measurements were carried out at pH 6.4-10.6 in the presence of 20 μM PLP, 2 mM DTNB, 0.06-3.0 μM eCBL (depending on the activity of the site-directed variant) and 6.25 mM L-Cth, for specific activity measurements, or 0.01-6.25 mM L-Cth, for the determination of $k_{cat}/K_m^{L\text{-}Cth}$. Specific activity versus pH measurements were performed in quadruplicate to provide an estimate of the experimental error associated with each point in the pH profile. The $k_{cat}/K_m^{L\text{-}Cth}$ versus pH

data were fit to the bell-shaped curve described by equation 5.2, where k_{cat}/K_m^{max} is the upper limit for $k_{cat}/K_m^{L\text{-}Cth}$ at the pH optimum (Aitken *et al.*, 2003).

$$k_{cat}/K_m = \frac{k_{cat}/K_m^{\max}}{1+10^{pK_{a1}-pH}+10^{pH-pK_{a2}}} \tag{5.2}$$

5.3.5. Inhibition of wild-type and site-directed variants of eCBL by AVG.

The IC_{50} values for inhibition of the eCBL enzymes by AVG were determined by measuring enzyme activity between 0.05 μM and 10 mM AVG. The enzyme and inhibitor were mixed and incubated at 25 °C for 10 min in assay buffer. Activity was subsequently measured at a L-Cth substrate concentration of 0.1 mM and the data were fit to equation 5.3 (Ejim *et al.*, 2007). Measurements were performed in quadruplicate for each enzyme. The parameters Act_{max}, Act_{mn}, S and IC_{50} of equation 5.3 correspond to the maximal enzyme activity, the minimal enzyme activity, the slope of the transition between the maximal and minimal activity plateaus and the midpoint of the transition, respectively.

$$Act = \frac{Act_{\max} - Act_{\min}}{1+\left(\frac{I}{IC_{50}}\right)^{S}} + Act_{\min} \tag{5.3}$$

Values for the dissociation constant K_I and the rate constant k_2 for the inhibition of eCBL by AVG were determined as described by Clausen *et al.*, (1997). In this model the enzyme and inhibitor do not form an initial, rapidly reversible enzyme-inhibitor complex (equation 5.4) (Clausen *et al.*, 1997).

$$E \underset{k_2}{\overset{k_1[I] \quad (slow)}{\rightleftharpoons}} EI \tag{5.4}$$

The wild-type eCBL and site-directed variant enzymes were incubated with 1.5 mM L-Cth and 0.005-7.5 mM AVG in assay buffer and the progress of the reactions was monitored for 30 min. Values of k_{obs} were determined from the fit of equation 5.5 to the progress curves. The resulting k_{obs} values were plotted versus inhibitor concentration and values of k_2 and K_i were obtained from fitting of the data to equation 5.6.

$$[P] = v_s t + \frac{(v_o - v_s)\left[1 - \exp^{-k_{obs}t}\right]}{k_{obs}} \tag{5.5}$$

$$k_{obs} = k_2 + \frac{k_2[I]}{K_i\left(1 + {[S]}/{K_m}\right)} \tag{5.6}$$

5.4. Results

All of the site-directed variants were soluble and yields were between 15-41 mg/L, which is comparable to the 56 mg/L reported for the wild-type enzyme (Farsi *et al.*, 2009). The data for the R58K, R372A and R372L variants could not be fit to the Michaelis-Menten equation as saturation kinetics were not observed within the solubility limit of the L-Cth substrate. Therefore, with the assumption that $K_m^{L\text{-}Cth} >>$ [L-Cth], the Michaelis-Menten equation was modified to obtain $k_{cat}/K_m^{L\text{-}Cth}$ values, but not independent estimates of k_{cat} and $K_m^{L\text{-}Cth}$, for these enzymes (Table 5.1). The specific activity versus pH profile of eCBL, and all of the site-directed variants investigated, is bell-shaped. Upon reaction of eCBL with AVG, the 424-nm peak of the internal aldimine form of the PLP cofactor shifts to 341 nm and an isobestic point at 386 nm is observed, as described by Clausen *et al.*, (1997).

5.4.1. The D116A,N and R59A,K variants.

The pH optima of eCBL-D116A and D116N are unchanged and the IC_{50} and K_i values, for inhibition by AVG, and the k_{cat} and $K_m^{L\text{-}Cth}$ values, for L-Cth hydrolysis, of these variants are within ~2-fold and 3-4-fold, respectively, of the wild-type enzyme (Tables 5.1 and 5.2). Similarly, the k_{cat}, IC_{50} and K_i values of R59A are within ~2-fold of the wild-type enzyme, the pH optima is unchanged and the $K_m^{L\text{-}Cth}$ of this variant is increased by only 5.7-fold. In contrast, while the k_{cat} of R59K is within ~2-fold of wild-type eCBL and the pH profile is unchanged, the $K_m^{L\text{-}Cth}$, IC_{50} and K_i values of R59K are increased by 8.4, 29 and 6.3-fold, respectively (Tables 5.1 and 5.2; Figure 5.3).

Table 5.1. Kinetic parameters of eCBL and site-directed variants.[a]

Enzyme	k_{cat} (s^{-1})	$K_m^{L\text{-}Cth}$ (mM)	$k_{cat}/K_m^{L\text{-}Cth}$ ($M^{-1}s^{-1}$)
eCBL	34.1 ± 0.6	0.18 ± 0.01	(1.9 ± 0.1) 10^5
R58A	9.7 ± 0.3	5.1 ± 0.3	(1.92 ± 0.05) 10^3
R58K[b]	n.s.	n.s.	385 ± 1
R59A	45.8 ± 0.4	1.02 ± 0.03	(4.5 ± 0.1) 10^4
R59K	36.7 ± 0.8	1.51 ± 0.09	(2.4 ± 0.1) 10^4
D116A	41.9 ± 0.7	0.67 ± 0.04	(6.2 ± 0.3) 10^4
D116N	37.9 ± 0.4	0.55 ± 0.02	(6.9 ± 0.2) 10^4
W340F	79 ± 1	1.35 ± 0.05	(5.9 ± 0.2) 10^4
R372A[b]	n.s.	n.s.	0.09 ± 0.04
R372K	8.1 ± 0.8	15 ± 2	550 ± 20
R372L[b]	n.s.	n.s	0.23 ± 0.03

[a]Kinetic parameters reported are for hydrolysis of L-Cth. Reaction conditions: 2 mM DTNB, 0.01-6.4 mM L-Cth and 0.068-6.6 μM wild-type or variant eCBL, depending on the activity of the enzyme, in assay buffer at 25 °C. The data were fit to the Michaelis-Menten equation to obtain k_{cat} and $K_m^{L\text{-}Cth}$ and equation 5.1 to obtain $k_{cat}/K_m^{L\text{-}Cth}$.

[b]n.s. indicates that $K_m^{L\text{-}Cth}$ exceeds the solubility limit of the L-Cth, such that $k_{cat}/K_m^{L\text{-}Cth}$ was determined via linear regression.

Table 5.2. Kinetic parameters for inhibition of eCBL and site-directed variants by AVG.

Enzyme	IC_{50} (μM)[a]	K_i (μM)[b]	k_2 (s^{-1})[b]	k_1 (s^{-1})[c]
eCBL	1.7 ± 0.2	1.9 ± 0.6	(5 ± 1) 10^{-4}	263
R58A	1.74 ± 0.08	6 ± 1	(2.0 ± 0.4) 10^{-3}	333
R58K	23 ± 1	55 ± 7	(3.5 ± 0.3) 10^{-3}	64
R59A	1.34 ± 0.05	2.7 ± 0.9	(1.3 ± 0.4) 10^{-3}	481
R59K	4.6 ± 0.3	12 ± 3	(6 ± 1) 10^{-4}	50
D116A	2.6 ± 0.4	3.9 ± 0.9	(4.2 ± 0.9) 10^{-4}	108
D116N	3.3 ± 0.6	2.7 ± 0.8	(2.6 ± 0.8) 10^{-4}	92
W340F	43 ± 6	40 ± 10	(7 ± 2) 10^{-4}	17.5
R372A	n.d.	n.d.	n.d.	
R372K	3500 ± 1400	9100 ± 400	(2.30 ± 0.02) 10^{-3}	0.25
R372L	n.d.	n.d.	n.d.	

[a]Reaction conditions for IC_{50} measurements: Enzyme (0.024-4.3 μM, depending on the activity of the variant) was incubated with 0.05-10^4 μM AVG in assay buffer at 25 °C for 10 min. Activity was subsequently measured (n=4) at a L-Cth substrate concentration of 0.1 mM and the data were fit to equation 5.3 to obtain the IC_{50} value for each enzyme.

[b]Reaction conditions for measurement of K_i and k_2: Wild-type eCBL and site-directed variants were incubated with 1.5 mM L-Cth and 0.005-7.5 mM AVG in assay buffer and the progress of the reactions was monitored for 30 min. The progress curves were fit to equation 5.5 to obtain k_{obs} values, which were plotted versus inhibitor concentration and fit to equation 5.6 to obtain the values of k_2 and K_i.

[c]Values of the rate constant k_1, for the association of eCBL and AVG were calculated using the equation $K_i = k_2/k_1$.

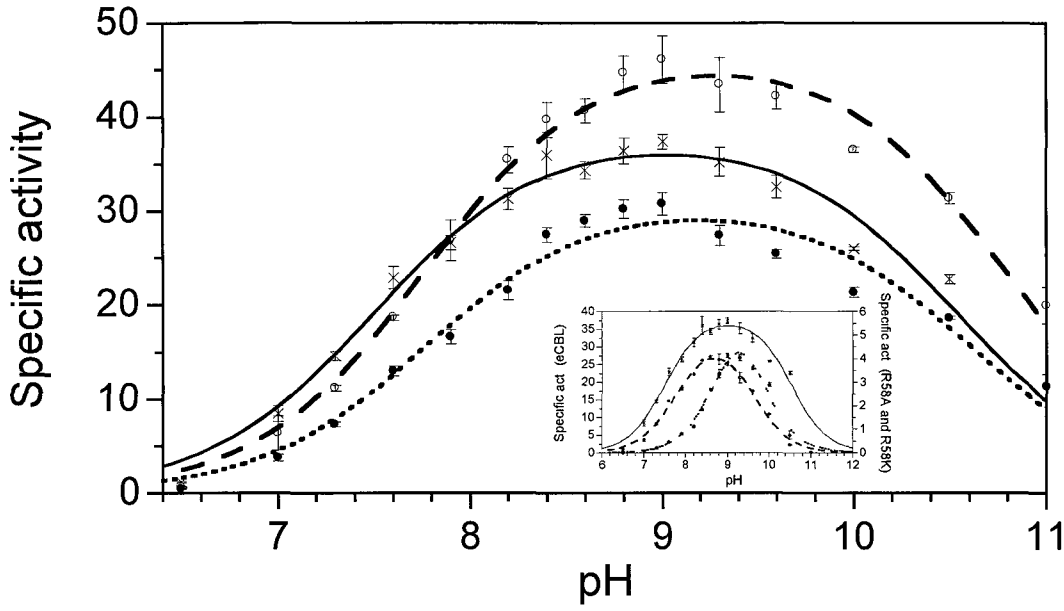

Figure 5.3. The pH dependence of specific activity for the hydrolysis of L-Cth catalyzed by eCBL (×) and the R59A (○) and R59K (●) site-directed variants. Inset: Comparison of the pH dependence of the specific activity of eCBL ( ) , R58A (○) and R58K (●). Reaction conditions: MBP buffer (50 mM MOPS, 50 mM Bicine and 50 mM proline), 20 uM PLP, 2 mM DTNB, 6.25 mM L-Cth and 68 nM eCBL, 0.96 μM R58A, 0.56 μM R58K, 58 nM R59A or 0.13 μM R59K. Measurements were performed in quadruplicate, as represented by the error bars.

5.4.2. The R58A and R58K variants.

The k_{cat} and $K_m^{L\text{-}Cth}$ of R58A are decreased 3.5-fold and increased 28-fold, respectively, and the $k_{cat}/K_m^{L\text{-}Cth}$ of R58K, which could not be saturated within the solubility limit of L-Cth, is increased ~500-fold (Table 5.1). In contrast, the IC_{50} and K_i values of R58A are within 3-fold of those of the wild-type enzyme, while those of R58K are increased by 14 and 29-fold, respectively (Table 5.2, Figure 5.4). Mutation of R58 results in a shift in the basic and the acidic limbs of the specific activity versus pH profiles of R58A and R58K, respectively. The pH optima of the R58A and R58K variants are correspondingly shifted to ~8.5-9 and 9-9.5, respectively, compared to 8.5-9.5 for the wild-type enzyme (Figure 5.3). Therefore, the effect of pH on the $k_{cat}/K_m^{L\text{-}Cth}$ of R58A and R58K, as well as R372K, which has an 345-fold reduction in $k_{cat}/K_m^{L\text{-}Cth}$ at pH 8.5, but an unaltered pH optimum, was determined (Figure 5.5). The values of pK_{a1} and pK_{a2}, corresponding to the acidic and basic limbs of the $k_{cat}/K_m^{L\text{-}Cth}$ versus pH profile, respectively, are presented in Table 5.3 The pK_{a1} values of R58A and R372K and the pK_{a2} values of R58K and R372K are similar to the wild-type enzyme, differing by only 0.01-0.24 pH units beyond the experimental error, confirming the trend observed in the specific activity versus pH profiles of these enzymes. In contrast, the pK_{a1} of R58K is increased 0.66 pH units and pK_{a2} of R58A is decreased by 0.67 pH units, a change of approximately 0.5 pH units beyond the experimental error in both cases (Table 5.3, Figure 5.5).

Table 5.3. Parameters determined from the $k_{cat}/K_m^{L\text{-}Cth}$ versus pH profiles of wild-type eCBL and the R58A, R58K and R372K site-directed variants.[a]

Enzyme	pK_{a1}	pK_{a2}
eCBL	8.28 ± 0.06	10.20 ± 0.06
R58A	7.93 ± 0.08	9.53 ± 0.09
R58K	8.94 ± 0.09	9.8 ± 0.1
R372K	8.44 ± 0.09	9.8 ± 0.1

[a]Kinetic measurements for the eCBL-catalyzed hydrolysis of L-Cth were carried out from pH 6.4-10.6 in MBP buffer containing 0.01-6.25 mM L-Cth, 20 μM PLP, 2 mM DTNB and 0.068-4.5 μM enzyme at 25 °C. The $k_{cat}/K_m^{L\text{-}Cth}$ versus pH data were fitted to equation 5.2 to obtain the values for pK_{a1} and pK_{a2}.

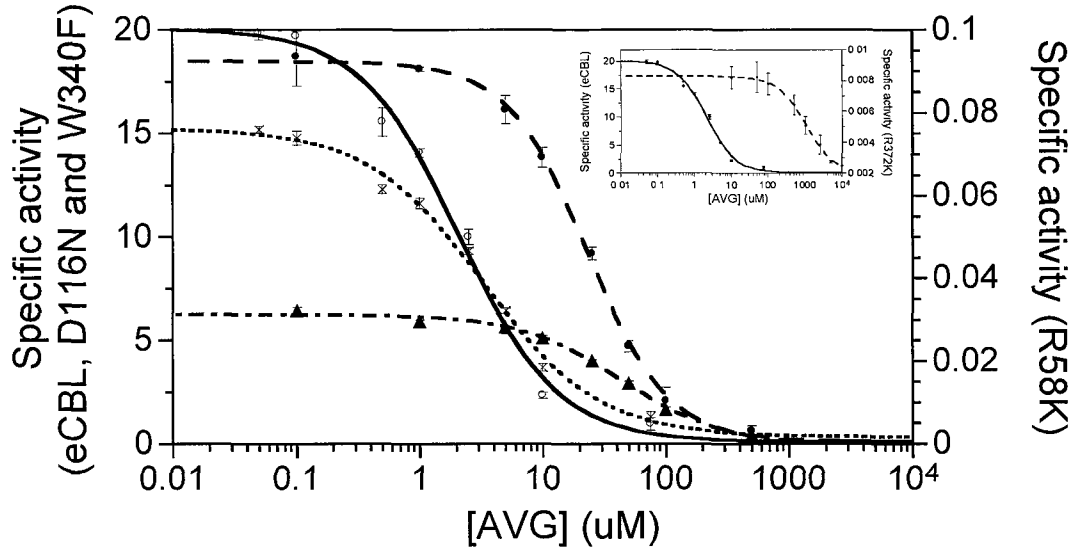

Figure 5.4. The dependence of enzyme activity on AVG concentration for wild-type eCBL (○) and the R58K (●), D116N (×) and W340 (▲) site-directed variants. Inset: Comparison of the effect of AVG inhibitor concentration on the activity of eCBL (○) and the R372K (◊) variant. Reaction conditions: The enzyme (32 nM eCBL, 4.3 μM R58K, 24 nM D116N, 57 nM W340 and 1.9 μM R372K) was mixed with 0.05-10^4 μM AVG in 50 mM Tris, pH 8.5, containing 20 μM PLP, and incubated at 25 °C for 10 min. Activity was subsequently measured in quadruplicate, as represented by the error bars, at a L-Cth substrate concentration of 0.1 mM and the data was fit to equation 5.3 to obtain the IC_{50} value for each enzyme.

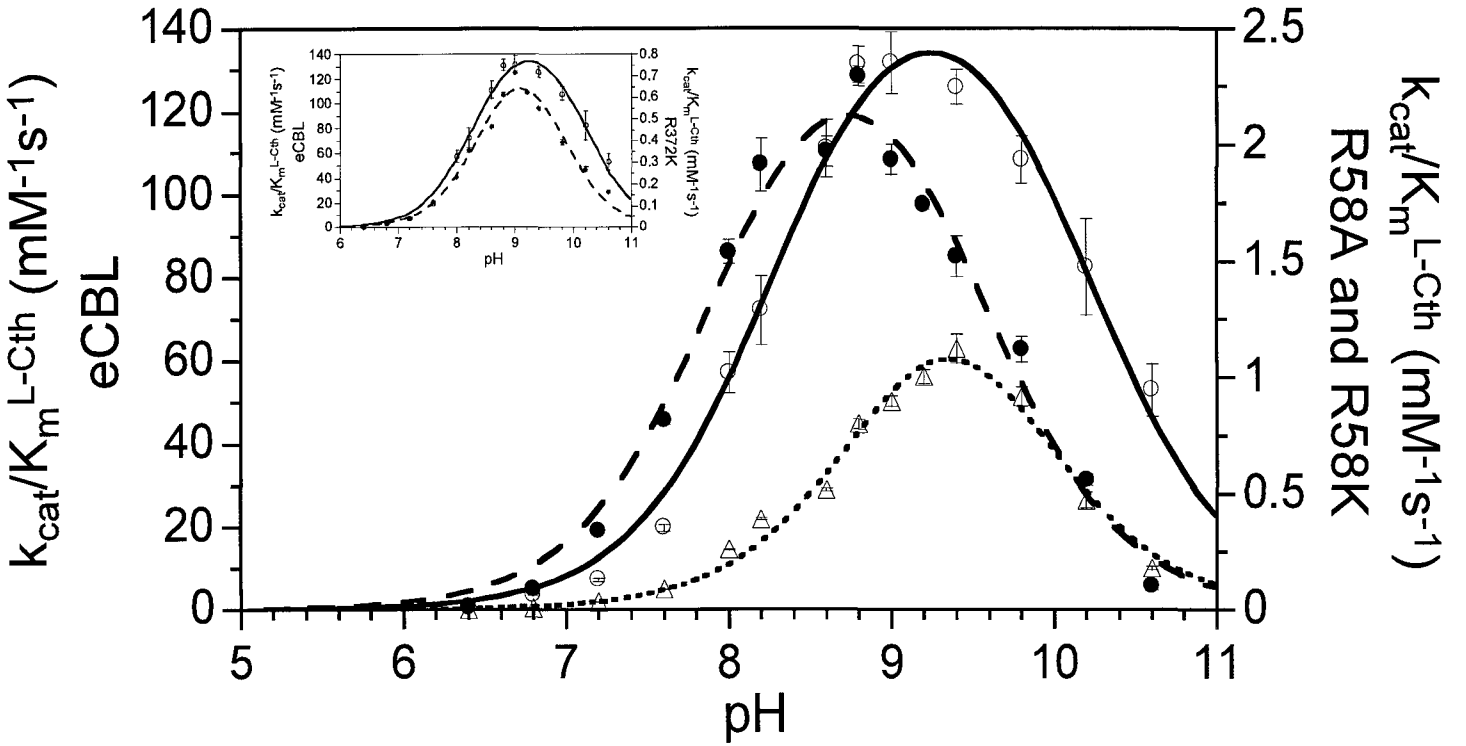

Figure 5.5. The pH dependence of $k_{cat}/K_m^{L\text{-}Cth}$ (mM^{-1}s^{-1}) for the hydrolysis of L-Cth catalyzed by eCBL (○) and the R58A (●) R58K (Δ) site-directed variants. Inset: Comparison of the pH dependence of $k_{cat}/K_m^{L\text{-}Cth}$ (mM^{-1}s^{-1}) for eCBL (○) and the R372K (♦) variant. Reaction conditions: MBP buffer (50 mM MOPS, 50 mM Bicine and 50 mM proline), 20 uM PLP, 2 mM DTNB, 0.01-6.25 mM L-Cth and 0.068-4.5 μM enzyme. The data were fit to equation 5.2.

5.4.3. The W340, R372A, R372L and R372K variants.

The k_{cat} of W340F is within ~2-fold of the wild-type enzyme and the pH profile of this variant is unchanged. In contrast, the $K_m^{L\text{-}Cth}$, for hydrolysis of L-Cth, and the IC_{50} and K_i values, for inhibition by of W340F AVG, are increased by 10, 25 and 21-fold, respectively (Tables 5.1 and 5.2, Figure 5.4). The k_{cat} and $K_m^{L\text{-}Cth}$ of R372K are decreased 4.2-fold and increased 83-fold, respectively, and the $k_{cat}/K_m^{L\text{-}Cth}$ of R372A and R372L, which could not be saturated within the solubility limit of L-Cth, 2.1 10^6 and 8.3 10^5-fold, respectively (Table 5.1). The pH optimum of ~8-9.5 of the R372K variant is similar to that of the wild-type enzyme. The low activity of R372A and R372L precluded the investigation of their activity as a function of pH as well as the reliable determination of inhibition parameters for these enzymes. The increases of 2100 and 4800-fold in IC_{50} and K_i, respectively, observed for R372K are the most drastic of the 10 variants investigated (Table 5.2 and Figure 5.4). Values of the rate constant k_1 for association of eCBL and AVG, calculated using the equation $K_i = k_2/k_1$, are within 5-fold of the wild-type enzyme, with the exception of the 15 and ~1000-fold increases in this parameter observed for the W340F and R372K variants (Table 5.2). Both of these mutations modify residues observed to interact with the α-carboxylate moiety of the inhibitor in the eCBL-AVG complex (Clausen *et al.*, 1997).

5.5. Discussion

The identity, position and flexibility of active-site residues are key determinants of both the substrate and reaction specificity of enzymes. This is particularly true of enzymes dependent on the catalytically versatile PLP cofactor. For example, the effect of a single conservative modification on reaction specificity is demonstrated by the β-elimination activity, not observed for the wild-type enzyme, of the T81A, S82A, T85A, Q157A,E,H, Y158F and S289A variants of yeast cystathionine β-synthase and the increased racemase and β-decarboxylase activities of the R292K variant of *E. coli* aspartate aminotransferase (eAATase), the archetypical PLP-dependent enzyme (Aitken and Kirsch, 2004; Quazi and Aitken, 2009; Vacca *et al.*, 1997). The γ-subfamily of fold-type I of PLP-dependent enzymes, including eCBL, eCGS and yCGL, provides a useful model system for the investigation of substrate and reaction specificity, as the overall structures and many active-site residues are conserved in these enzymes (Clausen *et al.*, 1996; Clausen *et al.*, 1998; Messerschmidt *et al.*, 2003). The characterization of a series of site-directed variants of five eCBL active-site residues (R58, R59, D116, W340 and R372) is the focus of the current study.

Clausen *et al.* have suggested, based on the structure of the eCBL-AVG complex, that the partitioning of bound substrate, or reactive intermediates, underlying reaction specificity, is related to the freedom of rotation about the Cα-Cβ bond of the substrate in the enzymes of the γ-subfamily (Clausen *et al.*, 1997). For example, methoxyvinylglycine (MVG) acts as either a substrate or an irreversible inhibitor of PLP-dependent enzymes, depending on the nature of the active site (Figure 5.1) (Clausen *et al.*, 1997; Miles, 1975; Rando, 1974; Rando *et al.*, 1976). Comparison of the reaction eCBL with L-Cth, MVG

and AVG demonstrates that the differing ability of active-site residues to form hydrogen bonds, tethering the distal portion of these molecules, has an important effect on the ability of the enzyme to catalyze their transformation. The distal methoxy group of MVG lacks the hydrogen bonding ability of AVG and L-Cth (Figure 5.1) and is predicted to have a correspondingly greater degree of mobility and rotational freedom within the active site. As a result, MVG is deaminated by eCBL (Clausen *et al.*, 1997). In contrast, AVG is a slow-binding inhibitor of eCBL because the distal amino moiety of AVG enables it to hydrogen bond to the side chain hydroxyl group of Y111, thereby adopting a conformation which results in the slowly-reversible formation of a ketimine intermediate (Figures 5.1 and 5.2) (Clausen *et al.*, 1997). The L-Cth substrate of eCBL possesses both distal amino and carboxylate groups (Figure 5.1) and is efficiently hydrolyzed to L-homocysteine and iminopropionate, *via* a β-elimination reaction, which does not include the ketimine intermediate observed upon reaction of eCBL with AVG.

5.5.1. Residue D116.

The structure of the eCBL-AVG complex provides a useful guide for the selection of residues to probe their role in binding of the L-Cth substrate (Figure 5.2) (Clausen *et al.*, 1997). However, the double bond of the β,γ-unsaturated inhibitor is not present in L-Cth and AVG does not possess the sulfur atom at the γ-position or the distal carboxylate group of the substrate (Figure 5.1). The ~2-fold greater B-factor of the distal portion of AVG, compared to the Cα region, demonstrates the relative mobility of this part of the inhibitor in the active site (Clausen *et al.*, 1997). Therefore, the binding mode observed for the distal portion of AVG may not be representative of the eCBL substrate (Figure

5.2) (Clausen *et al.*, 1997). Residue D116 is conserved as an aspartate in bacterial CBL sequences and as an arginine residue in bacterial CGS and eukaryotic CGL. An interaction between the corresponding R106 of eCGS and its *O*-succinyl-L-homoserine (L-OSHS) substrate was observed in docking studies, prior to energy minimization (Clausen *et al.*, 1998). The side chain of D116 is 8.3 Å from the distal amino group of the inhibitor in the eCBL-AVG complex (Figure 5.2). This residue was replaced with alanine and asparagine to investigate the possibility that a conformational change in the active site, upon binding of L-Cth, could bring D116 into contact with the distal portion of the substrate. However, in agreement with the structure of the eCBL-AVG complex, the 3-4-fold increases in the $K_m^{L\text{-}Cth}$ and the ≤2-fold increases in the IC_{50} and K_i values of the D116A,N variants demonstrates that this residue is not involved in binding AVG or the distal amino group of L-Cth (Tables 5.1 and 5.2) (Clausen *et al.*, 1997).

5.5.2. Residue W340.

The side chain nitrogen of W340 forms a hydrogen bond with the α-carboxylate group of both the trifluoroalanine and AVG inhibitors, but does not interact with the corresponding carbonyl group of N-hydrazinocarbonylmethyl-2-trifluoromethyl-benzamide (Figures 5.1 and 5.2) (Clausen *et al.*, 1996; Clausen *et al.*, 1997; Ejim *et al.*, 2007). Residue W340 is conserved in γ-proteobacterial CBL, but is replaced by a leucine residue in CGL from fungi and higher eurkaryotes. The 10-fold increase in $K_m^{L\text{-}Cth}$ and the 25 and 21-fold increases in IC_{50} and K_i for inhibition of eCBL-W340F by AVG support the proposed role for this residue in binding to the α-carboxylate groups of L-Cth and AVG (Tables 5.1 and 5.2) (Clausen *et al.*, 1997).

5.5.3. The role of arginine residues in the active-site of eCBL.

The three arginine residues in the eCBL active site were mutated in this study with the goal of probing the role of each in the binding of L-Cth. The α-carboxylate groups of AVG and trifluoroalanine, in the active sites of the eCBL-inhibitor complexes, both form a pair of hydrogen bonds to the side chain of R372 (Figure 5.2) (Clausen *et al.*, 1996; Clausen *et al.*, 1997). The low B-factor (~15 Å (Ejim *et al.*, 2007)) of the α-carboxylate group of the inhibitor in the eCBL-AVG complex is a result of the interaction with R372, as well as with the backbone amide nitrogen of S339 and the side chain of W340 (Clausen *et al.*, 1997). The 83-fold increase in the $K_m^{L\text{-}Cth}$ of R372K, the 2.1×10^6 and 8.3×10^5-fold increases in the $k_{cat}/K_m^{L\text{-}Cth}$ of the alanine and leucine substitution variants of R372 (Table 5.1), respectively, and the three order of magnitude increases in the IC_{50} and K_i values for inhibition of eCBL-R372K by AVG (Table 5.2) demonstrate the importance of this residue (Figure 5.2). The additional hydrogen bonds, and ~1 Å greater length, of the native arginine residue at position R372 of eCBL is expected to contribute to the two and three order of magnitude lower $K_m^{L\text{-}Cth}$ and K_i for AVG, respectively, of the native enzyme, compared to the R372K variant. The order of magnitude difference between these parameters is likely due to the distal carboxylate moiety of the substrate, which is lacking in AVG. The tyrosine, phenylalanine, alanine and lysine substitution variants of the corresponding R386 of eAATase also cause a reduction of at least three orders of magnitude in k_{cat}/K_m, demonstrating that replacement with lysine resulted in a similar effect as other non-conservative replacements (Danishefsky *et al.*, 1991; Graber *et al.*, 1995; Vacca *et al.*, 1997). Despite the lack of sequence similarity between AATase and CBL, the two enzymes share the common

catalytic core of fold-type I PLP-dependent enzymes as well as several active-site features (Clausen *et al.*, 1996). The 4-fold decrease in the k_{cat} of CBL-R372K contrasts with the 55-fold decrease in this parameter reported for AATase-R386K (Inoue *et al.*, 1989; Vacca *et al.*, 1997). Vacca *et al.*, proposed that the observed loss of activity of the R386K variant reflects differences in the binding orientation and conformation of the substrates, such that they are not optimally positioned for catalysis (Vacca *et al.*, 1997). Therefore, the 14-fold smaller decrease in the k_{cat} of eCBL-R372K likely reflects differences in the nature of the reactions catalyzed by these enzymes, as the hydrolysis of L-Cth is a facile reaction that, in contrast with the transamination of eAATase, does not require the generation of a ketimine intermediate or the binding of a second substrate.

Residues R58 and R59 have been alternatively proposed to interact with the distal carboxylate moiety of L-Cth by Messerschmidt *et al.*, (2003) and Clausen *et al.*, (1996), respectively. The corresponding residues of eCGS (L-OSHS + L-Cys → L-Cth) and yCGL (L-Cth → L-Cys + α-ketobutyrate + NH_3) are R48/R49 and R52/S53, respectively. Based on docking studies in the eCGS active site, the distal carboxylate group of L-OSHS and the α-carboxylate of L-Cys are proposed to interact with R48 and R49, respectively (Clausen *et al.*, 1998). Clausen *et al.*, observed that the salt bridge between E235 and R59 of eCBL is similar to that between eAATase residues D15 and R292, which also interacts with the distal carboxylate of anionic substrates, and proposed that eCBL-R59 could alternatively form an ion pair with E235 in the free enzyme and with the distal carboxylate group of L-Cth, upon substrate binding (Clausen *et al.*, 1996; Kirsch *et al.*, 1984). However, docking of L-Cth to the active site of eCBL has indicated that the distal carboxylate group of the substrate interacts with R58 (Messerschmidt *et al.*, 2003).

Comparison of the kinetic parameters obtained in this study for hydrolysis of the L-Cth substrate and inhibition by the AVG inhibitor, which lacks the distal carboxylate moiety of L-Cth (Figure 5.1), provides insight into the roles of R58 and R59. While the $K_m^{L\text{-}Cth}$ is increased 5.7 and 8.4-fold by mutation of R59 to alanine or lysine, a 28-fold increase in this parameter is observed for R58A and R58K could not be saturated within the solubility limit of L-Cth. In contrast, the K_i values for inhibition of R58A, R58K, R59A and R59K by AVG, were increased by only 3.2, 29, 1.4 and 6.3-fold respectively (Table 5.2). The similar changes, of less than one order of magnitude, in the $K_m^{L\text{-}Cth}$ and K_i values of R59A and R59K demonstrate that this amino acid is not directly involved in binding L-Cth and AVG. The observed minor effects on the kinetic parameters of these variants are likely due to loss of the R59-E235 interaction and the resulting alteration in active-site conformation. In contrast, the effect of the alanine and lysine substitutions of R58 on the hydrolysis of L-Cth is much greater than their effect on inhibition by AVG, demonstrating that it is R58 that interacts with the distal carboxylate of the substrate. Residue R58 also interacts with both the phosphate group of the PLP cofactor and the side chain hydroxyl of Y111 in the eCBL active site (Figure 5.2) (Clausen *et al.*, 1996). In the structure of the eAATase-methylaspartate complex the corresponding R292 forms two hydrogen bonds each with the side chain of D15 and the distal carboxylate group of the substrate analog. Tethering of the eCBL-R58 side chain by the phosphate group of PLP, similar to the R292-D15 interaction of eAATase, may provide rigidity to eCBL-R58 to enable the precise positioning of the distal portion of substrate. The role of arginine residues in the binding of anionic substrates, particularly carboxylate groups, has been observed in a wide range of enzymes (Hwang and Warshel, 1988; Kirsch *et al.*, 1984;

Mitchell *et al.*, 1992; Riordan *et al.*, 1977; Vacca *et al.*, 1997). As a result of the ~1-Å difference in the length of the lysine side chain and its inability to fulfill the number of hydrogen-bonding interactions formed by arginine, the ε-amino group of the R58K side chain cannot interact with both the phosphate moiety of the cofactor and the distal carboxylate group of the substrate in the same manner as R58. The 29-fold increase in the K_i for inhibition of R58K by AVG, which lacks a distal carboxylate group, may reflect a weakening in the interaction between Y111 and the distal amino group of AVG in the context of the R58K mutation.

Residue R58 may also be involved in modulating the nucleophilic character of an active-site residue, such as Y111, which forms a π-stacking interaction with the pyridine ring of the cofactor and has been proposed to abstract a proton from the α-amino group of L-Cth and donate a proton to aminoacrylate (Clausen *et al.*, 1996). The observed interaction between R58 with Y111 (Figure 5.2) may lower the pK_a of the latter, such that the side chain of Y111 exists as a phenolate ion in the pH 8.5-9.5 range, which is pH optimum of eCBL (Figure 5.3) (Dwivedi *et al.*, 1982a; Farsi *et al.*, 2009). Clausen *et al.*, have suggested that conformational changes in the active site, resulting from substrate binding, would be expected to increase the hydrophobicity of the active-site environment and weaken the R58-Y111 interaction (Clausen *et al.*, 1996; Clausen *et al.*, 1998). This would result in an increase in the pK_a of Y111, thereby facilitating a role for Y111 in proton transfer from the α-amino group of the L-Cth substrate, during transaldimination, to aminoacrylate to facilitate the release of the iminopropionate product. Correspondingly, a shift in the specific activity versus pH profiles was observed only for the R58A and R58K variants (Figure 5.3). Vacca *et al.*, reported a similar narrowing of

the specific activity versus pH profile for the corresponding R292K variant of eAATase, but not for R386K (eCBL-R372K), and proposed that the change may be due to deprotonation of K292, as the pK_a of lysine is lower than that of arginine (Vacca *et al.*, 1997). However, a similar mechanism is unlikely in the case of the eCBL-R58K variant, unless the interaction of R58 with the phosphate moiety of the PLP cofactor, is weakened or not formed in the R58K enzyme (Figure 5.2). The $k_{cat}/K_m^{L\text{-}Cth}$ versus pH profiles of R58A and R58K are also both narrower than that of the wild-type enzyme. The value of pK_{a2}, of the basic limb, of R58A is decreased by 0.66 pH units and pK_{a1}, of the acidic limb, of R58K is increased by 0.67 pH units (Figure 5.5, Table 5.3). The pK_a of the basic limb of the $k_{cat}/K_m^{L\text{-}Cth}$ versus pH profile of eCBL may correspond to the substrate, as it is within 0.6 pH units of the pK_a of 9.63 determined for one of the amino groups of L-Cth (Aitken and Kirsch, 2003). The observed increase in the pK_a of the acidic limb of the R58K variant may be due to the decreased ability of a lysine in this position to modulate the pK_a of Y111 to the same extent as R58 in the wild-type enzyme, as the ε-amino group of this residue cannot fulfill all of the hydrogen bonding interactions observed (phosphate moiety of the cofactor and side chain of Y111) and proposed (distal carboxylate group of L-Cth) for residue R58. However, the increase in pK_{a1} and decrease pK_{a2} observed for R58K and R58A, respectively, are distinct to the each variant, suggesting that the observed pK_a shifts may be an indirect effect resulting from a change in the conformation or charge distribution of the active site.

5.6. Conclusion

The CBL enzyme, which is unique to plants and bacteria, is an attractive target for the development of novel antimicrobial compounds because it is linked to a variety of cellular processes, including DNA replication, via the ubiquitous methyl donor *S*-adenosylmethionine. This study has identified R58, W340 and R372 as residues interacting with the distal and α-carboxylate groups, respectively, of the L-Cth substrate, information that will guide the design of inhibitors of this enzyme. For example, the addition of a distal carboxylate moiety to AVG would allow this compound to form a pair of hydrogen bonds with residue R58 in the active site of eCBL.

Chapter 6. Characterization of the Side-Chain Hydroxyl Moieties of Residues Y56, Y111, Y238, Y338 and S339 as Determinants of Specificity in *E. coli* Cystathionine β-Lyase.

6.1. Abstract

Cystathionine β-lyase (CBL) catalyzes the hydrolysis of L-cystathionine to produce L-homocysteine, pyruvate and ammonia. A series of site-directed variants of *Escherichia coli* CBL (eCBL) was constructed to investigate the roles of the hydroxyl moieties of active-site residues Y56, Y111, Y238, Y338 and S339 as determinants of specificity. The effect of the conservative phenylalanine and alanine substitutions on the $k_{cat}/K_m^{L\text{-}Cth}$ for the α,β-elimination of L-Cth ranges from a change of only 1.1-fold for Y338F to a reduction of three orders of magnitude for the alanine replacement variant of S339, which acts as a determinant of reaction specificity by tethering the catalytic base. Comparison of the kinetic parameters for L-Cth hydrolysis with those for inhibition of eCBL by aminoethoxyvinylglycine (AVG) indicates that Y238 interacts with the distal carboxylate group of the substrate. The 22 and 50-fold increases in the $K_m^{L\text{-}Cth}$ and K_i^{AVG} resulting from replacement of Y56 with phenylalanine suggest that this residue may interact with the distal amino group of these compounds, although an indirect role in binding is more likely. The near-native $k_{cat}/K_m^{L\text{-}Cth}$ and pH profile of eCBL-Y111F, demonstrate that residue Y111 does not play a role in proton transfer.

6.2. Introduction

The transsulfuration pathway converts L-cysteine (L-Cys), synthesized *de novo* by bacteria and plants, to L-homocysteine (L-Hcys), the precursor of L-methionine (L-Met). The L-cystathionine (L-Cth) product of cystathionine γ-synthase (CGS) is cleaved by cystathionine β-lyase (CBL), the second enzyme of the transsulfuration pathway, *via* an α,β-elimination reaction, to produce L-Hcys, pyruvate and ammonia (Figure 6.1). In contrast, cystathionine γ-lyase (CGL), which follows cystathionine β-synthase (CBS) in the reverse transsulfuration pathway of mammals and *Saccharomyces cerevisiae*, catalyzes the hydrolysis of L-Cth, *via* an α,γ-elimination reaction, to yield L-Cys, α-ketobutyrate and ammonia (Aitken and Kirsch, 2005; Aitken *et al.*, 2011). The enzymes CGS and CBL are targets for the development of herbicides and anti-microbial compounds because the transsulfuration pathway is unique to bacteria and plants (Clausen *et al.*, 1997; Clausen *et al.*, 1998; Ejim *et al.*, 2007).

Phylogenetic analysis has demonstrated that there are five structurally distinct families, or fold types, of PLP-dependent enzymes (Percudani and Peracchi, 2009). With the exception of CBS, which is a member of fold-type II, the enzymes of the transsulfuration pathways are members of the γ-subfamily of fold-type I. The striking structural similarity of the members of the γ-subfamily is illustrated by the ~1.5-Å r.m.s. deviation in the least squares superposition of ~350 C_α atoms of the protein backbones of *E. coli* CGS (eCGS), *E. coli* CBL (eCBL), *S. cerevisiae* CGL (yCGL) and *Trichomonas vaginalis* (*T. vaginalis*) methionine γ-lyase (tMGL), which share ~35% amino-acid sequence identity (Clausen *et al.*, 1996; Clausen *et al.*, 1998;

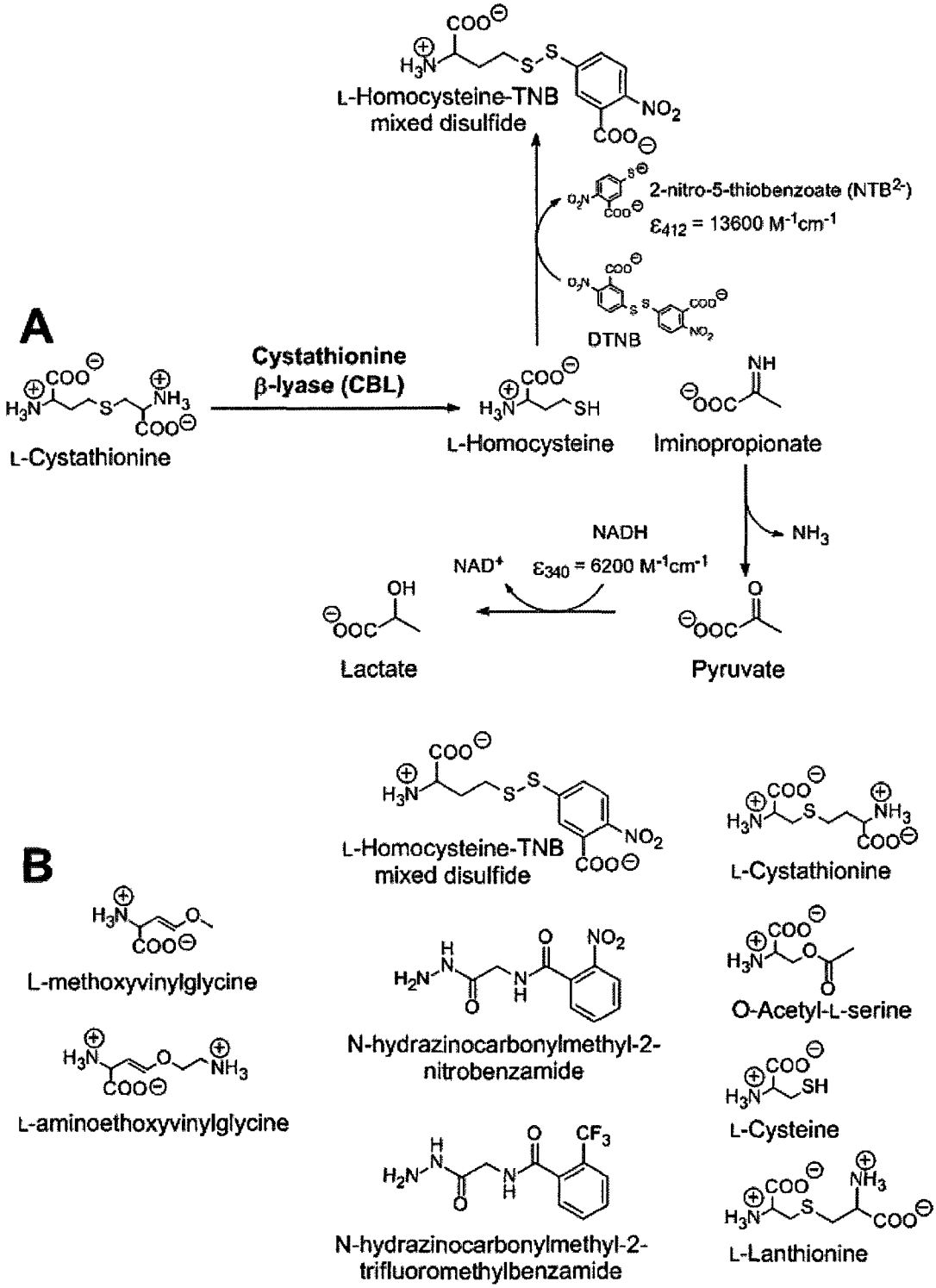
A
L-Homocysteine-TNB mixed disulfide
2-nitro-5-thiobenzoate (NTB2-)
ε412 = 13600 M-1cm-1
DTNB
Cystathionine β-lyase (CBL)
L-Cystathionine
L-Homocysteine
Iminopropionate
NADH
NAD+
ε340 = 6200 M-1cm-1
NH3
Lactate
Pyruvate
B
L-Homocysteine-TNB mixed disulfide
L-Cystathionine
L-methoxyvinylglycine
O-Acetyl-L-serine
N-hydrazinocarbonylmethyl-2-nitrobenzamide
L-aminoethoxyvinylglycine
L-Cysteine
N-hydrazinocarbonylmethyl-2-trifluoromethylbenzamide
L-Lanthionine

Figure 6.1. (**A**) The DTNB and LDH assays employed to measure the L-Cth hydrolysis activity eCBL. (**B**) The structures of L-Cth and the related compounds L-Cys, L-OAS, L-lanthionine and the slow-binding inhibitors of eCBL: AVG, N-hydrazinocarbonylmethyl-2-nitrobenzamide and N-hydrazinocarbonylmethyl-2-trifluoromethylbenzamide (Clausen *et al.*, 1997; Ejim *et al.*, 2007).

Goddall *et al.*, 2001; Messerschmidt *et al.*, 2003). The residues lining the active-site cavities are largely conserved among these enzymes, suggesting that differences in their substrate and reaction specificity are primarily the result of differences in the placement and mobility of active-site residues. Therefore, these enzymes provide a useful model system to investigate determinants of specificity, information which will facilitate the engineering of enzymes dependent on the catalytically versatile PLP cofactor.

The structure of eCBL in complex with the inhibitors aminoethoxyvinylglycine (AVG), N-hydrazinocarbonylmethyl-2-nitrobenzamide and N-hydrazinocarbonylmethyl-2-trifluoromethylbenzamide provide valuable insight into both the nature of contacts of the L-Cth substrate in the active site and the mechanism of this enzyme (Figure 6.1) (Clausen *et al.*, 1997; Ejim *et al.*, 2007). The interactions between the α-carboxylate group of L-Cth and AVG and the side chains of residues W340 and R372, observed in the structure of the eCBL-AVG complex, were confirmed by characterization of site-directed variants of these residues (Figure 6.2) (Clausen *et al.*, 1997; Lodha *et al.*, 2010). Lodha *et al.* (2010) also identified R58 as the residue which binds the distal carboxylate moiety of L-Cth, not present in AVG (Lodha *et al.*, 2010). There are four active-site tyrosines (Y56, Y111, Y238 and Y338) and a serine (S339) residue that is conserved in bacterial CBL sequences (Figure 6.2). Residues Y56, Y111 and S339 are also conserved in eCGS and yCGL, while Y238 and Y338 are replaced by asparagine and glutamate, respectively. The side chains of Y111, Y238 and Y338 of eCBL have been proposed to interact with the L-Cth substrate of eCBL (Clausen *et al.*, 1996; Clausen *et al.*, 1998; Messerschmidt *et al.*, 2003).

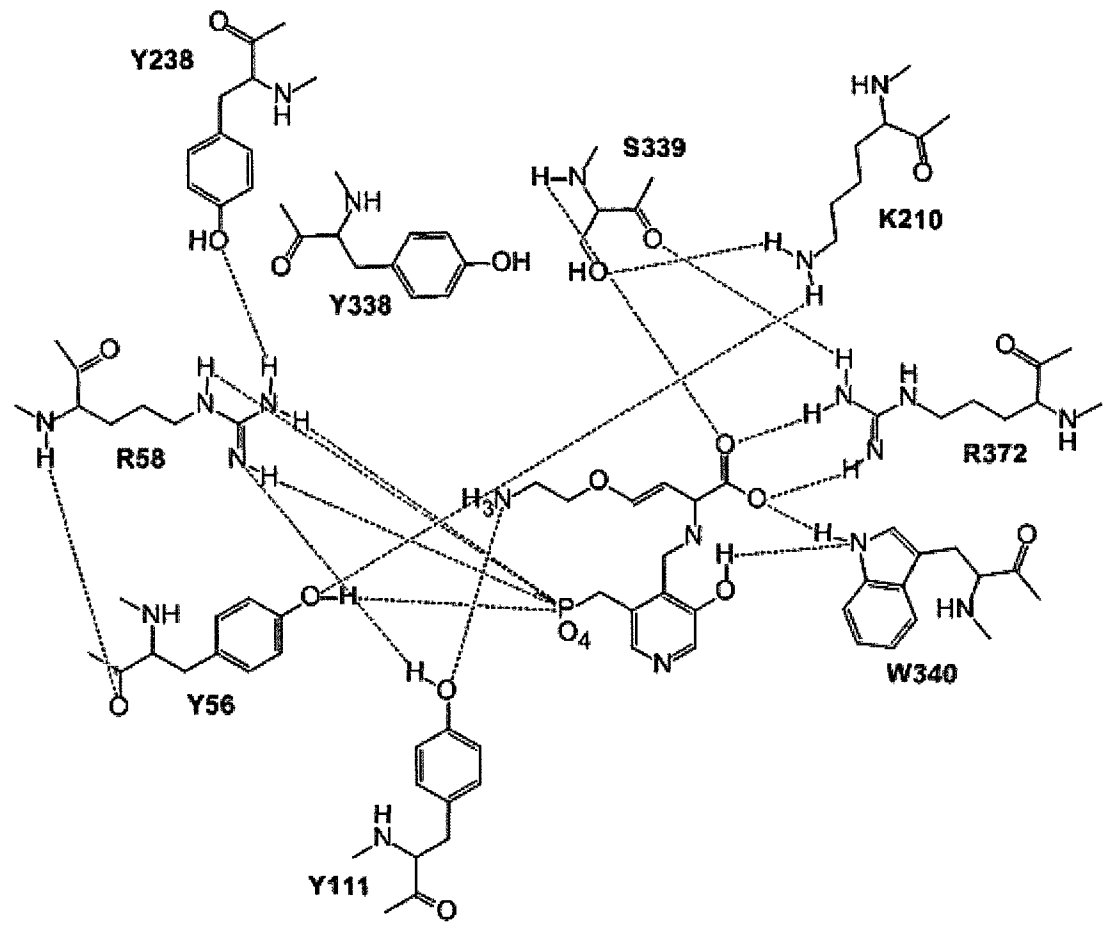

Figure 6.2. Observed contacts of AVG in the active-site of eCBL. The dotted lines represent putative hydrogen bond distances of ≤ 3.3 Å between heteroatoms. The image was constructed using ChemDraw and PDB entry 1CL2 (Clausen *et al.*, 1997).

A series of site-directed variants, removing only the side-chain hydroxyl group, of the eCBL active-site residues Y56, Y111, Y238, Y338 and S339 was constructed to investigate the roles of the hydrogen bonding interactions of these side chains (Figure 6.2). The drastic reduction in the turnover observed upon replacement of S339 with alanine demonstrates that this residue plays an essential role in catalysis. Substitution of Y238 with phenylalanine increases the $K_m^{L\text{-}Cth}$ and K_i^{AVG} by 15 and 2-fold, respectively, demonstrating that this residue participates in binding, with R58, the distal carboxylate moiety of the L-Cth substrate. In contrast, the 22-fold increase in the $K_m^{L\text{-}Cth}$ of Y56F does not indicate a direct interaction with the substrate.

6.3. Materials and Methods

6.3.1. Reagents.

O-acetyl-L-serine (L-OAS), L-aminoethoxyvinylglycine (AVG), L-Cth [*S*-(2-amino-2-carboxyethyl)-L-homocysteine], L-Cys, L-lactate dehydrogenase (LDH), β-nicotinamide adenine dinucleotide (β-NADH, reduced form) and L-Ser and were purchased from Sigma. Ni-NTA resin and 5,5'-Dithiobis(2-nitrobenzoic acid) (DTNB) were obtained from Qiagen and Pierce, respectively. Oligonucleotide primers were synthesized by Integrated DNA Technologies and site-directed mutants were sequenced by BioBasic prior to expression and purification.

6.3.2. Construction, expression and purification of site-directed variants.

Site-directed variants of eCBL were constructed, expressed and purified as described previously (Farsi *et al.*, 2009; Lodha *et al.*, 2010). The *E. coli* KS1000 *metC::cat* strain, in which the gene encoding eCBL is replaced with chloramphenicol acetyltransferase, was employed for expression to avoid contamination with the wild-type *E. coli* enzyme (Farsi *et al.*, 2009). The presence of the N-terminal, 6-His tag and linker, encoded by pTrc-99aAF, does not alter the kinetic properties of eCBL (Farsi *et al.*, 2009).

6.3.3. Determination of steady-state kinetic parameters.

Enzyme activity was measured using a Spectramax 340 microtiter plate spectrophotometer (Molecular Devices) in a total volume of 100 μL at 25 °C. The assay buffer was comprised of 50 mM Tris, pH 8.5, containing 20 μM PLP. The hydrolysis of L-Cth (0.01-6.25 mM) was detected via the reaction of 5,5'-dithiobis-(2-nitrobenzoic

acid) (DTNB) with the free thiol of the L-Hcys product (ε_{412} = 13,600 $M^{-1}s^{-1}$) and using the coupling enzyme L-lactate dehydrogenase (LDH), which reduces the pyruvate product to lactate, with the concomitant conversion of NADH to NAD^+ (ε_{340} = 6,200 $M^{-1}s^{-1}$) (Figure 6.1) (Ellman, 1959; Aitken *et al.*, 2003; Farsi *et al.*, 2009). A background reading was recorded before initiation of the reaction by the addition of eCBL (0.02-10.3 μM for DTNB assay or 0.12-16.2 μM for LDH assay, depending on the activity of the enzyme). Values of k_{cat} and K_m for the hydrolysis of L-Cth and L-OAS were obtained by fitting of the data to the Michaelis-Menten equation and k_{cat}/K_m was obtained independently from equation 6.1. The L-Cys hydrolysis data was fit to equation 6.2, which incorporates the $K_{mi}^{L\text{-}Cys}$ term for substrate inhibition by L-Cys, and $k_{cat}/K_m^{L\text{-}Cys}$ was obtained independently from equation 6.3. Data were fit by nonlinear regression with the SAS software package (SAS Institute, Cary, NC).

$$\frac{v}{[E]} = \frac{k_{cat}/K_m \times [S]}{1 + [S]/K_m} \tag{6.1}$$

$$\frac{v}{[E]} = \frac{k_{cat} \times [S]}{K_m^{L-Cys} + [S]\left(1 + [S]/K_m^{L-Cys}\right)} \tag{6.2}$$

$$\frac{v}{[E]} = \frac{k_{cat}/K_m \times [S]}{1 + [S]/K_m\left(1 + [S]/K_m^{L-Cys}\right)} \tag{6.3}$$

6.3.4. Evaluation of the pH dependence of wild-type and site-directed variants of eCBL.

The pH dependence of L-Cth hydrolysis by eCBL was determined using the continuous DTNB assay in a three-component buffer, comprised of 50 mM MOPS (pK_a = 7.2), 50 mM Bicine (pK_a = 8.3) and 50 mM proline (pK_a = 10.7) (Peracchi *et al.*, 1996; Jhee *et al.*, 2000). The kinetic measurements were carried out at pH 6.4-10.6 in the presence of 20 μM PLP, 2 mM DTNB, 0.06-3.0 μM eCBL (depending on the activity of the site-directed variant) and 6.25 mM L-Cth, for specific activity measurements, or 0.01-6.25 mM L-Cth, for the determination of $k_{cat}/K_m^{L\text{-}Cth}$. Specific activity versus pH measurements were performed in quadruplicate with the DTNB assay or in triplicate with the LDH assay to provide an estimate of the experimental error associated with each point in the pH profile. The $k_{cat}/K_m^{L\text{-}Cth}$ versus pH data were fit to the bell-shaped curve described by equation 6.4, where k_{cat}/K_m^{max} is the upper limit for $k_{cat}/K_m^{L\text{-}Cth}$ at the pH optimum (Aitken *et al.*, 2003).

$$k_{cat}/K_m = \frac{k_{cat}/K_m^{\max}}{1+10^{pK_{a1}-pH}+10^{pH-pK_{a2}}} \qquad (6.4)$$

6.3.5. Inhibition of wild-type and site-directed variants of eCBL by AVG.

The IC_{50}^{AVG} values for inhibition of the eCBL enzymes by AVG were determined by measuring enzyme activity between 5×10^{-5} - 10 mM AVG. The enzyme and inhibitor were mixed and incubated at 25 °C for 10 min in assay buffer. Activity was subsequently measured at a L-Cth substrate concentration of 0.1 mM and the data were fit to equation 6.5 (Ejim *et al.*, 2007). Measurements were performed in quadruplicate for each enzyme. The parameters Act_{max}, Act_{min}, S and IC_{50}^{AVG} of equation 6.5 correspond to the maximal

enzyme activity, the minimal enzyme activity, the slope of the transition between the maximal and minimal activity plateaus and the midpoint of the transition, respectively.

$$Act = \frac{Act_{max} - Act_{min}}{1 + \left(\frac{I}{IC_{50}}\right)^{S}} + Act_{min} \tag{6.5}$$

Values for the dissociation constant K_i^{AVG} and the rate constant k_2 for the inhibition of eCBL by AVG were determined using the model described by Clausen *et al.* (1997) in which formation of the enzyme-inhibitor complex is slow. The wild-type eCBL and site-directed variant enzymes were incubated with 1.5 mM L-Cth and 0.005-7.5 mM AVG in assay buffer and the progress of the reactions was monitored for 30 min. Values of k_{obs} were determined from the fit of equation 6.6 to the progress curves. The resulting k_{obs} values were plotted *versus* inhibitor concentration and values of k_2 and K_i^{AVG} were obtained from fitting of the data to equation 6.7. The K_i^{AVG} and k_2 of eCBL-S339A could not be accurately determined with the LDH assay due to its low activity.

$$[P] = v_s t + \frac{(v_o - v_s)\left[1 - \exp^{-k_{obs}t}\right]}{k_{obs}} \tag{6.6}$$

$$k_{obs} = k_2 + \frac{k_2[I]}{K_i\left(1 + [S]/K_m\right)} \tag{6.7}$$

6.4. Results

The five phenylalanine and alanine substitution variants were soluble with yields between 17-40 mg/L, which is similar to the 15-41 mg/L and 56 mg/L values reported for a series of arginine replacement variants of eCBL and the wild-type enzyme, respectively (Farsi *et al.*, 2009; Lodha *et al.*, 2010). The L-Cth-hydrolysis activity of the eCBL variants was measured with both the DTNB and LDH assays, which monitor production of the L-Hcys and pyruvate products, respectively (Figure 6.1). The kinetic parameters determined with these two assays were within less than 2-fold for all enzymes except Y111F, which is sensitive to the presence of DTNB. The values for both assays are presented in Table 6.1 and, unless otherwise stated, kinetic parameters of L-Cth hydrolysis and inhibition by AVG described in the text were determined with the LDH assay. The ability of each enzyme to catalyze the hydrolysis of L-OAS and L-Cys was also investigated to probe the role of the targeted residues as determinants of substrate specificity. The specific activity of L-Cth hydrolysis and the $k_{cat}/K_m^{L\text{-}Cth}$ versus pH profiles of the wild-type enzyme and the five site-directed variants investigated are bell-shaped.

6.4.1. The Y56F variant.

The k_{cat} and $K_m^{L\text{-}Cth}$ values, for L-Cth hydrolysis, of eCBL-Y56F are decreased 5.8-fold and increased 22-fold, respectively, resulting in a 130-fold decrease in catalytic efficiency (Table 6.1). The L-OAS-hydrolysis data of the Y56F variant could not be fit to the Michaelis-Menten equation, as saturation kinetics were not observed. Therefore, with the assumption that $K_m^{L\text{-}OAS} >>$ [L-OAS], the Michaelis-Menten equation was modified to

Table 6.1. Kinetic parameters for L-Cth hydrolysis and inhibition by AVG of eCBL and site-directed variants.

Enzyme		k_{cat} (s^{-1})[a]	$K_m^{L\text{-}Cth}$ (mM)[a]	$k_{cat}/K_m^{L\text{-}Cth}$ ($M^{-1}s^{-1}$)[a]	IC_{50}^{AVG} (μM)[b]	K_i^{AVG} (μM)[c]	k_2 (s^{-1})[c]
eCBL	DTNB	34.1 ± 0.6	0.18 ± 0.01	(1.9 ± 0.1) 10^5	1.74 ± 0.08	1.9 ± 0.6	(5 ± 1) 10^{-4}
	LDH	28.3 ± 0.2	0.188 ± 0.007	(1.50 ± 0.05) 10^5	2.8 ± 0.3	3 ± 2	(6 ± 3) 10^{-4}
Y56F	DTNB	10.4 ± 0.6	18 ± 1	(5.82 ± 0.09) 10^2	23 ± 1	188 ± 9	(2.5 ± 0.1) 10^{-3}
	LDH	4.85 ± 0.08	4.1 ± 0.1	(1.18 ± 0.02) 10^3	140 ± 30	142 ± 5	(2.1 ± 0.1) 10^{-3}
Y111F	DTNB	n.s.	n.s.	76 ± 1	1.34 ± 0.05	2.7 ± 0.9	(1.3 ± 0.4) 10^{-3}
	LDH	12.4 ± 0.1	0.67 ± 0.02	(1.86 ± 0.04) 10^4	1.61 ± 0.09	n.d.	n.d.
Y238F	DTNB	62.3 ± 0.5	4.59 ± 0.07	(1.36 ± 0.01) 10^4	4.6 ± 0.3	6.9 ± 0.3	(1.9 ± 0.1) 10^{-3}
	LDH	26.4 ± 0.3	2.88 ± 0.07	(9.2 ± 0.1) 10^3	5.8 ± 0.5	1.45 ± 0.08	(2.7 ± 0.1) 10^{-3}
Y338F	DTNB	157 ± 3	0.27 ± 0.02	(6.0 ± 0.5) 10^5	2.6 ± 0.4	5 ± 2	(2.1 ± 0.1) 10^{-3}
	LDH	46.9 ± 0.6	0.27 ± 0.01	(1.71 ± 0.07) 10^5	2.8 ± 0.2	1 ± 1	(2 ± 2) 10^{-4}
S339A	DTNB	(9.9 ± 0.2) 10^{-3}	0.11 ± 0.01	92 ± 8	3.3 ± 0.6 [DTNB]	2.7 ± 0.8	(2.6 ± 0.8) 10^{-4}
	LDH	(5.04 ± 0.06) 10^{-3}	0.087 ± 0.005	58 ± 3	n.d.	n.d.	n.d.

[a]Kinetic parameters reported are for hydrolysis of L-Cth. Reaction conditions: 0.01-6.4 mM, L-Cth, 0.02-10.3 μM (DTNB assay) or 0.12-16.2 μM (LDH assay) wild-type or variant eCBL (depending on the activity of the enzyme) and 2 mM DTNB to monitor L-Hcys production, or 1.5 mM NADH and 2.0 μM LDH, to monitor pyruvate production, in assay buffer at 25 °C. The data were fit to the Michaelis-Menten equation to obtain k_{cat} and $K_m^{L\text{-}Cth}$ and equation 6.1 to obtain $k_{cat}/K_m^{L\text{-}Cth}$.

[b]Reaction conditions for IC_{50}^{AVG} measurements: Enzyme (0.029-3.6 μM, depending on the activity of the variant) was incubated with 0.05-10^4 μM AVG in assay buffer at 25 °C for 10 min. Activity was subsequently measured, via the DTNB (n=4) and LDH-based coupled (n=3) assays at a L-Cth substrate concentration of 0.1 mM. the data were fit to equation 6.5 to obtain IC_{50}^{AVG}. The IC_{50}^{AVG} of the S339A variant could not be accurately determined with the LDH assay due to its low activity.

[c]Reaction conditions for measurement of K_i^{AVG} and k_2: Wild-type eCBL and site-directed variants (0.023-8.1 μM, depending on the activity of the variant) were incubated with 1.5 mM L-Cth and 0.005-7.5 mM AVG in assay buffer and the progress of the reactions was monitored for 30 min *via* the DTNB and LDH-based coupled assays. The progress curves were fit to equation 6.6 to obtain k_{obs} values, which were plotted versus inhibitor concentration and fit to equation 6.7 to obtain k_2 and K_i^{AVG}. The K_i^{AVG} and k_2 of the S339A variant could not be accurately determined with the LDH assay due to its low activity.

obtain $k_{cat}/K_m^{L\text{-}OAS}$, which is reduced 470-fold compared to the wild-type enzyme (Table 6.2). The k_{cat}, $K_m^{L\text{-}Cys}$, $K_i^{L\text{-}Cys}$ and $k_{cat}/K_m^{L\text{-}Cys}$, for L-Cys hydrolysis, of Y56F are all reduced, by 100, 12, 8 and 9-fold, respectively (Table 6.2, Figure 6.3). However, the low L-Cys hydrolysis activity of Y56F results in a lower quality fit of the data to equation 6.2 than the wild-type enzyme, raising the possibility that the reductions in $K_m^{L\text{-}Cys}$ and $K_i^{L\text{-}Cys}$ are an artifact. Although the IC_{50}^{AVG} and K_i^{AVG} values of eCBL-Y56F for inhibition by AVG differ by 4 and 2-fold, respectively, between the DTNB and LDH assays, a consistent trend of an increase in both values is observed. The IC_{50}^{AVG} and K_i^{AVG} values of Y56F, measured with the LDH assay, are both increased 50-fold (Table 6.1), compared to the wild-type enzyme. Substitution of Y56 with phenylalanine results in a shift in the acidic limb of the specific activity versus pH profile, relative to the wild-type enzyme. The pH optimum of eCBL-Y56F is correspondingly shifted to 9-9.5, compared to 8.5-9 for the wild-type enzyme (Figure 6.4). Therefore, the effect of pH on the $k_{cat}/K_m^{L\text{-}Cth}$ of Y56F was determined (Figure 6.4). The values of pK_{a1} and pK_{a2}, corresponding to the acidic and basic limbs of the $k_{cat}/K_m^{L\text{-}Cth}$ versus pH profile, respectively, are presented in Table 3. The values of pK_{a1} and pK_{a2} of the wild-type enzyme, measured with the LDH assay, are 8.0 ± 0.1 and 10.1 ± 0.1, while those of the Y56F variant are 8.7 ± 0.1 and 10.1 ± 0.1, respectively (Table 6.3). The pK_{a1} value of Y56F is consistently increased 0.7 pH units when measured with either assay.

6.4.2. The Y111F variant.

The k_{cat} and $K_m^{L\text{-}Cth}$ of Y111F are decreased 2.3-fold and increased 3.6-fold, respectively (Table 6.1). A unique feature of the Y111F variant is the difference in L-Cth-

Table 6.2. Kinetic parameters of eCBL and site-directed variants for the hydrolysis of L-OAS and L-Cys.[a]

Enzyme	k_{cat} (s^{-1})	$K_m^{L\text{-}OAS}$ (mM)	$k_{cat}/K_m^{L\text{-}OAS}$ ($M^{-1}s^{-1}$)	k_{cat} (s^{-1})	$K_m^{L\text{-}Cys}$ (mM)	$K_i^{L\text{-}Cys}$ (mM)	$k_{cat}/K_m^{L\text{-}Cys}$ ($M^{-1}s^{-1}$)
	L-OAS → acetate + pyruvate + NH_3			L-cysteine → H_2S + pyruvate + NH_3			
eCBL	0.280 ± 0.004	2.18 ± 0.09	128 ± 4	0.49 ± 0.02	0.24 ± 0.02	4.9 ± 0.5	2000 ± 100
Y56F	n.s.	n.s.	0.27 ± 0.02	0.0048 ± 0.0007	0.02 ± 0.01	0.6 ± 0.2	230 ± 80
R58A	0.57 ± 0.07	51 ± 8	11.2 ± 0.4	0.173 ± 0.007	0.36 ± 0.04	13 ± 2	480 ± 40
R58K	0.04 ± 0.01	31 ± 9	1.4 ± 0.1	n.d.	n.d.	n.d.	n.d.
R59K	0.69 ± 0.02	12.7 ± 0.6	54 ± 1	0.32 ± 0.01	0.28 ± 0.03	7.2 ± 0.7	1160 ± 80
Y111F	0.0131 ± 0.0007	13 ± 1	0.98 ± 0.05	0.17 ± 0.02	0.11 ± 0.02	0.65 ± 0.09	1500 ± 100
D116A	0.691 ± 0.009	2.6 ± 0.1	190 ± 20	0.58 ± 0.05	0.33 ± 0.06	4.1 ± 0.6	1700 ± 200
Y238F	0.250 ± 0.005	3.1 ± 0.2	81 ± 3	0.55 ± 0.03	0.46 ± 0.06	10 ± 1	1200 ± 100
Y338F	0.515 ± 0.006	2.79 ± 0.09	185 ± 4	0.39 ± 0.02	0.23 ± 0.03	4.2 ± 0.6	1700 ± 200
R372K	n.s.	n.s.	(1.0 ± 0.1) 10^{-6}	n.d	n.d	n.d.	n.d.

[a] Kinetic parameters reported are for hydrolysis of L-Cth. The activity of S339A for the hydrolysis of L-Cys and L-OAS is undetectable. Reaction conditions: 1.5 mM NADH, 2.0 μM LDH, 0.01-20 mM L-OAS or L-Cys and 2.6-7.7 μM eCBL enzyme, depending on the activity of the variant, in assay buffer at 25 °C. The L-OAS data were fit to the Michaelis-Menten equation to obtain k_{cat} and $K_m^{L\text{-}OAS}$ and equation 6.1 to obtain $k_{cat}/K_m^{L\text{-}OAS}$ and the L-Cys data were fit to equation 6.3 to obtain k_{cat} and $K_m^{L\text{-}Cys}$ and equation 6.4 to obtain $k_{cat}/K_m^{L\text{-}Cys}$. The notation n.d. indicates that the L-Cys hydrolysis activity of the R58K and R372K variants could not be detected.

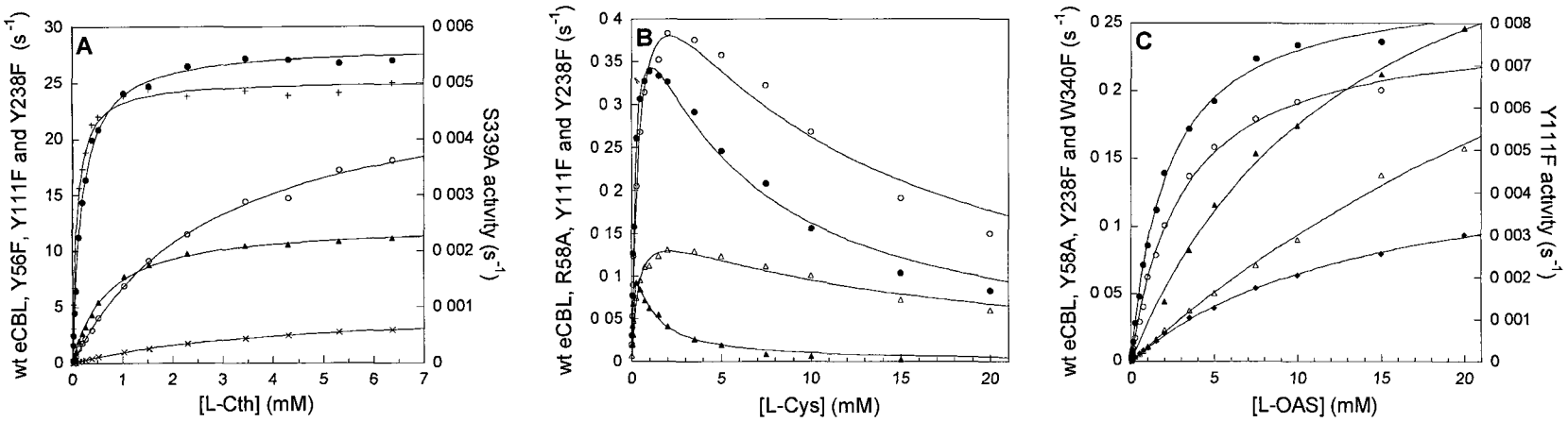

Figure 6.3. The dependence of (**A**) Wt-eCBL (●), Y56F (×), Y111F (▲), Y238F (○) and S339A (+), (**B**) Wt-eCBL (●), R58A (Δ), Y111F (▲) and Y238F (○) and (**C**) Wt-eCBL (●), R58A(Δ), Y111F (▲), Y238F (○) and W340F(♦) activity on the concentrations of (**A**) L-Cth, (**B**) L-Cys and (**C**) L-OAS.

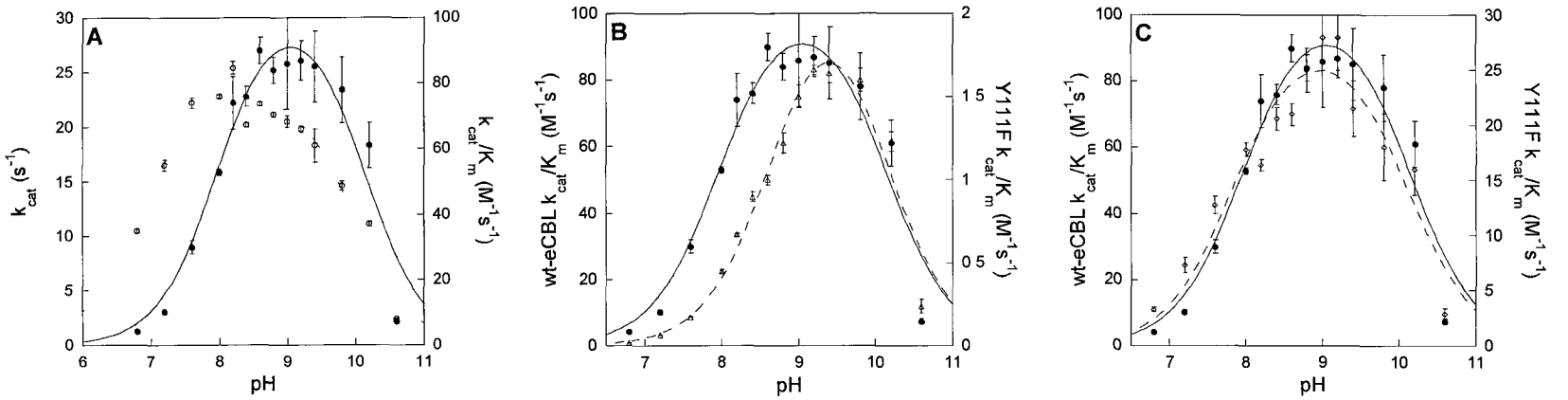

Figure 6.4. The pH dependence of L-Cth hydrolysis by wild-type eCBL and the Y56F and Y111F variants. (**A**) The pH dependence of k_{cat} (○, dotted line) and $k_{cat}/K_m^{L\text{-}Cth}$ (●, solid line) for eCBL. Comparison of the pH dependence of $k_{cat}/K_m^{L\text{-}Cth}$ for wild-type eCBL (●, solid line) and the (**B**) Y56F (Δ, dashed line) and (**C**) Y111F (◊, dashed line) variants. Reaction conditions: MBP buffer (50 mM MOPS, 50 mM Bicine and 50 mM proline), 20 uM PLP, 1.25 mM NADH, 1-6 μM LDH (concentration optimized for each pH) and 0.05-6.6 mM L-Cth and 0.11 wild-type eCBL, 0.93 μM Y11F or 7.9 μM S339A. The data were fit to equation 6.4.

Table 6.3. Parameters determined from the pH profiles of wild-type eCBL and the Y56F and Y111F variants.[a]

Enzyme	Assay	pK_{a1}	pK_{a2}
eCBL	DTNB	8.28 ± 0.06	10.20 ± 0.06
	LDH	8.0 ± 0.1	10.1 ± 0.1
Y56F	DTNB	9.01 ± 0.07	10.43 ± 0.09
	LDH	8.7 ± 0.1	10.1 ± 0.1
Y111F	DTNB	7.8 ± 0.3	9.7 ± 0.3
	LDH	7.8 ± 0.1	10.1 ± 0.1

[a]Kinetic measurements for the eCBL-catalyzed hydrolysis of L-Cth were carried out from pH 6.4-10.6 in MBP buffer containing 0.05-6.6 mM L-Cth, 20 μM PLP, 0.03-5.75 μM enzyme and 2 mM DTNB or 1.25 mM NADH and 1-6 μM LDH (concentration optimized for each pH) at 25 °C. The k_{cat} or $k_{cat}/K_m^{L\text{-}Cth}$ data were fitted to equation 6.4 to obtain the values for pK_{a1} and pK_{a2}.

hydrolysis activity observed with the LDH and DTNB assays, which measure the production of pyruvate and L-Hcys, respectively. Figure 6.5 shows that when pyruvate production is measured Y111F displays saturation kinetics, similar to the wild-type enzyme, while in the presence of DTNB the activity is reduced 20-fold at 6.27 mM L-Cth, the highest substrate concentration tested, and the enzyme is not saturated within the solubility limit of L-Cth. The L-Hcys formed upon hydrolysis of L-Cth reacts with DTNB to release TNB^- and produce the mixed disulfide of TNB and L-Hcys (TNB-Hcys), which is similar in overall structural form to N-hydrazinocarbonylmethyl-2-nitrobenzamide (Figure 6.1), an eCBL inhibitor with an IC_{50} of 4.5 μM (Ejim *et al.*, 2007). However, up to 100 μM TNB-Hcys, synthesized by reaction of equimolar L-Hcys and DTNB, has no effect on the activity of the wild-type enzyme and Y111F variant, suggesting that DTNB may be the component inhibiting the activity of Y111F. Despite the observed discrepancy in the kinetic parameters for L-Cth hydrolysis between the DTNB and LDH assays, the IC_{50}^{AVG} for inhibition of Y111F by AVG differs by only 1.2-fold when measured with the two assays. Additionally, the difference between the IC_{50}^{AVG} of the wild-type enzyme and Y111F variant is only 1.3 and 1.7-fold when measured with the DNTB and LDH assays, respectively. Although the Y111F substitution reduces the $k_{cat}/K_m^{L\text{-}Cys}$, for the α,β-elimination of L-Cys, by only 1.3-fold, the $K_i^{L\text{-}Cys}$ for substrate inhibition is decreased 7.5-fold (Figure 6.3B, Table 6.2), demonstrating that removal of the hydroxyl group of Y111 facilitates the binding of a second molecule of L-Cys to the eCBL active site. Although the Y111F substitution has no effect on the pH optimum of activity, as determined from measurement of specific activity *versus* pH, this variant was targeted for further analysis because of the role proposed for Y111 in proton transfer (Clausen *et al.*, 1996). The

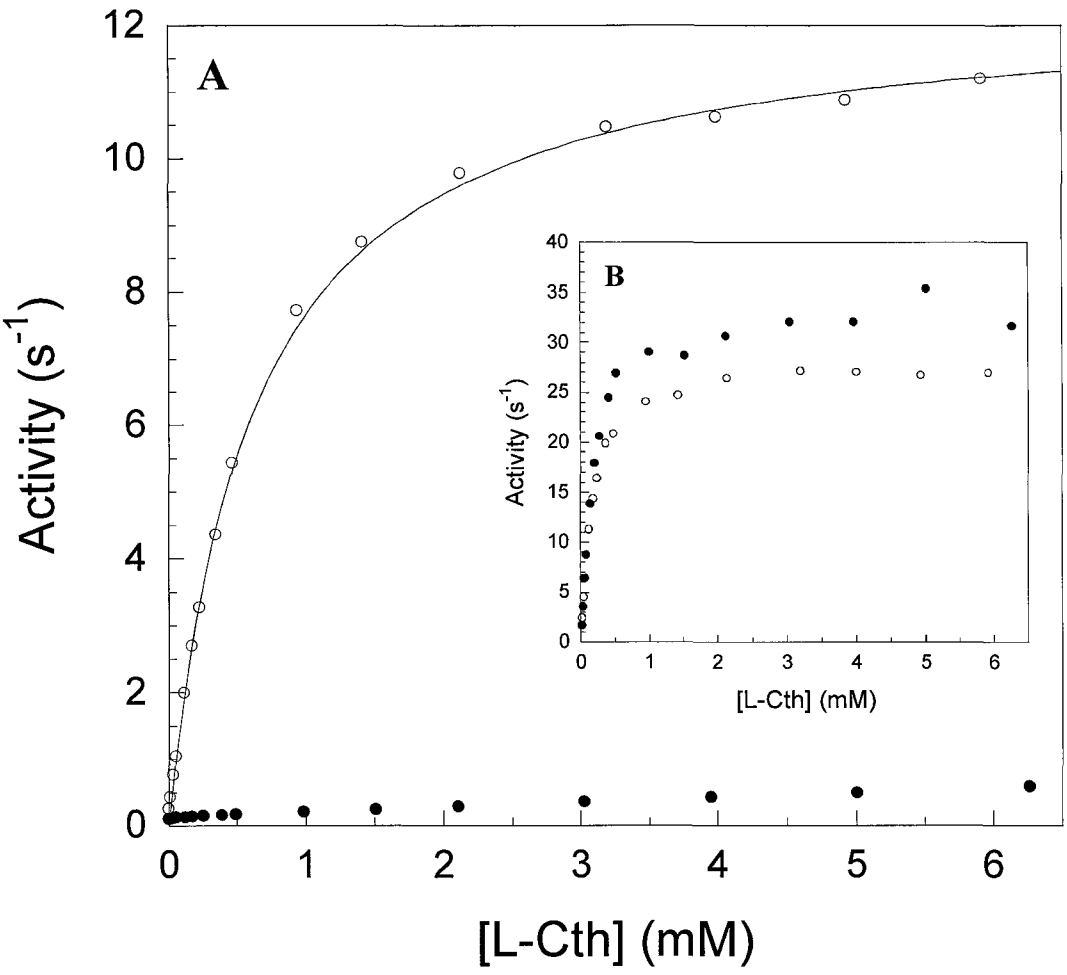

Figure 6.5. Comparison of the dependence of (**A**) Y111F and (**B**) wild-type eCBL activity on the concentration of L-Cth when measured with the DTNB (•) and LDH (○) assays. Reaction conditions: 50 mM Tris, pH 8.5, 20 μM PLP, 0.01-6.3 mM L-Cth, 0.05 μM eCBL or 2.5 μM Y111F, for the DNTB assay, or 0.1 μM eCBL or 0.9 μM Y111F, for the LDH assay, and either 2 mM DTNB or 1.3 mM NADH and 1.9 μM LDH.

Y111F substitution has no effect on the k_{cat} and $k_{cat}/K_m^{L\text{-}Cth}$ versus pH profiles of eCBL (Figure 6.4). The pK_{a1} and pK_{a2} of the $k_{cat}/K_m^{L\text{-}Cth}$ profile of the Y111F variant, measured with the LDH assay, are 7.8 ± 0.1 and 10.1 ± 0.1, which is within experimental error of the wild-type enzyme (Table 6.3).

6.4.3. The Y238F variant.

The k_{cat} of Y238F is identical to the wild-type enzyme (Table 6.1) and the specific activity and $k_{cat}/K_m^{L\text{-}Cth}$ versus pH profiles of this variant are unchanged. Although the $K_m^{L\text{-}Cth}$, for hydrolysis of L-Cth, of Y238F is increased 15-fold, the IC_{50}^{AVG} and K_i^{AVG} values, for inhibition by AVG, and the values of $K_m^{L\text{-}OAS}$ and $K_m^{L\text{-}Cys}$, for hydrolysis of L-OAS and L-Cys, respectively, are increased by only 2-2.5-fold (Tables 6.1 and 6.2). The distal carboxylate of L-Cth, the physiological substrate of eCBL, distinguishes it from AVG, L-OAS and L-Cys, which each possess a single carboxylate group. The substrate inhibition observed for wild-type eCBL, in the α,β-elimination of L-Cys, is reduced in the Y238F and R58A variants by 2 and 2.7-fold, respectively, supporting a role for both residues in binding the α-carboxylate group of the second L-Cys molecule, occupying the binding site of the distal portion of the physiological L- Cth substrate (Figure 6.3B, Table 6.2).

6.4.4 The Y338F variant.

The effect of substitution of Y338 with phenylalanine is negligible, as the steady state kinetic parameters for L-Cth, L-OAS and L-Cys hydrolysis and the IC_{50}^{AVG} and K_i^{AVG} values, for inhibition by AVG, are all within 2-fold of the corresponding values for the

wild-type eCBL enzyme (Tables 6.1 and 6.2). The pH profile and optimum of eCBL are also unchanged by the Y338F substitution.

6.4.5. The S339A variant.

The 2600-fold decrease in the $k_{cat}/K_m^{L\text{-}Cth}$ of S339A is dominated by a 5600-fold decrease in k_{cat} as the $K_m^{L\text{-}Cth}$ of S339A is also decreased, but by only 2.2-fold. This reduction in k_{cat}, by three orders of magnitude, distinguishes S339A as the other active-site variants investigated altered this parameter by only 1.1-5.8-fold (Table 6.1, Figure 6.3). The K_i^{AVG} is increased by the same 2.2-fold degree as the $K_m^{L\text{-}Cth}$ and the IC_{50}^{AVG} for inhibition by AVG, which could be measured with only the DTNB assay due to the low activity of this variant, was also increased by only ~2-fold. The low activity of the S339A variant precluded the measurement of L-OAS and L-Cys hydrolysis, as the k_{cat} of the wild-type enzyme for these substrates is two orders of magnitude below that for L-Cth hydrolysis. A unique feature of S339A is the 340-nm absorbance observed upon reaction with L-Cth (Figure 6.6). The wild-type eCBL and S339A enzymes were incubated with 3 mM L-Cth (150 molar equivalents) for 2 h, followed by dialysis to remove substrates and products. The enzymes were subsequently incubated with 20 mM pyruvate for 2 h, followed by dialysis to remove excess pyruvate, to return any pyridoxamine, produced by transamination of L-Cth, to the internal aldimine of PLP. Upon reaction of the wild-type enzyme with L-Cth the 424-nm peak, corresponding to the ketimine tautomer of the internal aldimine of the PLP cofactor, decreases in intensity, with a concomitant increase at 326 nm. In contrast, the 422-nm peak of S339A is shifted to 338 nm following reaction with L-Cth. The ratio between the 424 and 326-nm peaks of the wild-type enzyme, before

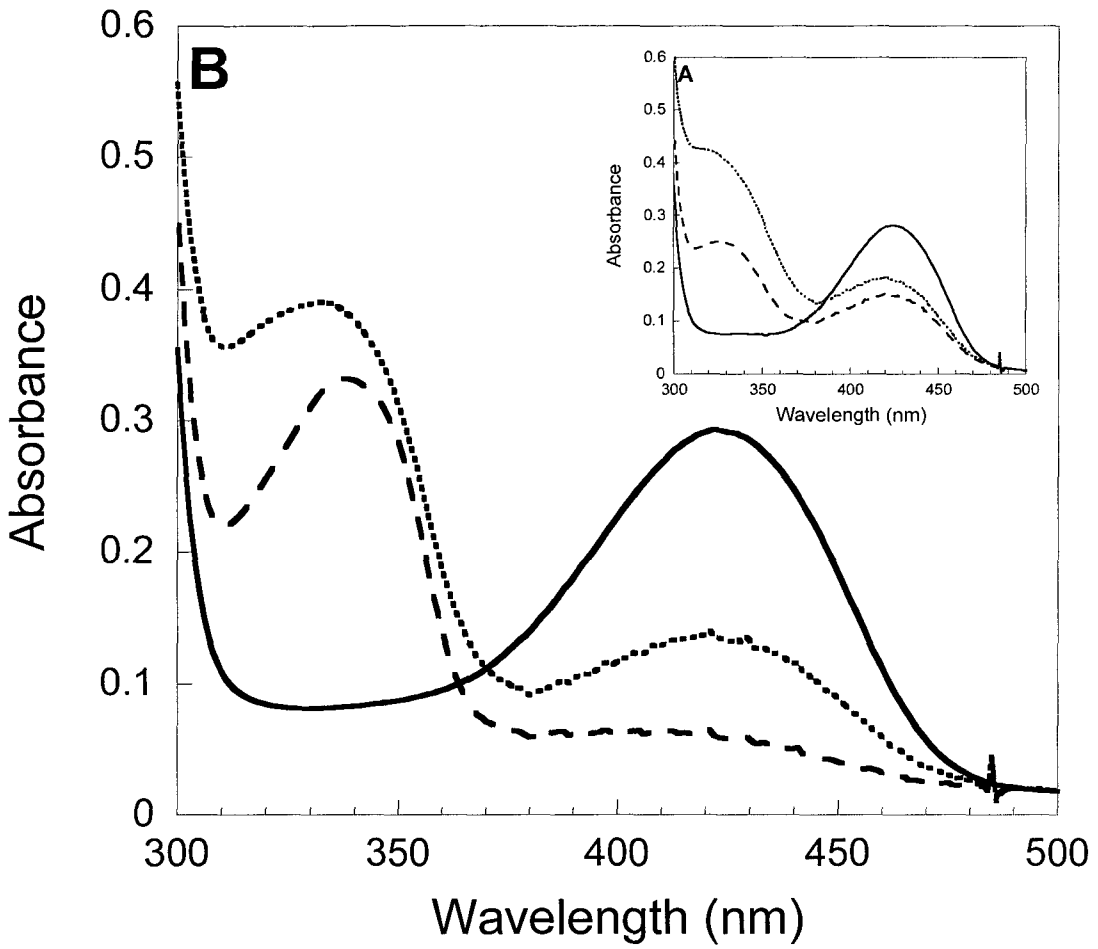

Figure 6.6. The effect of consecutive incubation with L-Cth and pyruvate on the PLP spectrum of (**A**) wild-type eCBL and (**B**) the S339A variant. The absorbance spectrum of the PLP cofactor of 20 μM enzyme was recorded before the addition of substrate (solid line), following a 2-h incubation with 3 mM L-Cth (dashed line) and following a 2-h incubation of the L-Cth-treated enzyme with 20 mM pyruvate (dotted line). The enzymes were dialyzed for one hour following both incubations to remove excess L-Cth and pyruvate.

and after reaction with L-Cth, and subsequent dialysis, is 3.7 and 0.6 respectively, while the corresponding ratios of the 422 and 338-nm bands of S339A are 3.6 and 0.2 (Figure 6.6). To investigate whether the 338-nm band of S339A corresponds to pyridoxamine, resulting from transamination of the L-Cth substrate, the effect of incubation with the keto-acid pyruvate was investigated. Reaction of the α-keto acid pyruvate with pyridoxamine would convert the latter to PLP, with the concomitant production of alanine. Incubation with 20 mM pyruvate for 2 h, followed by dialysis, had no effect on the 424-nm absorbance of the wild-type enzyme, as the slight increase in absorbance observed is due to residual pyruvate. In contrast, incubation with pyruvate resulted in a 2.3-fold increase in the intensity of the corresponding 422-nm band of S339A. The 2-h incubation was not sufficient to completely regenerate the PLP form of the enzyme as the 422-nm peak of the pyruvate-treated S339A enzyme is 2.2-fold lower than prior to reaction with L-Cth (Figure 6.6).

6.5. Discussion

Cystathionine β-lyase is a member of the γ-subfamily of the large and diverse fold-type I class of PLP-dependent enzymes (Percudani and Peracchi, 2009). Crystal structures are available for 14 enzymes from the γ-subfamily, including plant and *E. coli* CBL and CGS, yeast and human CGL, and methionine γ-lyase (MGL), homocysteine γ-lyase (HGL), *O*-acetylhomoserine sulfhydrylase (OAHSS) and *O*-succinylhomoserine sulfhydrylase (OSHSS) from Trichomonads and diverse bacterial species (Allen *et al.*, 2009a; Allen *et al.*, 2009b; Breitinger *et al.*, 2001.; Clausen *et al.*, 1996; Clausen *et al.*, 1998; Edwards *et al.*, 2010; Goodall *et al.*, 2001; Imigawa *et al.*, 2009a; Imigawa *et al.*, 2009b; Messerschmidt *et al.*, 2003; Ngo *et al.*, 2009; Nikulin *et al.*, 2008; Steegborn *et al.*, 1999; Sun *et al.*, 2009). Comparison of the amino-acid sequences and structures of these enzymes highlights their striking structural similarity and the conservation of key active-site residues. For example, while half of the 22 positions conserved between the 14 γ-subfamily structures correspond to glycine or hydrophobic residues, required for structural purposes, seven (corresponding to eCBL-Y56, R58, G86, D185, T209, K210 and R372) are situated in proximity to the cofactor. The active-site lysine (K210), conserved in all PLP-dependent enzymes catalyzing transformations of amino acid substrates, tethers the PLP cofactor *via* a Schiff base linkage and acts as the catalytic base (Eliot and Kirsch, 2004). Residues G86 and T209 form hydrogen bonds with the phosphate moiety of PLP and D185 interacts with the pyridinium nitrogen of the cofactor. Lodha *et al.*, (2010) identified R58 and R372 as the residues which bind with the distal and α-carboxylate groups, respectively, of the L-Cth substrate. Although the substrates of all γ-subfamily members possess an α-carboxylate group, those of OAHSS

and MGL do not include a distal carboxylate. Accordingly, the strict conservation of R58 is likely due to its additional role in tethering the phosphate group of the PLP cofactor. Similarly, the conserved tyrosine, corresponding to eCBL-Y56, also forms a hydrogen bond to the phosphate moiety of the cofactor (Clausen *et al.*, 1996). Other fold-type I enzymes, such as the extensively studied aspartate aminotransferase (AAT), also utilize a pair of arginine residues to bind dicarboxylic substrates, as well as an arginine and tyrosine to position the cofactor, *via* interaction with the phosphate moiety (Kirsch *et al.*, 1984). In contrast, other active-site residues proposed to play a role in substrate binding or catalysis in eCBL, such as Y111, Y238, Y338 and S339, vary between members of the γ-subfamily and may act as determinants of substrate or reaction specificity. Site-directed mutagenesis was employed to replace residues Y56, Y111, Y238 and Y338 with phenylalanine and S339 with alanine, to probe the roles of the side-chain hydroxyl of each. The structural similarity and subtle differences in active-site architecture between the enzymes of the γ-subfamily of fold-type I provides an interesting model system for the investigation of substrate and reaction specificity among enzymes dependent on the catalytically versatile PLP cofactor.

6.5.1. Residue Y338.

The presence of a tyrosine residue at position 338 (of eCBL) is unique to bacterial CBL sequences as this residue is a valine in the three available MGL structures, as well as *A. thaliana* CBL (AtCBL), and is replaced by a glutamate in eCGS and both yeast and hCGL (Allen *et al.*, 2009a; Allen *et al.*, 2009b; Breitinger *et al.*, 2001.; Clausen *et al.*, 1996; Clausen *et al.*, 1998; Goodall *et al.*, 2001; Messerschmidt *et al.*, 2003; Nikulin *et*

al., 2008; Sun *et al.*, 2009). The eCBL-Y338F substitution removes only the side-chain hydroxyl group and preserves the van der Waals contacts with active-site ligands observed in the structures of eCBL in complex with the inhibitors AVG, N-hydrazinocarbonylmethyl-2-nitrobenzamide and N-hydrazinocarbonylmethyl-2-trifluoro-methylbenzamide (Clausen *et al.*, 1997; Ejim *et al.*, 2007). The observed change of less than 2-fold in the kinetic parameters of the Y338F variant (Tables 6.1 and 6.2) indicates that elimination of the hydrogen bond between the side chains of Y338 and K42, and ensuing increased conformational flexibility of Y338, does not substantially alter the hydrophobic packing interactions of the aromatic ring, which are proposed to play a role in substrate and inhibitor binding (Clausen *et al.*, 1996; Clausen *et al.*, 1997; Ejim *et al.*, 2007). Interestingly, K42 is situated within a segment of eight amino acids in eCBL (residues 38-45), nCGS and MGL that is absent in eCGS, AtCBL and CGL sequences. A role for F55 and Y338, conserved as hydrophobic residues in eCBL and MGL structures and replaced by acidic residues in CGL and CGS, as determinants of reaction specificity in the α,β versus α,γ-elimination of L-Cth of eCBL and yeast CGL (yCGL) has been suggested (Messerschmidt *et al.*, 2003). However, although the interconversion of these residues in eCBL (F55D, Y338E), eCGS (D45F, E325Y) and yCGL (E48F, E333Y) reduces the catalytic efficiency of these enzymes, it does not modify their *in vivo* reaction specificity (Farsi *et al.*, 2009). While these residues may contribute to regulation of reaction specificity, the near-native kinetic parameters of the eCBL-Y338F variant, in combination with the lack of change in reaction specificity in the inter-conversion variants reported by Farsi *et al.*, (2009), demonstrate that they must act in concert with other residues to modulate the chemistry of the PLP cofactor.

6.5.2. Residues Y111 and Y238.

The structure of the eCBL-AVG complex provides a useful model for the design of inhibitors and interpretation of binding interactions (Clausen *et al.*, 1997). However, the binding mode observed for the distal portion of AVG may not be representative of the L-Cth because the β,γ-unsaturated inhibitor lacks rotational freedom about this bond, a sulfur atom at the γ-position and the distal carboxylate group of the substrate (Figure 6.1). Lodha *et al.* (2010) determined that the side chain of eCBL-R58 interacts with the distal carboxylate group of L-Cth, as the R58A substitution increased the $K_m^{L\text{-}Cth}$ and K_i^{AVG} by 30 and 3-fold, respectively. The side chain hydroxyl moieties of Y111 and Y238 are situated 2.8 and 4.2 Å, respectively, from the distal amino group of AVG (Figure 6.2) and the latter interaction is enabled by a bridging water molecule (Clausen *et al.*, 1997). The Y111F and Y238F substitution variants of eCBL were constructed to probe the roles of the hydroxyl groups of these residues.

Residue Y238 is conserved in bacterial CBL sequences, but is replaced by an asparagine residue in bacterial CGS and eukaryotic CGL, which also bind dicarboxylic substrates, and by isoleucine or leucine in MGL, the methionine substrate of which lacks a distal, hydrogen-bonding group. The $K_m^{L\text{-}Cth}$ of eCBL-Y238F is increased 15-fold while the IC_{50}^{AVG} and K_i^{AVG}, for inhibition by AVG, and the $K_m^{L\text{-}OAS}$ and $K_m^{L\text{-}Cys}$, for hydrolysis of L-OAS and L-Cys, respectively, are increased only ~2-fold. This indicates a role for eCBL-Y238F in binding to the distal carboxylate group of L-Cth, as this group is not present in AVG, L-Cys and L-OAS (Table 6.1). Similarly, the $K_m^{L\text{-}Cys}$, for the hydrolysis of L-Cys, of R58A is increased only 1.5-fold. The 23-fold increase in $K_m^{L\text{-}OAS}$ observed for R58A suggests that residue R58 may interact with the carbonyl oxygen of the acetate

moiety of L-OAS. The comparable, 2-3-fold, reductions in substrate inhibition by L-Cys observed for both Y238F and R58A (Figure 6.3B, Table 6.2) also indicates a common role for these residues in interacting with the distal portion of the L-Cth substrate, the binding site of which can be occupied by L-Cys.

Residue Y111 engages in a π-stacking interaction with the aromatic ring of the cofactor, an interaction common among fold-type I, PLP-dependent enzymes, as exemplified by W140 of *E. coli* AATase (*e*AATase) and H142 of Rhodobacter capsulatis 5-aminolevulinate synthase (ALAS) (Hayashi *et al.*, 1990; Astner *et al.*, 2005). Among the 14 structures for members of the γ-subfamily, a tyrosine is found in this position in 12 enzymes, including CGL, MGL and both plant and bacterial CBL and CGS, while a phenylalanine is present in *Mycobacterium tuberculosis* OSHSS and *Thermus thermophilus* OAHSS (Imagawa *et al.*, 2009; Edwards *et al.*, 2010). Therefore, the presence of an aromatic ring that can engage in π-stacking with the cofactor, rather than the specific identity of this residue, is the common element shared by all members of the γ-subfamily for which structures are available. Although Y111 interacts with the distal amino group of L-Cth in the eCBL-AVG complex, removing the hydroxyl group of this residue increases the IC_{50}^{AVG} and $K_m^{L\text{-}Cth}$ by less than 2-fold and 3.6-fold, respectively (Table 6.1), suggesting that the crystal structure may differ from the binding mode of the L-Cth substrate and from the eCBL-AVG complex in solution. Distinct features of the Y111F variant are the 7.5-fold decrease in $K_i^{L\text{-}Cys}$ for the α,β-elimination of L-Cys and the 250-fold difference between $k_{cat}/K_m^{L\text{-}Cth}$ values for the measurement of L-Cth hydrolysis with the DTNB and LDH assays, which monitor the production of L-Hcys and pyruvate, respectively. These results suggest that Y111 is an indirect determinant of substrate and

reaction specificity, as although removal of the hydroxyl group of this residue alters the K_m of L-Cth, L-Cys and L-OAS by only 2-6-fold, it enables a conformational change in the active site that allows inhibition of the enzyme by either DTNB or the L-Hcys-TNB mixed disulfide and facilitates the binding of a second molecule of L-Cys, to inhibit the production of pyruvate in favor of lanthionine (Tables 6.1 and 6.2, Figures 6.1 and 6.5). The production of lanthionine from L-Cys has also been reported for hCGL (Chiku *et al.*, 2009). The decrease of only ~2-fold in the k_{cat} of the L-Cth hydrolysis reaction (Table 6.1), in combination with the similarity in the $k_{cat}/K_m^{L\text{-}Cth}$ versus pH profiles of wild-type eCBL and the Y111F variant (Figure 6.4C, Table 6.3), demonstrate that Y111 does not participate in proton transfer from the α-amino group of the substrate to the aminoacrylate product, a role proposed on the basis of the proximity of the Y111 hydroxyl group to Cα of the substrate (Clausen *et al.*, 1996).

6.5.3. Residues Y56 and S339.

The conservation of eCBL-Y56 in all members of the γ-subfamily, as well as many enzymes of the broader fold-type I family, including AAT, ALAS and cystalysin, suggests the involvement of this residue in a process fundamental to the enzymes of this structural class (Cellini *et al.*, 2005; Toney and Kirsch, 1991a; Tan *et al.*, 1998). Conversely, the presence of a serine residue at the position corresponding to eCBL-S339 is restricted to 12 of the 14 structures for members of the γ-subfamily, including CGL, MGL and both plant and bacterial CBL and CGS, suggesting that this residue may act as a determinant of specificity. The side-chain hydroxyl groups of Y56 and S339 are 2.9 and 2.7 Å, respectively, from the ε-amino group of K210, the active-site lysine, in the eCBL-

AVG structure (Figure 6.2) (Clausen *et al.*, 1997). Tethering of the catalytic base in this manner is likely required to enforce reaction specificity, as protonation of position C4' of the cofactor could result in γ-elimination/replacement or transamination, as observed for eCGS and eAATase, respectively (Clausen *et al.*, 1997; Aitken *et al.*, 2003; Eliot and Kirsch, 2004). However, while the minor, 6-fold decrease in k_{cat} observed for the phenylalanine substitution variant of eCBL-Y56 demonstrates that this residue does not participate in catalysis, removal of the hydroxyl group of S339, by the S339A substitution, reduces the k_{cat} for L-Cth hydrolysis by 5600-fold while increasing $K_m^{L\text{-}Cth}$ by only 2-fold (Table 6.1), a result in keeping with a K210-tethering role for this residue. The 340-nm peak observed upon reaction of eCBL-S339A with 3 mM L-Cth is suggestive of pyridoximine (PMP) formation, resulting from protonation of C4' (Figure 6.6). In contrast, the L-Cth substrate is efficiently hydrolyzed by wild-type eCBL and Y56F, via a β-elimination reaction, which does not include the PMP intermediate observed upon reaction of this substrate with the S339A variant (Figure 6.6). This indicates that although the ε-amino group of K210 forms hydrogen bonds to the side chains of both Y56 and S339, only the latter acts as a determinant of reaction specificity, a conclusion in keeping with the conservation of residues corresponding to Y56 and S339 in the broader fold-type I and only the γ-subfamily, respectively. The Y56F substitution is unique among the variants investigated in this study in that it is the only one to exhibit a change in the activity *versus* pH profile (Figure 6.4). A similar increase of ~0.7 pH units in the pK_a value of the acidic limb (pK_{a1}) of the $k_{cat}/K_m^{L\text{-}Cth}$ *versus* pH profile is observed for both R58K and Y56F (Table 6.3) (Lodha *et al.*, 2010). Clausen *et al.*, (1996) suggested a role for R58 in modulating the pK_a of Y111 to enable the latter to transfer a

proton from the α-amino group of the L-Cth substrate, as it enters the active site, to the aminoacrylate leaving group to facilitate release of the iminopropionate product. However, the near wild-type activity and pH profile of Y111 do not support this hypothesis (Figure 6.4, Table 6.3). Therefore, the similar change in the acidic limb of the $k_{cat}/K_m^{L\text{-}Cth}$ versus pH profile is likely an indirect effect resulting from a change in the conformation or charge distribution of the active site resulting from a shift in the positioning of the negatively charged phosphate group of the cofactor, which is tethered in the eCBL active site by 7 hydrogen bonds, including one to Y56 and a pair to R58 (Figure 6.2).

Residues Y56 and S339 are restrained by direct and indirect, respectively, interactions with the cofactor. A 2.6-Å hydrogen bond to OP2 tethers Y56 to the phosphate moiety, while S339 is positioned by the adjacent W340, which interacts with O3` of the cofactor, and by a hydrogen bond between the backbone carbonyl of S339 and the side chain of R372 (Figure 6.2). Residues W340 and R372 form hydrogen bonds to the α-carboxylate group of the substrate or inhibitor bound in Schiff-base linkage with the cofactor in the active site of eCBL (Clausen *et al.* 1997; Lodha *et al.*, 2010). Residue W340, conserved in bacterial CBL, is replaced by a leucine residue in bacterial CGS and fungal and animal CGL sequences. Interestingly, substitution of either Y338 or W340 with phenylalanine results in a 2-3-fold increase in the k_{cat} for L-Cth hydrolysis, demonstrating that the interactions formed by these residues, which flank S339, are not essential for the positioning of the latter (Figure 6.2). Since both Y56 and S339 are restrained by interactions with the cofactor, it is unlikely that either residue adopts a conformation distinct from that observed in the eCBL-AVG complex (Clausen *et al.*,

1997). However, the similarity of the 21 and 28-fold increases in $K_m^{L\text{-}Cth}$ and 6 and 3-fold decreases in k_{cat} observed for the Y56F and R58A variants, respectively, evinces a common role in substrate binding for these residues (Table 6.1). The difference between the 30 and 3-fold increases in the $K_m^{L\text{-}Cth}$ and K_i^{AVG} values of the R58A variant imply that residue R58 binds the distal carboxylate group of L-Cth, not present in AVG (Lodha *et al.*, 2010). Although the K_i^{AVG} of Y56F is increased 50-fold (Table 6.1), suggesting that Y56 interacts with the distal amino group that is common to L-Cth and AVG (Figure 6.1), this contradicts the evidence of the eCBL-AVG structure in which the distal amino group of AVG is 2.8 and 6.5 Å from the side-chain hydroxyl groups of Y111 and Y56, respectively (Figure 6.2) (Clausen *et al.*, 1997). The residue corresponding Y56 of eCBL has been investigated in several fold-type-I enzymes. A common role in binding the phosphate group of PLP, thereby preventing cofactor dissociation, has been reported for Y71 of *Citrobacter freundii* (*C. freundii)* tyrosine phenol lyase (CfTPL), Y70 of *E. coli* AATase (eAATase), Y64 of *Treponema denticola* (*T. denticola*) cystalysin (Td-Cys) and Y121 of murine erythroid ALAS (Toney and Kirsch, 1991b; Chen *et al.*, 1995; Tan *et al.*, 1998; Cellini *et al.*, 2005). Residue Y71 also participates in the α,β-elimination reaction catalyzed by CfTPL, while the 12.5-fold decrease and 3-5-fold increases in the k_{cat} and K_m values of the phenylalanine substitution variant of the corresponding eAATase-Y70 show that this residue does not play an important role in substrate binding or catalysis (Toney and Kirsch, 1991a; Chen *et al.*, 1995). Cellini *et al.,* (2005) observed that, based on the crystal structures, eCBL-Y56 and Td-Cys-Y64 appear to guide the ε-amino group of the active-site lysine (Clausen *et al.*, 1996; Krupka *et al.*, 2000). However, this is not reflected in the modest 7 and 12-fold decreases in the k_{cat}/K_m and k_{cat} values for the α,β-

elimination of β-chloroalanine by Td-Cys-Y64F (Cellini *et al.*, 2005). Interestingly, the K_d^{PLP} and K_m for glycine of the corresponding Y121F variant of meALAS are increased 15 and 34-fold, while the k_{cat} is decreased by only 3-fold (Tan *et al.*, 1998). The glycine substrate of meALAS cannot form a hydrogen bond with the side-chain hydroxyl moiety of Y121. Therefore, Tan *et al.,* (1998) proposed that the observed increase in K_m is due to the increase in K_d^{PLP}. This presents an alternative explanation for the observed 22 and 50-fold increases in the $K_m^{L\text{-}Cth}$ and K_i^{AVG} values of eCBL-Y56F (Table 6.1) that does not require the formation of a hydrogen bond between the hydroxyl moiety of Y56 and the distal amino group of L-Cth or AVG. Additionally, the increased flexibility in positioning of the phenylalanine side chain of Y56F, due to loss of the restraining link to the phosphate moiety of the cofactor, may allow this residue to move toward the entrance of the active site, thereby impeding substrate binding.

6.6. Conclusion

Cystathionine β-lyase is an attractive target for the development of novel antimicrobial compounds because is unique to bacteria and plants. This study has identified Y238, a residue conserved in bacterial CBL sequences, as a determinant of substrate specificity. The identity, position and flexibility of active-site residues are key determinants of both the substrate and reaction specificity, particularly for enzymes dependent on the catalytically versatile PLP cofactor. For example, residue eCBL-S339, which is conserved among many members of the γ-subfamily, has been identified as a determinant of reaction specificity. In contrast, while the ability of an aromatic residue, corresponding to eCBL-Y111, to engage in a π-stacking interaction with the cofactor is a common feature of fold-type-I enzymes the specific identity of this residue varies and substitution of Y111 with phenylalanine only marginally impacts the physiological L-Cth hydrolysis reaction. However, the enhanced L-Cys substrate inhibition of Y111F suggests an indirect role, likely *via* modulation of active-site architecture, for this residue in specificity. The information resulting from this study will guide the design of inhibitors specific for bacterial CBL, a challenging target given the structural similarity of the γ-subfamily enzymes, as well as facilitate protein engineering studies aimed at modifying the substrate and reaction specificity of these enzymes.

Chapter 7. Exploration of the Active Site of *E. coli* Cystathionine γ-Synthase.

7.1. Abstract

Cystathionine γ-synthase (CGS) catalyzes the condensation of *O*-succinyl-L-homoserine and L-cysteine, to produce L-cystathionine and succinate, in the first step of the bacterial transsulfuration pathway. In the absence of L-cysteine the enzyme catalyzes the futile α,γ-elimination of L-OSHS, yielding succinate, α-ketobutyrate and ammonia. A series of 15 site-directed variants of *Escherichia coli* CGS (eCGS) was constructed to probe the roles of active-site residues D45, Y46, R48, R49, Y101, R106, E325, S326 and R361 in binding and catalysis. The effects of these mutations on the catalytic efficiency of the α,γ-elimination reaction range from a reduction of only ~2-fold for R49K and the E325A,Q variants to 370 and 1100-fold for R361K and R48K, respectively. A similar trend is observed for the $k_{cat}/K_m^{L\text{-}OSHS}$ of the physiological, α,γ-replacement reaction. The observed reductions in the catalytic efficiency of the Y46F, R48K, R106A,K and R361K variants are dominated by increases in $K_m^{L\text{-}OSHS}$, while that of S326A reflects the 40-and 360-fold decreases in the k_{cat} values for the α,γ-elimination and α,γ-replacement reactions, respectively. The results of this study suggest that the arginine residues at positions 48 and 106 and at position 361 of eCGS, conserved in bacterial CGS sequences, tether the distal and α-carboxylate moieties, respectively, of the L-OSHS substrate. In contrast, the $K_m^{L\text{-}Cys}$ is not markedly affected by the site-directed replacement of any of the nine residues investigated. The unique decreases in k_{cat} observed for the S326A variant reflect the role of this residue in tethering the side chain of K198, the catalytic base.

7.2. Introduction

Cystathionine γ-synthase (CGS) is the first enzyme of the transsulfuration pathway, which converts L-cysteine (L-Cys) to L-homocysteine (L-Hcys), the immediate precursor of L-methionine (L-Met) (Figure 7.1). The branch-point between L-Met and L-threonine biosynthesis is L-homoserine in bacteria and *O*-phospho-L-homoserine (L-OPHS) in plants. Therefore, the bacterial and plant CGS enzymes condense distinct forms of activated L-homoserine, *O*-succinyl-L-homoserine (L-OSHS) and L-OPHS, respectively, with L-Cys to produce L-cystathionine (L-Cth) (Aitken *et al.*, 2011). Structures are available for *Escherichia coli* CGS (eCGS) and *Nicotiana tabaccum* CGS (nCGS), as well as for the latter in complex with 3-(phosphonomethl)pyridine-2-carboxylic acid (PPCA), 5-carboxymethylthio-3-(3'-chlorophenl)-1,2,4-oxadiazol (CTCPO) and DL-E-2-amino-5-phosphono-3-pentenoic acid (APPA) (Figure 7.1) (Steegborn *et al.*, 2001). These enzymes are attractive targets for the development of novel anti-microbial compounds and herbicides because they are not present in mammals.

The enzymes of the γ-subfamily of fold-type I of PLP-dependent enzymes display remarkable structural similarity, as exemplified by the ~1.5 Å r.m.s. deviation between ~350 C_α atoms observed upon superposition of the structures of eCGS, *T. vaginalis* methionine γ-lyase (tMGL), yeast (*Saccharomyces cerevisiae*) cystathionine γ-lyase (yCGL) and *E. coli* CBL (eCBL), the second enzyme of the bacterial transsulfuration pathway (Messerschmidt *et al.*, 2003). These enzymes catalyze α,β and α,γ elimination and replacement reactions on similar amino acid substrates and share common active-site features, including the residues corresponding to Y46, R48, Y101, S326 and R361 of eCGS, as well as K198, the catalytic base In contrast, the acidic

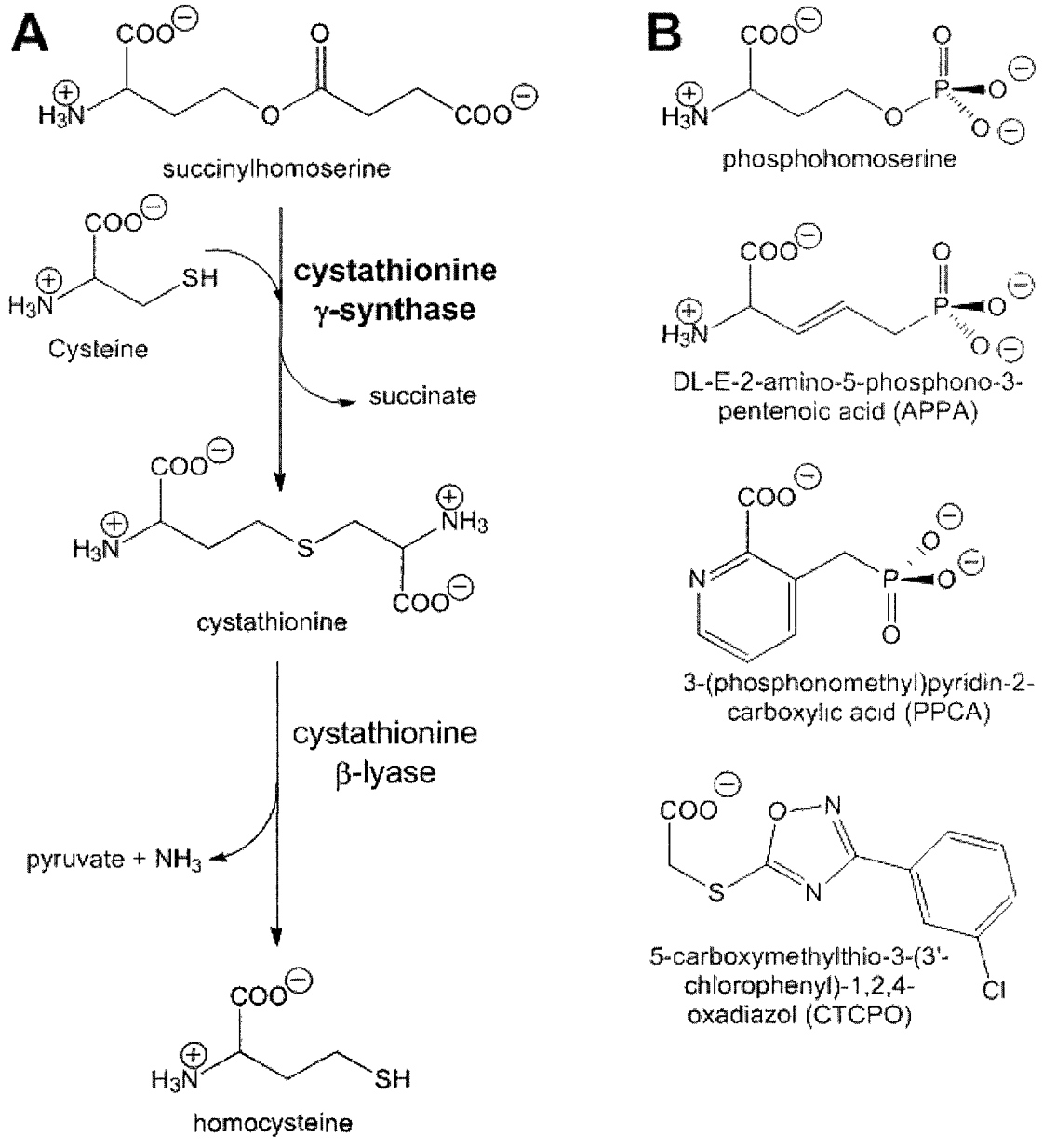

Figure 7.1. (**A**) The bacterial transsulfuration pathway and (**B**) the structures of the L-OSHS substrate and L-Cth product of eCGS and the nCGS inhibitors. (Steegborn *et al.*, 2001; Messerschmidt *et al.*, 200

residues, D45 and E325 of eCGS are shared by CGL sequences, but not by MGL and CBL and eCGS-R49 is common to bacterial CGS and CBL enzymes, but is replaced by a tyrosine residue in the plant enzyme nCGS. Interestingly, an arginine at position 106 of eCGS is conserved in bacterial and plant CGS enzymes, but while this residue is proposed to bind the distal carboxylate of L-OSHS, it does not interact with the phosphonate moiety of APPA, an L-OPHS analog, in the structure of the nCGS complex (Clausen *et al.*, 1998; Steegborn *et al.*, 2001).

The crystal structures of the plant nCGS in complex with the inhibitors CTCPO, PPCA and APPA (Figures 7.1 and 7.2) provides valuable insight into active site interactions (Steegborn *et al.*, 2001). However, the difference in the activated L-homoserine substrates and the active sites of the plant and bacterial enzymes complicates the use of these structures as a model for eCGS (Clausen *et al.*, 1998; Steegborn *et al.*, 1999; Steegborn *et al.*, 2001). Additionally, no information is available concerning the binding site of L-Cys. The side chains of R48, R106, Y101, S326 and R361 and those of E45, R49 and E325 are proposed to bind the L-OSHS and L-Cys substrates, respectively, of eCGS (Clausen *et al.*, 1998). Lodha *et al.,* (2010) demonstrated that residues R58 and R372 of eCBL, which correspond to eCGS-R48 and R361, bind the distal and α-carboxylate moieties of the L-Cth substrate, the product of CGS. A series of 15 site-directed variants of eCGS residues D45, Y46, R48, R49, Y101, R106, E325, S326 and R361 was constructed to probe the specific roles of these residues. The $K_m^{L\text{-}Cys}$ of all variants is within 3-fold of the wild-type enzyme, indicating that the nine targeted residues do not interact directly with the L-Cys substrate. In contrast, the observed increases in the $K_m^{L\text{-}OSHS}$ values of the R48K, R106A,K and R361K variants identify R48,

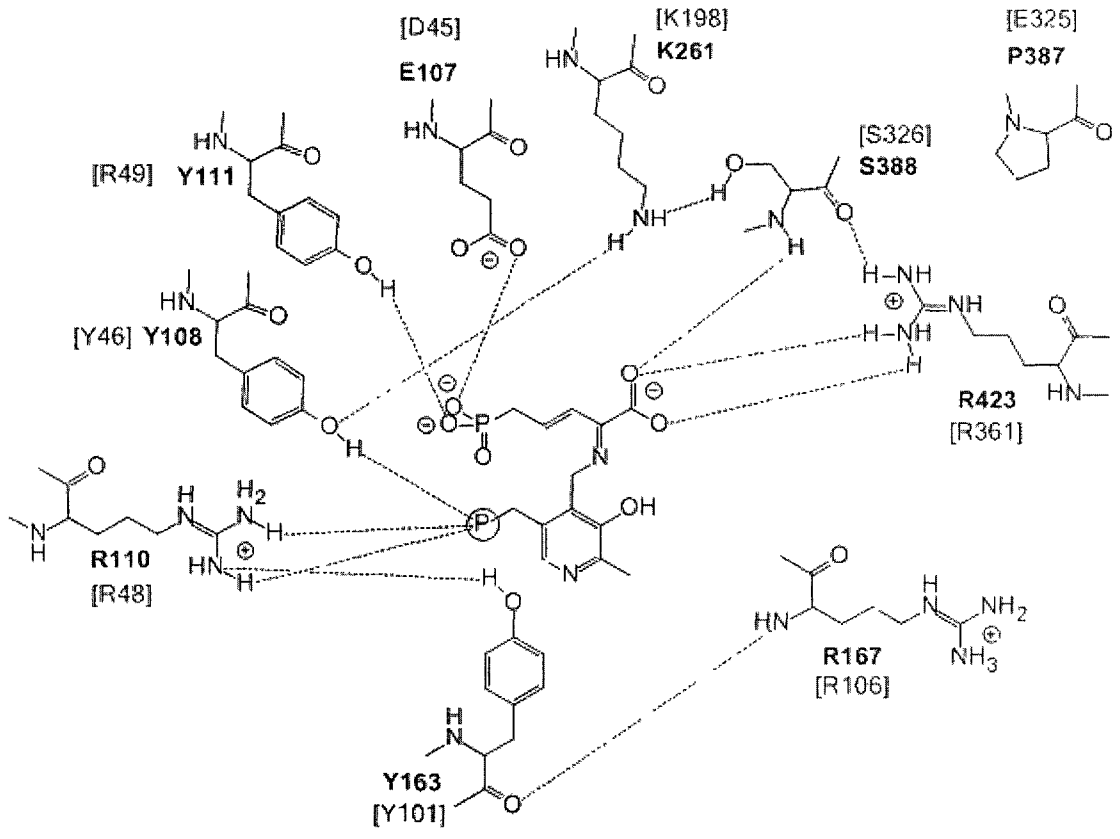

Figure 7.2. Observed contacts of APPA in the active-site of nCGS (Steegborn *et al.* 2001). The dotted lines represent putative hydrogen bond distances of ≤ 3.3 Å between heteroatoms. Corresponding nCGS and eCGS residues: nCGS-E107 (eCGS-D45), nCGS-Y108 (eCGS-Y56), nCGS-R110 (eCGS-R48), nCGS-Y111 (eCGS-R49), nCGS-Y163 (eCGS-Y101), nCGS-R167 (eCGS-R106), nCGS-K261 (eCGS-K198), nCGS-P387 (eCGS-E325), nCGS-S388 (eCGS-S326) and nCGS-R423 (eCGS-R361). The image was constructed using ChemDraw and PDB entry 1I41.

R106 and R361 as residues interacting with L-OSHS. The 40 and 360-fold decreases in the k_{cat} of the α,γ-elimination and replacement activities of the alanine replacement variant of S326 distinguish this residue, which does not participate in substrate binding, but guides the ε-amino group of K198, the catalytic base.

7.3. Materials and Methods

7.3.1. Reagents.

L-Cth, L-Cys, *O*-succinyl-L-homoserine (L-OSHS) and L-lactate dehydrogenase (LDH) were purchased from Sigma. Ni-NTA resin was obtained from Qiagen. Oligonucleotide primers were synthesized by Integrated DNA Technologies and mutants were sequenced by BioBasic prior to expression and purification. The C-terminally, 6-His-tagged eCBL and D-2-Hydroxyisocaproate dehydrogenase (HO-HxoDH) coupling enzymes employed in the eCGS γ-replacement and γ-elimination assays, respectively, were expressed and purified as described previously (Aitken and Kirsch, 2003; Aitken *et al.*, 2003).

7.3.2. Construction, expression and purification of site-directed variants.

Site-directed mutants of eCGS, constructed *via* the overlap-extension polymerase chain reaction method, were inserted into the pTrc-99aAF plasmid. The amino-terminal, 6-His tag and linker encoded by this vector enables affinity purification of the expressed enzymes and does not alter the kinetic parameters of eCGS. Wild-type and site-directed variants of eCGS were expressed in the *E. coli* KS1000 *metB::aadA* strain, in which the gene encoding eCGS is replaced by aadA, encoding resistance to streptomycin, to prevent contamination with the wild-type *E. coli* enzyme. The wild-type and site-directed mutants of eCGS were expressed and purified, *via* Ni-nitrilotriacetic acid affinity chromatography, as described by Farsi *et al.*, (2009).

7.3.3. Determination of steady-state kinetic parameters.

Enzyme activity was measured in a total volume of 100 µL at 25 °C on a Spectramax 340 microtiter plate spectrophotometer (Molecular Devices). The assay buffer was comprised of 50 mM Tris, pH 7.8, with 20 µM PLP. The formation of L-Cth, *via* the condensation of L-OSHS and L-Cys, was detected using the CBL-LDH coupled assay (Aitken *et al.*, 2003). A background reading was recorded, before initiation of the reaction by the addition of enzyme, in all assays. The data for the γ-replacement activity of eCGS were fitted to equations 7.1-7.3 for the modified ping pong mechanism described by Aitken *et al.* (2003), in which the E and R subscripts denote the γ-elimination and γ-replacement activities, respectively, to obtain k_{catR}, $K_{mR}^{L\text{-}Cys}$, $K_{mR}^{L\text{-}OSHS}$, $K_{iR}^{L\text{-}Cys}$, $k_{catR}/K_{mR}^{L\text{-}Cys}$ and $k_{catR}/K_{mR}^{L\text{-}OSHS}$. The independently-determined values of k_{catE} and $K_{mE}^{L\text{-}OSHS}$, for the γ-elimination activity, were substituted into equations 7.1-7.33 to reduce the number of kinetic parameters to be determined (Aitken *et al.*, 2003). Data were fit by nonlinear regression with the SAS software package (SAS Institute, Cary, NC).

$$\frac{v}{[E]} = \frac{k_{catE}K_{mR}^{L-Cys}[L-OSHS] + k_{catR}[L-OSHS][L-Cys]}{K_{mE}^{L-OSHS}K_{mR}^{L-Cys} + K_{mR}^{L-Cys}[L-OSHS] + K_{mR}^{L-OSHS}\left(1+\frac{[L-Cys]}{K_{iR}^{L-Cys}}\right)[L-Cys] + [L-OSHS][L-Cys]} \tag{7.1}$$

$$\frac{v}{[E]} = \frac{k_{catE}K_{mR}^{L-Cys}/K_{mR}^{L-OSHS}[L-OSHS] + k_{catR}/K_{mR}^{L-OSHS}[L-OSHS][L-Cys]}{K_{mE}^{L-OSHS}K_{mR}^{L-Cys}/K_{mR}^{L-OSHS} + K_{mR}^{L-Cys}/K_{mR}^{L-OSHS}[L-OSHS] + \left(1+\frac{[L-Cys]}{K_{iR}^{L-Cys}}\right)[L-Cys] + 1/K_{mR}^{L-OSHS}[L-OSHS][L-Cys]} \tag{7.2}$$

$$\frac{v}{[E]} = \frac{k_{catE}[L-OSHS] + k_{catR}/K_{mR}^{L-Cys}[L-OSHS][L-Cys]}{K_{mE}^{L-OSHS} + [L-OSHS] + K_{mR}^{L-OSHS}/K_{mR}^{L-Cys}\left(1+\frac{[L-Cys]}{K_{iR}^{L-Cys}}\right)[L-Cys] + 1/K_{mR}^{L-Cys}[L-OSHS][L-Cys]} \tag{7.3}$$

Values of k_{cat}, $K_m^{L\text{-}Cys}$ and $K_i^{L\text{-}Cys}$ for the R48K and R361K, for which $K_m^{L\text{-}OSHS}$ exceeds the solubility of L-OSHS, were determined from the fit of velocity versus L-Cys, at the highest concentration of L-OSHS employed, to equation 7.4, which incorporates the $K_i^{L\text{-}Cys}$ term for substrate inhibition by L-Cys. The parameter $k_{cat}/K_m^{L\text{-}Cys}$ was obtained independently from equation 7.5.

$$\frac{v}{[E]} = \frac{k_{cat} \times [S]}{K_m^{L-Cys} + [S]\left(1 + {[S]}/{K_m^{L-Cys}}\right)} \tag{7.4}$$

$$\frac{v}{[E]} = \frac{{k_{cat}}/{K_m} \times [S]}{1 + {[S]}/{K_m}\left(1 + {[S]}/{K_m^{L-Cys}}\right)} \tag{7.5}$$

The hydrolysis of L-OSHS was detected via the continuous γ-elimination assay, in which α-ketobutyrate is reduced, with concomitant oxidation of NADH (ε_{340} = 6,200 $M^{-1}s^{-1}$), by HO-HxoDH (Aitken *et al.*, 2003). Values of $k_{catE}^{L\text{-}OSHS}$ and $K_{mE}^{L\text{-}OSHS}$ were obtained by fitting of the data to the Michaelis-Menten equation and $k_{catE}/K_{mE}^{L\text{-}OSHS}$ was obtained independently from equation 7.6.

$$\frac{v}{[E]} = \frac{{k_{catE}}/{K_{mE}^{OSHS}} \times [S]}{1 + {[S]}/{K_{mE}^{OSHS}}} \tag{7.6}$$

7.4. Results

All of the 15 site-directed variants are soluble, possess detectable α,γ-elimination and replacement activities, with the exceptions of R48A and R361A, and are substrate inhibited by L-Cys, but not L-OSHS (Figure 7.3). Therefore, the α,γ-replacement data were fitted to a ping-pong model, incorporating both the minor α,γ-elimination reaction and inhibition by L-Cys, in which the release of succinate from L-OSHS precedes the binding of L-Cys and subsequent release of L-Cth (Aitken *et al.*, 2003).

7.4.1. The D45A,N, R49A,K, and E325A,Q variants.

The value of $K_{mR}^{L\text{-}Cys}$ is unchanged by site-directed substitutions targeting D45, R49 and E325 (Table 7.1). Although the k_{catR} of the α,γ-replacement activity is reduced 20-fold and $K_{mR}^{L\text{-}OSHS}$ is increased less than 2-fold by the R59A substitution (Table 7.1), the k_{catE} for the α,γ-elimination of L-OSHS is unchanged and $K_{mE}^{L\text{-}OSHS}$ is increased 6-fold, compared to the wild-type enzyme (Table 7.2). In contrast, the kinetic parameters of the R59K variant are identical to those of wild-type eCGS, within experimental error (Tables 7.1 and 7.2). The 4-9-fold reductions in the $k_{catR}/K_{mR}^{L\text{-}OSHS}$ and $k_{catR}/K_{mR}^{L\text{-}OSHS}$ of the alanine and asparagine replacement variants of D45 are the result of ~2-fold changes in k_{catR}, $K_{mR}^{L\text{-}OSHS}$ and $K_{mR}^{L\text{-}Cys}$, with the exception of the 6-fold increase in the $K_{mR}^{L\text{-}OSHS}$ of D45N. Similarly, the 6 and 5-fold decreases in $k_{catE}/K_{mE}^{L\text{-}OSHS}$ are dominated by ~4-fold increases in $K_{mE}^{L\text{-}OSHS}$. Interestingly, while the kinetic parameters of the α,γ-elimination activity are unaffected and the $k_{catR}/K_{mR}^{L\text{-}OSHS}$ and $k_{catR}/K_{mR}^{L\text{-}Cys}$ of eCGS are reduced only 2-3-fold by the alanine and glutamine substitutions of E325, the $K_{mR}^{L\text{-}OSHS}$

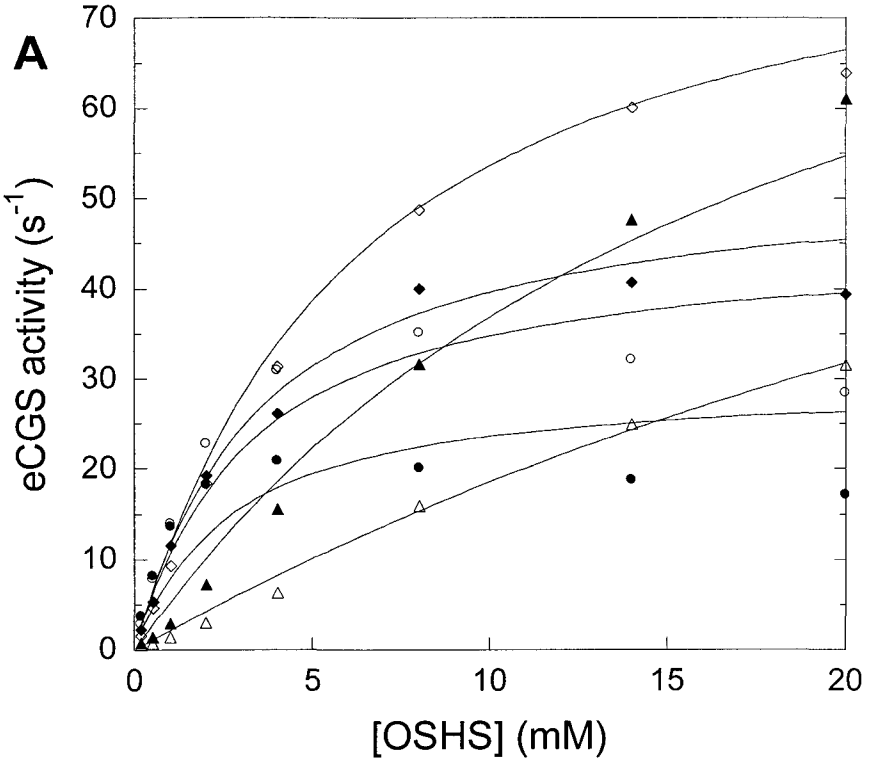
A
eCGS activity (s^{-1})
[OSHS] (mM)
0
10
20
30
40
50
60
70
0
5
10
15
20

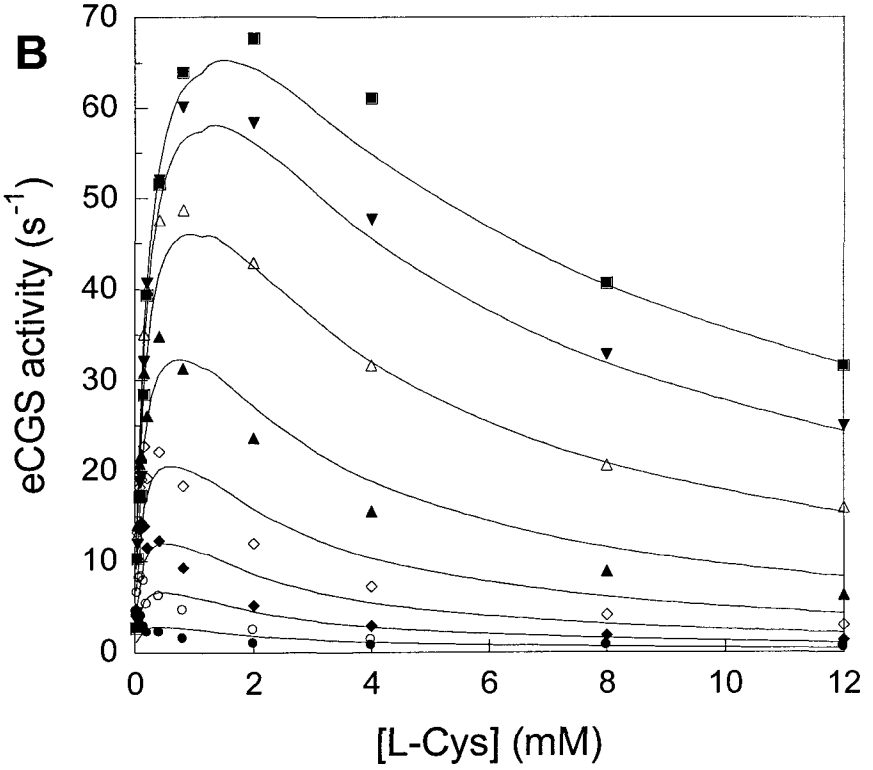
B
eCGS activity (s^{-1})
[L-Cys] (mM)
0
10
20
30
40
50
60
70
0
2
4
6
8
10
12

Figure 7.3. The dependence of wild-type eCGS activity on (**A**) L-OSHS concentration, measured at 0.075 mM Cys (●), 0.15 mM Cys (○), 0.2 mM Cys (♦), 0.8 mM Cys (◊), 4 mM Cys (▲), 12 mM Cys (Δ), and (**B**) L-Cys concentration, measured at 0.2 mM L-OSHS (●), 0.5 mM L-OSHS (○), 1 mM L-OSHS (♦), 2 mM L-OSHS (◊), 4 mM L-OSHS (▲), 8 mM L-OSHS (Δ), 14 mM L-OSHS (▼), 20 mM L-OSHS (■). Reaction conditions: 0.2-20 mM L-OSHS, 0.025-12 mM L-Cys, 1.3 mM NADH, 1.0 μM eCBL, 1.0 μM LDH and 0.05-0.1 μM wild-type or variant eCGS, depending on the activity of the enzyme, in assay buffer at 25 °C.

Table 7.1. Kinetic parameters for the condensation of L-OSHS and L-Cys by wild-type site-directed variants of eCGS.[a]

Enzyme	k_{catR} (s^{-1})	$K_{mR}^{L\text{-}OSHS}$ (mM)	$K_{mR}^{L\text{-}Cys}$ (mM)	$K_{iR}^{L\text{-}Cys}$ (mM)	$k_{catR}/K_{mR}^{L\text{-}OSHS}$ ($M^{-1}s^{-1}$)	$k_{catR}/K_{mR}^{L\text{-}Cys}$ ($M^{-1}s^{-1}$)
eCGS[b]	121 ± 5	2.5 ± 0.5	0.11 ± 0.01	0.33 ± 0.09	$(4.9 \pm 0.9) \times 10^4$	$(1.06 \pm 0.07) \times 10^6$
eCGS[c]	91 ± 8	3.0 ± 0.7	0.43 ± 0.06		$(3.0 \pm 0.6) \times 10^4$	$(3.2 \pm 0.2) \times 10^5$
eCGS	112 ± 5	4.4 ± 0.6	0.24 ± 0.02	1.2 ± 0.2	$(2.5 \pm 0.3) \times 10^4$	$(4.7 \pm 0.4) \times 10^5$
D45A	59 ± 5	11 ± 2	0.47 ± 0.06	0.9 ± 0.1	$(5.4 \pm 0.7) \times 10^3$	$(1.25 \pm 0.09) \times 10^5$
D45N	76 ± 9	26 ± 5	0.55 ± 0.09	1.6 ± 0.2	$(2.9 \pm 0.2) \times 10^3$	$(1.4 \pm 0.1) \times 10^5$
Y46F	6 ± 1	90 ± 20	0.6 ± 0.1	1.8 ± 0.2	71 ± 5	$(1.13 \pm 0.08) \times 10^4$
R48K[c]	0.15 ± 0.01	n.s.[d]	0.22 ± 0.03	2.5 ± 0.5	2.1 ± 0.1	$(6.8 \pm 0.6) \times 10^2$
R49A	5.7 ± 0.5	2.9 ± 0.6	0.12 ± 0.03	0.9 ± 0.3	No fit	$(5.5 \pm 0.7) \times 10^4$
R49K	120 ± 20	6 ± 2	0.32 ± 0.08	0.9 ± 0.3	$(2.0 \pm 0.5) \times 10^4$	$(3.7 \pm 0.6) \times 10^5$
Y101F	9.6 ± 0.2	1.9 ± 0.2	0.15 ± 0.01	0.34 ± 0.05	$(5.2 \pm 0.7) \times 10^3$	$(6.4 \pm 0.3) \times 10^4$
R106A	$0.34 \pm 0.02^{L\text{-}Cys}$ $0.44 \pm 0.03^{L\text{-}OSHS}$	40 ± 4	0.61 ± 0.07	6.8 ± 0.8	11.0 ± 0.5	$(5.6 \pm 0.4) \times 10^2$
R106K	5.3 ± 0.5	39 ± 5	0.65 ± 0.08	2.9 ± 0.3	$(1.4 \pm 0.1) \times 10^2$	$(8.2 \pm 0.5) \times 10^3$
E325A	59 ± 3	0.7 ± 0.2	0.17 ± 0.02	0.24 ± 0.07	$(9 \pm 2) \times 10^4$	$(3.5 \pm 0.4) \times 10^5$
E325Q	57 ± 3	1.1 ± 0.3	0.29 ± 0.04	0.26 ± 0.08	$(5 \pm 1) \times 10^4$	$(2.0 \pm 0.2) \times 10^5$
S326A	0.31 ± 0.02	21 ± 3	0.20 ± 0.04	2.3 ± 0.3	15 ± 1	$(1.6 \pm 0.2) \times 10^3$
R361K[c]	0.50 ± 0.04	n.s.[d]	0.22 ± 0.04	0.25 ± 0.4	5.4 ± 0.2	$(2.3 \pm 0.2) \times 10^3$

[a]Kinetic parameters reported are for condensation of L-OSHS and L-Cys. Reaction conditions: 0.1-50 mM L-OSHS, 0.025-20 mM L-Cys, 1.3 mM NADH, 1.0 μM eCBL, 1.0 μM LDH and 0.094-21.25 μM wild-type or variant eCGS, depending on the activity of the enzyme, in assay buffer at 25 °C. The data were fit to the equations 7.1-7.3.
[b]Kinetic parameters of eCGS reported by Aitken *et al.* (2003).
[c]Kinetic parmeters of eCGS reported by Farsi *et al.* (2009).
[d]n.s. indicates that $K_m^{L\text{-}OSHS}$ exceeds the solubility limit of the L-OSHS, such that $k_{cat}/K_m^{L\text{-}OSHS}$ was determined via linear regression, at the L-Cys concentration for which maximal activity was observed, and k_{cat}, $K_m^{L\text{-}Cys}$ and $K_i^{L\text{-}Cys}$ were determined from the fit of velocity versus L-Cys, at the highest concentration of L-OSHS employed, to equation 7.4.

Table 7.2. Kinetic parameters of the α,γ-elimination of L-OSHS by wild-type site-directed variants of eCGS.[a]

Enzyme	k_{catE} (s^{-1})	$K_{mE}^{L\text{-}OSHS}$ (mM)	$k_{catE}/K_{mE}^{L\text{-}OSHS}$ ($M^{-1}s^{-1}$)
eCGS[b]	1.80 ± 0.05	1.3 ± 0.1	(1.35 ± 0.09) × 10^3
eCGS[c]	2.02 ± 0.05	0.64 ± 0.09	(3.2 ± 0.4) × 10^3
eCGS	3.56 ± 0.05	1.27 ± 0.8	(2.8 ± 0.1) × 10^3
D45A	1.61 ± 0.04	3.7 ± 0.3	(4.3 ± 0.2) × 10^2
D45N	2.64 ± 0.05	4.6 ± 0.3	(5.8 ± 0.2) × 10^2
Y46F	1.8 ± 0.1	23 ± 2	78 ± 3
R48K	0.7 ± 0.2	230 ± 80	2.63 ± 0.03
R49A	1.60 ± 0.04	8.2 ± 0.4	(1.96 ± 0.06) × 10^2
R49K	2.99 ± 0.09	1.5 ± 0.2	(2.0 ± 0.2) × 10^3
Y101F	1.74 ± 0.04	6.3 ± 0.4	(2.8 ± 0.1) × 10^2
R106A	0.5 ± 0.02	25 ± 2	19.9 ± 0.8
R106K	0.99 ± 0.05	20 ± 2	51 ± 3
E325A	2.4 ± 0.1	1.5 ± 0.3	(1.6 ± 0.2) × 10^3
E325Q	2.5 ± 0.1	2.0 ± 0.3	(1.2 ± 0.1) × 10^3
S326A	0.093 ± 0.002	9.3 ± 0.6	10.0 ± 0.4
R361K	0.73 ± 0.06	97 ± 10	7.6 ± 0.2

[a]Kinetic parameters reported are for hydrolysis of L-OSHS. Reaction conditions: 0.1-50 mM L-OSHS and 1-26.25 μM wild-type or variant eCGS, depending on the activity of the enzyme, in assay buffer at 25 °C. The data were fit to the Michaelis-Menten equation to obtain k_{cat} and $K_m^{L\text{-}OSHS}$ and equation 7.4 to obtain $k_{cat}/K_m^{L\text{-}OSHS}$.
[b]Values for wild-type eCGS are from Aitken *et al.* (2003).
[c]Values for wild-type eCGS from Farsi *et al.* (2009).

and $K_{iR}^{L\text{-}Cys}$ values of E325A are both decreased 6-fold, while those of E325Q are decreased 4 and 5-fold, respectively (Tables 7.1 and 7.2, Figure 7.4).

7.4.2. The R48K, R106A,K and R361K variants.

The 140, 55, 1100 and 370-fold decreases in the catalytic efficiency of the α,γ-elimination activity of the R106A, R106K, R48K and R361K variants are dominated by 20, 16, 180 and 80-fold increases in $K_{mE}^{L\text{-}OSHS}$, respectively, as the k_{catE} is increased only 4-7-fold (Table 7.2). The $K_{mR}^{L\text{-}OSHS}$ and $K_{mR}^{L\text{-}Cys}$ values, for the physiological, α,γ-replacement activity, of the R106A and R106K variants are both increased, by 9 and 3-fold, respectively. In contrast, the ~300-fold decrease in the k_{catR} of R106A is 15-fold greater than that of R106K. The data for the R48K and R361K variants could not be fit to equations 7.1-7.3 as saturation kinetics were not observed within the solubility of the L-OSHS substrate. Therefore, with the assumption that $K_{mR}^{L\text{-}OSHS} >>$ [L-OSHS], the Michaelis-Menten equation was modified to obtain $k_{catR}/K_{mR}^{L\text{-}OSHS}$, at the concentration of L-Cys at which each enzyme displays maximal activity (Table 7.1). Values of k_{catR}, $K_{mR}^{L\text{-}Cys}$, $K_{iR}^{L\text{-}Cys}$ and $k_{catR}/K_{mR}^{L\text{-}Cys}$ were determined for the R48K and R361K variants from the fit of velocity versus L-Cys, at the highest concentration of L-OSHS employed, to equations 7.4 and 7.5. The $K_m^{L\text{-}Cys}$ and $K_i^{L\text{-}Cys}$ values of these enzymes are within 5-fold of wild-type eCGS, while the 750 and 220-fold decreases in k_{catR} make considerable contribution to the 12000 and 4600-fold reductions in $k_{catR}/K_{mR}^{L\text{-}OSHS}$ of the lysine substitution variants of R48 and R361 (Table 7.1).

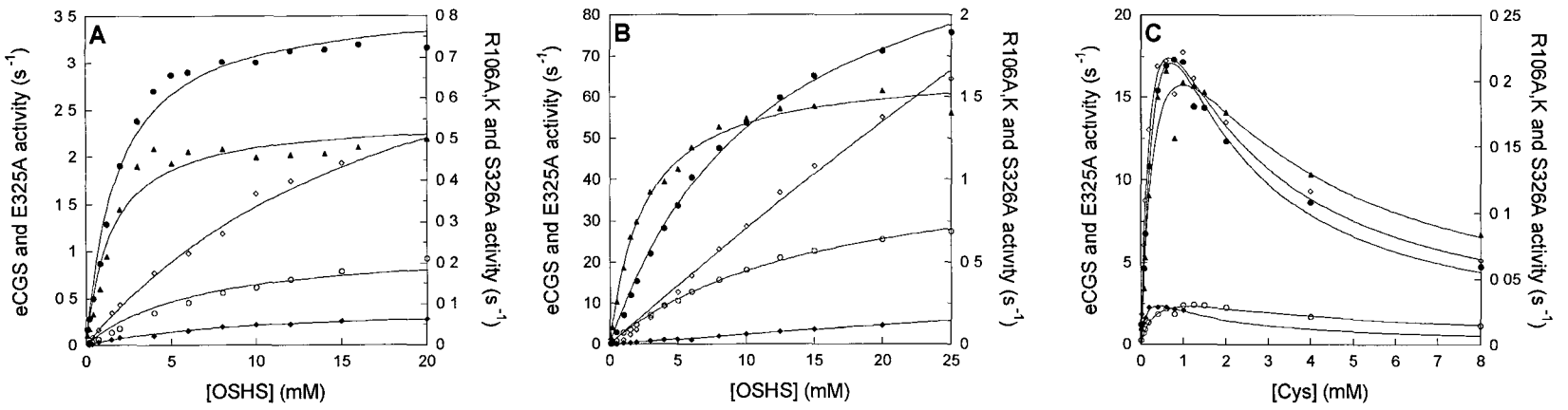

Figure 7.4. The dependence of the activity of wild-type eCGS (●) and the R106A (○), R106K (◊), E325A (▲) and S326A (♦) site-directed variants on substrate concentration. (**A**) The α,γ-elimination activity is plotted *versus* L-OSHS concentration. Reaction conditions: 0.1-50 mM L-OSHS and 1-26.25 μM wild-type or variant eCGS, depending on the activity of the enzyme, in assay buffer at 25 °C. The α,γ-replacement activity is plotted *versus* (**B**) L-OSHS and (**C**) L-Cys concentration. Reaction conditions: 0.1-50 mM L-OSHS (at 1 mM L-Cys), 0.025-20 mM L-Cys (at 10 mM L-OSHS), 1.3 mM NADH, 1.0 μM eCBL, 1.0 μM LDH and 0.05-21.25 μM wild-type or variant eCGS, depending on the activity of the enzyme, in assay buffer at 25 °C.

7.4.3. The Y46F, Y101F and S326A variants.

The 350-fold decrease in the $k_{catR}/K_{mR}^{L\text{-}OSHS}$ of the α,γ-replacement activity of eCGS-Y56F is comprised of equal, ~20-fold changes in k_{catR} and $K_{mR}^{L\text{-}OSHS}$, while the $K_{mR}^{L\text{-}Cys}$ is increased by only 3-fold. Although the k_{catE} of the minor α,γ-elimination activity of Y56F is unchanged, compared to the wild-type enzyme, a similar, 18-fold increase is observed for $K_{mE}^{L\text{-}OSHS}$. The k_{catE} and k_{catR} of eCGS-Y101F are reduced 2 and 12-fold, respectively. Interestingly, although the changes in K_m resulting from this substitution are within a factor of five of eCGS, the 5-fold increase in the $K_{mE}^{L\text{-}OSHS}$ contrasts with the 2 and 4-fold decreases in $K_{mR}^{L\text{-}OSHS}$ and $K_{iR}^{L\text{-}Cys}$. The 40 and 360-fold decreases in k_{catE} and k_{catR}, respectively, of eCGS-S339A are unique among the site-directed variants investigated and the corresponding $K_{mE}^{L\text{-}OSHS}$ and $K_{mR}^{L\text{-}OSHS}$ values are increased by only 7 and 5-fold, respectively (Tables 7.1 and 7.2).

7.5. Discussion

The enzymes of the γ-subfamily of fold-type I, including those of the transsulfuration pathways, comprise an exemplary model system for investigation of the structure-function relationships underlying substrate and reaction specificity in PLP-dependent enzymes. The structural similarity of CGS, CBL and CGL extends to the active site as five of the residues proposed to participate in substrate binding and catalysis are conserved in these three enzymes, from both prokaryotic and eukaryotic species (Messerschmidt *et al.*, 2003; Lodha *et al.*, 2010). These conserved positions include a pair of arginines (eCGS-R48 and R361), two tyrosines (eCGS-Y46 and Y101) and a serine residue (eCGS-S326). The conformation and orientation of substrate(s) within the active site as well as freedom of rotation about the C_α-C_β bond of the substrate have been proposed to be determinants of reaction specificity among the enzymes of the γ-subfamily (Clausen *et al.*, 1997; Lodha *et al.*, 2010). Therefore, exploration of the roles of active-site residues in these enzymes, dependent on the versatile PLP cofactor, is necessary in order to decipher to subtle and complex structure-function relationships of these structurally similar, but mechanistically distinct enzymes. Therefore, the characterization of a series of 15 site-directed variants of nine eCGS active-site residues (D45, Y46, R48, R49, Y101, R106, E325, S326 and R361) is the focus of the current study.

7.5.1. The D45A,N, R49A,K, and E325A,Q variants.

The acidic residues D45 and E325 and basic residue R49 were proposed by Clausen *et al.,* (1998) to interact with the α-amino and α-carboxylate groups,

respectively, of the L-Cys substrate. The near-native $K_{mR}^{L\text{-}Cys}$ values of the alanine substitution variants of these residues, which remove their hydrogen-bonding capacity, do not substantiate this theory (Table 7.1). The 20-fold reduction in the k_{catR} and the 6-fold increase in the $K_{mE}^{L\text{-}OSHS}$, of the α,γ-replacement and elimination reactions suggest that replacement of R49 with alanine subtly alters the architecture of the active site. The wild-type kinetic parameters of the R49K variant, unaltered despite the ~1-Å shorter side-chain of lysine, confirm that this residue does not play a direct role in substrate binding or catalysis. In contrast with the corresponding R59 of eCBL, which forms a salt bridge with residue E235 of the neighboring subunit of the catalytic dimer, the side chain of eCGS-R49 does not interact with other amino acids (Clausen *et al.*, 1998). The 4-9-fold reductions in the $k_{catE}/K_{mE}^{L\text{-}OSHS}$ and $k_{catR}/K_{mR}^{L\text{-}OSHS}$ of the D45A and D45N variants reflect minor, 2-4-fold changes in k_{cat} and $K_m^{L\text{-}OSHS}$ resulting from subtle alterations in active-site architecture or the positioning of water molecules. In contrast, Farsi *et al.*, (2009) reported that replacement of residue D45 with phenylalanine decreases k_{cat} by 16-fold and causes a 6-fold increase in $K_m^{L\text{-}Cys}$. These results suggest that, although this residue does not participate directly in substrate binding, it is situated in proximity to the L-Cys binding site. Similarly, the unique 4-6-fold decreases in the $K_{mR}^{L\text{-}OSHS}$ and $K_{iR}^{L\text{-}Cys}$ values of the alanine and glutamine substitutions of E325 (Table 7.1, Figure 7.4) indicate that this residue is located in the L-OSHS binding site, such that its negative charge deters L-Cys from binding in place of L-OSHS.

7.5.2. The R48K, R106A,K and R361K variants.

Docking studies with eCGS indicated roles for three arginine residues, R48/R106 and R361, in binding the distal and α-carboxylate moieties, respectively, of the L-OSHS substrate (Clausen *et al.*, 1998). This model is supported by the 180, ~20 and 80-fold increases in $K_{mE}^{L\text{-}OSHS}$ for the α,γ-elimination activity of the R48K, R106A,K and R361K variants, respectively (Table 7.2). Similarly, the $K_{mR}^{L\text{-}OSHS}$ value for the α,γ-replacement activity is increased 9-fold by substitution of R106 with alanine or lysine, while the R58K and R361K variants are not saturated within the solubility limit of L-OSHS (Table 7.1). Residue R106 of eCGS is conserved as an arginine in prokaryotic and eukaryotic CGS and CGL sequences and replaced by an aspartate in bacterial CBL (eCBL-D116). Substitution of the side chain of D116, located 8.3 Å from the distal amino group of AVG, does not modify the kinetic parameters of eCBL (Clausen *et al.*, 1997; Lodha *et al.*, 2010). Similarly, the side-chain of R167 of the plant nCGS enzyme, which corresponds to eCGS-R106 and eCBL-D116, is oriented away from the phosphonate moiety of the inhibitor in the eCGS-APPA complex (Figure 7.2), suggesting that while this residue likely does not bind the distal phosphate group of the L-OPHS substrate, it may interact with the α-carboxylate of L-Cys (Steegborn *et al.*, 2001). In contrast, the 9 and ~20-fold increases in the $K_{mR}^{L\text{-}OSHS}$ and $K_{mE}^{L\text{-}OSHS}$ values of the R106A,K variants, demonstrate that this residue interacts with the distal portion of the larger L-OSHS substrate of eCGS (Tables 7.1 and 7.2, Figure 7.1). The α-carboxylate group of APPA forms a pair of hydrogen bonds to the side chain of R423 of nCGS, which corresponds to eCGS-R361 (Figure 7.2) (Steegborn *et al.*, 2001). The 80-fold increase in the $K_{mE}^{L\text{-}OSHS}$ and lack of L-OSHS saturation observed for the α,γ-replacement activity of R361K

(Tables 7.1 and 7.2), support the proposed role of R361 in L-OSHS binding. An identical 80-fold increase in $K_m^{L\text{-}Cth}$ has been reported for the corresponding R372K variant of eCBL, which also interacts with the α-carboxylate moiety of the inhibitor in the eCBL-AVG complex (Clausen *et al.*, 1997; Lodha *et al.*, 2010). The 220-fold decrease in the kcat of the α,γ-replacement activity of eCGS-R361K is in keeping with the 55-fold decrease in this parameter reported for the corresponding AATase-R386K (Inoue *et al.*, 1989; Vacca *et al.*, 1997), but contrasts with the 4-fold decrease in the k_{cat} of CBL-R372K (Lodha *et al.*, 2010). The observed reductions in the activity of the eCGS and eAATase variants reflects differences in the binding orientation and conformation of the substrates, such that they are not optimally positioned for catalysis (Vacca *et al.*, 1997). In contrast, the substantially smaller decrease in the k_{cat} of eCBL-R372K reflects the facile nature of the α,β-elimination of L-Cth, which, when compared to the transamination of eAATase and α,γ-replacement reaction of eCGS, does not require the generation of a ketimine intermediate or the binding of a second substrate. Suboptimal positioning and conformation of L-OSHS within the active site of eCGS is also proposed to explain the observed 300 and 750-fold decreases in the k_{catR} of the R106A and R48K variants.

7.5.3. The Y46F, Y101F and S326A variants.

Clausen *et al.*, (1998) proposed that residues Y101 and S326 participate in binding the distal and α-carboxylate groups, respectively, of L-OSHS, a model which is not supported by the minor, 2 and 5-fold changes in $K_{mR}^{L\text{-}OSHS}$ of the Y101F and S326A variants, respectively (Table 7.1). The tyrosine at position 46 of eCGS was targeted for

investigation in this study because phenylalanine substitution variants of the corresponding residue in diverse fold-type I enzymes, including Y56 of eCBL (Chapter 6 of this thesis), Y70 of *E. coli* aspartate aminotransferase, Y121 of murine erythroid aminolevulinate synthase (meALAS), Y71 of *C. freundii* tyrosine phenol lyase and Y64 of *T. denticola* cystalysin, have been reported to impact substrate binding (Toney and Kirsch, 1991; Chen *et al.*, 1995; Tan *et al.*, 1998; Cellini *et al.*, 2005). The 20-fold decrease in k_{catR} and 20-fold increases in $K_{mR}^{L\text{-}OSHS}$ and $K_{mE}^{L\text{-}OSHS}$ of eCGS-Y46F (Table 7.1) are of similar magnitude as the 6-fold decrease in k_{cat} and 20-fold increase in $K_m^{L\text{-}Cth}$ of the corresponding Y56F variant of eCBL (Table 6.1). Based on the similar, 15-fold increase in the K_m for glycine of the corresponding meALAS-Y121F variant, Tan *et al.* (1998) proposed that the observed increase in K_m is due to the increase in K_d^{PLP} of the cofactor, rather than a direct interaction with the substrate, as glycine does not possess a side chain. Given that the hydrogen bond between the phosphate moiety of the cofactor and residue Y121 of meALAS, is conserved in eCBL and eCGS, the observed increases in the K_m values of the corresponding Y56F and Y46F variants, may also reflect the absence of this link rather than a direct interaction with the substrate. The 2-12-fold changes in the kinetic parameters of eCGS-Y101F demonstrate that Y101 is not involved in catalysis, indicating that the role proposed for this residue in proton transfer between the α-amino group of L-OSHS and the succinate leaving group is not observed (Clausen *et al.*, 1998). The 40 and 360-fold decreases in k_{catE} and k_{catR}, respectively, of eCGS-S326A are unique among the site-directed variants investigated (Tables 7.1 and 7.2). Residue S326 is proposed to guide and tether the ε-amino group of K198, the catalytic base. The presence of a serine residue in this position is unique to the enzymes of the γ-

subfamily of fold-type I. A 5600-fold decrease in k_{cat} for the hydrolysis of L-Cth has been observed for the corresponding S339A variant of eCBL (Table 6.1). The 140-fold greater effect of the S339A substitution on the k_{cat} of α,β-elimination activity of eCBL, compared to the α,γ-elimination activity of eCGS is insightful. The ε-amino group of eCBL-K210 must be more strictly restrained than the corresponding eCGS-K198 because protonation of C4' of the cofactor is required in the α,γ-elimination reaction of eCGS, but must be prevented in eCBL.

7.6. Conclusion

Cystathionine γ-synthase is an attractive target for the development of novel antimicrobial compounds because it is unique to plants and bacteria and it catalyzes the first reaction in the transsulfuration pathway. The design of effective inhibitors of the bacterial CGS enzyme requires an in-depth characterization of the active-site residues participating in substrate binding. This study has identified R48/R106 and R361 as residues interacting with the distal and α-carboxylate groups, respectively, of the L-OSHS substrate. However the negligible effect of the 15 site-directed variants on $K_m^{L\text{-}Cys}$ demonstrates that the nine residues investigated do not directly participate in L-Cys binding. A residue that will be targeted to expand this study is eCGS-N227, corresponding to eCBL-Y238, which has been shown to interact with the distal carboxylate of the substrate in Chapter 6 of this thesis.

8. CONCLUSION

Modern medical and agricultural practices are rapidly exhausting the pool of effective anti-infective agents, a problem compounded by the observation that the last novel class of antibiotic compounds was discovered more than two decades ago. The current generation of antibiotics is a result of minor modifications to existing therapeutics. The lack of novel antimicrobial compounds reflects the established tendency to target the major cellular processes that distinguish prokaryotic pathogens from their mammalian hosts. These targets include the enzymes involved in cell wall biosynthesis, protein, DNA and RNA synthesis and the folate cycle (Hurdle *et al.,* 2011). Since amino acid biosynthesis is strictly controlled in micro-organisms and up-regulated to allow rapid growth during an infection, targeting the anabolic pathways of the essential amino acids, defined from the perspective of human nutrition, for the development of inhibitors is a viable option for expansion of the repository of conventional anti-microbial targets (Ejim *et al.*, 2007).

The enzymes catalyzing transformations of amino acids are generally dependent on the pyridoxal 5'-phosphate (PLP) cofactor. Despite decades of research, the question of how the protein component of these enzymes regulates the chemistry of this versatile cofactor, to select for only one of the plethora of possible reactions, remains an important area of investigation. The enzymes of the transsulfuration and reverse transsulfuration pathways, which interconvert L-Cys and L-Hcys, the precursors of glutathione and of L-Met and SAM biosynthesis, respectively, provide an excellent model system to investigate the structure-function relationships that underlie substrate and reaction specificity in PLP-dependent enzymes. Additionally, studies on *Salmonella enterica* and

E. coli have shown increased expression of genes related to methionine biosynthetic pathway during infection, demonstrating that the enzymes of the transsulfuration pathway are suitable targets for the development of antimicrobial compounds (Becker *et al.*, 2006 and Wei *et al.*, 2001). The transsulfuration pathway of plants and bacteria, which converts L-Cys and *O*-activated-L-homoserine, to L-Hcys, pyruvate, ammonia and phosphate or succinate, is comprised of the enzymes cystathionine-γ-synthase (CGS) and cystathionine-β-lyase (CBL). In contrast, cystathionine-β-synthase (CBS) precedes cystathionine-γ-lyase (CGL) in the yeast and mammalian reverse transsulfuration pathway, which converts L-Ser and L-Hcys to L-Cys, α-ketobutyrate and ammonia. These enzymes catalyze side-chain rearrangements of similar amino acid substrates, L-Cys, L-Hcys, L-Cth, L-Ser and *O*-activated-L-homoserine, *via* distinct α,β or α,γ-elimination or replacement reactions. Site-directed replacement of specific active-site residues, proposed to be involved in substrate and/or cofactor binding, of the *E. coli* CGS, CBL and yeast CBS enzymes was performed to define their roles in the modulation of substrate and reaction specificity. The knowledge resulting from this work will guide the development of therapeutics, including novel anti-infective compounds and treatments for the genetic disease homocystinuria, as well as facilitate the engineering of specificity in the enzymes of the γ-subfamily of the large and diverse fold-type I class of PLP-dependent enzymes.

The reported characterization of the L-Ser binding site of the CBS enzyme by Aitken and Kirsch, (2004) demonstrated the involvement of ytCBS residues S82, T81 and Q157 in L-Ser binding and reaction specificity. The role of S289 in regulating the chemistry of the cofactor, *via* interaction with the pyridinium nitrogen, and the E1cB mechanism of the α,γ-replacement reaction catalyzed by ytCBS were subsequently

demonstrated by Quazi and Aitken, (2009). Chapters 3 and 4 of this thesis describe the continuation of this work by probing the L-Hcys binding site and the role of residue N84, which forms a hydrogen bond to the phenolic O3' of the cofactor. Five active-site residues of ytCBS, capable of forming hydrogen bonds to the α-amino and α-carboxylate groups of L-Hcys, were selected on the basis of their location at the mouth of the active site and through *in silico* docking studies. The 18-fold increase in the $K_m^{L\text{-}Hcys}$ of H138F suggests that this residue plays an indirect, possibly water-mediated, role in binding L-Hcys. The recent structure of the *D. melanogaster* enzyme confirmed the earlier proposal that this enzyme undergoes a conformational change, involving the rigid-body movement of the small subdomain of the catalytic domain, to result in closure of the active site, thereby protecting reactive intermediates from solvent (Aitken and Kirsch, 2004; Koutmos *et al.*, 2010). The residues corresponding to Y158 and Y248 of ytCBS are shifted upon substrate binding and closure of the active site in dCBS. As a result, the role of these two residues, not evident in the earlier structures of the open conformation of hCBS, is elucidated by the structure of the dCBS-L-Ser complex. The residue corresponding to ytCBS-Y158 shifts ~1-2.1 Å and that corresponding to ytCBS-Y248 shifts ~4.2-4.7 Å and rotates ~90° when the two available hCBS structures are compared to those of dCBS and the dCBS-L-Ser complex (Meier *et al.*, 2001; Taoka *et al.*, 2002; Koutmos *et al.*, 2010). The repositioning of these residues and formation of hydrogen bonds between Y248 and the side-chain hydroxyl groups of Y158 and the serine substrate demonstrates the role of the former in substrate binding and in bridging the active-site (Meier *et al.*, 2001; Taoka *et al.*, 2001; Koutmos *et al.*, 2010). The observed ~100-fold reduction in the k_{cat} of ytCBS-Y248F, in combination with the lack of α,β-elimination

activity observed for this variant, suggest that although Y248 plays an important, but not essential, role in the β-replacement reaction of ytCBS, likely by facilitating the elimination of the hydroxyl leaving group, it is not a determinant of reaction specificity (Lodha *et al.*, 2009).

The interaction between the distal carboxylate group of L-Cth and the ε-amino group of K112, predicted on the basis of *in silico* docking, is not reflected in the near wild-type values of the K_m of L-Hcys of site-directed variants of this residue. However, the 50 and 90-fold increases in the K_m of L-Ser of the K112L and K112R substitutions, respectively, are of similar magnitude to that observed for the S82A variant of ytCBS (Aitken and Kirsch, 2004; Lodha *et al.*, 2009). The corresponding stOASS-S69 and dCBS-S121 move ~7 Å upon ligand-induced closure of the active site and the spectral characteristics of the alanine-replacement variant of stOASS-S69 indicate that the active site remains partially open following substrate binding (Burkhard *et al.*, 1999; Tian *et al.*, 2010). Residue hCBS-K177, which corresponds to K112 of ytCBS, is involved in a hydrogen-bonding network (S147-K177-E304-K384 of hCBS) that bridges the opposing sides of the active-site cleft. This network of interactions, maintained in the open and closed conformations of the dCBS active site, links the mobile loop of residues (146-150 of hCBS), which interacts with the α-carboxylate group of the L-Ser substrate, with loops 296-316 and 374-388, which cover a large portion of the active-site surface (Meier *et al.*, 2001). The knowledge of the CBS active site derived from the work described in chapters 3 and 4 will guide future experiments probing the complex regulation of CBS. Additionally, it expands our understanding of the mechanism of homocystinuria-

associated mutations of this enzyme, information that is essential for the development of therapeutics for this metabolic disease.

Detailed steady-state and presteady-state characterizations of *E. coli* CGS have demonstrated the complexity of the α,γ-replacement reaction catalyzed by this enzyme (Brzovic *et al.*, 1990; Aitken *et al.*, 2003). The development of continuous assays for the α,γ-elimination and replacement activities of eCGS and for the α,β-elimination activity of eCBL has enabled studies probing the structure-function relationships that define the specificity of these enzymes (Aitken *et al.*, 2003). Farsi *et al.,* (2009) determined that the interconversion of a pair of conserved aromatic residues of eCBL (F55 and Y338) and the corresponding acidic D45 and E325 of eCGS is not sufficient to modify the reaction specificity of these enzymes, a theory that had been proposed on the basis of comparison of the active sites of these structurally similar enzymes (Messerschmidt *et al.*, 2003). Chapters 5-7 of this thesis describe the continuation of this work in the detailed characterization of a selection of active-site residues, proposed to interact with the substrate(s) and cofactor, of eCGS and eCBL.

While the eCBL-AVG and nCGS-APPA complexes provide useful models of substrate binding, AVG lacks the distal carboxylate group of L-Cth and the interactions of the distal succinate moiety of L-OSHS, as well as those of L-Cys, cannot be predicted based on the structure of the L-OPHS-analog (APPA) in complex with the plant nCGS enzyme (Clausen *et al.*, 1997). Chapters 5 and 6 describe the investigation of site-directed variants of eCBL residues Y56, R58, R59, Y111, D116, Y238, Y338, S339, W340 and R372, proposed to be involved in substrate binding. The effect of targeted substitutions of

a similar selection of active-site residues of eCGS (D45, Y46, R48, R49, Y101, R106, E325, S326 and R361) is presented in chapter 7.

The differential impact of the alanine and lysine substitutions of eCBL-R58, compared to R59, on the hydrolysis of L-Cth and reaction with AVG identify the former as interacting with the distal carboxylate moiety of the L-Cth substrate. The corresponding R48 of eCGS was also investigated. The inactivity of the eCGS-R48A variant, in combination with the lack of saturation with the L-OSHS substrate, observed for eCGS-R48K, demonstrate that this residue plays a similar role in substrate binding as eCBL-R58. Comparison of the kinetic parameters for L-Cth hydrolysis with those for inhibition of eCBL by AVG indicates that residue Y238 also binds the distal carboxylate group of the substrate. The 20-50-fold increases in the $K_m^{L\text{-}Cth}$ and K_i^{AVG} of eCBL-Y56F and in the $K_m^{L\text{-}OSHS}$ of the α,γ-elimination and replacement activities of the corresponding eCGS-Y46F substitution suggest that this residue may interact with the distal amino group of these compounds. However, an indirect role in binding, mediated by the observed hydrogen bond between the side-chain hydroxyl group of this residue and the phosphate moiety of the PLP cofactor, observed in both enzymes, is more likely (Clausen *et al.*, 1996; Clausen *et al.*, 1998).

A role for residue eCBL-R58 in modulation of the pK_a of Y111 has been proposed to facilitate proton transfer between the α-amino group of L-Cth substrate and the iminopropionate product of eCBL (Clausen *et al.*, 1996). However, the observed ~0.6 pH unit increase in the pK_a of the acidic limb and decrease in the pK_a of the basic limb of the $k_{cat}/K_m^{L\text{-}Cth}$ versus pH profiles of R58K and R58A, respectively, are likely the result of conformational changes in the active site resulting from mutation of R58 (Lodha *et al.*,

2010). Additionally, the near-native $k_{cat}/K_m^{L\text{-}Cth}$ and pH profile of eCBL-Y111F, demonstrate that residue Y111 does not play a role in proton transfer. The guanindino group of eCBL-R58 forms two hydrogen bonds with the phosphate moiety of the PLP cofactor (Clausen *et al.*, 1996; Clausen *et al.*, 1997). This interaction anchors the side chain of R58, providing rigidity and precisely positioning the distal portion of the L-Cth substrate with respect to the cofactor. Tethering of the distal carboxylate and amino groups of L-Cth has been proposed to be a determinant of reaction specificity, *via* partitioning of bound substrate or reactive intermediates (Clausen *et al.*, 1997). Residue D116 of eCBL corresponds to eCGS-R106, proposed to interact with the distal carboxylate group of L-OSHS (Clausen *et al.*, 1998; Brzovic *et al.*, 1990). Although D116 is conserved as asparate in bacterial CBL sequences, mutation of this residue to alanine or asparagine has negligible effect on the kinetic parameters of eCBL, demonstrating that this residue does not interact with the distal amino group of L-Cth (Lodha *et al.*, 2010). In contrast, substitution of eCGS-R106 with alanine or lysine increases the $K_m^{L\text{-}OSHS}$ for the α,γ-elimination and replacement activities by 10-20-fold, indicating that this residue, conserved in bacterial and plant CGS, plays a minor role in binding the distal carboxylate moiety of L-OSHS. The $K_m^{L\text{-}Cys}$ was not impacted by any of the 15 site-directed substitutions of the nine eCGS active-site residues investigated. Therefore, the model proposed by Clausen *et al.* (1998) for binding of the α-amino and α-carboxylate groups of the L-Cys substrate by D45/E325 and R361, respectively, is not supported by the biochemical characterization of these residues.

The eCBL-AVG and nCGS-APPA structures demonstrates that, typical of fold-type I enzymes, the α-carboxylate moiety of the ligand interacts with an active-site

arginine residue (Clausen *et al.*, 1997; Ejim *et al.*, 2007). Replacement of eCBL-R372 with either alanine or leucine results in a drastic, six-order-of- magnitude decrease in catalytic efficiency for the hydrolysis of L-Cth. The corresponding three-order of magnitude increase in the IC_{50} of AVG of these variants demonstrates that R372 plays an essential role in binding the α-carboxylate group of both compounds (Lodha *et al.*, 2010). The conserved R361 of eCGS was also targeted for investigation. The inactivity of the eCGS-R361A variant, in combination with the lack of saturation with the L-OSHS substrate, observed for eCGS-R361K, demonstrate that this residue plays a similar role in substrate binding as eCBL-R372. Replacement of the corresponding eAATase-R386, which binds the α-carboxylate group of its aspartate substrate, produces a similar effect and the R375A substitution of hCGL abolishes H_2S production from L-Cys (Vacca *et al.*, 1997; Huang *et al.*, 2010). The hydrogen bond between the side-chain of eCBL residue W340 and the α-carboxylate group of the inhibitor in the eCBL-AVG complex is secondary to the role of R372 in substrate and inhibitor binding, as demonstrated by the 10 and 25-fold increases in the K_m of L-Cth and IC_{50} of AVG of the W340F variant (Lodha *et al.*, 2010). This residue is conserved as tryptophan and leucine in CBL and CGL/CGS sequences, respectively.

The 40-and 360-fold decreases in the k_{cat} values for the α,γ-elimination and α,γ-replacement reactions, respectively, observed for eCGS-S326A and the corresponding 5600-fold decrease in the k_{cat} of L-Cth hydrolysis by eCBL-S339A are unique among the site-directed variants of these enzymes. A similar role in tethering the side chain of the active-site lysine residue, which acts as the catalytic base, is proposed for eCBL-S339 and eCGS-S326. The presence of a serine residue in this position is unique to the

enzymes of the γ-subfamily of fold-type I. The 140-fold greater effect of the S339A substitution on the k_{cat} of α,β-elimination activity of eCBL, compared to the α,γ-elimination activity of eCGS suggests that the ε-amino group of eCBL-K210 must be more strictly restrained than the corresponding eCGS-K198. This is likely because protonation of C4' of the cofactor is required in the α,γ-elimination reaction of eCGS, but must be prevented by eCBL, a model supported by the observed formation of pyridoxamine, an intermediate in PLP-catalyzed transamination reactions, following incubation of the S339A variant with the L-Cth substrate of eCBL. This intermediate is not observed upon reaction of the wild-type eCBL enzyme with L-Cth.

The similarities and differences observed between the effects of site-directed variants of active-site residues on the kinetic parameters of eCGS and eCBL can guide the design of specific inhibitors for these enzymes. A pair of conserved arginine residues anchors the distal and proximal regions of the di-carboxylic substrates of eCBL (R58 and R372) and eCGS (R48 and R361). These common residues can form a pair of salt bridges to enhance inhibitor binding affinity. In contrast, substitution of eCGS-R106 impacts binding of the distal region of the L-OSHS substrate, a trend not observed for the corresponding D116 of eCBL. Additionally, eCBL-Y238 and W340, which are replaced by aspargine and leucine, respectively, in eCGS (N227 and L327), interact with the distal and proximal carboxylate groups of L-Cth, respectively. Two further residues that distinguish the active sites of these enzymes are F55 and Y338 of eCBL, which correspond to D45 and E325 of eCGS. Inhibitors for eCBL and eCGS should employ R58/R48 and R372R361 to provide an anchor in the active site, while the interaction with

residues F55, D116, Y238, Y338 and W340 of eCBL and the corresponding D45, R106, N227, E325 and L327 of eCGS can be exploited to enhance specificity.

The studies described in chapters 3-7 of this thesis have employed site-directed mutagenesis to explore the active sites of the PLP-dependent enzymes of the transsulfuration pathways. Among these four enzymes, CBS is the unique representative of fold-type II. Factors determining active-site dynamics and the shielding of reactive intermediates are determinants of α,β-replacement versus elimination specificity in fold-type II enzymes, as exemplified by ytCBS, stTrpS and stOASS. In contrast, active-site architecture and the specific conformation in which substrates are bound likely regulate reaction specificity in eCBL, eCGS and yCGL, the fold-type-I enzymes of the transsulfuration pathways. A thorough understanding of the mechanisms controlling substrate and reaction specificity is a necessary step to enable the engineering of PLP-dependent enzymes. This work is also essential for the development of novel antimicrobial compounds and of therapeutics for genetic diseases, including homocystinuria.

9. REFERENCES

Abe, K., and Kimura, H. (1996). The possible role of hydrogen sulfide as an endogenous neuromodulator. *Journal of Neuroscience, 16*(3), 1066-1071.

Adams, E. (1969). Fluorometric determination of pyridoxal phosphate in enzymes. *Analytical Biochemistry, 31*(1), 118-122.

Ahmed, S. A., Ruvinov, S. B., Kayastha, A. M., and Miles, E. W. (1991). Mechanism of mutual activation of the tryptophan synthase alpha and beta subunits. analysis of the reaction specificity and substrate-induced inactivation of active site and tunnel mutants of the beta subunit. *Journal of Biological Chemistry, 266*(32), 21548-21557.

Aitken, S. M., and Kirsch, J. F. (2003). Kinetics of the yeast cystathionine β-synthase forward and reverse reactions: continuous assays and the equilibrium constant for the reaction. *Biochemistry, 42*(2), 571-578.

Aitken, S. M., Kim, D. H., and Kirsch, J. F. (2003). *Escherichia coli* cystathionine γ-synthase does not obey ping-pong kinetics. Novel continuous assays for the elimination and substitution reactions. *Biochemistry, 42*(38), 11297-11306.

Aitken, S. M., and Kirsch, J. F. (2004). Role of active-site residues Thr81, Ser82, Thr85, Gln157, and Tyr158 in yeast cystathionine β-synthase catalysis and reaction specificity. *Biochemistry, 43*(7), 1963-1971.

Aitken, S. M., and Kirsch, J. F. (2005). The enzymology of cystathionine biosynthesis: Strategies for the control of substrate and reaction specificity. *Archives of Biochemistry and Biophysics, 433*(1), 166-175.

Aitken, S.M., Lodha, P.L. and Morneau, D.J.K. (2011). The enzymes of the transsulfuration pathways: active-site characterizations. *Biochimica et Biophysica Acta (BBA) - Proteins & Proteomics*. In press.

Allen, T.W., Sridhar, V., Prasad, S.G., Han, Q., Xu, M., Tan, Y., Hoffman, R.M. and Ramaswamy, S. (2009a). Methionine γ-lyase from *Trichomonas vaginales.* Unpublished crystal structure. PDB accession: 1PFF

Allen, T.W., Sridhar, V., Prasad, S.G., Han, Q., Xu, M., Tan, Y., Hoffman, R.M. and Ramaswamy, S. (2009b). Crystal Structure of L-methionine α,γ-lyase. Unpublished crystal structure. PDB accession: 1PG8

Alting, A. C., Engels, W., van Schalkwijk, S., and Exterkate, F. A. (1995). Purification and characterization of cystathionine β-lyase from *Lactococcus lactis* subsp.

cremoris B78 and its possible role in flavor development in cheese. *Applied and Environmental Microbiology, 61*(11), 4037-4042.

Aono, S., Honma, Y., Ohkubo, K., Tawara, T., Kamiya, T., and Nakajima, H. (2000). CO sensing and regulation of gene expression by the transcriptional activator CooA. *Journal of Inorganic Biochemistry, 82*(1-4), 51-56.

Astner, I., Schulze, J. O., van den Heuvel, J., Jahn, D., Schubert, W. D., and Heinz, D. W. (2005). Crystal structure of 5-aminolevulinate synthase, the first enzyme of heme biosynthesis, and its link to XLSA in humans. *EMBO Journal, 24*(18), 3166-3177.

Avraham, T., Badani, H., Galili, S., and Amir, R. (2005). Enhanced levels of methionine and cysteine in transgenic alfalfa (*Medicago sativa* L.) plants over-expressing the arabidopsis cystathionine γ-synthase gene. *Plant Biotechnology Journal, 3*(1), 71-79.

Awata, S., Nakayama, K., Suzuki, I., Sugahara, K., and Kodama, H. (1995). Changes in cystathionine γ-lyase in various regions of rat brain during development. *Biochemistry and Molecular Biology International, 35*(6), 1331-1338.

Bachmann, B. J., Low, K. B., and Taylor, A. L. (1976). Recalibrated linkage map of *Escherichia coli* K-12. *Bacteriological Reviews, 40*(1), 116-167.

Bailey, G. B., Chotamangsa, O., and Vuttivej, K. (1970). Control of pyridoxal phosphate enzyme reaction specificity studied with alpha-dialkylamino acid transaminase. *Biochemistry, 9*(16), 3243-3248.

Bashford, D. and D. Case. (2000). Generalized born models of macro-molecular solvation effects. *Annual Review of Physical Chemistry, 51*, 129-152.

Belfaiza, J., Parsot, C., Martel, A., de la Tour, C. B., Margarita, D., Cohen, G. N., *et al.* (1986). Evolution in biosynthetic pathways: Two enzymes catalyzing consecutive steps in methionine biosynthesis originate from a common ancestor and possess a similar regulatory region. *Proceedings of the National Academy of Sciences of the United States of America, 83*(4), 867-871.

Berzelius, J.J. (1833). Calculus urinairs. *Traite Chem. 7*, 424.

Binkley, F. (1951). Synthesis of cysathionine by preparations from rat liver. *Journal of Biological Chemistry, 191*(2), 531-534.

Binkley, F., Christensen, G. M., and Jensen, W. N. (1952). Pyridoxine and the transfer of sulfur. *Journal of Biological Chemistry, 194*(1), 109-113.

Blumenstein, L., Domratcheva, T., Niks, D., Ngo, H., Seidel, R., Dunn, M. F., *et al.* (2007). βQ114N and βT110V mutations reveal a critically important role of the substrate alpha-carboxylate site in the reaction specificity of tryptophan synthase. *Biochemistry, 46*(49), 14100-14116.

Borcsok, E., and Abeles, R. H. (1982). Mechanism of action of cystathionine synthase. *Archives of Biochemistry and Biophysics, 213*(2), 695-707.

Bradford, M. M. (1976). A rapid and sensitive method for the quantitation of microgram quantities of protein utilizing the principle of protein-dye binding. *Analytical Biochemistry, 72,* 248-54.

Braunstein, A. E., and Kritzman, M. G. (1937) *Biokhimiya, 2,* 859-874.

Braunstein, A. E., and Kritzman, M. G. (1946) *Nature, 158.* 102

Braunstein, A. E.,and M.M. Shemyakin. (1953) *Biokhimiya 18,* 393 - 411.

Breitinger, U., Clausen, T., Ehlert, S., Huber, R., Laber, B., Schmidt, F., *et al.* (2001). The three-dimensional structure of cystathionine β-lyase from arabidopsis and its substrate specificity. *Plant Physiology, 126*(2), 631-642.

Brenton, D. P., Cusworth, D. C., and Gaull, G. E. (1965). Homocystinuria. Biochemical studies of tissues including a comparison with cystathioninuria. *Pediatrics, 35,* 50-56.

Brown, G. B., and du Vigneaud, V. (1941). The synthesis of s-(β-amino-β-carboxyethyl)-homocysteine. *Journal of Biological Chemistry, 137*(2), 611-615.

Bryce, C. F. A. (1979). SAM - semantics and misunderstandings. *Trends in Biochemical Sciences, 4*(3), N62-N63.

Brzovic, P., Holbrook, E. L., Greene, R. C., and Dunn, M. F. (1990). Reaction mechanism of *Escherichia coli* cystathionine γ-synthase: Direct evidence for a pyridoxamine derivative of vinylgloxylate as a key intermediate in pyridoxal phosphate dependent γ-elimination and γ-replacement reactions. *Biochemistry, 29*(2), 442-451.

Burkhard, P., Rao, G. S., Hohenester, E., Schnackerz, K. D., Cook, P. F., and Jansonius, J. N. (1998). Three-dimensional structure of O-acetylserine sulfhydrylase from *Salmonella typhimurium. Journal of Molecular Biology, 283*(1), 121-133.

Burkhard, P., Tai, C. H., Ristroph, C. M., Cook, P. F., and Jansonius, J. N. (1999). Ligand binding induces a large conformational change in O-acetylserine sulfhydrylase from *Salmonella typhimurium. Journal of Molecular Biology, 291*(4), 941-953.

Butz, L. W., and du Vigneaud, V. (1932). The formation of a homologue of cystine by the decomposition of methionine with sulfuric acid. *Journal of Biological Chemistry, 99*(1), 135-142.

Cammarata, P. S., and Cohen, P. P. (1950). The scope of the transamination reaction in animal tissues. *The Journal of Biological Chemistry, 187*(1), 439-452.

Carroll, W. R., Stacy, G. W., and du Vigneaud, V. (1949). α-Ketobutyric acid as a product in the enzymatic cleavage of cystathionine. *Journal of Biological Chemistry, 180*(1), 375-382.

Carson, N. A., Cusworth, D. C., Dent, C. E., FIeld, C. M., NeilL, D. W., and Westall, R. G. (1963). Homocystinuria: A new inborn error of metabolism associated with mental deficiency. *Archives of Disease in Childhood, 38*, 425-436.

Carson, N. A., and Neill, D. W. (1962). Metabolic abnormalities detected in a survey of mentally backward individuals in Northern Ireland. *Archives of Disease in Childhood, 37*, 505-513.

Cellini, B., Bertoldi, M., Montioli, R. and Voltattorni, C.B. (2005). Probing the role of Tyr64 of *Treponema denticola* cystalysin by site-directed mutagenesis and kinetic studies. *Biochemistry, 44,* 13970-13980.

Chen, H.-Y., Demidkina, T. V. and Phillips, R. S. (1995). Site-directed mutagenesis of tyrosine 71 to phenylalanine in *Citrobacter freundii* tyrosine phenol-lyase: Evidence for dual roles of tyrosine 71 as a general acid catalyst in the reaction mechanism and in cofactor binding. *Biochemistry, 34*, 12276-12283.

Chenna, R., Sugawara, H., Koike, T., Lopez, R., Gibson, T. J., Higgins, D. G., Thompson, J. D. (2003). Multiple sequence alignment with the Clustal series of programs. *Nucleic Acids Research, 31*(13),3497-500.

Cherney, M. M., Pazicni, S., Frank, N., Marvin, K. A., Kraus, J. P., and Burstyn, J. N. (2007). Ferrous human cystathionine β-synthase loses activity during enzyme assay due to a ligand switch process. *Biochemistry, 46*(45), 13199-13210.

Chiku, T., Padovani, D., Zhu, W., Singh, S., Vitvitsky, V., and Banerjee, R. (2009). H_2S biogenesis by human cystathionine γ-lyase leads to the novel sulfur metabolites lanthionine and homolanthionine and is responsive to the grade of hyperhomocysteinemia. *Journal of Biological Chemistry, 284*(17), 11601-11612.

Chopra, I., Hesse, L., and O'Neill, A. J. (2002). Exploiting current understanding of antibiotic action for discovery of new drugs. *Journal of Applied Microbiology, 92*, 4S-15S.

Christen, P., Jaussi, R., Juretic, N., Mehta, P. K., Hale, T. I., and Ziak, M. (1990). Evolutionary and biosynthetic aspects of aspartate aminotransferase isoenzymes and other aminotransferases. *Annals of the New York Academy of Sciences, 585*, 331-338.

Christen, P., and Mehta, P. K. (2001). From cofactor to enzymes. the molecular evolution of pyridoxal-5'-phosphate-dependent enzymes. *Chemical Records, 1*(6), 436-447.

Clausen, T., Huber, R., Laber, B., Pohlenz, H. D., and Messerschmidt, A. (1996). Crystal structure of the pyridoxal-5'-phosphate dependent cystathionine β-lyase from *Escherichia coli* at 1.83 A. *Journal of Molecular Biology, 262*(2), 202-224.

Clausen, T., Huber, R., Messerschmidt, A., Pohlenz, H. D., and Laber, B. (1997). Slow-binding inhibition of *Escherichia coli* cystathionine β-lyase by L-aminoethoxyvinylglycine: A kinetic and X-ray study. *Biochemistry, 36*(41), 12633-12643.

Clausen, T., Huber, R., Prade, L., Wahl, M. C., and Messerschmidt, A. (1998). Crystal structure of *Escherichia coli* cystathionine γ-synthase at 1.5 A resolution. *The EMBO Journal, 17*(23), 6827-6838.

Clausen, T., Wahl, M. C., Clausen, T., Wahl, M. C., Fuhrmann, J. C., Laber, B., *et al.* (1999). Cloning, purification and characterisation of cystathionine γ-synthase from nicotiana tabacum. *Biological Chemistry, 380*(10), 1237-1242.

Dancs, G., Kondrak, M., and Banfalvi, Z. (2008). The effects of enhanced methionine synthesis on amino acid and anthocyanin content of potato tubers. *BMC Plant Biology, 8*(1), 65.

Danishefsky, A. T., Onnufer, J. J., Petsko, G. A., and Ringe, D. (1991). Activity and structure of the active-site mutants R386Y and R386F of *Escherichia coli* aspartate aminotransferase. *Biochemistry, 30*(7), 1980-1985.

Datko, A. H., Giovanelli, J., and Mudd, S. H. (1974). Homocysteine biosynthesis in green plants. *Journal of Biological Chemistry, 249*(4), 1139-1155.

Delavier-Klutchko, C., and Flavin, M. (1965a). Enzymatic synthesis and cleavage of cystathionine in fungi and bacteria. *Journal of Biological Chemistry, 240*(6), 2537-2549.

Delavier-Klutchko, C., and Flavin, M. (1965b). Role of a bacterial cystathionine β-cleavage enzyme in disulfide decomposition. *Biochimica et Biophysica Acta (BBA) - Enzymology and Biological Oxidation, 99*(2), 375-377.

Dominy, J. E., and Stipanuk, M. H. (2004). New roles for cysteine and transsulfuration enzymes: Production of H_2S, A neuromodulator and smooth muscle relaxant. *Nutrition Reviews, 62*(9), 348-353.

Droux, M., Ravanel, S., and Douce, R. (1995). Methionine biosynthesis in higher plants .II. purification and characterization of cystathionine β-lyase from spinach chloroplasts. *Archives of Biochemistry and Biophysics, 316*(1), 585-595.

du Vigneaud, V., Chandler, J. P., Moyer, A. W., and Keppel, D. M. (1939). The effect of choline on the ability of homocystine to replace methionine in the diet. *Journal of Biological Chemistry, 131*(1), 57-76.

du Vigneaud, V., Dyer, H. M., and Kies, M. W. (1939). A relationship between the nature of the vitamin b complex supplement and the ability of homocystine to replace methionine in the diet. *Journal of Biological Chemistry, 130*(1), 325-340.

Dunathan, H. C. (1966). Conformation and reaction specificity in pyridoxal phosphate enzymes. *Proceedings of the National Academy of Sciences of the United States of America, 55*(4), 712-716.

Dunathan, H. C., and Voet, J. G. (1974). Stereochemical evidence for the evolution of pyridoxal phosphate enzymes of various function from a common ancestor. *Proceedings of the National Academy of Sciences of the United States of America, 71*(10), 3888-3891.

Dunathan, H. C., Davis, L., Kury, P. G., and Kaplan, M. (1968). Stereochemistry of enzymic transamination. *Biochemistry, 7*(12), 4532-4537.

Dunaway-Mariano, D. (2008). Enzyme function discovery. *Structure, 16*(11), 1599-1600.

Dwivedi, C. M., Ragin, R. C., and Uren, J. R. (1982a). Cloning, purification, and characterization of β-cystathionase from *Escherichia coli. Biochemistry, 21*(13), 3064-3069.

Dwivedi, C. M., Ragin, R. C., and Uren, J. R. (1982b). Cloning, purification, and characterization of β-cystathionase from *E. coli. Biochemistry, 21*(13), 3064-3069.

Edwards, T.E., Gardberg, A.S. and Sankaran. B. (2010). Crystal structure of O-succinyl-homoserine sulfhydrylase from *Mycobacterium tuberculosis* covalently bound to pyridoxal-5-phosphate. Unpublished crystal structure. PDB accession: 3NDN.

Ejim, L. J., Blanchard, J. E., Koteva, K. P., Sumerfield, R., Elowe, N. H., Chechetto, J. D., *et al.* (2007). Inhibitors of bacterial cystathionine β-lyase: Leads for new antimicrobial agents and probes of enzyme structure and function. *Journal of Medicinal Chemistry, 50*(4), 755-764.

Eliot, A. C., and Kirsch, J. F. (2004). Pyridoxal phosphate enzymes: Mechanistic, structural, and evolutionary considerations. *Annual Review of Biochemistry, 73*, 383-415.

Ellman, G. L. (1959). Tissue sulfhydryl groups. *Archives of Biochemistry and Biophysics, 82*(1), 70-77.

Eto, K., Asada, T., Arima, K., Makifuchi, T., and Kimura, H. (2002). Brain hydrogen sulfide is severely decreased in alzheimer's disease. *Biochemical and Biophysical Research Communications, 293*(5), 1485-1488.

Farsi, A., Lodha, P. H., Skanes, J. E., Los, H., Kalidindi, N., and Aitken, S. M. (2009). Interconversion of a pair of active-site residues in *Escherichia coli* cystathionine γ-synthase, *E. coli* cystathionine β-lyase, and *S. cerevisiae* cystathionine γ-lyase and development of tools for the investigation of their mechanisms and reaction specificity. *Biochemistry and Cell Biology, 87*(2), 445-457.

Federiuk, C. S., and Shafer, J. A. (1983). A reaction pathway for transimination of the pyridoxal 5'-phosphate in D-serine dehydratase by amino acids. *The Journal of Biological Chemistry, 258*(9), 5372-5378.

Ferguson, D.M. and Raber D.J. (1989). A New Approach to Probing Conformational Space with Molecular Mechanics: Random Incremental Pulse Search. *Journal of the American Chemical Society, 111*, 4371-4378.

Finkelstein, J. D., and Martin, J. J. (1984). Methionine metabolism in mammals. distribution of homocysteine between competing pathways. *Journal of Biological Chemistry, 259*(15), 9508-9513.

Finkelstein, J. D. (1974). Methionine metabolism in mammals: The biochemical basis for homocystinuria. *Metabolism: Clinical and Experimental, 23*(4), 387-398.

Finkelstein, J. D. (2000). Homocysteine: A history in progress. *Nutrition Reviews, 58*(7), 193-204.

Finkelstein, J. D., Kyle, W. E., Martin, J. J., and Pick, A. (1975). Activation of cystathionine synthase by adenosylmethionine and adenosylethionine. *Biochemical and Biophysical Research Communications, 66*(1), 81-87.

Flavin, M., and Slaughter, C. (1964). Cystathionine cleavage enzymes of *Neurospora*. *Journal of Biological Chemistry, 239*(7), 2212-2219.

Fleming, A. (1929). On the antibacterial action of cultures of a *Penicillium* with special reference to their use for the isolation of *B. infuenzae*. *British Journal of Experimental Pathology 10*, 226-236.

Frimpter, G. W. (1965). Cystathioninuria: Nature of the defect. *Science, 149*(3688), 1095-1096.

Gallagher, D. T., Gilliland, G. L., Xiao, G., Zondlo, J., Fisher, K. E., Chinchilla, D., *et al.* (1998). Structure and control of pyridoxal phosphate dependent allosteric threonine deaminase. *Structure, 6*(4), 465-475.

Gentry-Weeks, C. R., Spokes, J., and Thompson, J. (1995). β-Cystathionase from *Bordetella avium*. *Journal of Biological Chemistry, 270*(13), 7695-7702.

Gerritsen, T., Vaughn, J. G., and Waisman, H. A. (1962). The identification of homocystine in the urine. *Biochemical and Biophysical Research Communications, 9*(6), 493-496.

Glasner, M. E., Gerlt, J. A., and Babbitt, P. C. (2006). Evolution of enzyme superfamilies. *Current Opinion in Chemical Biology, 10*(5), 492-497.

Goodall, G., Mottram, J. C., Coombs, G. H. and Lapthorn, A. J. (2001). Methionine γ-lyase from *Trichomonas vaginales.* Unpublished crystal structure. PDB accession: 1E5F.

Goldberg, J. M., Swanson, R. V., Goodman, H. S., and Kirsch, J. F. (1991). The tyrosine-225 to phenylalanine mutation of *Escherichia coli* aspartate aminotransferase results in an alkaline transition in the spectrophotometric and kinetic pKa values and reduced values of both k_{cat} and K_m. *Biochemistry, 30*(1), 305-312.

Graber, R., Kasper, P., Malashkevich, V. N., Sandmeier, E., Berger, P., Gehring, H., *et al.* (1995). Changing the reaction specificity of a pyridoxal-5'-phosphate-dependent enzyme. *European Journal of Biochemistry / FEBS, 232*(2), 686-690.

Guggenheim, S., and Flavin, M. (1969a). Cystathionine γ-synthase. *Journal of Biological Chemistry, 244*(22), 6217-6227.

Guggenheim, S., and Flavin, M. (1969b). Cystathionine γ-synthase from *Salmonella*. *Journal of Biological Chemistry, 244*(13), 3722-3727.

György, P. (1934). Vitamin B_2 and the pellagra-like dermatitis in rats [8]. *Nature, 133*(3361), 498-499.

Hacham, Y., Matityahu, I., Schuster, G., and Amir, R. (2008). Overexpression of mutated forms of aspartate kinase and cystathionine γ-synthase in tobacco leaves resulted in the high accumulation of methionine and threonine. *The Plant Journal, 54*(2), 260-271.

Hacham, Y., Song, L., Schuster, G., and Amir, R. (2007). Lysine enhances methionine content by modulating the expression of S-adenosylmethionine synthase. *The Plant Journal, 51*(5), 850-861.

Halgren, T.A. (1999*a*). MMFF VI.MMFF94s options for energy minimization studies. *Journal of Computational Chemistry, 20*, 720-729.

Halgren, T.A. (1999b). MMFF VII. Characterization of MMFF94, MMFF94s, and other widely available force feilds for conformational energies and for intermolecular-interaction energies and geometries. *Journal of Computational Chemistry, 20*, 730-748.

Harris, H., Penrose, L. S., and Thomas, D. H. H. (1959). Cystathioninuria. *Annals of Human Genetics, 23*(4), 442-453.

Harris, S. A., and Folkers, K. (1939). Synthesis of vitamin B_6. *Journal of the American Chemical Society, 61*(5), 1245-1247.

Harris, S. A., Stiller, E. T., and Folkers, K. (1939). Structure of vitamin B_6. II. *Journal of the American Chemical Society, 61*(5), 1242-1244.

Hayashi, H. (1995). Pyridoxal enzymes: Mechanistic diversity and uniformity. *Journal of Biochemistry, 118*(3), 463-473.

Higuchi, R., Krummel, B., and Saiki, R. (1988). A general method of in vitro preparation and specific mutagenesis of DNA fragments: Study of protein and DNA interactions. *Nucleic Acids Research, 16*(15), 7351-7367.

Higuchi, R. (1990). PCR protocols: a guide to methods and applications. *Editied by* M.A. Innis, D.H. Gelfand, J.J. Sninsky and T.J. White. San Diego, Academic Press: 177-83.

Holbrook, E. L., Greene, R. C., and Krueger, J. H. (1990). Purification and properties of cystathionine γ-synthase from overproducing strains of *Escherichia coli*. *Biochemistry, 29*(2), 435-442.

Huang, S., Chua, J. H., Yew, W. S., Sivaraman, J., Moore, P. K., Tan, C. H., *et al.* (2010). Site-directed mutagenesis on human cystathionine-γ-lyase reveals insights into the modulation of H_2S production. *Journal of Molecular Biology, 396*(3), 708-718.

Hurdle, J. G., O'Neill, A. J., Chopra, I., and Lee, R. E. (2011). Targeting bacterial membrane function: An underexploited mechanism for treating persistent infections. *Nature Reviews Microbiology, 9*(1), 62-75.

Hwang, J. K., and Warshel, A. (1988). Why ion pair reversal by protein engineering is unlikely to succeed. *Nature, 334*(6179), 270-272.

Hyde, C. C., Ahmed, S. A., Padlan, E. A., Miles, E. W., and Davies, D. R. (1988). Three-dimensional structure of the tryptophan synthase alpha 2 beta 2 multienzyme complex from *Salmonella typhimurium*. *Journal of Biological Chemistry, 263*(33), 17857-17871.

Ikawa, M., and Snell, E. E. (1954). Synthesis and biological activity of homologs of pyridoxal and pyridoxamine. *Journal of the American Chemical Society, 76*(3), 637-638.

Imigawa, T., Utsunomiya, H., Agari, Y., Satoh, S. and Tsuge, H. (2009a). The crystal structure of *O*-acetylhomoserine-2 from *Thermus thermophilus* HB8. Unpublished crystal structure. PDB accession: 2CB1.

Imagawa, T., Kousumi, Y., Tsuge, H., Utsunomiya, H., Ebihara, A., Nakagawa, N., Yokoyama, S. and Kuramitsu, S. (2009b). Crystal structure of o-acetyl homoserine sulfhydrylase from *Thermus thermophilus.* Unpublished crystal structure. PDB accession: 2CTZ.

Inoue, Y., Kuramitsu, S., Inoue, K., Kagamiyama, H., Hiromi, K., Tanase, S., *et al.* (1989). Substitution of a lysyl residue for arginine 386 of *Escherichia coli* aspartate aminotransferase. *The Journal of Biological Chemistry, 264*(16), 9673-9681.

Jackson, R. W., and Block, R. J. (1932). The metabolism of cystine and methionine. *Journal of Biological Chemistry, 98*(2), 465-477.

Jager, J., Moser, M., Sauder, U., and Jansonius, J. N. (1994). Crystal structures of *Escherichia coli* aspartate aminotransferase in two conformations. Comparison of an unliganded open and two liganded closed forms. *Journal of Molecular Biology, 239*(2), 285-305.

Janosik, M., Kery, V., Gaustadnes, M., Maclean, K. N., and Kraus, J. P. (2001). Regulation of human cystathionine β-synthase by S-adenosyl-L-methionine: Evidence for two catalytically active conformations involving an autoinhibitory domain in the C-terminal region. *Biochemistry, 40*(35), 10625-10633.

Jansonius, J. N. (1998). Structure, evolution and action of vitamin B_6-dependent enzymes. *Current Opinion in Structural Biology, 8*(6), 759-769.

Jansonius, J. N., Eichele, G., Ford, G. C., Kirsch, J. F., Picot, D., Thaller, C., *et al.* (1984). Three-dimensional structure of mitochondrial aspartate aminotransferase and some functional derivatives: Implications for its mode of action. *Biochemical Society Transactions, 12*(3), 424-427.

Jenkins, W. T., and Sizer, I. W. (1957). Glutamic aspartic transaminase. *Journal of the American Chemical Society, 79*(10), 2655-2656.

Jhee K. H., Yang L. H., Ahmed S. A., McPhie P., Rowlett R., and Miles E. W. (1998). Mutation of an active site residue of tryptophan β-synthase (serine 377) alters cofactor chemistry, *Journal of Biological Chemistry, 273*(19), 11417-11422.

Jhee, K. H., McPhie, P., and Miles, E. W. (2000*a*). Yeast cystathionine β-synthase is a pyridoxal phosphate enzyme but, unlike the human enzyme, is not a heme protein. *The Journal of Biological Chemistry, 275*(16), 11541-11544.

Jhee, K., McPhie, P., and Miles, E. W. (2000*b*). Domain architecture of the heme-independent yeast cystathionine β-synthase provides insights into mechanisms of catalysis and regulation. *Biochemistry, 39*(34), 10548-10556.

Jhee, K., Niks, D., McPhie, P., Dunn, M. F., and Miles, E. W. (2001). The reaction of yeast cystathionine β-synthase is rate-limited by the conversion of aminoacrylate to cystathionine. *Biochemistry, 40*(36), 10873-10880.

Jimenez-Sanchez, G., Childs, B., and Valle, D. (2001). Human disease genes. *Nature, 409*(6822), 853-855.

John, R. A. (1995). Pyridoxal phosphate-dependent enzymes. *Biochimica et Biophysica Acta (BBA) - Protein Structure and Molecular Enzymology, 1248*(2), 81-96.

Johnston, M., Jankowski, D., Marcotte, P., Tanaka, H., Esaki, N., Soda, K., *et al.* (1979). Suicide inactivation of bacterial cystathionine γ-synthase and methionine γ-lyase during processing of L-propargylglycine. *Biochemistry, 18*(21), 4690-4701.

Kabil, Ö., and Banerjee, R. (1999). Deletion of the regulatory domain in the pyridoxal phosphate-dependent heme protein cystathionine β-synthase alleviates the defect observed in a catalytic site mutant. *Journal of Biological Chemistry, 274*(44), 31256-31260.

Kack, H., Sandmark, J., Gibson, K., Schneider, G., and Lindqvist, Y. (1999). Crystal structure of diaminopelargonic acid synthase: Evolutionary relationships between pyridoxal-5'-phosphate-dependent enzymes. *Journal of Molecular Biology, 291*(4), 857-876.

Kaplan, M. M., and Flavin, M. (1965). Enzymatic synthesis of L-cystathionine from the succinic ester of L-homoserine. *Biochimica Et Biophysica Acta (BBA) - General Subjects, 104*(2), 390-396.

Kaplan, M. M., and Flavin, M. (1966a). Cystathionine γ-synthetase of *salmonella*. *Journal of Biological Chemistry, 241*(19), 4463-4471.

Kaplan, M. M., and Flavin, M. (1966b). Cystathionine γ-synthetase of *salmonella*. *Journal of Biological Chemistry, 241*(24), 5781-5789.

Kashiwamata, S., and Greenberg, D. M. (1970). Studies on cystathionine synthase of rat liver. Properties of the highly purified enzyme. *Biochimica Et Biophysica Acta, 212*(3), 488-500.

Katz, Y. S., Galili, G., and Amir, R. (2006). Regulatory role of cystathionine γ-synthase and *de novo* synthesis of methionine in ethylene production during tomato fruit ripening. *Plant Molecular Biology, 61*(1-2), 255-268.

Kerr, D., and Flavin, M. (1969). Inhibition of cystathionine γ-synthase by S-adenosylmethionine: A control mechanism for methionine synthesis in *Neurospora*. *Biochimica et Biophysica Acta (BBA) - General Subjects, 177*(1), 177-179.

Kery, V., Poneleit, L., and Kraus, J. P. (1998). Trypsin cleavage of human cystathionine β-synthase into an evolutionarily conserved active core: Structural and functional consequences. *Archives of Biochemistry and Biophysics, 355*(2), 222-232.

Khersonsky, O., Roodveldt, C., and Tawfik, D. S. (2006). Enzyme promiscuity: Evolutionary and mechanistic aspects. *Current Opinion in Chemical Biology, 10*(5), 498-508.

Kirsch, J. F., Eichele, G., Ford, G. C., Vincent, M. G., Jansonius, J. N., Gehring, H., *et al.* (1984). Mechanism of action of aspartate aminotransferase proposed on the basis of its spatial structure. *Journal of Molecular Biology, 174*(3), 497-525.

Kirsch, J. F., and Toney, M. D. (1990). Bronsted analysis of enzymatic proton transfer reactions through site-directed mutagenesis. *Annals of the New York Academy of Sciences, 585*, 48-57.

Kong, Y., Wu, D., Bai, H., Han, C., Chen, J., Chen, L., *et al.* (2008a). Enzymatic characterization and inhibitor discovery of a new cystathionine γ-synthase from helicobacter pylori. *Journal of Biochemistry, 143*(1), 59-68.

Kong, Y., Zhang, L., Yang, Z., Han, C., Hu, L., Jiang, H., *et al.* (2008b). Natural product juglone targets three key enzymes from helicobacter pylori: Inhibition assay with crystal structure characterization. *Acta Pharmacologica Sinica, 29*(7), 870-876.

Koshland, D. E. (1958). Application of a theory of enzyme specificity to protein synthesis. *Proceedings of the National Academy of Sciences of the United States of America, 44*(2), 98-104.

Koutmos, M., Kabil, O., Smith, J. L., and Banerjee, R. (2010). Structural basis for substrate activation and regulation by cystathionine β-synthase (CBS) domains in

cystathionine β-synthase. *Proceedings of the National Academy of Sciences, 107*(49), 20958-20963.

Kraus, J. P., Janosik, M., Kozich, V., Mandell, R., Shih, V., Sperandeo, M. P., *et al.* (1999). Cystathionine β-synthase mutations in homocystinuria. *Human Mutation, 13*(5), 362-375.

Kuhn, R., and Wendt, G. (1938). Über das antidermatitische Vitamin der Hefe. *Berichte der deutschen chemischen Gesellschaft, 71*(4), 780–782.

Kuhn, R., Westphal, K., Wendt, G., and Westphal, O. (1939). Synthese des adermins. *Die Naturwissenschaften, 27*(27), 469-470.

Kutzbach, C., and Stokstad, E. L. R. (1971). Mammalian methylenetetrahydrofolate reductase partial purification, properties, and inhibition by S-adenosylmethionine. *Biochimica Et Biophysica Acta (BBA) - Enzymology, 250*(3), 459-477.

Laster, L., Mudd, S. H., Finkelstein, J. D., and Irreverre, F. (1965). Homocystinuria due to cystathionine synthase deficiency: The metabolism of L-methionine. *The Journal of Clinical Investigation, 44*(10), 1708-1719.

Lepkovsky, S. (1938). Crystalline factor i. *Science , 87*(2251), 169-170.

Leuchtenberger, W., Huthmacher, K., and Drauz, K. (2005). Biotechnological production of amino acids and derivatives: Current status and prospects. *Applied Microbiology and Biotechnology, 69*(1), 1-8.

Levy, H. L., Mudd, S. H., Uhlendorf, B. W., and Madigan, P. M. (1975). Cystathioninuria and homocystinuria. *Clinica Chimica Acta; International Journal of Clinical Chemistry, 58*(1), 51-59.

Likos, J. J., Ueno, H., Feldhaus, R. W., and Metzler, D. E. (1982). A novel reaction of the coenzyme of glutamate decarboxylase with L-serine O-sulfate. *Biochemistry, 21*(18), 4377-4386.

Lodha, P. H., Jaworski, A. F., and Aitken, S. M. (2010). Characterization of site-directed mutants of residues R58, R59, D116, W340 and R372 in the active site of E. coli cystathionine β-lyase. *Protein Science : A Publication of the Protein Society, 19*(3), 383-391.

Lodha, P. H., Shadnia, H., Woodhouse, C. M., Wright, J. S., and Aitken, S. M. (2009). Investigation of residues Lys112, Glu136, His138, Gly247, Tyr248, and Asp249 in the active site of yeast cystathionine β-synthase. *Biochemistry and Cell Biology = Biochimie Et Biologie Cellulaire, 87*(3), 531-540.

Longenecker, J. B. (1957a). The comparative activities of metal ions in promoting pyridoxal-catalyzed reactions of amino acids. *Journal of the American Chemical Society, 79*(1), 142-145.

Longenecker, J. B., Ikawa, M., and Snell, E. E. (1957b). The cleavage of alpha-methylserine and alpha-methylolserine by pyridoxal and metal ions. *The Journal of Biological Chemistry, 226*(2), 663-666.

Mackenzie, C. G., Chandler, J. P., Keller, E. B., Rachele, J. R., Cross, N., and du Vigneaud, V. (1949). The oxidation and distribution of the methyl group administered as methionine. *Journal of Biological Chemistry, 180*(1), 99-111.

Maclean, K. N., Janosik, M., Oliveriusova, J., Kery, V., and Kraus, J. P. (2000). Transsulfuration in *Saccharomyces cerevisiae* is not dependent on heme: Purification and characterization of recombinant yeast cystathionine β-synthase. *Journal of Inorganic Biochemistry, 81*(3), 161-171.

Mandeles, S., Koppelman, R., and Hanke, M. E. (1954). Deuterium studies on the mechanism of enzymatic amino acid decarboxylation. *The Journal of Biological Chemistry, 209*(1), 327-336.

Matsuo, Y., and Greenberg, D. M. (1958). A crystalline enzyme that cleaves homoserine and cystathionine. I. isolation procedure and some physicochemical properties. *The Journal of Biological Chemistry, 230*(2), 545-560.

McClure, G. D., and Cook, P. F. (1994). Product binding to the alpha-carboxyl subsite results in a conformational change at the active site of O-acetylserine sulfhydrylase-A: Evidence from fluorescence spectroscopy. *Biochemistry, 33*(7), 1674-1683.

McCully, K. S. (2004). Homocysteine, vitamins, and prevention of vascular disease. *Military Medicine, 169*(4), 325-329.

McCully, K.S. (2005). Hyperhomocysteinemia and arteriosclerosis: historical perspectives. *Clinical Chemistry and Laboratory Medicine, 43*(10), 980-986.

Meier, M., Janosik, M., Kery, V., Kraus, J. P., and Burkhard, P. (2001). Structure of human cystathionine β-synthase: A unique pyridoxal 5′-phosphate-dependent heme protein. *EMBO Journal, 20*(15), 3910-3916.

Meier, M., Oliveriusova J., Kraus J.P. and Burkhard P. (2003). Structural insights into mutations of cystathionine β-synthase. *Biochimica et Biophysica Acta, 1647*(1-2), 206-213.

Meister, A. (1955). Transamination. *Advances in Enzymology and Related Subjects of Biochemistry, 16*, 185-246.

Messerschmidt, A., Worbs, M., Steegborn, C., Wahl, M. C., Huber, R., Laber, B., *et al.* (2003). Determinants of enzymatic specificity in the cys-met-metabolism PLP-dependent enzymes family: Crystal structure of cystathionine γ-lyase from yeast and intrafamiliar structure comparison. *Biological Chemistry, 384*(3), 373-386.

Metzler, D. E., Ikawa, M., and Snell, E. E. (1954). A general mechanism for vitamin B_6-catalyzed reactions. *Journal of the American Chemical Society, 76*(3), 648-652.

Miles, E. W. (1975). A new type of pyridoxal-P enzyme catalyzed reaction: The conversion of β, γ-unsaturated amino acids to saturated alpha-keto acids by tryptophan synthase. *Biochemical and Biophysical Research Communications, 66*(1), 94-102.

Miles, E. W. (1995). Tryptophan synthase. structure, function, and protein engineering. *Sub-Cellular Biochemistry, 24*, 207-254.

Mitchell, J. B., Thornton, J. M., Singh, J., and Price, S. L. (1992). Towards an understanding of the arginine-aspartate interaction. *Journal of Molecular Biology, 226*(1), 251-262.

Mörner, K. A. H. (1899). Cystin, ein spaltungsprodukt der hornsubstanz. *Hoppe-Seyler's Zeitschrift für physiologische Chemie, 28*(5-6), 595-617.

Mudd, S. H., Finkelstein, J. D., Irreverre, F., and Laster, L. (1964). Homocystinuria: An enzymatic defect. *Science , 143*, 1443-1445.

Mudd, S. H., Finkelstein, J. D., Irreverre, F., and Laster, L. (1965). Transsulfuration in mammals. *Journal of Biological Chemistry, 240*(11), 4382-4392.

Mueller, J. H. (1922a). Studies on cultural requirements of bacteria. I. *Journal of Bacteriology, 7*(3), 309-324.

Mueller, J. H. (1922b). Studies on cultural requirements of bacteria. II. *Journal of Bacteriology, 7*(3), 325-338.

Mueller, J. H. (1923). A new sulfur-containing amino-acid isolated from the hydrolytic products of protein. *Journal of Biological Chemistry, 56*(1), 157-169.

Munke, M., Kraus, J. P., Ohura, T., and Francke, U. (1988). The gene for cystathionine β-synthase (CBS) maps to the subtelomeric region on human chromosome 21q and to proximal mouse chromosome 17. *American Journal of Human Genetics, 42*(4), 550-559.

Navidpour, L., Shadnia H., Shafaroodi H., Amini M., Dehpourd A.R. and Shafiee A. (2007). Design, synthesis, and biological evaluation of substituted 2-alkylthio-1,5-

diarylimidazoles as selective COX-2 inhibitors. *Bioorganic and Medicinal Chemistry, 15*, 1976-1982.

Ngo, H.P.T., Kim, J.K., Kim, H.S., Jung, J.H., Ahn, Y.J., Kim, J.G., Lee, B.M., Kang, H.W. and Kang, L.W. (2009). Crystal structure of XometC, a cystathionine γ-lyase-like protein from *Xanthomonas oryzae*. Unpublished crystal structure. PDB accession: 3E6G.

Nikulin, A., Revtovich, S., Morozova, E., Nevskaya, N., Nikonov, S., Garber, M. and Demidkina, T. (2008). High-resolution structure of methionine γ-lyase from *Citrobacter freundii. Acta Crystallographica Section D Biological Crystallography, 64*, 211-218.

Ono, B., Heike, C., Yano, Y., Inoue, T., Naito, K., Nakagami, S., *et al.* (1992). Cloning and mapping of the CYS4 gene of *Saccharomyces cerevisiae*. *Current Genetics, 21*(4-5), 285-289.

Ono, B., Kijima, K., Inoue, T., Miyoshi, S., Matsuda, A., and Shinoda, S. (1994). Purification and properties of *Saccharomyces cerevisiae* cystathionine β-synthase. *Yeast (Chichester, England), 10*(3), 333-339.

Ono, B., Shirahige, Y., Nanjoh, A., Andou, N., Ohue, H., and Ishino-Arao, Y. (1988). Cysteine biosynthesis in *Saccharomyces cerevisiae*: Mutation that confers cystathionine β-synthase deficiency. *The Journal of Bacteriology, 170*(12), 5883-5889.

Osborne, T. B. (1902). Sulphur in protein bodies. *Journal of the American Chemical Society, 24*(2), 140-167.

Owens, L. D., Guggenheim, S., and Hilton, J. L. (1968). Rhizobium-synthesized phytototoxin: An inhibitor of β-cystathionase in *Salmonella typhimurium*. *Biochimica et Biophysica Acta, 158*(2), 219-225.

Pankey, G. A., and Sabath, L. D. (2004). Clinical relevance of bacteriostatic versus bactericidal mechanisms of action in the treatment of gram-positive bacterial infections. *Clinical Infectious Diseases, 38*(6), 864-870.

Park, Y. M., and Stauffer, G. V. (1987). Cloning and characterization of the metC gene from *Salmonella typhimurium* LT2. *Gene, 60*(2-3), 291-297.

Peracchi, A., Bettati, S., Mozzarelli, A., Rossi, G. L., Miles, E. W., and Dunn, M. F. (1996). Allosteric regulation of tryptophan synthase: Effects of pH, temperature, and alpha-subunit ligands on the equilibrium distribution of pyridoxal 5'-phosphate-L-serine intermediates. *Biochemistry, 35*(6), 1872-1880.

Perault, A. M., Pullman, B., and Valdemoro, C. (1961). Electronic aspects of the reactions of pyridoxal phosphate enzymes. *Biochimica et Biophysica Acta, 46*, 555-575.

Percudani, R., and Peracchi, A. (2003). A genomic overview of pyridoxal-phosphate-dependent enzymes. *EMBO Reports, 4*(9), 850-854.

Pogribna, M., Melnyk, S., Pogribny, I., Chango, A., Yi, P., and James, S. J. (2001). Homocysteine metabolism in children with Down syndrome: In vitro modulation. *American Journal of Human Genetics, 69*(1), 88-95.

Quazi, F., and Aitken, S. M. (2009). Characterization of the S289A,D mutants of yeast cystathionine β-synthase. *Biochimica et Biophysica Acta (BBA) - Proteins and Proteomics, 1794*(6), 892-897.

Rando, R. R. (1974). β, γ unsaturated amino acids as irreversible enzyme inhibitors. *Nature, 250*(467), 586-587.

Rando, R. R., Relyea, N., and Cheng, L. (1976). Mechanism of the irreversible inhibition of aspartate aminotransferase by the bacterial toxin L-2-amino-4-methoxy-trans-3-butenoic acid. *The Journal of Biological Chemistry, 251*(11), 3306-3312.

Ravanel, S., Job, D., and Douce, R. (1996). Purification and properties of cystathionine β-lyase from *Arabidopsis thaliana* overexpressed in *Escherichia coli*. *The Biochemical Journal, 320*(Pt 2), 383-392.

Reed, L. J., Cavallini, D., Plum, F., Rachele, J. R., and du Vigneaud, V. (1949). The conversion of methionine to cystine in a human cystinuric. *Journal of Biological Chemistry, 180*(2), 783-790.

Riordan, J. F., McElvany, K. D., and Borders, C. L.. (1977). Arginyl residues: Anion recognition sites in enzymes. *Science , 195*(4281), 884-886.

Robert, K., Vialard, F., Thiery, E., Toyama, K., Sinet, P., Janel, N., *et al.* (2003). Expression of the cystathionine β synthase (CBS) gene during mouse development and immunolocalization in adult brain. *Journal of Histochemistry and Cytochemistry, 51*(3), 363-371.

Roberts, W. (1874). Studies on biogenesis. *Philosophical Transactions of the Royal Society of London, 164*, 457-477.

Rothberg, S., and Steinberg, D. (1957). Studies on the mechanism of enzymatic decarboxylation. *Journal of the American Chemical Society, 79*(12), 3274-3278.

Rowbury, R. J., and Woods, D. D. (1964). O-succinylhomoserine as an intermediate in the synthesis of cystathionine by *Escherichia coli*. *Journal of General Microbiology, 36*(3), 341-358.

Selim, A. S. M., and Greenberg, D. M. (1959). An enzyme that synthesizes cystathionine and deaminates L-serine. *Journal of Biological Chemistry, 234*(6), 1474-1480.

Severina, I. S. (1998). Role of soluble guanylate cyclase in the molecular mechanism underlying the physiological effects of nitric oxide. *Biochemistry. 63*(7), 794-801.

Shadnia, H., J.S. Wright and J.M. Anderson. 2009. Interaction force diagrams: New insight into ligand-receptor binding. *Journal* of *Computer-Aided Molecular Design, 23*(3), 185-194.

Shlaes, D.M. (2010). *Antibiotics: The Perfect Storm*. NewYork: Springer. ISBN: 9048190568

Shaw, J. P., Petsko, G. A., and Ringe, D. (1997). Determination of the structure of alanine racemase from bacillus stearothermophilus at 1.9-Å resolution. *Biochemistry, 36*(6), 1329-1342.

Singh, S., Madzelan, P., and Banerjee, R. (2007). Properties of an unusual heme cofactor in PLP-dependent cystathionine β-synthase. *Natural Product Reports, 24*(3), 631-639.

Snell, E. E. (1953). Summary of known metabolic functions of nicotinic acid, riboflavin and vitamin B_6. *Physiological Reviews, 33*(4), 509-524.

Steegborn, C., Clausen, T., Sondermann, P., Jacob, U., Worbs, M., Marinkovic, S., *et al.* (1999). Kinetics and inhibition of recombinant human cystathionine γ-lyase. *Journal of Biological Chemistry, 274*(18), 12675-12684.

Steegborn, C., Laber, B., Messerschmidt, A., Huber, R., and Clausen, T. (2001). Crystal structures of cystathionine γ-synthase inhibitor complexes rationalize the increased affinity of a novel inhibitor. *Journal of Molecular Biology, 311*(4), 789-801.

Steegborn, C., Messerschmidt, A., Laber, B., Streber, W., Huber, R., and Clausen, T. (1999). The crystal structure of cystathionine γ-synthase from *Nicotiana tabacum* reveals its substrate and reaction specificity. *Journal of Molecular Biology, 290*(5), 983-996.

Stipanuk, M. H. (1986). Metabolism of sulfur-containing amino acids. *Annual Review of Nutrition, 6*, 179-209.

Subapriya, R., and Nagini, S. (2005). Medicinal properties of neem leaves: A review. *Current Medicinal Chemistry. Anti-Cancer Agents, 5*(2), 149-146.

Sugio, S., Petsko, G. A., Manning, J. M., Soda, K., and Ringe, D. (1995). Crystal structure of a D-amino acid aminotransferase: How the protein controls stereoselectivity. *Biochemistry, 34*(30), 9661-9669.

Sukhareva, B. S., Dunathan, H. C., and Braunstein, A. E. (1971). The stereochemistry of the abortive transmination shown by glutamate decarboxylase. *FEBS Letters, 15*(3), 241-244.

Sun, Q., Collins, R., Huang, S., Holmberg-Schiavone, L., Anand, G. S., Tan, C., *et al.* (2009). Structural basis for the inhibition mechanism of human cystathionine γ-lyase, an enzyme responsible for the production of H_2S. *Journal of Biological Chemistry, 284*(5), 3076-3085.

Tan, D., Barber, M.J., and Ferreira, G.C. (1998). The role of tyrosine 121 in cofactor binding of 5-aminolevulinate synthase. *Protein Science, 7*,1208-1213.

Taoka, S., Lepore, B. W., Kabil, O., Ojha, S., Ringe, D., and Banerjee, R. (2002). Human cystathionine β-synthase is a heme sensor protein. Evidence that the redox sensor is heme and not the vicinal cysteines in the CXXC motif seen in the crystal structure of the truncated enzyme. *Biochemistry, 41*(33), 10454-10461.

Tarver, H., and Schmidt, C. L. A. (1939). The conversion of methionine to cystine: experiments with radioactive sulfur. *Journal of Biological Chemistry, 130*(1), 67-80.

Tazuya, K., Yamada, K., Nakamura, K., and Kumaoka, H. (1987). The origin of the sulfur atom of thiamin. *Biochimica et Biophysica Acta (BBA) - General Subjects, 924*(1), 210-215.

Teague, B., Asiedu, S., and Moore, P. K. (2002). The smooth muscle relaxant effect of hydrogen sulphide in vitro: Evidence for a physiological role to control intestinal contractility. *British Journal of Pharmacology, 137*(2), 139-145.

Tian, H., Guan, R., Salsi, E., Campanini, B., Bettati, S., Kumar, V. P., Karsten W.E., Mozzarelli A., and Cook P.F. (2010). Identification of the structural determinants for the stability of substrate and aminoacrylate external schiff bases in O-acetylserine sulfhydrylase-A. *Biochemistry, 49*(29), 6093-6103.

Thompson, G. A., Datko, A. H., and Mudd, S. H. (1982). Methionine synthesis in lemna: Inhibition of cystathionine γ-synthase by propargylglycine. *Plant Physiology, 70*(5), 1347-1352.

Tomlinson, R. V., Kuhlman, D. P., Torrence, P. F., and Tieckelmann, H. (1967). Precursors of the pyrimidine and thiazole rings of thiamine. *Biochimica et Biophysica Acta (BBA) - General Subjects, 148*(1), 1-10.

Toney, M.D. and Kirsch, J.F. (1991a). Tyrosine 70 fine-tunes the catalytic efficiency of aspartate aminotransferase. *Biochemistry. 30*, 746-7461.

Toney, M.D. and Kirsch, J.F. (1991b). Kinetics and equilibria for the reactions of coenzymes with wild-type and the Y70F mutant of *Escherichia coli* aspartate aminotransferase. *Biochemistry. 30*, 7461-7466.

Toney, M. D. (2005). Reaction specificity in pyridoxal phosphate enzymes. *Archives of Biochemistry and Biophysics, 433*(1), 279-287.

Turbeville, T. D., Zhang, J., Hunter, G. A., and Ferreira, G. C. (2007). Histidine 282 in 5-aminolevulinate synthase affects substrate binding and catalysis. *Biochemistry, 46*(20), 5972-5981.

Tyndall, J. (1876). The optical deportment of the atmosphere in relation to the phenomena of putrefaction and infection. *Philosophical Transactions of the Royal Society of London, 166*, 27-74.

Ueno, H., Likos, J. J., and Metzler, D. E. (1982). Chemistry of the inactivation of cytosolic aspartate aminotransferase by serine O-sulfate. *Biochemistry, 21*(18), 4387-4393.

Vacca, R. A., Giannattasio, S., Graber, R., Sandmeier, E., Marra, E., and Christen, P. (1997). Active-site arg --> lys substitutions alter reaction and substrate specificity of aspartate aminotransferase. *Journal of Biological Chemistry, 272*(35), 21932-21937.

Voet, D., Voet, J. G., and Pratt, C. W. (2002.). *Fundamentals of biochemistry.* John Wiley & Sons Inc., New York.

Voet, J. G., Hindenlang, D. M., Blanck, T. J., Ulevitch, R. J., Kallen, R. G., and Dunathan, H. C. (1973). The stereochemistry of pyridoxal phosphate enzymes. The absolute stereochemistry of cofactor C'4 protonation in the transamination of holoserine hydroxymethylase by D-alanine. *Journal of Biological Chemistry, 248*(3), 841-842.

Weeks, C. L., Singh, S., Madzelan, P., Banerjee, R., and Spiro, T. G. (2009). Heme regulation of human cystathionine β-synthase activity: Insights from fluorescence and raman spectroscopy. *Journal of the American Chemical Society, 131*(35), 12809-12816.

Wei, Y., Lee, J. M., Richmond, C., Blattner, F. R., Rafalski, J. A., and LaRossa, R. A. (2001). High-density microarray-mediated gene expression profiling of *Escherichia coli*. *Journal of Bacteriology, 183*(2), 545-556.

Wirtz, M., and Droux, M. (2005). *Synthesis of the sulfur amino acids: Cysteine and methionine*. Springer Netherlands.

Wollaston, W. H. (1810). On cystic oxide, a new species of urinary calculus. *Philosophical Magazine Series 1, 100*, 223-230.

Wood, W. A., and Gunsalus, I. C. (1951). D-alanine formation; a racemase in *Streptococcus faecalis*. *The Journal of Biological Chemistry, 190*(1), 403-416.

Yamagata, S., D'Andrea, R. J., Fujisaki, S., Isaji, M., and Nakamura, K. (1993). Cloning and bacterial expression of the CYS3 gene encoding cystathionine γ-lyase of *Saccharomyces cerevisiae* and the physicochemical and enzymatic properties of the protein. *The Journal of Bacteriology, 175*(15), 4800-4808.

Yano, T., Mizuno, T., and Kagamiyama, H. (1993). A hydrogen-bonding network modulating enzyme function: Asparagine-194 and tyrosine-225 of *Escherichia coli* aspartate aminotransferase. *Biochemistry, 32*(7), 1810-1815.

Yanofsky, C., and Reissig, J. L. (1953). L-serine dehydrase of *Neurospora*. *The Journal of Biological Chemistry, 202*(2), 567-577.

Yao, M., Ose, T., Sugimoto, H., Horiuchi, A., Nakagawa, A., Wakatsuki, S., *et al.* (2000). Crystal structure of L-aminocyclopropane-L-carboxylate deaminase from hansenula saturnus. *Journal of Biological Chemistry, 275*(44), 34557-34565.